CYCLIC TEARING INVESTIGATIONS ON CARBON STEEL AND STAINLESS STEEL NUCLEAR PIPING COMPONENTS

By

SUNEEL KUMAR GUPTA

(ENGG01200704004)

Bhabha Atomic Research Centre, Mumbai

A thesis submitted to the

Board of Studies in Engineering Sciences

In partial fulfillment of requirements

for the Degree of

DOCTOR OF PHILOSOPHY

of

HOMI BHABHA NATIONAL INSTITUTE

March, 2015

Homi Bhabha National Institute

Recommendation of Vice Voce Committee

As members of the Vice Voce Committee, we certify that we have read the dissertation prepared by SUNEEL KUMAR GUPTA entitled "Cyclic Tearing Investigations on Carbon Steel and Stainless Steel Nuclear Piping Components" and recommend that it may be accepted as fulfilling the thesis requirement for the award of Degree of Doctor of Philosophy.

Chairman-	**Prof. V. K. Suri** **HBNI, Mumbai**	**Date:** March 05, 2015
Guide / Convener-	**Prof. J. Chattopadhyay** **HBNI, Mumbai**	**Date:** March 05, 2015
Co-Guide-	**Prof. A. K. Ghosh** **HBNI, Mumbai**	**Date:** March 05, 2015
Examiner-	**Prof. Amitava De** **IITB, Mumbai**	**Date:** March 05, 2015
Technical Adviser-	**Mr. Vivek Bhasin** **HBNI, Mumbai**	**Date:** March 05, 2015
Member-	**Prof. R. K. Singh** **HBNI, Mumbai**	**Date:** March 05, 2015
Member-	**Prof. P. V. Varde** **HBNI, Mumbai**	**Date:** March 05, 2015

Final approval and acceptance of this thesis is contingent upon the candidate's submission of the final copies of the thesis to HBNI.

We hereby certify that we have read this thesis prepared under our direction and recommend that it may be accepted as fulfilling the thesis requirement

Date: March 05, 2015

Place: Mumbai

Dr. J. Chattopadhyay, Guide **Dr. A. K. Ghosh, Co-Guide**

STATEMENT BY AUTHOR

This dissertation has been submitted in partial fulfillment of requirements for an advanced degree at Homi Bhabha National Institute (HBNI) and is deposited in the Library to be made available to borrowers under rules of the HBNI.

Brief quotations from this dissertation are allowable without special permission, provided that accurate acknowledgement of source is made. Requests for permission for extended quotation from or reproduction of this manuscript in whole or in part may be granted by the Competent Authority of HBNI when in his or her judgment the proposed use of the material is in the interests of scholarship. In all other instances, however, permission must be obtained from the author.

(Suneel Kumar Gupta)

DECLARATION

I, hereby declare that the investigation presented in the thesis has been carried out by me. The work is original and has not been submitted earlier as a whole or in part for a degree / diploma at this or any other Institution / University.

(Suneel Kumar Gupta)

LIST OF PUBLICATIONS ARISING FROM THE THESIS

Journal

1. **Suneel K. Gupta**, Vivek Bhasin, K. K. Vaze, A.K. Ghosh, H. S. Kushwaha, "Experimental Investigations on Effects of Simulated Seismic Loading on LBB Assessment of High Energy Piping ",ASME-Journal of Pressure Vessel and Technology, Vol.-129, 2007
2. **Suneel K. Gupta**, V. Bhasin, J. Chattopadhyay, A.K. Ghosh, K. K. Vaze, "A proposal on cyclic tearing based stability assurance for LBB demonstration of nuclear piping", International Journal of Pressure Vessel and Piping, vol-119, pp 69-86, July 2014
3. **Suneel K. Gupta**, V. Bhasin, J. Chattopadhyay, A.K. Ghosh, K. K. Vaze, "Cyclic-tearing behaviour and J-R curves of Indian NPP pipes under displacement controlled cyclic loading", IJPVP , 2013. (Under review Sep. 2014)

Conference

4. **Suneel K. Gupta**, Vivek Bhasin, J. Chattopadhyay, A.K. Ghosh, "Cyclic Tearing Assessment of PHT Piping Material of PHWRs", Interquadrennial Conference of The International Congress on Fracture (IQCICF-08), August 2008
5. **Suneel K. Gupta**, V. Bhasin, J. Chattopadhyay, K. K. Vaze, A.K. Ghosh, H. S. Kushwaha, "Cyclic Tearing of Through Wall Cracked Pipes made of Carbon Steel", 20th International Conference on Structural Mechanics in Reactor Technology (SMiRT 20), Division-II, Paper 1861 Espoo, Finland, August 9-14, 2009
6. **Suneel K. Gupta**, V. Bhasin, J. Chattopadhyay, A.K. Ghosh, K. K. Vaze, "Tearing-Fatigue behavior of circumferential through wall cracked stainless steel pipes under reversible cyclic loading", First International Conference on Structural Integrity (ICONS-2014), Kalpakkam, India, February 4-7 , 2014

Others

7. **Suneel K. Gupta**, Vivek Bhasin, K.K. Vaze, A.K. Ghosh and H.S. Kushwaha, " Effect of Cyclic Loads on LBB Assessment of High Energy Piping", BARC Newsletter, Issue no. 283, pp. 14-20, August 2007

(Suneel Kumar Gupta)

ACKNOWLEDGEMENT

I express my deep gratitude to my thesis guides, Prof. J. Chattopadhyay and Prof. A.K. Ghosh, of Homi Bhabha National Institute (HBNI), Mumbai, for their guidance and encouragement during my PhD. study. Their instructions and support have always been a tremendous help during the preparation of this thesis. It is a great pleasure and a great experience to conduct this thesis under their guidance.

I would like to express my great gratitude to my technical advisor, Mr. Vivek Bhasin, Head, Reactor Structures Section (RSS), of Reactor Safety Division (RSD), Bhabha Atomic Research Centre (BARC), Mumbai, for his supervision and encouragement during my PhD study. His broad and profound knowledge, his integral view on research, and his warm and encouraging smile have made a deep impression on me. Working under his supervision provided great learning in the broader area of structural integrity.

I extend my gratitude and thanks to Mr. K.K.Vaze, Director of Reactor Design and Development Group, BARC, Mr. H.S. Kushawaha, R.R. Fellow and former Director of Health safety and Environment group, BARC, and Dr. R. K. Singh (Head, RSD, BARC) for their initiative, inspiration and guidance to pursue this work.

I wish to thank to all the scientific and technical staff of Center for Design and Manufacture (CDM), BARC who have contributed in fabrication of pipe and pipe weld specimens required for this programme.

The tests in this study have been conducted at Structural Engineering Research Centre (SERC), Chennai, India as a consultancy funded project of BARC. I gratefully acknowledge the contribution of engineers and other staff of Fatigue Testing Laboratory (FTL) of SERC, Chennai for undertaking the testing work on BARC supplied pipe specimens as per specified loading and acquire specified data during the test.

I greatly acknowledge the contribution of the engineers and other staffs of Electronics & Instrumentation Services Division (EISD) of BARC who have developed the image-based technology along with a GUI based user-friendly software which was used for crack growth measurement in the current study.

I also acknowledge the contribution of Mr. Sunil Satpute, RSD, BARC, for his support in carrying out the image acquisition and their analysis to measure the crack growth.

My sincere thanks are due to my friends and fellow colleagues of Reactor Safety Division who assisted me during the need.

Lastly but definitely not the least, I express my heart felt deep gratitude to my wife Jyoti, daughter Shreya and son Shreyas. I dedicate this thesis to my family who has always been behind me and always been a source of support in my life.

Table of contents

List of Figures

List of Tables

List of Abbreviations

ADINA	:	Automatic Dynamic Incremental Nonlinear Analysis, FE software
AHWR	:	Advanced Heavy Water Reactor
ASME	:	American Society of Mechanical Engineers
ASTM	:	American Society for Testing and Standards
BCL	:	British Columbus Laboratory
CEA	:	French, Atomic Energy Centre
CMOD	:	Crack Mouth Opening Displacement
CMOD	:	Crack Mouth Opening Displacement
CRIEPI	:	Central Research Institute of Electric Power Industry
CS	:	Carbon Steel
CSB	:	Carbon Steel Base
CSW	:	Carbon Steel Weld (conventional method SMAW)
CT	:	Compact Tension
CTFAD	:	Cyclic Tearing Failure Assessment Diagram
CTOD	:	Crack Tip Opening Displacement
DEGB	:	Double-Ended Guillotine Break
ECCS	:	Emergency Core Cooling Systems
EPFM	:	Elastic Plastic facture Mechanics
EPRI	:	Electric Power Research Institute
FEM	:	Finite Element Method
GE	:	General Electric
GTAW	:	Gas Tungsten Arc Welding
IAEA	:	International Atomic Energy Agency
IPIRG	:	International Piping Integrity Research Group
LBB	:	Leak Before Break
LEFM	:	Linear Elastic Fracture Mechanics
LLD	:	Load Line Displacement
LOCA	:	Loss Of Coolant Accident
LPD	:	Load Point Displacement
LSC	:	Leakage Size Crack

LVDT	:	Linear variable Differential Transformer
NB	:	Nominal Bore
NGW	:	Narrow Groove Weld (hot wire GTAW)
NOC	:	Normal Operating Conditions
NPP	:	Nuclear Power Plant
NPP	:	Nuclear Power Plants
NRC	:	Nuclear Regulatory Commission, USA
NSC	:	Net Section Collapse
NUREG	:	NRC reports
OBE	:	Operation Basis Earthquake
PHT	:	Primary Heat Transport piping
PHWR	:	Pressurized Heavy Water Reactor
PWR	:	Pressurized Water Reactor
RSK	:	German Commission on Reactor Safety
SENB	:	single edge notch bend
SERC	:	Structural Engineering Research Centre
SMAW	:	Shielded Metal Arc Welding
SS	:	Stainless Steel
SSB	:	Stainless Steel Base
SSE	:	Safe Shut-down Earthquake
SSW	:	Stainless Steel Weld (conventional method SMAW)
TWC	:	Through Wall Cracked
USNRC	:	U.S. Nuclear Regulatory Commission
ADINA	:	Automatic Dynamic Incremental Nonlinear Analysis, FE software

List of Symbols

E	:	Young's modulus
σ_y	:	Yielding Stress
σ_u	:	Ultimate Tensile Strength
σ_f	:	Flow Stress defined as $0.5*(\sigma_y + \sigma_u)$
K	:	Stress Intensity Factor
J	:	J-integral
J_a	:	applied J-integral
J_R	:	Material's Resistance J-integral
J_i	:	J initiation, i.e. fracture crack initiation toughness
T	:	Tearing Modulus, i.e. $(dJ/da)*(E/\sigma_o^2)$
T_a	:	applied Tearing Modulus
a	:	Crack length per crack tip
Δa	:	Average Crack growth per crack tip
J_{mat}	:	Material J-integral
T_{mat}	:	Material Tearing Modulus
R	:	Load ratio, i.e. (Minimum load)/(Maximum Load)
J_{cyc}	:	Material J-integral from quasi-static cyclic loading tests
J_{mono}	:	Material J-integral from quasi-static monotonic loading tests
J_{dyn}	:	Material J-integral from dynamic monotonic loading tests
$J_{dyn,cyc}$	:	Material J-integral from dynamic cyclic loading tests
ΔJ	:	Range Cyclic J-integral
A	:	Crack Area
Π	:	Potential Energy
w	:	Strain Energy Density
T_i	:	Component of Traction Vector
u_i	:	Component of Displacement Vector
a_i	:	Half of machined notch length
θ_i	:	Half of machined notch angle
θ	:	Half crack angle (after fatigue pre-cracking)
P_c	:	Theoretical plastic collapse load

R_m	:	Mean radius of pipe
t	:	Average thickness of pipe
D_o	:	Nominal Outer diameter of pipe
I	:	Second moment of inertia of cross section
EI	:	Rigidity of pipe
P	:	Total load
Z	:	outer span
L	:	inner span
M	:	Moment, i.e. P(Z-L)/4
Δ_{Total}	:	Total Load line displacement (LLD) as recorded during test
Δ_{NC}	:	LLD of un-cracked pipe
Δ_{MC}	:	LLD due to the machine and fixture members in load path
C_M	:	Machine compliance
ϕ or ϕ_{tot}	:	Total rotation of a cracked pipe between the load points, i.e. inner span
ϕ_{NC}	:	Total rotation of an un-cracked pipe
ϕ_C	:	Part of total rotation due to crack
ϕ_{el} , ϕ_{pl}	:	elastic and plastic part of ϕ_C
B_3	:	Pipe geometry function Zahoor et. al.[32]
δ	:	Applied displacement increment after each cyclic in incremental displacement cyclic tearing tests
δ_m	:	Cyclic displacement δ given as % of load line displacement, Δ_i, at crack initiation in corresponding monotonic fracture tests
P_{max}	:	Maximum load point in Disp. Cyclic or monotonic pipe fracture test
M_{max}	:	Maximum moment in Disp. Cyclic or monotonic pipe fracture test
$N_{M\text{-}max}$	:	number of cycles to reach M_{max}
$M_{max}^{Cyclic\ test}$	:	M_{max} , Maximum moment in incremental disp. cyclic pipe fracture test
Δ_{amp}	:	applied displacement amplitude of in fully reversing cyclic displacement tests
$M_{max,app}$	:	Maximum Moment applied in each cycle
N_f	:	Number of cycles to Instability in load controlled cyclic test or total

		number of cyclic applied in displacement controlled cyclic tests
$M_{max}^{Monotonic\ Test}$	:	M_{max} of monotonic fracture test
M_{crit}	:	Critical moment, Moment capacity under monotonic loading
$\phi_{M\text{-}max}$	:	Total pipe rotation at M_{max} point in a cyclic or monotonic pipe test
$\phi_{M-max}^{monotonic\ test}$	:	Total pipe rotation at M_{max} point in a monotonic pipe test
$\Delta a_{M\text{-}max}$	:	Crack growth up to M_{max} point in a cyclic or monotonic pipe test
χ	:	crack growth rate, $da/d\phi$, obtained beyond the $\phi_{M\text{-}max}$ point where the slope of Δa vs ϕ curve becomes nearly constant in a monotonic / disp. cyclic test
J, J_{el} , J_{pl}	:	Total, elastic and plastic parts of the J-integral
f_b	:	Pipe geometry function, [32]
$J_{i,pl}$	:	plastic components of i^{th}–cycle the J-integral
$\phi_{i,pl}$	:	Plastic part of i^{th}–cycle ϕ_C
η	:	a function to multiply the area under the load vs. plastic load-point-deflection curve to get the plastic component of the J –integral
γ	:	a function to correct the plastic J-integral evaluated by η function in crack growth situations
h	:	Crack weakening function,[32]
M_{amp}	:	amplitude of cyclic moment loading
M_{mean}	:	Mean part of cyclic moment loading
$J_{max,i}$, $J_{max,el}$, $J_{max,el,i}$	:	Total, elastic and plastic part of maximum cyclic J-integral in i^{th} cycle
ΔJ_i, $\Delta J_{el,i}$, $\Delta J_{pl,i}$	:	Total, elastic and plastic part of range of cyclic J-integral in i^{th} cycle
ΔK_i	:	Equivalent SIF, $\sqrt{(E\Delta J_i)}$, obtained from elastic plastic ΔJ_i
C, m	:	Paris law constants
ΔM_i	:	Range of applied moment in i^{th} cycle
σ_o	:	reference stress, generally taken equal to yield stress
a_o	:	the initial crack length, after fatigue pre-cracking
a	:	current crack length measured at outer surface
Δa	:	Crack growth, $=(a- a_o)$
θ_i	:	Half crack angle at end of i^{th} cycle loading

$\phi_{i,pl}^{min}$, $\phi_{i,pl}^{max}$	:	Plastic rotations, ϕ_{pl} corresponding to starting and end loading point of i^{th} cycle
$J'_{i,pl}$	:	Plastic part of cyclic J-integral calculated for i^{th} cycle loading (positive half of loading branch of i^{th} cycle hysteresis loop)
$M_{max,\ Cyclic\ Load}$	:	Maximum of applied cyclic load to a through wall cracked pipe
$M_{Montonic\ Capacity}$	:	monotonic moment capacity of a through wall cracked pipe, i.e. M_{Crit}
β	:	load reduction factor, ratio of cyclic load, $M_{max,\ Cyclic\ Load}$ to $M_{Monotonic\ Capacity}$
β_M	:	load reduction factor corresponding to best-fit curve
β_L	:	load reduction factor corresponding to lower bound fit curve
Δa_{cyc}	:	Total crack growth in a cycle
Δa_{fat}	:	Fatigue crack growth in a cycle
Δa_{ter}	:	ductile tearing crack growth in a cycle

1 Introduction

The “Leak-before-break (LBB)” concept is widely applied on the high energy primary coolant loop piping, and to limited extent in secondary piping, of PHWR / PWR type nuclear power plant (NPP). The LBB approach [1-19] through application of fatigue and fracture mechanics principles, demonstrates that the double-ended guillotine rupture or equivalent break of these piping is very unlikely. Implementation of LBB concept provides early warning before any major break in pressure boundary occurs. It allows taking timely measures to prevent accident and keep the integrity of these piping intact, which in turn minimizes chances of radioactive material release inside the reactor building. This concept therefore, serves as rational basis for neglecting the consequences of pipeline breaks, such as reactive and active forces due to coolant jet outflow, its impingement onto equipment, piping and various structures, as well as possible dynamic effects associated with pipeline movement or whipping due to postulated breaks. As a result the design is simplified and facilitates easy access for maintenance and inspections. This in turn leads to reduced radiation exposure during operation and maintenance.

“Modification of General Design Criterion 4 (GDC-4): Requirements for Protection against Dynamic Effects of Postulated Pipe Ruptures”, [2], released by the U.S. Nuclear Regulatory Commission (USNRC) in 1986, uniquely defines the leak-before-break case and requirements. At present, broadly two approaches are used for LBB demonstration of piping of NPPs; one is based on the American procedure NUREG-1061 [1], Standard Review Plan, Section 3.6.3 of NUREG-0800 [3], IAEA-TECDOC [4, 5] and the other is based on German Siemens procedure [4,6]. Both of these procedures use systematic fatigue, fracture and plastic collapse assessment principles.

In LBB assessment it is ensured that material is ductile and tough, free from objectionable flaws/cracks and has adequate margin against different modes of failure. This is usually referred as level-1 of LBB and is achieved by adhering to standard design codes, sound design and manufacturing practices and rigorous quality assurance. Further, as level-2 LBB analysis, a credible sized part-through flaw is postulated, assuming it might have escaped detection during pre-service inspection. Assessments are done to ensure that under different service loads until end of life, it will not grow to a size where breakage may occur before the leak. Finally in level-3 LBB analysis, it is essential to demonstrate the stability of candidate pipe by postulating a leakage size through wall crack at the worst location. The worst location is decided based on magnitude of stresses and/or material toughness consideration. The leakage size crack (LSC) is the one that leads to reliable detection leakage under normal operation loading conditions. A safety margin is ensured on LSC with respect to the critical through wall crack. The critical through wall crack is evaluated based on monotonic ductile fracture and plastic collapse modes of failure~~s~~ under maximum credible loads during design basis earthquake event. Here, the pipe stability analysis considers the earthquake load as a one-time applied load monotonically increasing to its equivalent maximum magnitude value. Hence the present practice is based on monotonic fracture / plastic collapse failure modes and ensures stability for one cycle of equivalent maximum magnitude load associated with an earthquake event. The cyclic nature of earthquake load and associated **Cyclic-Tearing** failure mode (tearing-fatigue regime) are not explicitly considered while demonstrating fracture stability of a through wall cracked pipe during LBB analysis.

In designing the nuclear components [20, 21], a minimum of 10 cycles of equivalent maximum magnitude of induced load during an earthquake event, are considered. In Indian

NPP, one Safe Shutdown Earthquake (SSE) event (comprising of 10 cycles) and five Operating Basis Earthquake (OBE) events (comprising of 10 cycles per event) are considered in design. In view of this, the fracture stability or LBB assessment of the candidate pipe should be demonstrated for reasonable number of cycles and should be based on the cyclic tearing failure mode.

The literature survey (discussed in Chapter-2) has shown that relatively limited work was done in area of fracture stability assessment under cyclic loading conditions. These investigators have recognized the deleterious cyclic tearing damage under a cyclic loading event. Although, these proposed a cyclic J-R curve approach to account for cyclic loading damage effects but it could not be widely used/practiced due to; i) strong dependence of cyclic J-R curve on applied loading history which in turn depends on piping layout, NPP site etc., ii) it is independent of number of loading cycles of a cyclic loading event and iii) the transferability of the cyclic J-R curve from the specimen level fracture test to component level test is not verified / established yet.

Despite the large efforts (discussed in detail in Chapter-2) to understand and develop procedures to account for the loading history effects in stability analysis, the cyclic tearing failure mode is not explicitly taken care of in present guides/practices [1-19] of stability demonstration of a cracked pipe. This may be due to un-availability of simple, reliable and easily implementable procedure to demonstrate the fracture stability of cracked pipes for specified number of cycles as required in level-3 of LBB analysis.

1.1 Problem Definition and Objectives

The above discussion clearly brings out that the presently available procedures of stability analysis of cracked pipes, does not explicitly account for cyclic tearing damage. However, the existence of significant influence of cyclic tearing damage on fracture stability of pipe under cyclic seismic loading is well recognised by previous investigators. In view of this, there is a need to develop an independent alternative assessment approach to consider cyclic tearing damage for a specified number of cycles of a cyclic loading event and which could directly be implemented in existing fracture stability assessment procedures. The present work is an effort in this direction and aimed at developing an easily implementable method to demonstrate stability against cyclic tearing mode of failure. The major objectives are:

(a) Understanding of the synergic fatigue-fracture failure of carbon and stainless steel pipes under reversible cyclic loading

(b) Generate the components level cyclic and monotonic J-R curves directly from tests on pipe used in Indian nuclear power plants. The generated data would be useful in studying the issue of transferability of J-R curve from specimen to component.

(c) Quantification of the deleterious impact of reversible cyclic loading in relation with corresponding monotonic fracture behaviours under both load and displacement controlled conditions

(d) Development of Crack Growth assessment methodology for combined fatigue-tearing crack growth under reversible cyclic loading conditions.

(e) Development of a Fracture Stability assessment method for cyclic tearing failure mode. Development of cyclic tearing based criteria for LBB assessment of Nuclear Power Plants piping components.

1.2 Methodology and work plan

A two-step methodology is considered. In the first step the cyclic tearing damage is quantified in relation to corresponding monotonic fracture behaviour for wide range of variable which are likely to affect the phenomena and which covers likely variations in nuclear power plant piping. In the second-step, post-tests analytical studies are carried out to understand dependence of cyclic tearing damage on the considered parameters and to develop a simply implementable assessment approach to consider cyclic tearing damage for a specified number of cycles of a cyclic loading event into fracture stability assessment.

The work plan based on above methodology, pursued to achieve major objective can be divided into following four sections. The Section-I generates comprehensive tests data from a set of extensive large-scale piping tests under monotonic and cyclic four-point bending. Different pipe sizes materials, crack sizes and loading conditions are covered. The Section-II uses the experimental data from section-I to derive the J-R curves from the pipe tests and investigates them in relation to those from monotonic pipe tests. The Section-III examines different methods available for predicting the crack growth component response. The 2D finite element analysis carried out to understand evolution of plastic zone under reversible loading conditions. The Section-IV attempts to develop a new approach to demonstrate fracture stability for specified number of reversible loading cycles. These four sections are briefly described below:

1.2.1 Section-1: Experimental Program on Carbon and Stainless Steel Pipes of Indian Nuclear Power Plants

This section consists of an extensive programme involving large number of cyclic tearing and monotonic fracture tests on cracked straight pipes having a through wall circumferential (TWC) crack. These tests cover wide range of pipe sizes, crack sizes, pipe material, welding types, and loading conditions. The work in this section consisted of: designing the test matrix; test setup for reversible cyclic loading tests; pipe specimen fabrication i.e. preparation of welds and machine notches; fatigue pre-cracking of pipe specimens to generate sharp cracks; cyclic tearing / monotonic fracture tests with continuous recording of the load, load line displacement, crack growth using imaging technique, crack mouth opening displacement until the instability or end of test; processing of the test recorded data to evaluate salient fracture parameters; discussion and presentation of the salient test results, observations of crack growth patterns in different pipe material categories and comparison of moment-rotations (M-ϕ) under different loading histories.

1.2.2 Section-2: Investigations on "Pipe fracture behaviour and J-R curves under displacement controlled cyclic loading"

This section consists of processing and analysing the large data of displacement controlled cyclic and corresponding monotonic fracture tests, obtained from section-1 experimental programme on carbon and stain less steel pipes. The work in this section consisted of: (a) Analysing the displacement controlled cyclic tearing test data to evaluate parameters, like maximum moment capacity and corresponding rotation, crack tearing in rising and drooping portion of M-ϕ curve, number of cycles to reach maximum moment; (b) investigations on the pipe fracture behaviour, that is moment-rotation (M-ϕ) and crack growth behaviour, under incremental cyclic (gradually building) displacement loading and monotonically increasing displacement loading is investigated; (c) development of a relation to assess the impact of displacement controlled cyclic loading on the on the extent of tearing or on its maximum moment capacity; (d) evaluation and comparisons of monotonic and cyclic J-R curves for all material categories

1.2.3 Section-3: Investigation on "Pipe crack growth and stability behaviour under load controlled cyclic loading"

In this section the load controlled cyclic tearing and corresponding monotonic fracture tests data on carbon and stain less steel pipes are investigated to understand the pipe fracture behaviour under load controlled cyclic loading. The crack growth calculations and stability assessment under has been carried out. The work in this section consists of: (i) study of the pipe fracture behaviour under load controlled reversible cyclic loading, importance of load ratio, load amplitude and number of cycles of loading in instability assessment; (ii) the crack growth assessment using methodology available in literature; (iii) finite element studies on standard CT specimen to assess suitability of envelope curve usages under fully reversible cyclic loading, to understand the effect of reverse plasticity on crack tip plasticity; (iv) development and validation of a procedure for crack growth and instability assessment for reversible load controlled cyclic loading.

1.2.4 Section-4: Development of a Cyclic Tearing Failure Assessment Diagram (CTFAD) and a proposal for stability assurance for LBB analysis of nuclear piping

This section consists of development of a simple concept to accounts for the cyclic tearing damage into current monotonic integrity assessment procedure. The critical loads obtained from the load-controlled cyclic tearing experiments are correlated with number of cycles of load application. These have been studied in relation with corresponding monotonic fracture tests conducted on identical pipe. The deleterious impact of cyclic nature of loading on the stability of a cracked pipe has been quantified in term of a load reduction factor. A cyclic tearing failure assessment diagram (CTFAD) and a cyclic tearing based stability analysis method has been developed with an aim to include the number of load cycles as one of the parameters in fracture integrity assessment of a cracked pipe. In context of the developed proposal, considerations of existing safety margins and effects of other associated matters like earthquake loads nature, cyclic plasticity, piping system compliance and dynamic strain ageing has been discussed.

1.3 Summary of work

To achieve the above stated objective, a systematic experimental study has been carried out. This study is focused to single out and quantify the deleterious effect of the cyclic character of applied load on stability assessment of a circumferential through wall cracked pipe. The test program involved extensive number of cyclic tearing and corresponding monotonic fracture tests on large sized pipe components. Tests have been conducted on seamless pipes made from carbon steel (CS of SA-333 Gr.6) and austenitic stainless steel (SS of SA-312 Type 304LN) material. The CS is the material of the Primary Heat Transport (PHT) system piping of Indian Pressurized Heavy Water Reactors (IPHWRs) while the SS is the proposed material for the Main Heat Transport Piping (MHT) system of Indian Advanced Heavy Water Reactor (AHWR). The tests have been carried out on pipes of two different base material (SSB and CSB) and three different girth weld configurations/combinations. The circumferential through wall notch was machined at weld centre line of the girth welded pipe and in base metal at centre of actual pipe. The girth welded pipe specimens were prepared by joining two seamless pipe pieces using two different welding techniques namely Shielded Metal Arc Welding (SMAW) with conventional groove (CSW and SSW) and Gas Tungsten Arc Welding (GTAW) with narrow Groove (NGW). The NGW procedure is the proposed welding technique for stainless steel piping of AHWR. The pipes specimens named as CSB, CSW, SSB, SSW and NGW, are regarded as five material categories and covered reasonable variation in fracture toughness. A series of monotonic fracture tests have also been conducted to obtain the base line data under monotonically increasing load conditions corresponding to each cyclic tearing test. The pipe size, material, crack size and crack location used are identical in cyclic and monotonic fracture tests. These tests covered reasonable variation in pipe size, crack size, crack location, load history, loading control type, weld techniques and nuclear piping material etc. The piping system is subjected to mixture of load controlled and displacement controlled conditions. Therefore, the cyclic fracture tests were done under both the pure load controlled as well as pure displacement controlled loading conditions. In addition to these, limited data on similar tests on STS410 Japanese carbon steel has also been included in current investigation.

The displacement controlled cyclic tearing tests of all five material categories along with corresponding monotonic fracture tests on identical pipes, have been analysed. The displacement controlled cyclic loading tests shown very high tearing crack growth leading to DEGB under step wise build-up of cyclic displacement loading. The relative comparisons of the pipe fracture behaviour obtained from cyclic displacement and corresponding monotonic fracture tests. A small decrease in the maximum moment but large decrease in corresponding displacement value is observed when compared to those obtained in monotonic fracture test on identical pipe. The cyclic J-R curves of all five material categories have shown significant decrease in fracture resistance under cyclic loading conditions. Smaller the cyclic displacement increment step resulted in larger drop in cyclic J-R curve.

The load controlled cyclic tearing tests have been conducted to assess the pipe crack growth and fracture stability behaviour during an earthquake event and they in general are treated as load controlled and of fully reversing cyclic in nature. They revealed that the pipe may fail by unstable tearing in very few cycles under fully reversible load with a magnitude much below the monotonic capacity of pipe. The unstable failure of pipe us preceded by large crack growth. The crack growth and number of cycles before unstable failure are found correlated with applied loading. Larger compressive load in reverse direction (that is when larger negative load ratio) caused cyclic damage and resulted in accelerated crack growth. This happened due to re-sharpening of crack tip and sharpening/flattening of otherwise voids under compressive loads / compressive plasticity.

Each of the load controlled cyclic tearing test results have been assessed in relation to corresponding monotonic fracture test conducted on identical pipe. The effect of number of load cycles and cyclic tearing damage on stability of a pipe is quantified in term of a load reduction factor (β). The β factor is defined as ratio of magnitude of cyclically applied load to the load capacity of the identical pipe under monotonically increasing load. A Cyclic Tearing Failure Assessment Diagram (CTFAD) is developed from β factors. A lower bound CTFAD curve equation (β_L) is proposed for fracture stability assessment under cyclic loading. The β_L factor usage enables the existing procedures of stability assessment to demonstrate the integrity for specified number of load cycles. Based on CTFAD and proposed equation, load reduction factors are proposed to rule out the unstable failure of a cracked pipe for different number of load cycles associated with different levels of earthquakes.

The thesis has been structured into seven chapters. The scope and significance of the research and the motivation behind the present investigation are briefed in Chapter-1. The salient literature background related to the current investigation has been presented in Chapter-2. The Chapter-3 presents details of the experimental program, methodology, and salient results. Chapter-4 presented the investigation on the cyclic / monotonic J-R curves and the pipe fracture behaviour under displacement controlled cyclic loading. The pipe fracture stability and crack growth behaviour under load controlled conditions are discussed in Chapter-5. Attempts have been made to assign explanations, reasons and justification for the observed results which are presented in graphical/tabular form. The Chapter-6 presented how the cyclic tearing damage is quantified and singled out from other aspects which affect the fracture stability behaviour of pipe. A cyclic fracture stability assessment method is proposed here. An overview of the conclusions derived from this work has been summarized briefly in Chapter-7 together with some proposed future work related to this area. All references quoted throughout the dissertation have been given after Chapter-7.

2 Literature Review

2.1 Introduction

This chapter deals with philosophy and methodology of designing pressurised piping for leak before break (LBB) condition; the terminologies of stability assessment of cracked pipes using elastic-plastic fracture mechanics, plastic collapse procedures and various parameters such as stress intensity factor (K), crack mouth opening displacement (CMOD), J-integral and tearing modulus T etc. have been defined and explained in brief. The currently used stability analysis procedures for leak-before break evaluation of pressure piping system is also described in brief.

The literature status on the following topic are covered: the LBB background and currently followed methodologies; investigations and consideration of the load history effects on the ductile fracture of pipe; the engineering need and the concepts behind development of cyclic J and ΔJ integral, cyclic J-R curves with their limitations; impact of geometric constraint, dynamic strain ageing, piping system compliance etc. on fracture assessment etc.. This section incorporates summary of outcomes from the two large programmes taken up by International Piping Integrity Research Group (IPIRG) and Central Research Institute for Electric Power Industry (CRIEPI), Japan in this area. Additionally many other associated issues like, impact of geometry / constraints, dynamic strain ageing, piping system compliance, and material’s cyclic plasticity behaviour on fracture stability assessment and LBB demonstration have been discussed.

Finally the limitation of presently available assessment methods and appraisal of the problem undertaken for present investigation are highlighted.

2.2 Leak-Before-Break (LBB)

Leak-before-break (LBB) is a term that has been used for decades in reference to a methodology that means that a leak will be discovered prior to a fracture occurring in service. LBB is most often used in high energy pipe lines of nuclear power plant piping and also being applied in many other places like gas and oil pipelines etc. The basic idea of LBB is to exclude any potential for pipe break and then prove that the critical crack which occurred in spite of the exclusion of all detrimental mechanisms will be safely detectable within reasonable time. Early detection enables shut down of the reactor in the case of a nuclear power plant.

Presently the primary piping of NPPs worldwide is demonstrated to meet LBB requirements. The LBB assessment of pressurized primary piping is done for two reasons. One is to provide assurance that there would be early warning before any major break in pressure boundary occurs. In this regard the calculations also help in serving design basis of leak monitoring devices, etc. The second important reason is to arrive at design simplifications to minimize design and operational penalty (i.e. the radiation exposure during in-service inspection). This is due to the fact that rupture of the pipe does not form design basis of pipe supports, jet shield, pipe whip restraints etc. This in turn leads to lesser operation stress and removal of jet shield, pipe whip restraints improves the accessibility to pipes which leads to lesser radiation exposure during in service inspection.

2.2.1 LBB Background

Historically, a hypothetical double-ended guillotine break (DEGB) of largest size high energy pipe line has been considered as the most severe accident namely loss of coolant accident (LOCA), while designing the NPP. Originally the postulation of DEGB was to provide a design basis for sizing the reactor containment system. However, later it was extended to the design of the high energy piping system, resulting in the construction of massive pipe whip restraints and jet impingement shields, simply because no alternate acceptable design basis was available. The DEGB postulate was further extended to the design for environmental qualification and even in the sizing of the emergency core cooling systems (ECCS).

For many years, the commercial nuclear industry has recognized that a DEGB is highly unlikely even under severe accident loads and that a design basis LOCA based on DEGB is an unnecessary and undesirable design restriction. The LBB methodology has been accepted as a technically justifiable approach for eliminating postulated DEGB in high energy piping systems. This conclusion resulted from extensive research, development and rigorous evaluations in the area of fatigue, fracture, material and component tests, defect inspection and leak detection technologies, by the U.S. Nuclear Regulatory Commission (USNRC), the German Commission on Reactor Safety (RSK) and the commercial nuclear power industry since the early 1970s.

2.2.2 LBB Methodology

The methodology to demonstrate LBB compliance is based on advanced fracture / fatigue mechanics techniques and includes critical flaw size evaluation; leakage calculation; crack propagation analysis; ultrasonic flaw detection/sizing; leak detection; and service experience. "Modification of General Design Criterion 4 (GDC-4): Requirements for Protection against Dynamic Effects of Postulated Pipe Ruptures", [2], released by the USNRC in 1984, uniquely defines the leak-before-break case. LBB assessment involves three levels. The complete LBB assessment calls for generation of complete material property database and understanding of material degradation mechanisms owing to ageing and environment (level-1), fatigue analysis (level-2), leak rate and fracture analysis (level-3). In level-1 it is ensured that material is ductile/tough and free from objectionable flaws/cracks. This is usually achieved by adhering to standard design codes, sound design and manufacture practices and rigorous quality assurance. In level-2 a credible sized part-through flaw is postulated, assuming it might have escaped detection during pre-service inspection. Assessments are done to assure that under different service loads it will not grow to a size where breakage may occur before the leak. In level-3, as a worst-case assumption, it is postulated that a through-wall crack exists with maximum credible size such that flow through can be detected using leakage monitoring system under normal operating conditions (NOC) loads. Such postulated crack is called as Leakage Size Crack (LSC). LSC is postulated, at all the potential locations and rigorous fracture assessment is performed for demonstration of LBB capability and safety margin against fracture failure, under postulated design basis accident event loading which in several countries, as in India also, is Safe Shutdown Earthquake (SSE). Presently LBB is applied worldwide in high energy piping of nuclear power plant and requirements and methodology are well documented in several guides/reports like USNRC LBB guide NUREG 1061 Vol-3 [1], Standard Review Plan, Section 3.6.3 of NUREG-0800 [3], IAEA-TECDOC [4, 5], Russian LBB guide[6], French LBB Guide [7], British R-6 method [8], German LBB concept [9-11], European LBB practices [12], NUREG-6765 on LBB technical basis [13], Korean practice [14], India [15], China [16,17] and recent developments in France [18, 19] etc..

From all above documents/reports it is clear that the most important and indispensable requirement for LBB is the stability demonstration of a leaking pipe.

"The piping system with a through wall crack, providing enough leakage for reliable detection by installed leak monitoring systems, shall remain stable during a severe earth quake event considered in design basis loading of piping system"

This requirement calls for integrity/stability demonstration of a through wall cracked (LSC size) pipe under normal operating conditions as well as under combined normal plus earthquake loading.

2.3 Stability analysis of cracked pipes

The nuclear power plant piping components are invariably made of ductile materials, like low C-Mn steel or austenitic stainless steel, and their failure is governed either by ductile fracture or by plastic collapse when they are subjected to large loading. Hence, the critical or ultimate load/moment (M_U or M_C) is taken as minimum of unstable ductile fracture/tearing load (M_f) or plastic collapse moment (M_p). The unstable ductile tearing load is assessed using the elastic plastic fracture mechanics while the plastic collapse load assessment is based on limit load analysis and net section plasticity. In the past huge effort were made to develop stability assessment procedures for the cracked pipe subjected to axial and bending loading. A brief background of these efforts in context of LBB is given below:

2.3.1 Background

The research and developments during 1960s, led to development of elastic plastic fracture mechanics parameters like CTOD [22] and J-integral [23] which later become the predominant method to characterize elastic-plastic fracture in the nuclear industry. During 1970s-80s, the research and developments efforts led to development of stability analysis procedures specially J-integral based solutions for piping fracture analysis, standardization of the J-R curve testing method to develop elastic-plastic fracture toughness of piping materials, and validation of the J solutions for cracked pipe using pipe experiments typically done under simple quasi-static loading. The J-integral tearing modulus fracture instability methodology got recognised and came into use. The tearing modulus (T) is a dimensionless parameter that is proportional to slope of the J-integral vs. Crack length (or growth) curve, $T \propto dJ/da$.

2.3.2 Elastic Plastic Fracture Mechanics

Elastic Plastic Fracture Mechanics (EPFM) is used when large plastic zone is formed ahead of crack tip. EPFM demands a careful understanding of the crack tip plasticity and currently there are main two methods of ductile fracture assessment. These are: (i) Crack tip opening displacement (CTOD), suggested by Wells [22] and is popular in Europe (ii) J-integral proposed by Rice [23] and is widely used in the United States. Both these fracture parameters are discussed below:

2.3.2.1 J-Integral

In 1968, Dr. James Rice [23] first proposed the J-integral as an elastic-plastic fracture mechanics (EPFM) methodology. It provided the basis for EPFM fracture mechanics methodology well beyond the validity limits of Linear Elastic Fracture Mechanics (LEFM). Since then, this parameter has become the predominant method to characterize elastic-plastic fracture in the nuclear industry. The J integral has been used to characterise the crack driving force, crack tip stress field and the strain energy release rate during crack growth under elastic plastic. Thus the J integral can be viewed as both an energy parameter and a stress intensity parameter for non-linear materials. The J-integral as energy parameter is defined as

$$J = \frac{d\Pi}{dA} \tag{2.1}$$

Where ‘Π’ is the potential energy and ‘A’ is crack area. The potential energy is given as difference of the strain energy stored in the body and the work done by external forces. The integral as a path independent parameter is defined as

$$J = \int_{\Gamma} \left(w\, dy - T_i \frac{\partial u_i}{\partial x} ds \right) \tag{2.2}$$

Where ‘w’ is the strain energy density and ‘T_i’ are component of traction vector. The ‘u_i’ is the displacement vector and the ds is a length increment along an arbitrary contour path ‘Γ’ taken as clockwise around the tip of the crack (see Figure 2.1(a)). The basic J-integral parameter was extended further to account for toughness changes with crack growth, resulting in what is known as the J-resistance curve.

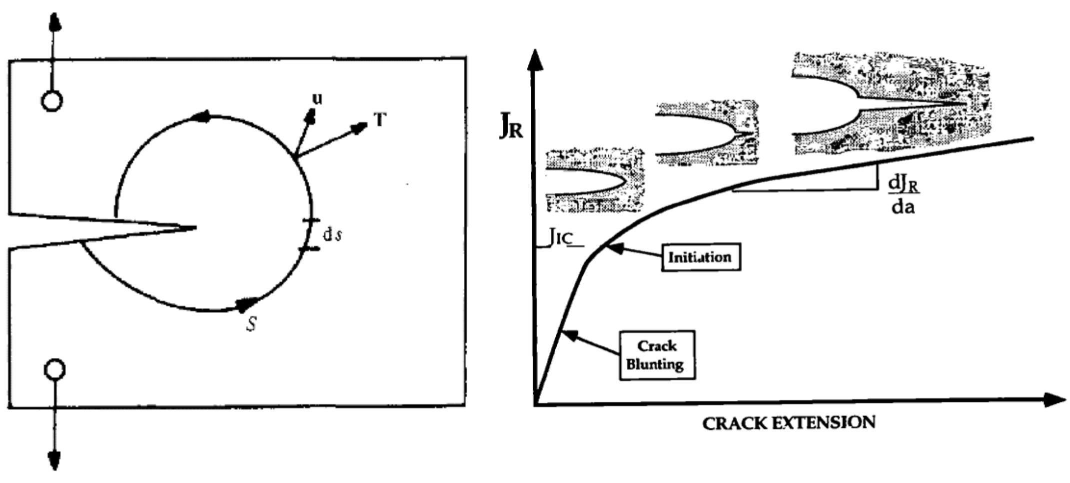

Figure 2.1:(a) Schematic of an arbitrary contour around the crack tip of a CT specimen; (b) Schematic of a typical J-R curve of ductile material (Ref. [25])

2.3.2.2 ***Crack Tip Opening Displacement (CTOD)***

Wells [22] proposed that the failure of a cracked component can be characterized by Crack Tip Opening Displacement (CTOD) theory based on the study of fracture specimens that degree of crack blunting in proportion of the material ductility. The CTOD or Crack Mouth Opening Displacement (CMOD) is defined as the opening of the crack faces in the vicinity of a sharp crack tip and is a measure for the plastic strain ahead of the crack-tip.

The Shih [24] analysis shows mat there is a unique relationship between J and CTOD/CMOD for a given material. Thus these two quantities are equally valid crack tip characterizing parameters for elastic-plastic materials.

2.3.2.3 ***Tearing Modulus***

The J-integral is used with Tearing Modulus T (J-Tearing method) in elastic plastic fracture assessment [41].The J-integral, as crack driving force or as material resistance to crack growth, changes with extension of crack. The rate of change of J-integral has significance while assessing stability of crack growth. The slope of J_{app} - Δa (or J_R - Δa) curve is usually quantified by a dimensionless parameter called Tearing Modulus. It is defined as:

$$T = \frac{E}{\sigma_0^{\,2}} \frac{dJ}{da} \tag{2.3}$$

Where E is the elastic modulus and σ_o is the flow stress of the material.

2.3.2.4 ***Crack growth resistance curve (J-R curve)***

Many materials with high toughness display increasing fracture resistance with crack growth characterized by a rising J-R curve. The material’s resistance to crack growth is quantified by the J-resistance (J-R) curve and is evaluated by performing fracture tests on small sized cracked specimens such as compact tension, CT and single edge notch bend, SENB etc. or piping components such as cracked pipes or elbows etc.. A typical J_R-Δa curve plot is shown in Figure 2.1(b).

2.3.2.5 <u>J-Tearing Analysis</u>

In the application of elastic plastic fracture mechanics (EPFM) for fracture assessment of NPP piping, the J-tearing theory is an established concept for calculation of maximum load carrying capacity of the pipe. It is based on the ductile tearing i.e. on the fact that fracture instability occurs at higher applied loads and after some amount of stable crack growth in ductile and tough materials. The initiation of crack growth is characterised by following equation:

$$\mathrm{J_a} \geq \mathrm{J}_i \tag{2.4}$$

Here 'J_a' is the applied J-integral and is obtained from the analysis of cracked component geometry under specified loading. The 'J_i' in the fracture crack initiation toughness and is obtained from standard fracture tests on small specimens made from same material. The fracture instability based on J-tearing theory is characterized by following equations.

$$J_a(\Delta a) \geq J_R(\Delta a) \tag{2.5}$$

$$T_a(\Delta a) \geq T_R(\Delta a) \tag{2.6}$$

To evaluate the instability load, the applied J-integral, 'J_a', and the tearing modulus, 'T_a', are respectively compared with those obtained from material J_R-Δa curve. The material J_R-Δa (or J_{mat}-T_{mat}) curve can be extrapolated beyond the maximum Δa obtained in specimen fracture test [26].

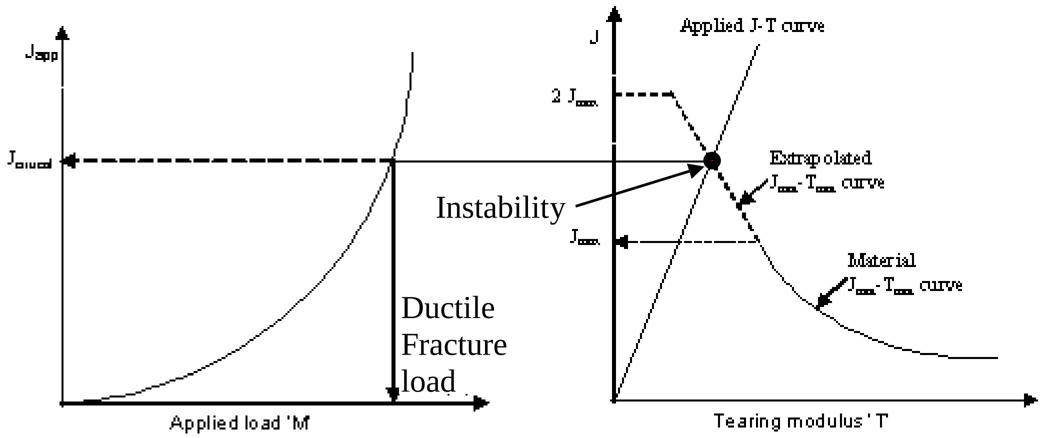

Figure 2.2 : Schematic of ductile fracture assessment using J-tearing analysis

2.3.3 Plastic Collapse

The plastic collapse is a competing failure mode to ductile fracture for cracked components made of ductile material. Here the failure is characterised when gross plasticity deformation or yielding occurs in the section containing crack which leads to unbounded / large deformations in the structure component leading to instability (see Figure 2.3). The plastic collapse assessment methods are well developed [27-31]

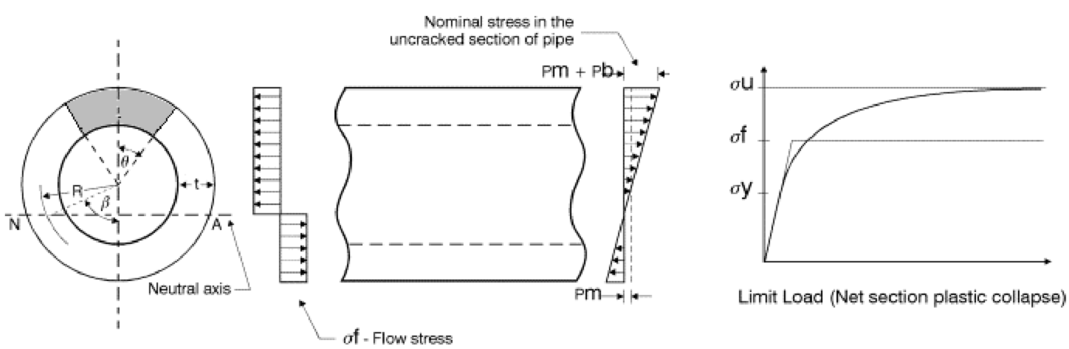

Figure 2.3: A schematic showing plastic collapse

2.3.4 Stability Analysis Methods: LBB level-3

Current leak-before-break analyses involve assessing the load-carrying capacity of through-wall cracked pipe. These assessments assume that the load is increased in a quasi-static fashion until the instability owing to fracture or plastic collapse occurs. The load carrying capacity of a pipe is taken as minimum of the critical load obtained for two competing mode of failures namely unstable ductile tearing and plastic collapse. In case of ductile materials, ductile tearing failure mode based critical load may be higher than that evaluated based on plastic collapse. Hence for ductile materials, both ductile fracture and plastic collapse mode of failure are considered in stability analysis of cracked piping components for demonstration of their compliance to LBB. Currently several methodologies of stability assessment are available in literature, codes and guides [6-8, 32-42]. The material's tensile, fatigue and fracture properties required in these methodologies are obtained by performing small specimen tests following the testing standards [43-45]. These stability assessment methodologies can be grouped into three broad categories as given below:

(a) J-integral based methods: This is a fracture mechanics based methodology which does not implicitly consider the possibility of plastic collapse mode of failure. Here, the criterion is primarily derived based on ductile tearing mode of failure with the calculation of J-integral by following methods:

(i) GE-EPRI J-Tearing Method

(ii) A-16 method

(iii) LBB-NRC Method

(iv) LBB.BCL1 Method

(v) LBB.BCL2 Method

(vi) Finite Element Method

The technical basis of above (iv and v) analyses methods was developed in the Degraded Piping Program of USNRC. Other methods GE/EPRI [32, 36-37] and LBB.NRC [42] analyses are based on the J-integral/tearing modulus theory. The A-16 [7] method is developed by French CEA as part of RCC-M code appendix. As such, (i - v) fall under the category of J-estimation schemes. These J-estimation schemes are relatively simple to use compared to finite element analysis.

b) Plastic collapse/instability based methods: Here, the criterion is primarily derived based on net section plastic collapse or the plastic instability mode of failure.

(i) Limit Load Method

(ii) Modified Limit Load Method

(iii) Moments Method

c) Double criteria approach: Here, the criterion considered both fracture as well as plastic collapse mode of failure.

(i) R-6 method [8]

(ii) ASME Section XI, Z-Factor method [38]

(iii) ASME Section XI, FAD method [38]

2.4 Load history effects on fracture stability cracked piping

The discussions in previous section have shown that the fracture stability assessment of cracked piping under quasi-static monotonic loading conditions is well understood and the analyses procedures / methodologies are well developed, validated and have been used in LBB analysis worldwide since last 2-3 decades. However these analyses/methodologies do not explicitly account for load history and load cycle effects on stability of cracked piping. In this section the existing literature has been reviewed in context of impact of load history effects onto fracture stability assessment of cracked piping. An earthquake event, which is considered in designing and LBB demonstration of the piping system of NPPs, induces reversible dynamic cyclic loading. In view of this the effects of load history and the number of loading cycles, on stability analysis of piping is a very important aspect of LBB compliance. A leaking pipe, which is considered safe based on monotonic load stability analysis procedures (sec.2.3.4), may fail in very few cycles of repetitive dynamic loading.

While reviewing various regulatory guides and documents on LBB [1-19] practised in different countries, it is observed that most of these documents are silent on consideration of the load history effects on the fracture/tearing stability assessment of a cracked pipe. Although some of them (e.g. NUREG-1061 vol.3 [1]) have identified its importance, however, no suggestions have been made to account for the degradation during cyclic loading. Below is an extract from NUREG 1061 [1]

…."The ductile fracture mechanics and experimental J-R curve techniques discussed in the report assume that loads are applied in a monotonically increasing fashion. In reality, under seismic loading conditions fully reversed cyclic loading could be anticipated. To date little work has been performed to evaluate the load history effects

on ductile fracture."….. (Section 10.4 of [1])

The review of all the current leak-before-break (LBB) [1-19] documents and in-service flaw stability evaluation criteria [38], showed that the fracture evaluations are typically based on a quasi-static monotonic J-R curve data. The earthquake loading, however is dynamic cyclic in nature.

2.4.1 Background

In view of above, in recent past two large experimental and analytical programmes, namely International Piping Integrity Research Group (IPIRG) programme (from 1986 - 1997), [46 to 61], and a programme (1991-1997) by Central Research Institute of Electric Power Industry (CRIEPI) Japan, [62-66], have put huge effort to understand and develop procedures to account for loading history effects in crack growth and stability analysis in the tearing – fatigue region. The IPIRG tests [13, 56-58] have shown that seismic inertial loading can produce complete fracture instability. The reversible cyclic nature of the earthquake load was found to have substantial deleterious effects on fracture, rather than its dynamic nature. IPIRG programme presented two approaches to account for the cyclic loading effect on ductile tearing assessment of cracked pipe. First one is based on the low cycle fatigue crack growth using the Dowling's ΔJ-integral while the other modifies the J-R curve, named as Cyclic J-R curve, to account for load-history effects. In CRIEPI programme a procedure for crack growth calculation and stability assessment was proposed. This was based on cyclic J_{max} and ΔJ integrals, evaluated from load - displacement envelope curve of the cyclic tearing test.

In addition to above research programmes, limited work was reported by other investigators which are primary based on tearing fatigue tests on CT specimen to study material behaviour under cyclic loading. Salient observations from these research works are discussed in following sections:

2.4.2 IPIRG Program (1986-97)

The International Piping Integrity Research Group (IPIRG) [46 to 61] who shared a common interest, was an international group formed and managed by the U.S. Nuclear Regulatory Commission and funded by a consortium of organizations from nine nations: Canada, France, Italy, Japan, Sweden, Switzerland, Taiwan, the United Kingdom, and the United States. One of the objectives of the IPIRG programs was to investigate the behaviour of circumferentially flawed piping systems subjected to high-rate repetitive loadings typical of seismic events.

Prior to IPIRG-1 program, the nuclear piping fracture research in the international community had focused on relatively large cracks in straight pipe and welds joining straight pipe under simple monotonic loading. As a result, the technology for predicting the behaviour of such cracks is relatively established. However, no efforts had been undertaken to determine if using quasi-static material properties was appropriate to use for integrity assessment of components subjected to cyclic type of loading e.g. earthquake. Under IPIRG-1 program there were three main experimental efforts undertaken in the area of load history effects on fracture resistance. These are:

(1) The simplest involved through-wall-cracked pipe tests conducted under four-point bending under different loading conditions. The IPIRG-l Program evaluated the separate and combined effects of dynamic and single-frequency cyclic loading on

circumferentially cracked pipe in four-point-bending experiments and in pipe system experiments. During the IPIRG-1, a series of circumferential through-wall-cracked pipe fracture experiments were conducted with the intent of investigating the separate effects of dynamic and cyclic loading on the fracture toughness of typical ferritic carbon and austenitic stainless steels. The results from both the load-history effects on fracture and the piping system evaluations showed that reversed cyclic loading during ductile tearing had a large effect on the apparent toughness of the material. The dynamic load effects were negligible for the TP304 steel, but tended to marginally reduce the toughness and load-capacity of the A106 B pipe material [35]. The investigations attempted to quantify the effect of cyclic and dynamic nature of loading on quasi-static monotonic fracture toughness of material. The quasi-static cyclic J (for fully reversed loading) and the dynamic monotonic J were related (see Figure 2.4) with the corresponding quasi-static monotonic J data [60].

(2) The second type pipe tests, slightly complicated, were conducted with internal pressure, an initial dead-weight load, and inertial loads. In these tests, once the pipe reached the maximum load, it only took two to four cycles to reach DEGB [35].

(3) The third type was major fracture tests of the IPIRG- 1 program. These were conducted on piping system conducted at PWR conditions with a relatively large diameter pipe [59]. Here, in all the experiments, the surface crack penetrated the pipe wall and grew unstably until it got arrested at the ends of the surface crack. Subsequent cyclic loading caused additional through-wall crack growth to produce a double- ended break [59]. The comparison of the maximum loads from

the pipe system and the quasi-static pipe experiments were also investigated in IPIRG-1 program [58]. The ratio of the maximum loads of the system experiments to the quasi-static experiments versus the quasi-static yield-to-ultimate strength ratio is shown in Figure 2.5(a) (reproduced from [58]). Here it may be noted that, in most cases, the pipe system maximum loads are lower than the quasi-static monotonic bend tests maximum loads. The effect of the different stress components (i.e., primary membrane, Primary bending, secondary thermal expansion, and secondary seismic anchor motion) in pipe system tests test and the comparison of the total maximum loads with that in the quasi-static experiments is shown in Figure 2.5(b) (reproduced from [58]). These tests were analysed and the margins were evaluated using various popular fracture analyses methods, like NSC, ASME Sec-XI, R-6 and J-Tearing etc. The fracture margins, defined as the ratio of maximum stress measured in the test and predicted by analytical methods, for both the IPIRG pipe system experiments as well as the companion quasi-static experiments, are shown in Figure 2.5(a and c) (reproduced from [58, 59 and 62]).

The results from IPIRG-1 program, both the load-history effects on pipe fracture and the piping system evaluations gave significant insight into the real behaviour needed to realistically assess the leak-before-break (LBB) and in-service flaw evaluations. These experiments showed that reversed cyclic loadings caused a significant decrease in the apparent toughness of the cracked pipe.

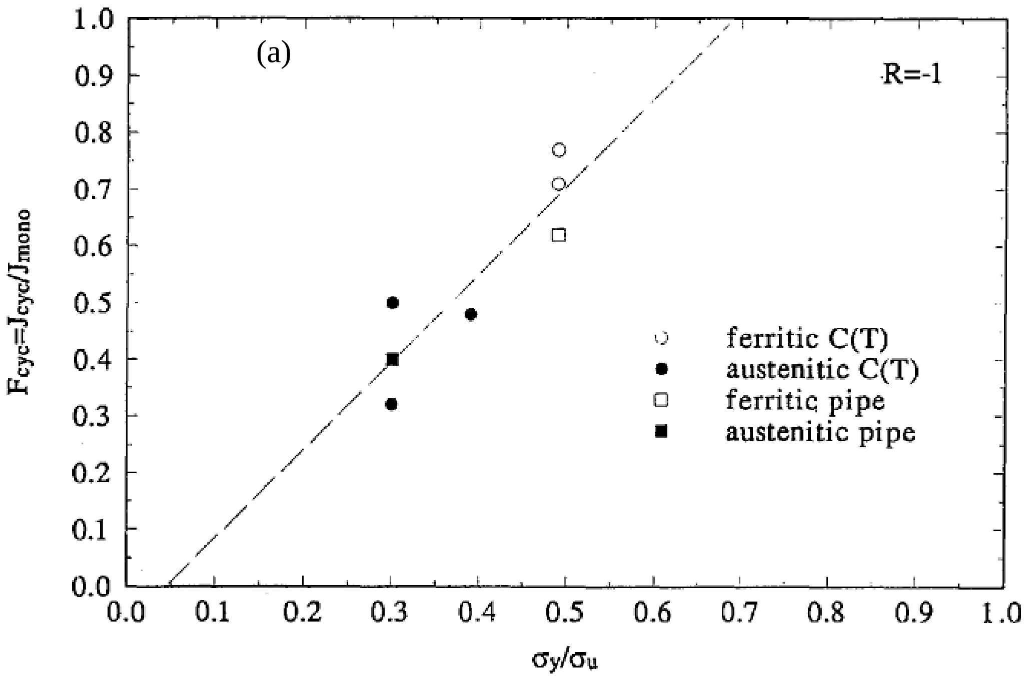

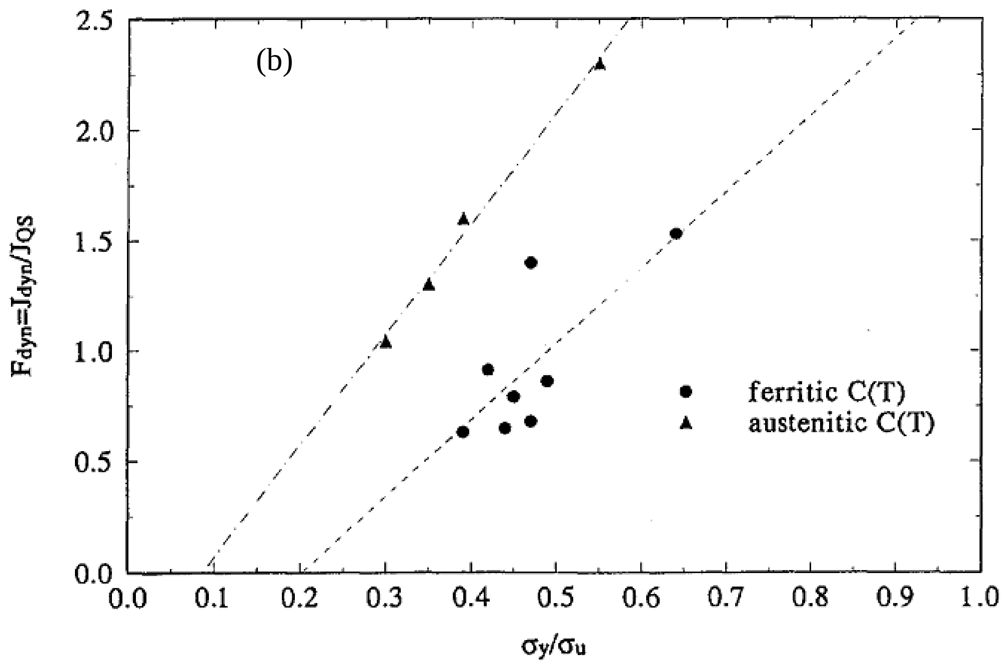

Figure 2.4: (a) The effect of cyclic loading on fracture toughness; [ref. 60] (b) the effect of dynamic loading rate on fracture toughness [ref. 60]

(a) Ratio of IPIRG-l pipe system maximum loads to the companion quasi-static pipe test maximum load versus quasi-static yield-to-ultimate strength, all data at 288C (ref. [58])

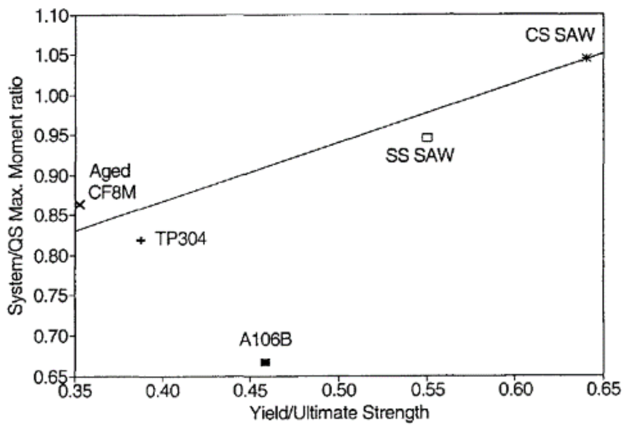

(b) Bar chart showing the fracture behaviour of the IPIRG-I pipe-system experiments (ref. [58]) Comparison of maximum loads for IPIRG-l pipe system tests and companion quasi- static tests (CSBM=AI06 B base metal, SSBM=TP304 base metal, ACS=aged CF8M, CSW= carbon steel SAW, SSW=stainless steel SAW)

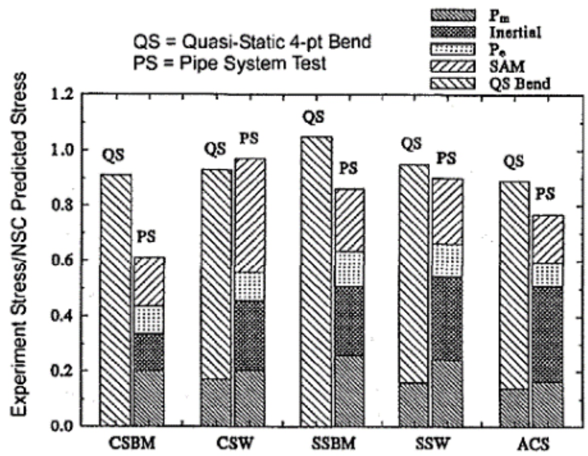

(c) Range of inherent fracture margins for pipe system and quasi-static experiments (ref. [59])

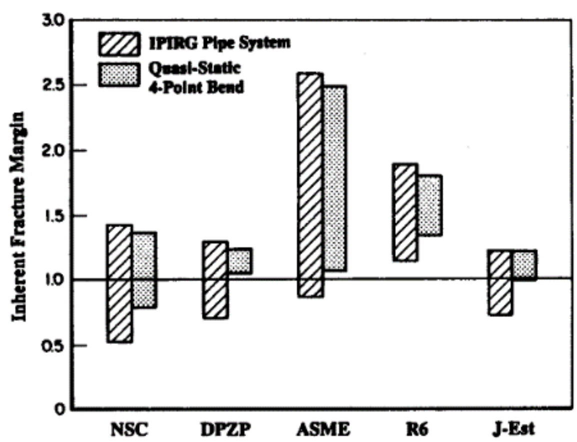

Figure 2.5: Salient results from IPIRG piping system and standalone pipe fracture tests

Second International Piping Integrity Research Group (IPIRG-2) Program was built on what was learnt during the IPIRG-1 program. The task 1 and task 3 of IPIRG-2 program were on further studies on dynamic cyclic fracture assessment of cracked pipe and piping system. These are briefly

(a) **IPIRG-2 Task 1:** In this task tests were conducted on pipe system (loop) with flaws in straight pipe / welds, under a simulated seismic loading history as opposed to the single-frequency loading used in the IPIRG-1program. The investigations were focused on the effects of complex load histories with variable amplitudes and multiple frequency content such as in a seismic event.

(b) **IPIRG-2 Task 3:** This task dealt with cyclic and dynamic load effects on fracture toughness. The investigations were focused on the resolution of differences in toughness values observed between laboratory specimen and full-scale pipe experimental data resulting from load history effects, such as the cyclic and dynamic loading effects that can occur during a seismic event.

2.4.2.1 Summary of outcomes from IPIRG program in context of present study

The salient observations reported from IPIRG programme [46-61] related to stability assessment under seismic load are given below:

(a) NUREG 6233-1 [57], NUREG 6233-4 [56], NUREG 6452 [61], G. Wilkowski et al. [58] and NUREG 6765 [13] reported that the inertial loading produced complete fracture instability in only a few cycles past maximum load. The inertial stresses produced in these experiments were similar to load-controlled stresses for fracture stability analyses. The load-carrying capacity of a cracked pipe subjected to a simulated seismic load history is no worse than that of a cracked pipe subjected to the single-frequency excitation. In IPIRG-1 program, the ratios of maximum loads obtained in the system experiments to that obtained in the quasi-static monotonic bend tests [58], in most cases, are less than 1, see Figure 2.5(a and b).

(b) The stress ratio (minimum/maximum stress) for a cracked pipe system at SSE loading should conservatively be assumed to be -1, because cracked pipe has a more negative stress ratio than un cracked pipe. [61]

(c) The investigations, NUREG-6440 [53] showed weak interaction between the dynamic and cyclic effects. NUREG-6438 [50] reported that the cyclic nature of the loading has substantial effect on the fracture resistance of the material than that of dynamic nature. Hence the deleterious damage due to cyclic nature of load dominates. NUREG 6233-2 [54] reported reduction in the load-carrying capacity, and apparent toughness under quasi-static incremental displacement loading test with load ratio equal to -1.

(d) Marschall et. al. [51], compared the monotonic static and monotonic dynamic strength and J-R curve from IRIRG-1 programme and have shown that the quasi-static material property data are adequate for in-service and LBB analysis of SS and CS pipes. In other word the dynamic nature of load, in general is found to have insignificant effect on fracture resistance.

(e) In IPIRG program, NUREG 6765[13], a set of curves were developed which relate the ratio of cyclic J to monotonic J-integral (J_{cyc}/J_{mono}) with applied load ratio and material toughness. These studies showed that J_{cyc} depend on loading history as well as material toughness.

(e) The cyclic plastic loading prior to crack initiation and during ductile crack growth causes a toughness degradation effect [53]. The toughness of all nuclear piping materials reduced under cyclic loading. The stress ratio, displacement increment, cyclic plasticity, cyclic crack growth, and initial toughness govern the amount of degradation. A correction factor was developed between yield/ultimate strength ratio versus toughness under dynamic and with R = -1 cyclic loading relative to the toughness under quasi-static monotonic loading [53, 61] (see Figure 2.4 and Figure 2.6). The effect of the R-ratio on the J-R curve appears to saturate to a minimum value at an R-ratio of -1. At R = 0, there is negligible effect, i.e., equal to the monotonic J-R curve. The transition of the J-R curve from R = 0 to -1 appears to be sensitive to the material toughness [53, 58].

(f) In order to obtain comparable J-R curves from CT specimens and TWC pipe under cyclic loading, the CT tests should be conducted with the same stress ratio and the same normalized cyclic plastic displacement. During crack growth, the cyclic plastic displacement needs to be changed to account for geometry effects in order to provide similitude between cracked pipe and specimens.

(g) The IPIRG programme [53] presented basic analysis approach to account for cyclic tearing. Here two approaches were presented to predict the effect of cyclic loading effect on ductile tearing and load carrying capacity of cracked pipe. The first one was based on the low cycle fatigue crack growth using the Dowling's ΔJ-integral method along with the extrapolated Paris law. The other was based on the modification of J-R curve, named as Cyclic J-R curve which accounts for load-history effects.

(h) The analytical assessment of cyclic tearing tests in the IPIRG programme had used procedures similar to monotonic fracture assessment except replacing the load-displacement curve with the envelope curve which was obtained from the incremental displacement controlled cyclic fracture tests.

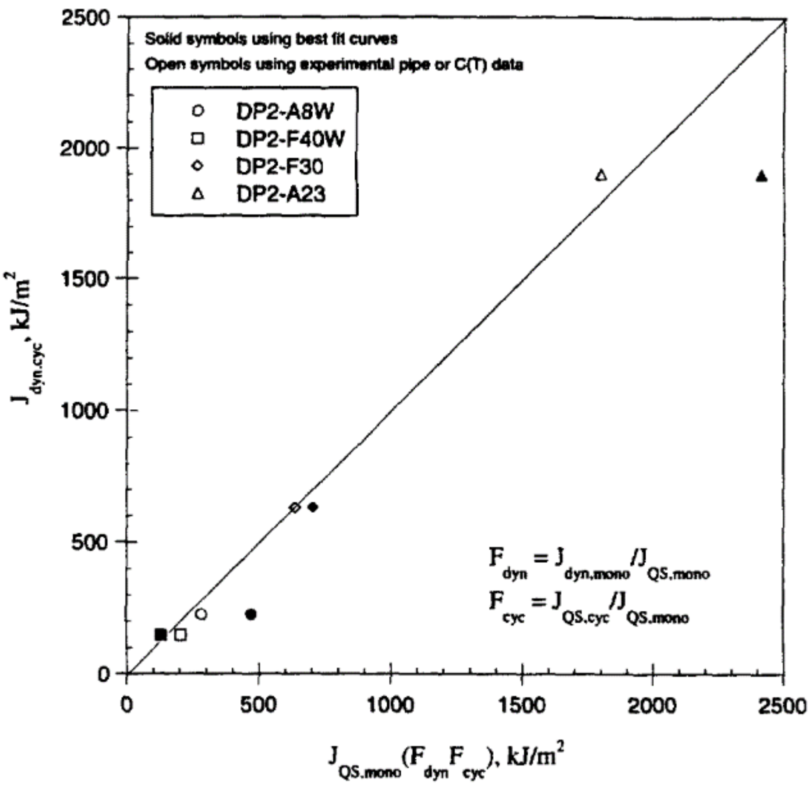

Figure 2.6: Experimental J versus calculated J for dynamic, cyclic(R=-1) experiments (ref. [35])

2.4.3 CRIEPI program (1991-97)

The Japanese participants in the above IPIRG program were CRIEPI. CRIEPI, as a Japanese representative, played a major role in managing the program among Japanese members. CRIEPI has carried out several tasks additional to the IPIRG program, on Japanese piping material and to look at some of the aspects which are not covered in IPIRG program. The CRIEPI programme [62-65] also confirmed the IPIRG finding of significant influence of fully reversed loading on the cyclic fracture stability. The salient observation / outcome of CRIEPI programme is given below:

(a) A series of fracture tests was conducted on circumferentially cracked carbon steel (STS410) pipes at high temperature (285°) under the four-types of dynamic bending loadings (monotonic load, cyclic loads with constant amplitude, increasing amplitude and random amplitude, see Figure 2.7).

(b) Monotonic pipe tests showed that the dynamic (strain rate) effect was negligible for this material and fracture load was well predicted by the tensile properties of the material.

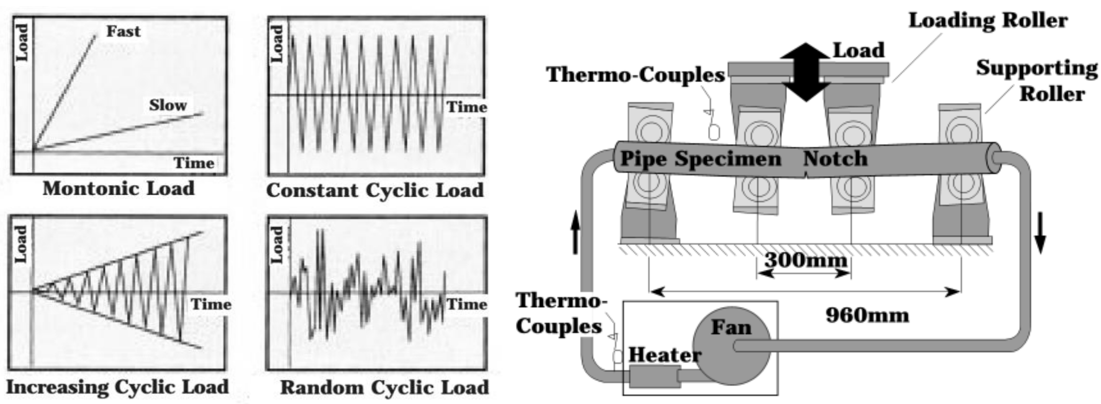

Figure 2.7: CRIEPI Test Facility and Loading Conditions (Ref. [62])

(c) CRIEPI proposed an evaluation method for dynamic pipe failure to predict the crack initiation, stable crack propagation and unstable pipe failure, based on the fracture mechanics approach, the J-integral based parameter.

(d) A cyclic J_{max} integral and cyclic ΔJ integral based procedure was proposed for crack growth calculation and stability assessment. Both the J_{max} and ΔJ integral were evaluated from the load - displacement envelope curve of the cyclic tearing test.

2.4.4 Other investigations

Salient observations from the limited work by several other investigators, in area of fatigue-tearing under cyclic loading other investigators which are primarily based on tearing fatigue tests on CT specimen, have been given below:

(a) I. Milne [68] has studied ductile tearing in presence of fatigue associated with variable amplitude loading and in conjunction with R-6 provisions. It is suggested that in fatigue-tearing regime, tearing should be regarded as causing an acceleration of the fatigue crack growth rate, than the fatigue causing a reduction in the material's resistance to tearing. The ductile instability condition is still determined by the pure tearing resistance curve, but the fatigue crack growth to that state is more rapid.

(b) Marschall and Wilkowski, [69], Chang et al [70, 71] and other investigators, have reported that the cyclic J-R curve based on load-displacement envelope of cyclic test strongly depends on loading parameters such as load ratio, displacement increment etc..

(c) Recently Singh et al [72], Roy et al [73, 74], have discussed cyclic fracture studies on CT specimens. These studies clearly brought out; i) the significant drop in cyclic J-R curve under fully reversing loads and ii) the dependence of cyclic J-R curve on loading history. Qualitatively these observations are in agreements with that from components cyclic tearing tests of IPIRG programme. However the quantitative observations have to be verified in view of issues of transferability of the J-R curve from the specimen fracture test to components level

2.4.5 Summary of past research on load history effect of fracture behaviour

The recent LBB document (2002), NUREG 6765 [13] has presented comprehensive review and compiled nearly all the developments of technical basis for LBB evaluations, lessons learned from past LBB applications and the research results (1985-2001) in area of Leak-Before-Break evaluation procedures. In addition to several other aspects, this report has thoroughly reviewed all the salient work (1985-2001), in the area of load history or cyclic load effects on the fracture stability behaviour of typical nuclear pipes, piping system and also on the fracture toughness J-R curve of typical nuclear piping materials. Below is an extract from NUREG 6765 [13]

..........“In summary, although cyclic loads can be detrimental to fracture resistance, there is no clear way as to how to account for them. Perhaps the best way would be to conduct a probabilistic study on seismic load functions, and use that to assess the magnitude of the degradation effect versus frequency of occurrence. One could then establish a cyclic toughness correction based on the mean result of that study.”………
(Section 5.3.3.2 of [13])

This clearly indicate that despite the huge efforts to develop procedures to account for the loading history effects in stability analysis, the cyclic tearing failure mode is not explicitly taken care of in present guides/practices [1-19] of stability demonstration of a cracked pipe. This also indicate the un-availability of simple, reliable and easily implementable procedure to demonstrate the fracture stability of cracked pipes including the load history effects and for specified number of cycles as required in level-3 of LBB analysis

2.5 Cyclic J and ΔJ Integral

The IPIRG and CRIEPI programmes and other past investigators have used Cyclic J and ΔJ integrals to develop analysis methodologies for assessing the crack growth and fracture behaviour of materials under cyclic loading conditions.

Lamba [75] in 1975, first proposed J-integral application under cyclic loading and presented its formulation. Dowling and Begley [76] in 1976 first proposed use of ΔJ-integral for fatigue crack growth modelling in presence of gross plasticity. K Tanaka, 1983 [77], Lambert,1988 [78], have provided mathematical frame work to estimate cyclic J and ΔJ integral for 2D and its physical significance for fatigue crack growth was discussed using Dugdale model. However, the applicability of the J-integral to cyclic loadings conditions is questioned and controversial. The J-integral evaluation procedure, prescribed in ASTM E 1820-09 [44] and other standards, violated the theoretical definition of J-integral due to periodic partial unloading, however to have an engineering solution it has been accepted by consensus [79]. Afterward, in IPIRG, CRIEPI and several other investigations used cyclic J and ΔJ integral for fatigue crack growth modelling under elastic-plastic conditions.

2.5.1 Cyclic J-R curve for fracture and Cyclic ΔJ Integral for FCG assessment

As reported above, the concept of cyclic J and ΔJ integral was developed during 1975-1990, [75-79]. However, the concept of cyclic J-R curve characterizing material's fracture resistance under cyclic loading is of recent origin [74, 80-85]. Only a few international laboratories have worked on this problem and the available literature on cyclic J-R behaviour of materials is very limited. Mogami et al. [80] have first proposed cyclic

J-integral tests to simulate the deleterious effects of periodic load reversals. K Mogami et al. [80] have studied the fatigue crack growth and tearing instability behaviour of STS 42 carbon steel and A508 low alloy steel under cyclic loading. Here the ΔJ and J_{max} were used for modelling of crack growth.

Several investigators [69-74] have reported that the cyclic J-R curve strongly depends on loading parameters such as load ratio (R), displacement increment (δ). To understand the impact of cyclic loading on cyclic J-integral, the studies generally divided broadly into two categories viz., tests conducted with a load ratio, $R \geq 0$ and $R<0$.

S Kaiser [81], B K Neale and E K Proddle [82] have studied the fatigue-crack growth and stable tearing under cyclic loading with positive load ratio, $R \geq 0$. S Kaiser [81] has conclusively shown the influence of number of unloading cycles on the J-R curve obtained from CT specimens tests (see Figure 2.8). The J-R curve is strong function of cyclic displacement increment and number of loading cycles. However, when this data is corrected for the fatigue part of the crack growth during unloading (fatigue crack growth in each cycle subtracted from the total crack extension of that cycle), the resulting J-R curves (see Figure 2.9), now fall into the scatter band of monotonic J-R tests.

B. Skallerud and Z L Zhang [84] have investigated failure of structures due to fatigue-tearing crack growth, under severe cyclic loading. Here the fatigue part of the crack growth was computed using Dowling's cyclic ΔJ integral while the ductile tearing crack growth computed using Gurson-Tvergard model. All these have studies [81-84] observed significant increase in crack growth due to concurrent fatigue cycling. The crack growths were found in reasonable agreement with the sum of predicted fatigue crack growth and stable tearing component for the tests conducted with a load ratio, $R \geq 0$.

C.W.Marschall and G. Wilkowski, [69] have reviewed several experimental and analytical studies carried out to understand effect of cyclic loading on ductile fracture resistance. It is shown that the crack tearing under cyclic loading with R-ratio greater than 0, the total crack extension is just summation of crack extension due to monotonic ductile tearing, Δa_{mono} (obtained from a monotonic J-R curve test) and fatigue crack growth, Δa_{cyc} (estimated using fatigue crack growth analysis). While for negative R-ratios the total crack extension exceeded the d $\Delta a_{mono}+ \Delta a_{cyc}$. The difference in measured tearing with that of estimated tearing clearly showed additional tearing/degradation taking place due to compressive loading which is not being accounted for in the above calculation procedure.

During 1990s, in the IPIRG programme, CRIEPI investigations and several other studies reported above, the cyclic J-R curve was considered in cyclic fracture assessment studies. Rahman et al.[85] have shown that the cyclic ΔJ is an effective parameter to describe the low cycle fatigue crack growth in cracked pipe fracture analysis.

2.5.2 Limitations of Cyclic J-R curve

The above literature review has clearly brought out that the cyclic J-R curves following limitations of cyclic J-R curves:

(a) The cyclic J-R curve is found dependent on loading parameters such load ratio, displacement increment etc. The loading history at a location in piping depends on several factors such as, input earthquake spectra, piping layout etc. Hence development of generalised procedure or rule is difficult.

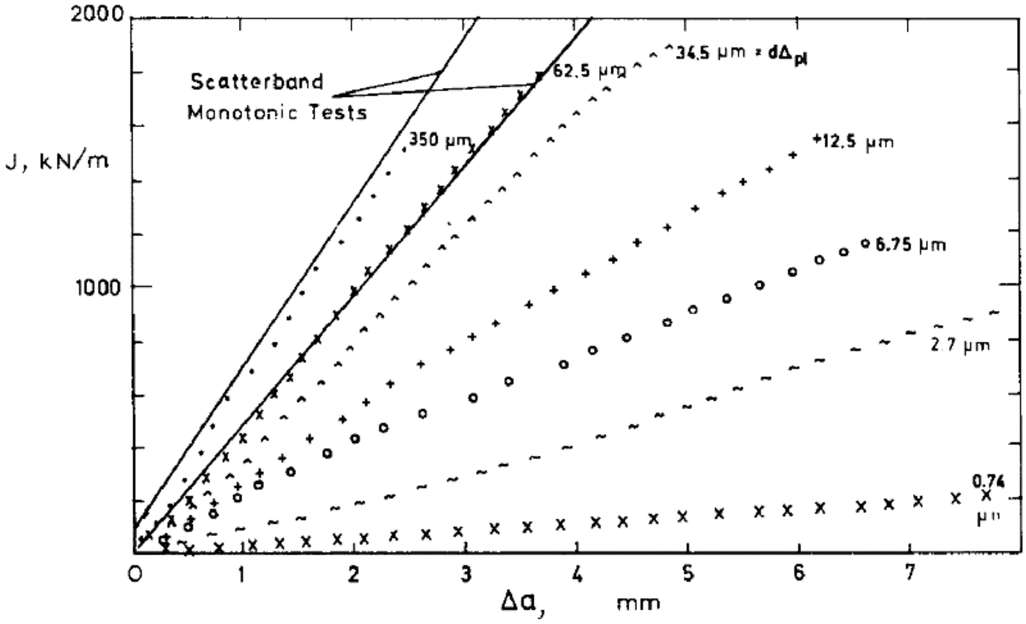

Figure 2.8: Influence of the numbers of unloading on the J-R-curve. CT-specimen of material OX 812. (Ref. S Kaiser [81])

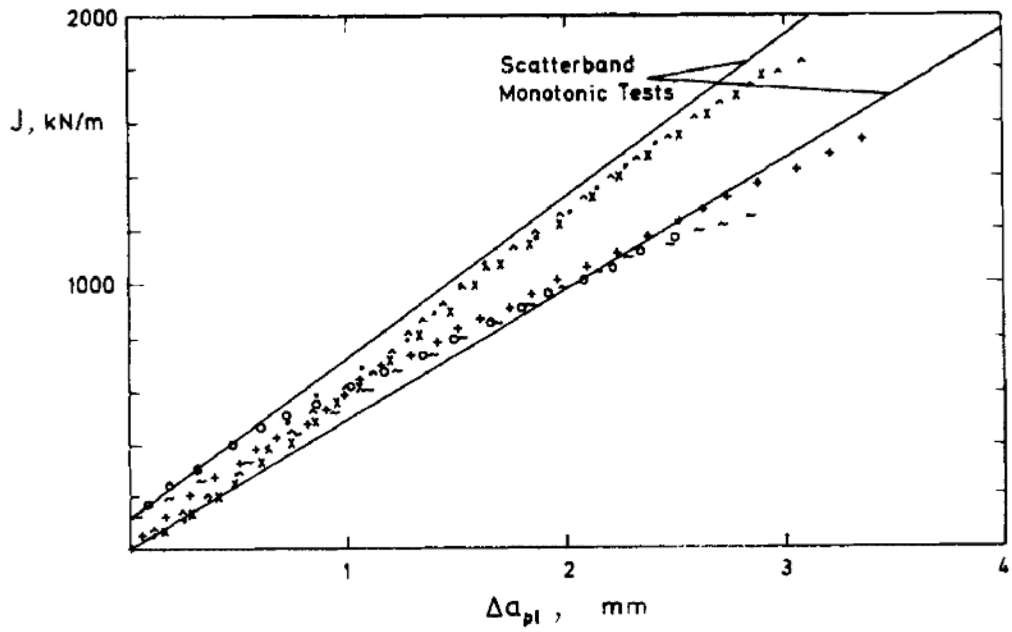

Figure 2.9: Data of Figure 2.8 but with the crack growth during unloading subtracted from the total crack extension. (Ref. S Kaiser [81])

(b) Most of the studies on cyclic J-R are performed on the small size specimens. The application of cyclic J-R curves generated from specimens to large size piping components in view of difference in their constraints, have not been investigated. Hence application of the quantitative observations from the CT specimen tests have to be verified in view of issues of transferability of the J-R curve from the specimen fracture test to components level

2.6 Effects of geometry constraint on J-R curves

The crack initiation toughness and J-R curve used in J-Tearing analysis are, in general, obtained from standard fracture specimens following ASTM standard-1820 [44]. Here the J-integral is assumed to characterize the crack-tip stress field and one unique J-R curve is assumed sufficient to characterize the material. However, now it is well understood and established [86-90] that the J-R curves are geometry dependent. In view of the influence of crack-tip constraint or stress triaxiality on ductile fracture, the transferability of specimen J-R curve data to a component level is an issue. In most cases, standard ASTM specimens are such; they maintain high level of constraint, to ensure predominantly plane strain conditions at the crack tip. However, real structures generally be low-constraint geometries and hence use of the specimen J-R curve lead to conservative assessment. However if the real component geometry have higher constraints than that of specimen used to obtain J-R, the fracture assessment would lead to un-conservative condition.

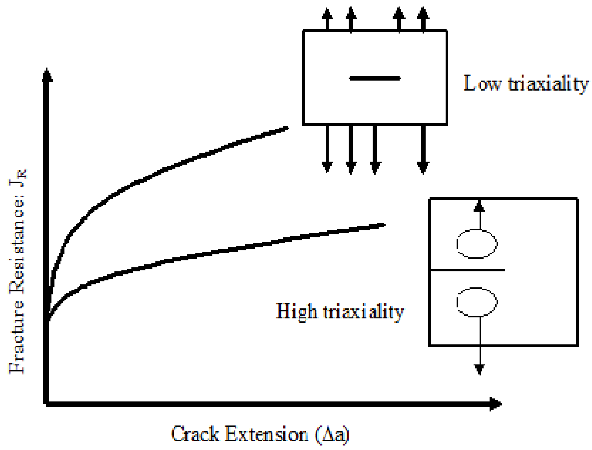

Figure 2.10: Schematic showing the effect of geometry constraint on fracture resistance, J-Δa curve

2.7 Dynamic Strain Ageing

Dynamic strain ageing (DSA) is a phenomenon observed in many carbon steels at light-water reactor operating temperatures ranges, 150-450°C [91-96]. The DSA involves interactions between highly mobile nitrogen and carbon atoms dissolved in the steel and moving dislocations associated with plastic strain. At certain combinations of strain rate and temperature, these interactions can lower the crack-growth resistance and can cause a stably growing crack to become temporarily unstable. In general, an increase in the ultimate tensile strength and a decreasing trend of ductility properties with increase in temperature is observed. Dynamic strain aging is a time and temperature dependent phenomenon. Alteration in the strain rate can shift the occurrence of DSA phenomenon from one temperature range to another. It has been observed by these investigators that DSA has detrimental effect on fracture toughness behaviour of a material. Both the fracture initiation toughness and the resistance to crack propagation are found to decrease in the DSA operative range. DSA occurs under specific combination of temperature and strain rate and such test conditions must prevail for the degradation of fracture toughness properties.

2.8 Piping system compliance effects on fracture assessment

In conventional fracture stability assessment, the cracked pipe is assumed to have free rotations at its ends (infinite compliance of the connected piping), and subjected to the bending load. However, in reality the piping system is indeterminate since the ends of the pipe are connected to the rigid pressure vessels etc. Hence, the piping on the either side of the cracked section has finite compliance or non-zero stiffness (rotational). In piping system, the presence of crack causes moment redistribution and may result in some reduction of moment at its location. The reason for the moment redistribution is the indeterminacy of the piping system. This leads to change in the applied J-integral, crack mouth opening displacement (CMOD) and applied tearing modulus (T) curve. Nestell and Coward [97] had first included the effect of compliance in the stability criteria and derived an equation for applied tearing modulus. Afterward several investigators [98-100] studied the effect of piping system compliance on J-Tearing analysis. Simplified equations / graphs were developed to account for the piping compliance into stability assessment. These studies have also shown that any beneficial effect due to compliance is strong function of the system stiffness at crack location. However, the piping system experiments carried out as part of IPIRG programme (see 2.4.2) have not shown any significant advantage in the maximum load capacity of the piping system with respect to stand alone pipe.

On the other hand E Smith [102-103] have shown the deleterious effect of the piping compliance on assessment of crack opening area which is important in evaluation of leakage size crack, LSC. Estimation of the size of the crack that gives a measureable leakage under normal operating condition is a key requirement of LBB. It requires calculations of crack opening area which, in general, is performed on cracked pipe (ends free) and subjecting it to elastically calculated loads for the untracked piping system.

However, E Smith [102-103], has shown that this procedures does not account for the effects of piping system stiffness (owing to facts that a piping system is restrained, i.e. built in at its ends into large sized components) and leads to under-prediction of leakage size crack associated with a specific leakage area and therefore this has potential to jeopardise any leak-before-break argument.

The above literature has shown that considerations of the piping system compliance may be favourable in stability assessment but un-favourable in assessment of leakage size crack.

2.9 Appraisal of the problem and key issues

In designing the nuclear components [38], a minimum of 10 cycles of equivalent maximum magnitude of induced load during an earthquake event, are considered. In Indian NPP, one Safe Shutdown Earthquake (SSE) event (comprising of 10 cycles) and five Operating Basis Earthquake (OBE) events (comprising of 10 cycles per event) are considered in design. In view of this, the fracture stability or LBB assessment of the candidate pipe should be demonstrated for reasonable number of cycles and the load history effects on failure shall be considered. Currently used crack tearing and fracture assessment method as outlined in several LBB documents [1-19] does not explicitly account for damage due to the repeated cycles of such load. These consider the earthquake load as once applied non-cyclic load, which monotonically increases up to its maximum magnitude. The ductile fracture load or the critical crack size evaluation is based on the monotonic ductile fracture and uses the J-R curves evaluated under monotonic loading conditions. However it is known that under the large magnitude reversible cyclic loads (during SSE), the realistic failure mode is due to combined tearing-fatigue damage. Such failure is termed as **Cyclic Tearing.**

The literature survey (discussed in section 2.4) has shown that significant work was done in area of fracture stability assessment under cyclic loading conditions. These investigators have recognized the deleterious cyclic tearing damage under a cyclic loading event. Although, these proposed a cyclic J-R curve approach to account for cyclic loading damage effects but it could not be widely used/ practised due to following key reasons;

(a) The Cyclic J-R curve has strong dependence on the loading history: The loading history at a location in piping depends on several factors such as, input earthquake spectra, piping layout etc. Hence development of generalised procedure or rule is difficult.

(b) The Cyclic J-R curve is independent of number of loading cycles of a cyclic loading event

(c) The transferability of the cyclic J-R curve from the specimen level fracture test to component level test is not verified / established yet. Application of the quantitative observations from the CT specimen tests have to be verified in view of issues of transferability of the J-R curve from the specimen fracture test to components level.

(d) Analytical assessment would involve modelling of the cyclic plasticity and combined tearing-fatigue regime crack growth under reversible cyclic loading. These are yet not well developed, nor widely validated.

In view of these issues, there is a need to develop an independent, alternative assessment approach to consider cyclic tearing damage for a specified number of cycles of a cyclic loading event and which could directly be implemented in existing fracture stability assessment procedures.

3 Experimental Program on Carbon and Stainless Steel Pipes of Indian Nuclear Power Plants

3.1 Introduction

The material and pipes selected for the experimental study are from those piping products used in Indian NPPS. Two material categories are selected, namely, a nuclear grade AISI 304LN (ASME SA 312 type 304LN) stainless steel (SS) and a low carbon manganese (C-Mn) carbon steel (CS) ASME SA 333 Gr 6 steel. In addition to pipe of these two different base materials, the girth welded pipe specimens using three different weld configurations are also investigated. The selected carbon steel pipes and pipe weld are used in fabrication of primary heat transport piping (PHT) of Indian Pressurised Heavy Water Reactors (PHWRs) while the stainless steel pipe and pipe weld are proposed materials for the main heat transport (MHT) piping of Indian Advanced Heavy Water Reactor (AHWR). In both the reactor types, PHWRs and AHWR, the leak before break (LBB) compliance is demonstrated for their primary piping that is PHT and MHT respectively. A severe earthquake event, i.e. SSE, is considered as the design basis accident for these piping. In view of recognition of significant damage due cyclic tearing (see section 2.4) and it being neglected in the present LBB practices (see section 2.3.4), the present investigations is done with an emphasis on characterization of cyclic tearing damage in such a manner that it can be used to account for the cyclic nature of earthquake loading in LBB fracture assessment.

This chapter presents details of the experimental program carried out to generate data for investigations on the cyclic tearing behaviour of pipe in relation with corresponding monotonic fracture. A comprehensive test programme is carried out involving large number of cyclic tearing and monotonic fracture tests on cracked straight pipes having a through wall circumferential (TWC) crack. These tests covered wide range of pipe sizes, crack sizes, pipe material, welding types and loading conditions. This chapter also describes details of the test specimen geometries, pipe material, test matrix, test setup for reversible cyclic loading tests, welds procedures used in fabrication of welded specimens, fatigue pre-cracking of pipe specimens to generate sharp cracks; cyclic tearing / monotonic fracture testing, continuous measurements of the load, load line displacement, crack growth, crack mouth opening displacement until the instability or end of test.

The work reported in this chapter are: (i) Test details covering the sizes, material description / characterisation, specimen fabrication, test setup arrangement, test loadings and test measurements (ii) conduct of cyclic and monotonic fracture tests and generation of tests data on the selected pipes and its weldments and (iii) processing of the recorded test data to evaluate salient fracture parameters (iv) important test results, observations of crack growth patterns in different pipe material categories and comparison of moment-rotations (M-ϕ) under different loading histories.

3.2 Objectives

The test program has been designed to realise the following objectives:

(a) To single out and quantify the deleterious impact of cyclic nature of loading on the load carrying capacity of a cracked pipe

(b) To quantify reduction in the load carrying capacity as function of number of load cycles under load controlled as well as under displacement controlled conditions.

(c) To develop a simple / implementable method to account for cyclic tearing damage into stability assessment during the LBB design of NPPs piping components.

(d) To study the crack tearing growth assessment and cyclic J-R under cyclic tearing conditions.

The cyclic tearing tests have been planned such that the cyclic loading effect can be studied in relation with corresponding monotonic fracture tests on an identical pipe. This is due to the fact that the fracture stability assessment of cracked pipe under monotonic loading is reasonably established; procedures/methods are well documented [6-8, 32-42], widely validated and used (see 2.3.4).

3.3 Test details

In this programme, a series of about 45 numbers of cyclic tearing tests and monotonic fracture tests have been conducted on straight pipes having a circumferential Through Wall Crack (TWC).

3.3.1 Test Specimens

The test programme has covered wide range of pipe sizes, crack size.

3.3.1.1 __Pipe sizes__

The pipe sizes considered are listed below: (Here 'Do' is nominal outer diameter and 't' is thickness of pipe)

(i) 6″ NB Sch. 120 (Do=168.2 mm ; t=14.27 mm)

(ii) 8″ NB Sch. 100 (Do=215 mm; t=15.08 mm)

(iii) 12″ NB Sch.100 (Do=323.8 mm; t=21.43 mm)

(iv) 12″ NB Sch.120 (Do=323.8; t=25.4 mm)

(v) 16″ NB Sch.100 (Do=406.4 mm; t=26.18 mm).

The 8″ NB, 12″ NB and 16″ NB size of carbon steel pipe, selected above are used in different pipe lines of Indian PHWRs. The 6″ NB and 12″ NB size of stainless steel pipe, selected above are proposed pipe sizes for main heat transport piping of Indian AHWR.

3.3.1.2 Crack sizes / location

Wide range of reference circumferential through wall crack sizes (2θ) is considered:

(i) 60° (in 6″, 8″ and 12″ pipes)

(ii) 90° (in 8″ and 12″ pipe)

(iii) 120° (in 16″ pipe)

The typical TWC orientation is shown in Figure 3.1. The crack sizes are given in terms of total angle (2θ) subtended, by the TWC, at the pipe centre (see Figure 3.1). The crack sizes have been selected keeping in mind the leakage size cracks determined in the LBB analysis of Indian NPPs and the maximum loading capacity of the test machine.

Crack Location: Two crack locations have been considered:

(i) In the base metal for seamless pipe (in middle of pipe length). Here the test is referred as CSB for carbon steel pipes and SSB for stainless steel pipes.

(ii) In weld metal (at the center of circumferential weld) of two seamless pipes joined by girth weld. Here the test is referred as CSW for carbon steel pipes and SSW or NGW for stainless steel pipes depending of the welding procedure (conventional / narrow gap) used to make the girth weld to join the two pipe pieces (see Figure 3.1)

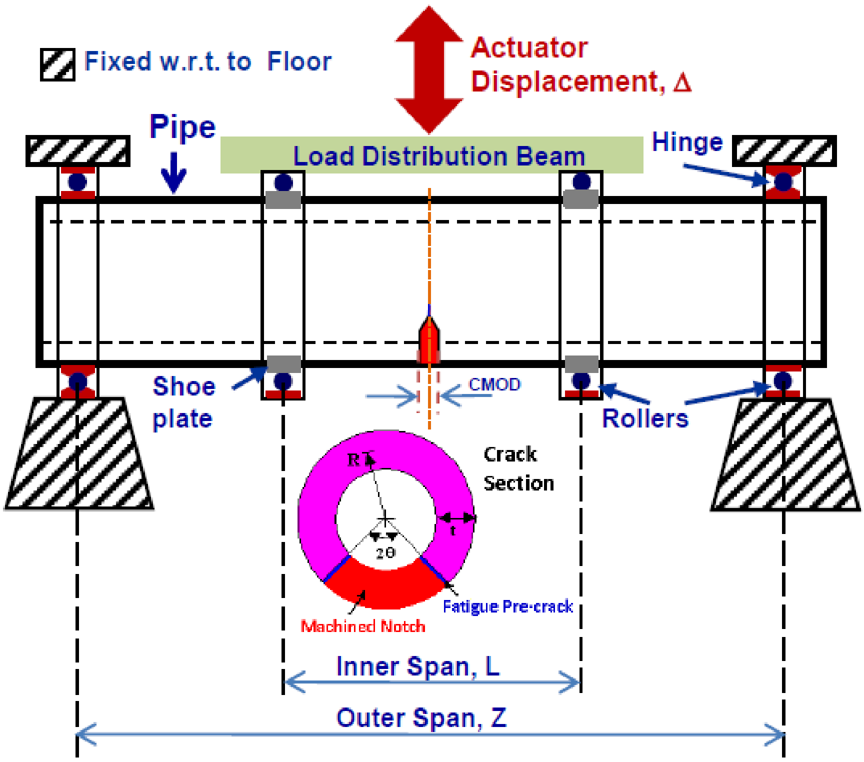

Figure 3.1: Schematic of cyclic tearing test setup

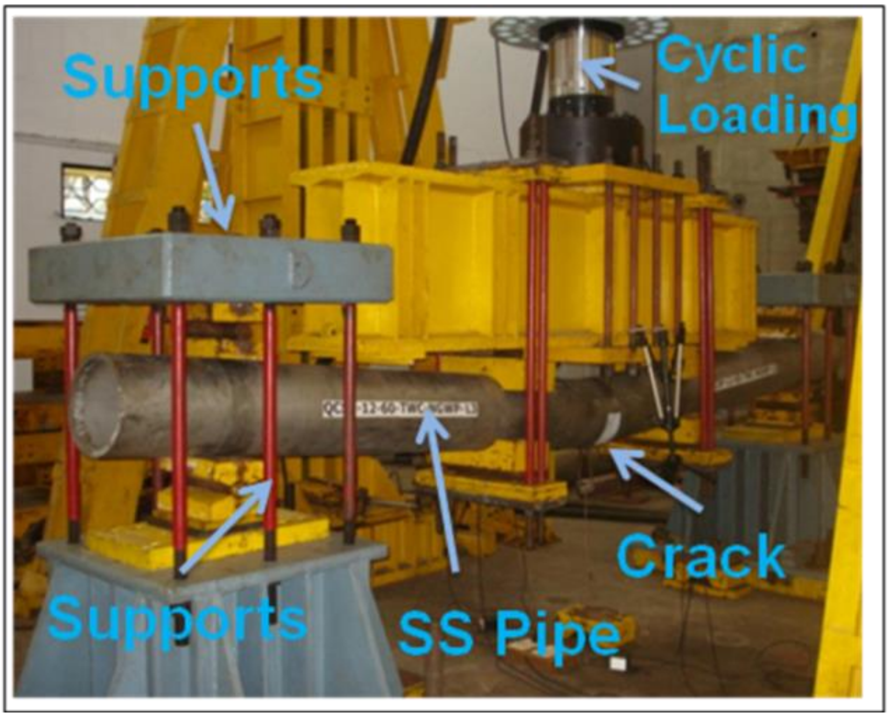

Figure 3.2: Photograph of cyclic tearing test setup

3.3.1.3 <u>Specimen Fabrication</u>

Through wall circumferential notch has been machined, by milling, in all the pipe specimens. The width of the initial machined notches is found between 2-4 mm. In order to generate sharp crack front, ahead of machined notches, these pipes have been subjected to low amplitude load cycling, before the actual tests. The test specimen designation, pipe material, diameter, thickness notch location (base or weld), machined notch length, notch mouth opening, inner pan and the outer span have been listed in Table 3.3 for carbon steel pipes and in Table 3.4 for stainless pipes. The realistic sharp and tight cracks are generally generated using the fatigue pre-cracking. In present investigations also, after notch machining all the pipe specimens are subjected to low magnitude (to contain crack tip plasticity) cyclic loading until initiation and growth of a fatigue crack at root of machined notch. The details of fatigue pre-cracking are given in sec. 3.4.1.

3.3.2 Test Materials

Tests have been conducted on seamless pipes made from carbon steel (CS of SA-333 Gr.6) and austenitic stainless steel (SS of SA-312 Type 304LN) material. The CS is the material of the Primary Heat Transport (PHT) system piping of Indian Pressurized Heavy Water Reactors (IPHWRs) while the SS is the proposed material for the Main Heat Transport Piping (MHT) system of Indian Advanced Heavy Water Reactor (AHWR).

In addition to base metal pipe, the tests have also been carried out on the pipe having a girth weld at the centre. The circumferential through wall notch is machined at weld centre line of the girth welded pipe and in base metal at centre of actual pipe. The girth welded pipe specimens have been prepared by joining two seamless pipe pieces using two different welding techniques namely Shielded Metal Arc Welding (SMAW) with conventional groove and Gas Tungsten Arc Welding (GTAW). In case of carbon steel the welding technique / procedure used is same as used in PHT piping of Indian PHWRs. In case of stainless steel two welding techniques are considered, one is based on SMAW with convention groove and the second is based on GTAW with narrow groove. The GTAW with narrow grove is the proposed welding techniques being for stainless steel piping of AHWR. The pipe tests in the present program can be grouped into following five material categories:

(i) Carbon Steel Base (CSB): Carbon-manganese steel that is SA-333 Gr.6 conforming to material specifications of PHT piping of Indian PHWRs

(ii) Stainless Steel Base (SSB): Austenite stainless steel, that is grade SA-312 Type 304LN conforming to specifications of proposed material for primary loop piping of AHWR

(iii) Carbon steel weld (CSW): SA333Gr6 Carbon steel Pipe with girth weld; root pass GTAW filler pass SMAW

(iv) Stainless steel weld (SSW): SS Type 304LN Stainless steel Pipe with conventional girth weld; root pass GTAW filler pass SMAW

(v) Narrow groove weld (NGW): SS Type 304LN Stainless Steel Pipe with narrow groove girth weld; hot wire GTAW

No post-weld heat treatment was applied to the welded specimens. The effect of any residual stress would be negligible since the large crack sizes and loading magnitudes cause significant plasticity ahead of crack.

The chemical composition of these materials is given in Table 3.1. Typical microstructure of as-received carbon steel and stainless steel materials are shown in Figure 3.3. In the microstructure of SA-333 Gr.6 base metal ferrite-pearlite bands are observed. The orientation of these bands is along the pipe axis, that is, along longitudinal direction. The average ferrite grain size is about 15 μm. The micrographs of SS304 base metal shows austenite grains and an average austenite grain size of 80 μm. Table 3.2 lists the typical tensile properties for both base and weld materials, of these pipe specimens. Figure 3.4 shows the typical stress-strain curve for both the base materials.

3.3.2.1 Welding procedures

Pipe Circumferential Welds of SA-333 Gr.6 Pipes (CSW): Root pass by GTAW process followed by filler passes by SMAW process. The weld procedure specifications (WPS) and QA used are same as used for welding of Indian PHWR primary piping. This is referred to as CSW.

Pipe Circumferential Welds of SS 304LN Pipes: Two different welding techniques have been considered in the test programme.

> In one case the conventional groove SMAW is adopted. In this, the groove size is as per conventional design. The root pass is by GTAW process followed by filler passes by SMAW process. This is referred to as SSW.
>
> In second case Narrow Groove (NG) GTAW is adopted. In this weld type the narrow groove design is adopted and the gap is within 12 mm for both 6″ NB Sch 120 and 12″ NB Sch 120 pipes. The welding is by hot wire pulsed GTAW technique and is done by automatic orbital welding machine. This is referred to as NGW. The WPS and QA used are same as planned for primary piping of proposed Indian AHWR. It is proposed welding technique for AHWR in order to ensure longer life of the pipe weldments. This welding technique (that is narrow grove full GTAW using hot wire pulsed technique) [104-106], results in less heat input, low residual stresses, low shrinkage and higher

fracture resistance. Lesser heat input also ensures higher margins against low temperature sensitization. Low residual stresses minimize chances of IGSCC; high fracture resistance would ensure higher margins against design basis accident loads. Figure 3.5 shows the photographs of both SSW and NGW pipe weldments prepared on 6″ size SS pipe.

3.3.3 Test Loading

The IPIRG and CRIEPI programme has shown that the reversing cyclic nature of the earthquake loads is the main reason for deleterious damage than that due to its dynamic nature. Also the interaction between the dynamic and the cyclic nature of loading is very weak. The dynamic effects and cyclic effects on the material J-R curve were found to be additive and hence can be dealt individually. In view these reported observations, all the tests in current programme were conducted under quasi-static reversible cyclic loading.

The piping system is subjected to mixture of load controlled and displacement controlled conditions. In IPIRG-1 program [58, 59-61], the effect of the different stress components (i.e., primary membrane, primary bending, secondary thermal expansion, and secondary seismic anchor motion) on the fracture behaviour are studied. The inertial and dead weight load in these tests considered as primary since they behaved as load controlled while the thermal expansion (TAM) loads and seismic anchor movement (SAM) load are considered as displacement controlled. Therefore, in the present programme the cyclic fracture tests have been conducted under pure load controlled as well as pure displacement controlled conditions. These are two possible extremes. The real piping system behaviour will lie somewhere in-between.

Table 3.1: Chemical composition of materials (in weight %)

Material	C	Mn	Si	P	S	Cr	Ni	N	Mo	Nb
SA-333 Gr. 6 CSB (Base)	0.14	0.9	0.25	0.016	0.018	0.08	0.05	0.01	-	-
SA-333 Gr. 6 CSW (Weld)	0.27	1.20	0.43	0.021	0.017	0.04	0.01	0.01	-	-
SS 304LN SSB (Base)	0.013	1.57	0.36	0.025	0.001	18.6	8.46	0.11	-	-
SS 304LN SSW (Weld)	0.03	1.66	0.56	0.021	0.01	19.8	11.06	0.1	-	-
SS 304LN NGW (Weld)	0.02	1.76	0.37	0.016	.005	19.52	9.91	0.1	0.24	-

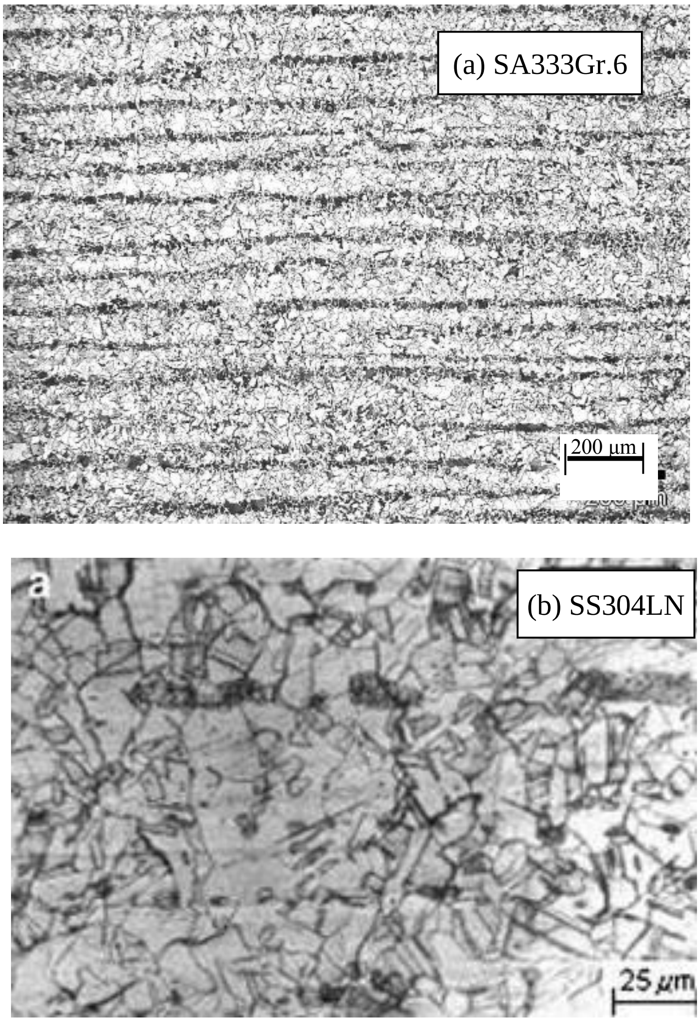

Figure 3.3: Typical microstructure of SA-333 Gr.6 and SS304LN base material, in as received condition

(a)

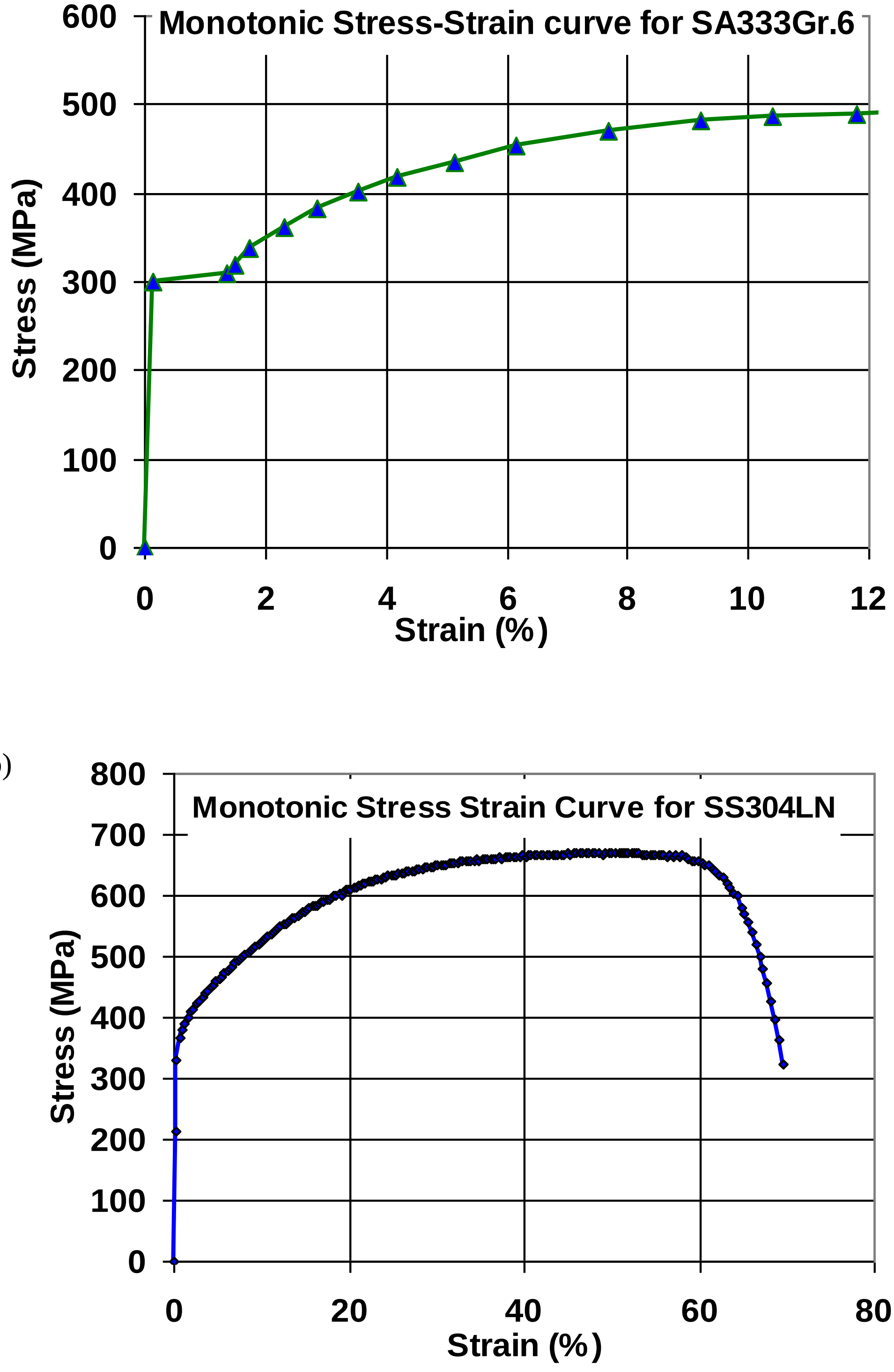

(b)

Figure 3.4: Typical monotonic stress-strain response of the material: (a) Carbon Steel: SA-333 Gr.6 (b) Stainless Steel: SS304LN

Table 3.2: Typical mechanical properties of SA-333 Gr.6 and SS 304LN base and weld material

Material Properties#	Pipe Size	Yield Strength σ_y (MPa)	Ultimate Strength σ_u (MPa)	Elongation (%)	Young's Modulus E (GPa)
SA-333 Gr. 6 CSB (Base)	8″ NB pipe	288	420	36.7	203
	12″ and 16″ NB pipe	312	459	41	203
SA-333 Gr. 6 CSW (Weld)	8″ NB pipe	302	450	18.7	203
SS 304LN SSB (Base)	6″ NB Pipe	318	650	67	195
SS 304LN SSW (Weld)	6″ NB Pipe	450	593	42	195
SS 304LN NGW (Weld)	6″ and 12″ NB Pipe	320	653	-	195

Note: # CSB= Carbon Steel base; CSW=Carbon steel weld; SSB= Stainless Steel Base; SSW=Stainless steel weld using SMAW with conventional groove; NGW= Stainless steel weld using GTAW with narrow groove

(a) NGW Pipe

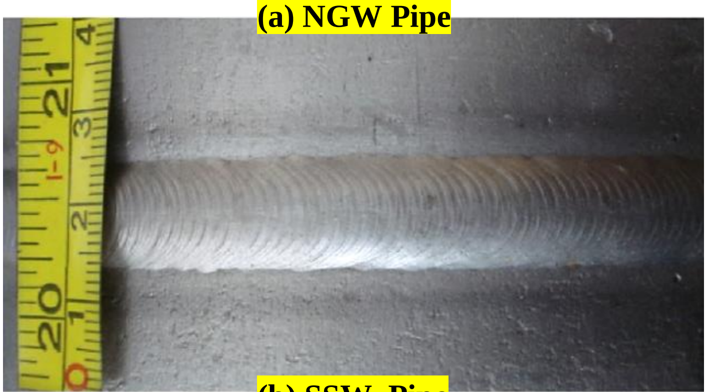

(b) SSW Pipe

Figure 3.5: Pictures of typical weld (a) NGW and (b) SSW done on stainless steel pipes

3.3.4 Test Setup

Figure 3.1 and Figure 3.2 show respectively the schematic and photograph of the four point bend test setup for cyclic loading. The tests setup has been design in such a way that it will load the pipe specimen in standard four point bend in both direction of loading.

At outer span or support points in each of the loading direction, a hinge and a roller type support arrangement (see Figure 3.1 and Figure 3.2) have been made to ensure simply supported conditions while applying load. Hence, in each direction loading one end support is hinge while the other end is roller. This has ensured a pure bending loading of the pipe between the two loading points, i.e. inner span. On each end, the pipe specimen is tied between the hinge and roller support assembly using a bottom and a top support block and six numbers of tie rods. At both side support point, a line contact between the pipe specimen and the flat face of hinge/roller assembly, over adequate length has ensured distribution of support reactions over a small region.

A steel distribution beam has been used to apply the load / displacement at two points (inner span). This distribution beam, in turn, is connected with a servo hydraulic actuator. Load distribution shoe blocks having radius same as test pipe has been used at inner span loading points. At loading points, these shoes ensured surface contact with pipe and hence distributed applied load over reasonable surface area of pipe at load point location. Roller assembly at each of the loading points in both the loading directions have been used to ensure free rotation of pipe with respect to rigid load distribution beam at both loading point.

The above described test setup has enabled to carry out cyclic tearing test under pure four point bend loading and also have prevented local denting of pipe due to force concentration.

3.4 Test procedure

The pipe tests have been conducted under quasi-static loading conditions, at room temperature and without internal pressure. The four point bending load test set up has been used for both the monotonic and cyclic tearing tests. The pipe specimens are first fatigue pre cracked to generate a sharp and tight natural crack prior to actual test. After fatigue pre-cracking, the cyclic and monotonic fracture tests have been carried out under different loading conditions. Tests are conducted under both the load as well as displacement control conditions (see section3.3.3). These are two asymptotic extremes loading conditions on piping during an earthquake event. Depending on the piping system compliance and layout, the real loading on it during an earthquake event, is mixture of both load and displacement controlled conditions. The displacement controlled loading are of concern since may causes unacceptable large tearing. On the other hand the load control situation may cause unstable tearing / failure of cracked pipe. Hence both has been considered. All the important variables (e.g. load, load-line displacement, CMOD, crack images etc.) have been recorded during the tests.

3.4.1 Fatigue pre cracking

Through wall circumferential notch has been machined, by milling, in all the pipe specimens. In order to generate sharp crack front, ahead of machined notches, these pipes have been subjected to low amplitude load cycling, before the actual tests. This fatigue pre-cracking step resulted in formation of sharp crack and small amount of growth (about 1^o to 2^o or 3 to 6 mm) at each notch tip. During fatigue pre-cracking step, the load ratio is kept constant and its actual value lies between 0.1 and 0.2 for different pipe specimens. The maximum load during pre-cracking is kept constant and its magnitude is kept below

40% of theoretical plastic collapse load. The theoretical plastic collapse load is evaluated using following equation [32].

$$P_c = \frac{4M_C}{Z-L} = \frac{4}{Z-L} * 4R^2 t\sigma_f \left(\cos\frac{\theta_i}{2} - \frac{1}{2}\sin\theta_i\right) \quad (3.1)$$

Where 'Z' and 'L' are outer and inner span respectively, 'R' is the mean radius and 't' is the thickness of pipe and 'σ_f' is pipe material flow stress and 'θ_i' is the half of machined notch angle. 'M_C' is plastic collapse moment of a crack pipe. When pipe crack section is subjected to M_C bending moment, the entire ligament will have plastic flow condition.

The fatigue pre-cracking has been carried out in four point bend loading setup which provides simply supported conditions and pure bending loading within the length of inner span. Since the fatigue pre-cracking loading is only in one direction, the upper supports plates have not been used. The final crack sizes, after fatigue pre-cracking are given in Table 3.5 and Table 3.6. The fatigue pre cracking, in all the test specimens, have generated sufficiently long, very tight and natural crack tip which further grows during the fracture tests and would provide crack closure effects during compressive loading. No shim is inserted into machined notch gap. After fatigue pre-cracking, the cyclic and monotonic fracture tests have been carried out under different loading conditions as described in following sections.

3.4.2 Load controlled Cyclic Tearing Tests

The load controlled tests have been carried out with the aim of investigating the importance of the number of large stress amplitude cycles associated with an earthquake, in unstable failure of cracked pipe. The pipe has been subjected to quasi-static cyclic loading with constant load amplitude and constant load ratio as shown in Figure 3.6 (a). The frequency is kept below 0.008 Hz. The load amplitude is selected between 60% and 95% of the monotonic fracture load data (see section 3.4.5 and Table 3.10). The details related to test number, pipe sizes, pipe material / weld type; machined notch size, fatigue pre cracking, final crack sizes and location are listed in Table 3.3 to Table 3.6. The applied load amplitude, load ratio and number of cycles to instability/failure along with key geometry and crack dimensions are listed in Table 3.7. The results from these tests would reveal the influence of number of load cycles, load ratio, mean load and maximum load on the crack growth and instability behaviour of cracked pipes.

3.4.3 Incremental displacement controlled Cyclic Tearing Tests

The incremental displacement controlled cyclic tearing tests have been conducted with the aim of quantifying effect of reversible cyclic loading on reduction of fracture resistance and acceleration of stable crack tearing growth. The pipe is subjected to constant displacement increment after every cycle, while the load ratio is kept constant throughout the experiment. In this category of tests, displacement increment is controlled when the specimen is loaded in crack opening direction and load is controlled in the reverse direction loading in order to maintain the constant load ratio. The Figure 3.6 (b) shows the loading scheme where δ is the displacement increment given in each cycle while crack opens and R is the load ratio controlled while unloading and reverse loading of the pipe. The details related to test number, pipe sizes, pipe material / weld type; machined notch size, fatigue pre cracking, final crack sizes and location are listed in Table 3.3 to Table 3.6. The applied cyclic displacement increment (δ), load ratio (R), measured maximum moment (M_{max}) and number of cycles (N_{M-max}) to reach M_{max}, along with key geometric and crack dimensions are listed in Table 3.8 The results from these tests reveal the influence of cyclic loading and the cyclic displacement increment (δ) on M_{max} (the pipe capacity load) and amount of cyclic tearing crack growth. These, in turn, quantify effect on energy absorbing capacity or fracture resistance curve (J-R curves) of cracked pipes.

3.4.4 Fully Reversible displacement controlled Cyclic Tearing Tests

The reversible displacement controlled cyclic tearing tests have been conducted with aim to understand the effect of reversible displacement controlled cyclic loading on cyclic tearing behaviour of material. The pipe has been subjected to fully reversible quasi-static cyclic loading with constant displacement amplitude. The displacement amplitude is selected between 80% and 95% of the LLD at maximum load in the corresponding monotonic fracture test. In this category of tests, displacement increment is controlled in both directions of loading. The Figure 3.6 (c) shows the loading scheme where Δ_{amp} is the displacement amplitude applied in each cycle while crack opens and the displacement ratio is kept as -1 while unloading and reverse loading of the pipe. The details related to test number, pipe sizes, pipe material / weld type; machined notch size, fatigue pre cracking, final crack sizes and location are listed in Table 3.3 to Table 3.6. The applied cyclic displacement amplitude Δ_{amp}, load ratio, maximum moment (M_{max}) and number of cycles to reach M_{max}, along with key geometric and crack dimensions are listed in Table 3.9. The results from these tests reveal the reversible cyclic displacement loading impact on M_{max} and the cyclic tearing crack growth.

3.4.5 Monotonic fracture Tests

The monotonic fracture tests have been conducted with an aim of obtaining base line data under monotonically increasing load conditions. The pipe sizes, material and crack sizes are identical in cyclic and monotonic fracture tests. The monotonic fracture tests have been conducted under displacement controlled loading. In these tests the displacement is applied incrementally with partial unloading (up to 25%). The loading scheme is similar to that of displacement controlled cyclic load tests. However, load ratio is kept greater than 0.75. The Figure 3.6 (d) shows the loading scheme where δ is the displacement increment given in each cycle while crack opens and R is the load ratio controlled while partial unloading of the pipe. The details related to test number, pipe sizes, pipe material / weld type, crack sizes and location and maximum moment (M_{max}) are listed in Table 3.10. The results of these tests have provided the bases line data of monotonic fracture behaviour of the identical pipes on which the cyclic fracture tests are conducted. The experimental obtained maximum load carrying capacity $M_{max}^{Monotonic\ Test}$ under quasi-static monotonically increasing load is an important parameter used in investigation of pipe capacities under cyclic loading conditions.

3.5 Test measurements

During all the cyclic and monotonic fracture tests, extensive instrumentation is done to measure the following parameters time history from the test

- Applied load
- Load Line Displacement (LLD)
- Crack Mouth Opening Displacement (CMOD)
- Crack extension at both the Crack Tips
- Deformation of Pipe (using a set of LVDTs)

All the above parameters are continuously monitored and recorded during the test. The applied load is recorded using the in-built load cell (in actuator) and the LLD is measured using the in-built Linear Variable Displacement Transducer (LVDT) of actuator. The CMOD data is recorded using the clip gauge. The initial CMOD values in these tests is equal to the width of machined notch, as shown in Figure 3.1, and are given in Table 3.3 and Table 3.4. The crack extension at both crack tips, and corresponding load, LLD and CMOD are obtained from image analysis technique. The Load, LLD and CMOD data recorded using images are redundant and obtained for correspondence with the crack growth data. About 3 to 4 linear variable displacement transducers (LVDTs) are placed below the pipe to measure its displacements, at different sections along the span. These LVDTs helps in ascertaining the compliance of the loading structure between the pipe and the actuator LVDT.

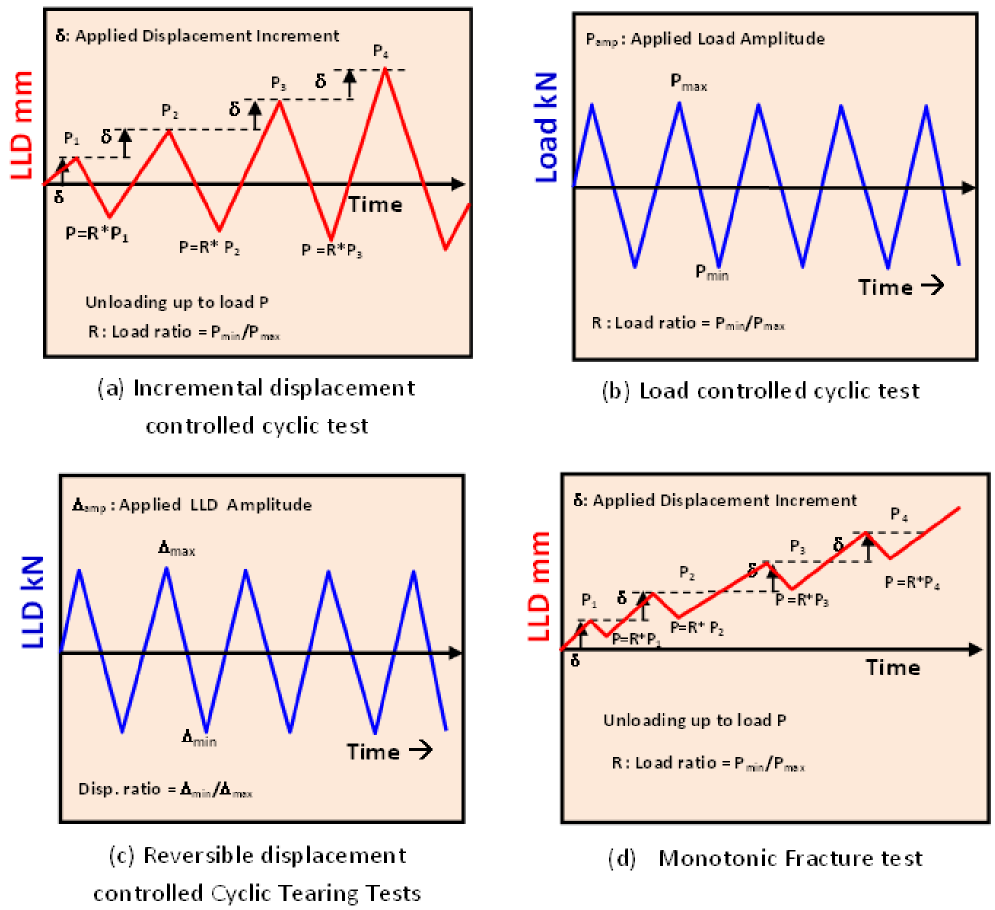

Figure 3.6: Schematic of the Loading Schemes for used for different type of tests

Table 3.3: Details of pipe and notch geometries of carbon steel pipe specimens

Sr. No.	Test Name	Material	Notch Location	Do	t	Notch Length, $2a_i$, mm	Notch Width mm	Inner Span L, mm	Outer span, Z, mm
1	QCSP-8-60-L1-CSB	SA-333 Gr.6	Base	219.5	15.5	119	3.9	860	2500
2	QCSP-8-60-L2-CSB	SA-333 Gr.6	Base	220	15.31	120	4	860	2500
3	QCSP-8-60-L3-CSB	SA-333 Gr.6	Base	219	15.4	119	3.7	860	2500
4	QCSP-8-60-L4-CSB	SA-333 Gr.6	Base	219	15.66	119	4	860	2500
5	QCSP-8-60-L5-CSB	SA-333 Gr.6	Base	219.9	15.6	123	4.1	860	2500
6	QCSP-8-90-L6-CSB	SA-333 Gr.6	Base	219	15.51	178	4	860	2500
7	QCSP-8-60-L1-CSW	SA-333 Gr.6	Weld	219	15.99	120	4	860	2500
8	QCSP-8-60-L2-CSW	SA-333 Gr.6	Weld	219	16.08	120	4	860	2500
9	QCSP-8-60-L3-CSW	SA-333 Gr.6	Weld	219	16.09	121	4	860	2500
10	QCSP-8-60-L4-CSW	SA-333 Gr.6	Weld	219	16.01	120	4	860	2500
11	QCSP-8-60-D1-CSB	SA-333 Gr.6	Base	219	15.63	120	4	860	2500
12	QCSP-8-60-D2-CSB	SA-333 Gr.6	Base	219	15.23	118	4	860	2500
13	QCSP-8-60-D1-CSW	SA-333 Gr.6	Weld	219	16.55	120	4	860	2500
14	QCSP-12-90-L1-CSB	SA-333 Gr.6	Base	324	21.64	264	3.9	1200	4600
15	QCSP-16-120-L1-CSB	SA-333 Gr.6	Base	405	26.54	432	4	1620	5600
16[a]	SP-8-60-M1-CSB (SPBMTWC8-1)	SA-333 Gr.6	Base	219	15.2	115	4	1480	4000
17[a]	SP-8-90-M2-CSB (SPBMTWC8-2)	SA-333 Gr.6	Base	219	15.2	170	4	1480	4000
18	SP-8-60-M-CSW	SA-333 Gr.6	Weld	219	16.2	256	4	1480	4000
19	SP-12-90-M-CSB	SA-333 Gr.6	Base	324	21.3	270	4	5000	1300
20	SP-16-120-M-CSB	SA-333 Gr.6	Base	406	26.2	430	4	1480	5820

Note: [a] Tests data from Chattopadhayay [107-108]

Table 3.4: Details of pipe and notch geometries of stainless steel pipe specimens

Sr. No.	Test Name	Material	Notch Location	Do	t	Notch Length, $2a_i$, mm	Notch Width mm	Inner Span L, mm	Outer span, Z, mm
1	QSSP-6-60-L1-SSB	SS304 LN	Base	168	14.7	90	2.8	800	1800
2	QSSP-6-60-L2-SSB	SS304 LN	Base	168	14.6	94	2.9	800	1800
3	QSSP-6-60-L3-SSB	SS304 LN	Base	168	14.76	89	2	680	1700
4	QSSP-6-60-L4-SSB	SS304 LN	Base	168	14.31	89	2	680	1700
5	QSSP-6-60-L1-SSW	SS304 LN	Weld	168	14.64	93	2	800	1800
6	QSSP-6-60-L2-SSW	SS304 LN	Weld	168	14.75	96	2	800	1800
7	QSSP-6-60-L3-SSW	SS304 LN	Weld	168	14.52	93.5	2	800	1800
8	QSSP-6-60-L4-SSW	SS304 LN	Weld	168	14.65	92	3.5	680	1700
9	QCSP-6-60-D1-SSB	SS304 LN	Base	168	14.8	91	2.8	800	1800
10	QCSP-6-60-D2-SSB	SS304 LN	Base	168	14.5	91	2.8	680	1800
11	QCSP-6-60-D1-SSW	SS304 LN	Weld	168	14.95	91	3	800	1800
12	QCSP-6-60-D2-SSW	SS304 LN	Weld	168	15.07	92	3.5	680	1700
13	QCSP-6-60-D3-SSW	SS304 LN	Weld	169	14.72	92	3.5	680	1700
14	SP-6-60-M-SSW	SS304 LN	Weld	168	14.79	92	3.5	680	1700
15	SP-6-60-M-NGW	SS304 LN	Weld	170	15.087	90	3	760	1780
16	QCSP-6-60-L1-NGW	SS304 LN	Weld	170	15.1	90	3	790	1780
17	QCSP-6-60-L2-NGW	SS304 LN	Weld	170	15.05	88	3	790	1780
18	QCSP-6-60-L3-NGW	SS304 LN	Weld	170	14.55	89	3	790	1780
19	QCSP-6-60-D1-NGW	SS304 LN	Weld	170	14.56	89	3	790	1780
20	QCSP-6-60-D2-NGW	SS304 LN	Weld	170	14.66	90	3	790	1780
21	SP-12-60-M-NGW	SS304 LN	Weld	324	22.24	170	3	1300	4000
22	QCSP-12-60-L2-NGW	SS304 LN	Weld	324	22.23	168	3	1300	4000
23	QCSP-12-60-L3-NGW	SS304 LN	Weld	324	22.52	167	3	1300	4000
24	QCSP-12-60-L4-NGW	SS304 LN	Weld	324	22.35	168	3	1300	4000
25	QCSP-12-60-L5-NGW	SS304 LN	Weld	324	22.16	170	3	1300	4000
26	QCSP-12-60-D1-NGW	SS304 LN	Weld	324	22.25	169	3	1300	4000
27	SP-6-60-M-SSB	SS 304LN	Base	170	15.08	90	2	680	1700

Table 3.5: Details of fatigue pre-cracking and final crack sizes of carbon steel pipe specimens

Sr. No.	Test Name	Frequency Hz.	Cyclic Load		No of Cycles	Initial Notch angle*, θ_i	Final Crack Angle*, θ
			Min, kN	Max. kN			
1	QCSP-8-60-L1-CSB	2	75	7.5	54980	31.06	33.24
2	QCSP-8-60-L2-CSB	2	75	7.5	58813	31.25	33.91
3	QCSP-8-60-L3-CSB	2	75	7.5	21352	31.13	33.75
4	QCSP-8-60-L4-CSB	2	75	7.5	29606	31.13	33.73
5	QCSP-8-60-L5-CSB	2	75	7.5	25328	32.05	33.74
6	QCSP-8-90-L6-CSB	2	60	6	21769	46.57	48.51
7	QCSP-8-60-L1-CSW	2	80	8	14593	31.39	33.23
8	QCSP-8-60-L2-CSW	2	80	8	14000	31.39	33.10
9	QCSP-8-60-L3-CSW	2	80	8	22500	31.66	33.69
10	QCSP-8-60-L4-CSW	2	75	7.5	24000	31.39	32.57
11	QCSP-8-60-D1-CSB	2	75	7.5	140269	31.39	32.62
12	QCSP-8-60-D2-CSB	2	75	7.5	6200	30.87	32.33
13	QCSP-8-60-D1-CSW	2	75	7.5	36752	31.39	33.25
14	QCSP-12-90-L1-CSB	2	100	10	8902	46.69	47.40
15	QCSP-16-120-L1-CSB	2	110	11	18750	61.12	61.68
16[a]	SP-8-60-M1-CSB (SPBMTWC8-1)	1.5-3	27.4	2.74	680000	30	32.8
17[a]	SP-8-90-M2-CSB (SPBMTWC8-2)	2-10	21.5	2.15	1626000	45	46.9
18	SP-8-60-M-CSW	-	-	-	-	30	32
19	SP-12-90-M-CSB	-	-	-	-	45.3	47.8
20	SP-16-120-M-CSB	5	67.9	6.79	101000	60.7	63.1

Note: * Half Crack Angle; [a] Tests data from Chattopadhayay [107-108]

Table 3.6: Details of fatigue pre-cracking and final crack sizes of stainless steel pipe specimens

Sr. No.	Test Name	Frequency Hz.	Cyclic Load		No of Cycles	Initial Notch angle*, θ_i	Final Crack Angle*, θ
			Min, kN	Max. kN			
1	QSSP-6-60-L1-SSB	2	90	15	17488	30.69	32.06
2	QSSP-6-60-L2-SSB	2	85/90	8.5/15	80500/100956	32.06	33.43
3	QSSP-6-60-L3-SSB	2	135	22.5	10209	30.35	32.91
4	QSSP-6-60-L4-SSB	2	135	22.5	11257	30.35	33.38
5	QSSP-6-60-L1-SSW	2	90	15	16470	31.72	33.08
6	QSSP-6-60-L2-SSW	2	90	15	512186	32.74	34.11
7	QSSP-6-60-L3-SSW	2	90	15	75238	31.89	33.25
8	QSSP-6-60-L4-SSW	2	90	15	62500	31.38	33.23
9	QCSP-6-60-D1-SSB	2	90	15	18902	31.04	33.16
10	QCSP-6-60-D2-SSB	2	90	15	18420	31.04	32.99
11	QCSP-6-60-D1-SSW	2	90	15	40958	31.04	33.56
12	QCSP-6-60-D2-SSW	2	90	15	38000	31.38	33.96
13	QCSP-6-60-D3-SSW	2	90	15	39420	31.19	33.42
14	SP-6-60-M-SSW	2	90	15	60150	31.38	33.40
15	SP-6-60-M-NGW	1.5	90	9	18500	30.33	31.83
16	QCSP-6-60-L1-NGW	2	90	15	120000	30.33	32.86
17	QCSP-6-60-L2-NGW	2	90	15	42500	29.66	31.74
18	QCSP-6-60-L3-NGW	2	90	15	46000	30.00	31.75
19	QCSP-6-60-D1-NGW	2	90	15	50000	30.00	32.02
20	QCSP-6-60-D2-NGW	2	90	15	65000	30.33	32.56
21	SP-12-60-M-NGW	0.6	160	16	18000	30.06	31.10
22	QCSP-12-60-L2-NGW	0.9	160	16	18000	29.71	30.77
23	QCSP-12-60-L3-NGW	0.9	160	16	17493	29.53	30.53
24	QCSP-12-60-L4-NGW	0.9	160	16	16305	29.71	30.59
25	QCSP-12-60-L5-NGW	0.9	160	16	15000	30.06	31.01
26	QCSP-12-60-D1-NGW	0.9	160	16	14000	29.89	30.86
27	SP-6-60-M-SSB	0.5	94.55	9.46	7500	30.33	33.03

Note: * Half Crack Angle

3.5.1 Crack growth measurement

During the fracture tests of cracked pipes, the acquisition of crack growth data is very important as it is essential to evaluate various fracture parameters. However, there are several uncertainties in the currently used techniques to measure the crack growth during fracture tests on large size ductile pipes. Unlike in small specimens (like CT, TPB etc.), the compliance function for large components like pipes & elbows etc. are not known. Further, it is known that the crack growths in carbon steel and stainless pipes may go out-of-plane of the crack and the angle at which it grows cannot be anticipated in advance. This imposes further limitation on compliance and other potential drop based method like DCPD used for crack growth measurement under such conditions. Additionally, due to excessive plasticity ahead of crack tip, electrical resistance of material changes, which, in turn, affects the potential drop in the DCPD technique. Therefore, in the present investigation, an image based technique has been used to crack growth. Image technique has an advantage over the conventional techniques (e.g., ACPD or DCPD) of measurement of crack-growth, as it captures the angle at which the crack has grown out-of-plane in addition to the actual amount of crack growth. In this technique, the images of growing crack are acquired using CCD cameras using appropriate hardware and software and subsequently, images are processed to obtain the crack growth and its angle. The present technique of measurement, however, creates 2D images of the piping components which are actually 3D in shape, i.e. the image seen on the 2D imaging plane of the CCD area sensor is a projection of the actual 3D structure. Four CCD cameras capture images of two crack tip positions, digital display of load/LLD and CMOD simultaneously. This correlates the crack tip position with the load, LLD and CMOD.

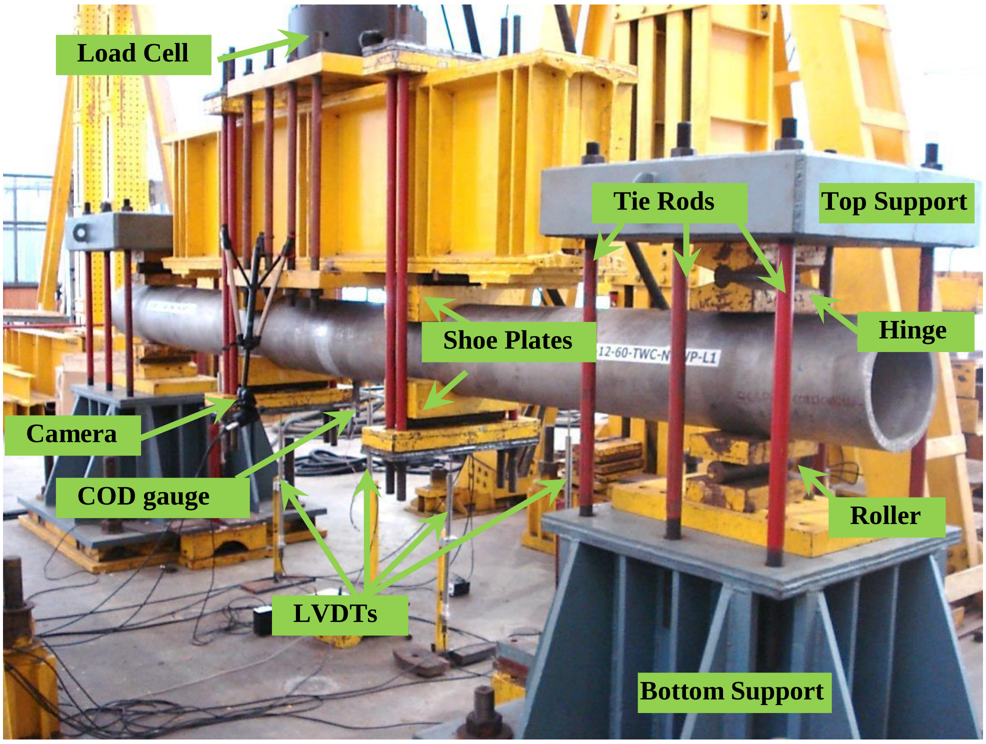

Figure 3.7: Picture of cyclic tearing test setup and different instrumentations

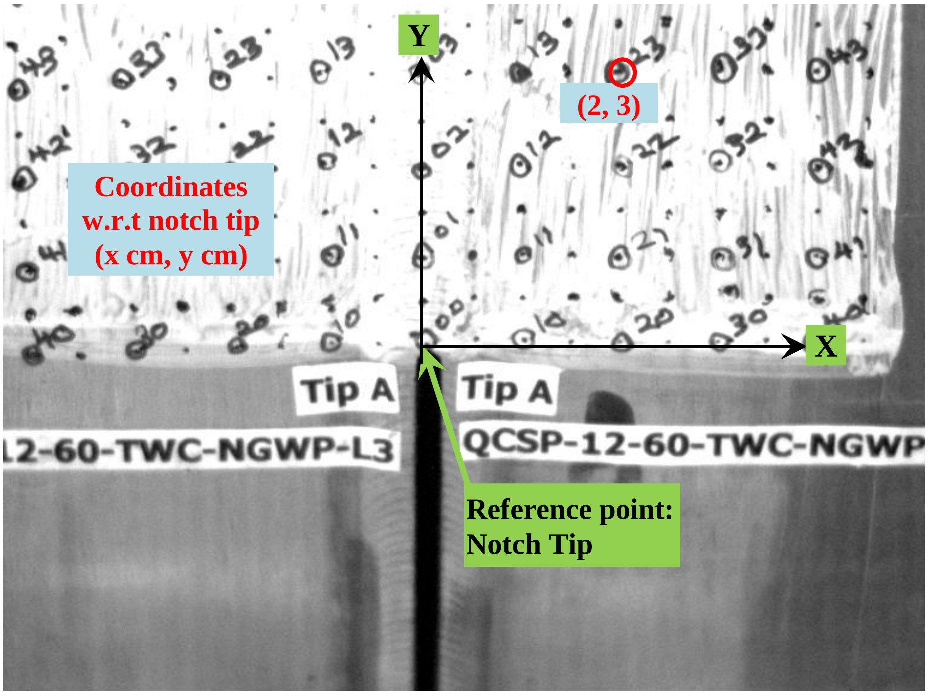

Figure 3.8: Image of dot pattern and point numbering made ahead of crack tip on pipe specimen outer surface

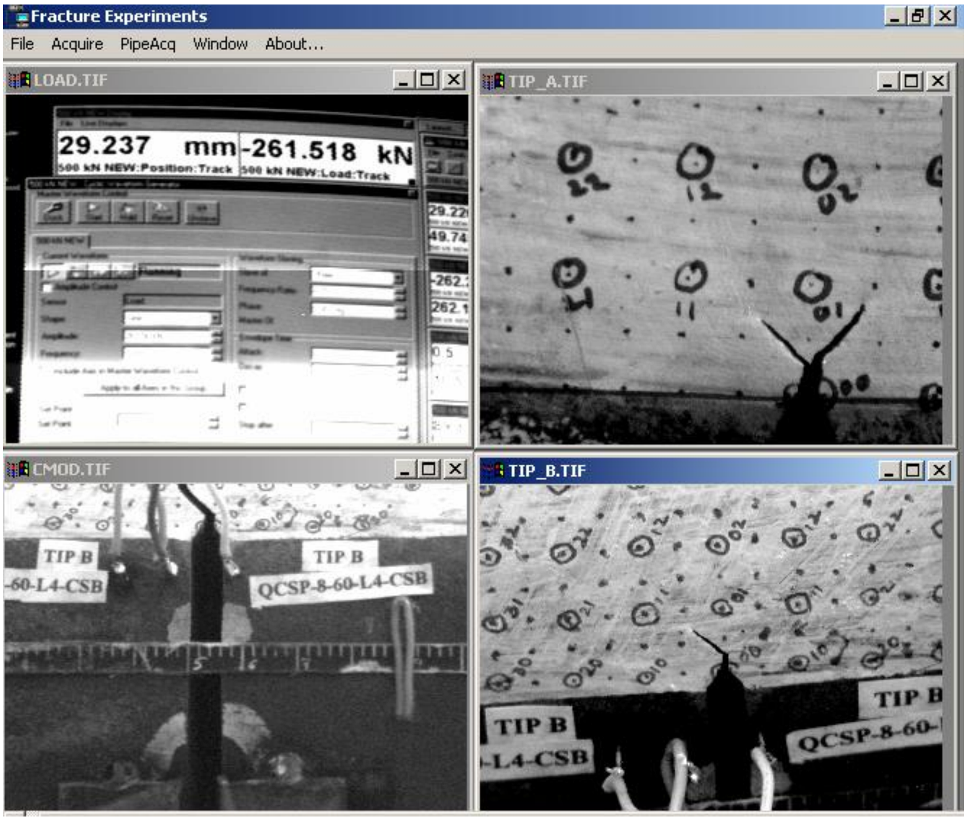

Figure 3.9: The typical display of online image acquisition system containing four child windows on computer screen captured during cyclic test.

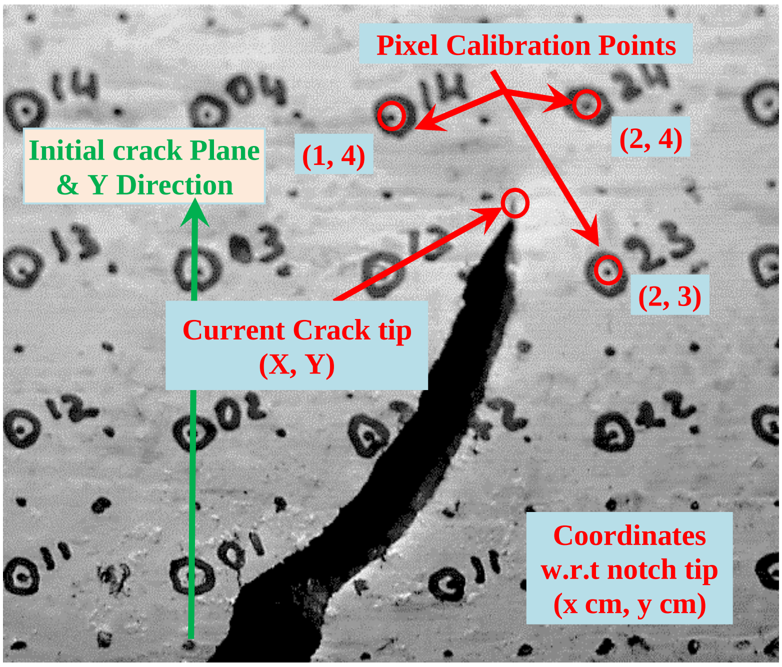

Figure 3.10: Crack growth evaluation from the captured images.

The outer surface ahead of both the crack tips (tip of the machined notch) in TWC cracked pipe specimen is painted (very thin layer of white paint) and then an orthogonal grid mesh with a pitch of 5 mm in both circumferential and an axial direction is made on the painted surface. The orthogonal grid mesh has been done using a template and black marker pen. The extent of meshing ahead of crack tip is about 100-140 mm in circumferential direction at each crack tip and about 60 mm in longitudinal direction on either side of each crack tip. Each node of the mesh was numbered such that it gives the coordinate of each node w.r.t. crack tip at any stage (see Figure 3.8). Every alternate dot is encircled. These encircled dots of 10 mm pitch are used to calibrate the acquired 2D images for computation of the actual 3D distance on pipe surface and are numbered in a particular fashion as shown in Figure 3.8. The first digit in the numbers indicates the x coordinates in 'cm' unit and the second digit indicates the y coordinate in 'cm' unit. The axes are as shown.

Two cameras are focussed towards the two crack tips, tip-A and tip-B, one is focussed at the centre of crack plane to obtain the images of the crack tips and crack mouth to measure Crack Opening Displacement (COD). A scale was mounted on the crack mouth centre to measure CMOD from the images. CMOD was measured in terms of pixels and converted to crack length in millimetre during the processing of crack images. It may be noted that image based COD measurements are in addition to the COD gauge measurement. The fourth camera is focussed towards the digital display of the actuator controller to record the images of load, actuator displacement (LLD) and time / cycle number corresponding to the crack growth at every step of loading. This camera is used as a master and the other three cameras are synchronized with this. For simultaneous acquisition of images from these four cameras during fracture experiments a GUI based user-friendly software developed by EISD of BARC is used. The four images are captured almost synchronously by clicking one key. The maximum delay is about 600 ms as against the load cycle time period of about 120s. Figure 3.9 shows a typical display of four child windows on the computer screen. The four child windows titled LOAD, COD, Tip-A and Tip-B show live images of the actuator controller panel, crack mouth opening, crack Tip-A and crack Tip-B respectively.

The images of the crack tips have been processed through the image analysis software to measure the crack tip extension. Three encircled dots are selected surrounding the crack tip as shown in Figure 3.10. Knowing the pixel coordinates of these three encircled dots along with their geometric coordinates (as indicated in Figure 3.10), the coordinates of the crack tip can be interpolated. This provides the x direction and y-coordinates of the current crack tip with respect to initial notch tip. The y-direction crack growth (the projected crack growth in the initial crack plane) is obtained after subtracting the fatigue pre cracking part (known from fatigue-pre cracking) at that crack tip.

3.5.2 Moment and rotation calculations:

The load and LLD of two tests may be compared if their inner and outer spans during the tests are kept same. However, for comparative study among different tests, the Load-LLD data is converted into the Moment (M) and rotation (ϕ) data which is independent of the test setup, i.e. inner / outer spans, and depends only on material, pipe and crack geometry. The moment and rotation are evaluated using equations as given below:

Moment (M): it is the bending moment acting in the crack plane or inner span (in case of four point bend test setup).

$$M = \frac{P(Z-L)}{4} \tag{3.2}$$

Where, P is the measured load by load cell; Z and L are outer and inner span respectively.

Rotation (ϕ): it is the pipe rotation at the loading point (inner span ends) with respect to the initial pipe configuration. It is function of the LLD, inner and outer span length (L and Z) and machine compliance. Since the machine and fixture member in the load path are very rigid, the machine compliance displacement observed are found insignificant in comparison to recorded LLDs. The total pipe rotation between the two loading point were back calculated from the measured LLD (Δ_{Total}). Procedure given below has been used to calculate the total pipe rotations.

$$\Delta_{C} = \Delta_{Total} - \Delta_{NC} - \Delta_{MC} \tag{3.3}$$

$$\Delta_{NC} = \frac{P(Z-L)^2(Z+2L)}{48EI} \tag{3.4}$$

$$\Delta_{MC} = C_M P \tag{3.5}$$

Where, the Δ_{NC} is the load line displacement when there no crack present in the pipe, in other words it is the non-crack component of load line displacement. The Δ_{MC} is the load line displacement owing to finite stiffness of the machine members in the loading path. C_M is the effective compliance of load train. The total crack rotation, ϕ_C (see Figure 3.11) is then evaluated using equations given below

$$\phi_{NC} = 2 * \frac{P(Z-L)L}{8EI} = 2 * \frac{ML}{2EI} \tag{3.6}$$

$$\phi_{C} = 2 * \tan^{-1}\frac{2\Delta_C}{Z-L} \tag{3.7}$$

$$\phi = \phi_C + \phi_{NC} \tag{3.8}$$

$$\phi_{pl} = \phi_C - \phi_{el} \tag{3.9}$$

$$\phi_{el} = \frac{B_3 M}{\pi R^2 t E} \tag{3.10}$$

The 'ϕ_{NC}' is the rotation of un-cracked pipe between two loading points and the 'ϕ_C' is the total increase in pipe rotation between two loading points due to presence of crack. The 'ϕ' is the total pipe rotation between two loading points. The 'B_3' is a geometry function and available in Zahoor et. al.[32]. In different pipe size tests, inner and outer span were different. Appropriate inputs have been used while making calculation using above described procedure.

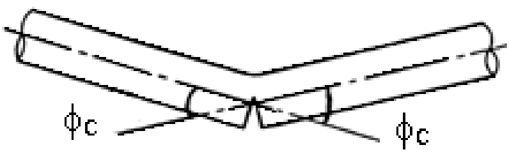

Figure 3.11: Schematic showing the total crack rotation angle (ϕ_C)

3.6 Test Results

Data recorded using various transduces such as COD Gauge, LLD, Load cell, LVDT and crack tip images have been processed and CMOD, load line displacement, load and crack growth at both the tips have been obtained. For each type of four test categories under different loading conditions as discussed in section 3.4, typical results showing the load, LLD and CMOD versus cycles/time and Load-LLD, Load-CMOD plots are given below:

3.6.1 Load controlled Cyclic Tearing Tests

Majority of the tests conducted in this programme belong to this category. This is because of great importance to know the number of allowable loading cycles associated with an earthquake event in stability in instability assessment of cracked pipe. The tests in this category are conducted as per the loading scheme given in section 3.4.2. Table 3.7 gives the salient details of applied loading and results obtained from pipe tests.

The typical variation of different parameters like load, LLD, CMOD, crack growth etc. have been plotted in Figure 3.12 to Figure 3.17 showing complete results of a test namely QCSP-8-60-L2-CSB. These figures plot evolution of load line displacement, CMOD and crack growth when a load controlled reversible loading is applied. Figure 3.12 plots the variation of applied load with time for the pipe specimen, QCSP-8-60-L2-CSB. The load amplitude and the load ratio are kept constant during the tests. Figure 3.13 and Figure 3.14 plot the LLD and CMOD versus number of loading cycles. These have shown that the maximum values of LLD / CMOD corresponding to maximum Load (when crack opens) remains nearly constant (or in some cases increase slightly) during initial cycles, while they increase rapidly in later cycles near to instability. This shows that depending on the load amplitude and number of loading cycles, the contribution of the fatigue and ductile tearing to the crack growth changes. In initial cycles, it is dominated by fatigue alone where ductile tearing contribution is insignificant. However in the later cycles near to instability, in addition to fatigue crack growth, the ductile tearing also becomes significant and in fact ductile tearing-fatigue synergy governs. The test pipe had stable cyclic crack growth up to 18 cycles and had unstable failure in 19th cycle when the crack size become large enough or the remaining ligament was not able to sustain applied load and sudden unstable failure took place. Figure 3.15 plots the load versus LLD and Figure 3.16 plots load versus CMOD behaviour of the tests QCSP-8-60-L2-CSB. These figures show the cycle by cycle evolution of hysteresis loop load versus LLD and load versus CMOD. It can be clearly seen that the width of the loop increase with number of cyclic showing cycle by cycle increase in the damage including loss in stiffness owing to the increase in crack size.

Table 3.7: Results and loading details of the load controlled cyclic tearing tests (all tests at room temperature)

Sr. No	Test No.	Material	Crack Location	Do (mm)	Half Crack Angle θ, (degree)	Maximum Moment applied in each cycle $M_{max,app}$ (kN.m)	Load Ratio, R	Cycles to Instability, N_f
1	QCSP-8-60-L1-CSB	SA-333 Gr.6	Base	219.5	33.24	141.07	-0.5	44
2	QCSP-8-60-L2-CSB	SA-333 Gr.6	Base	220	33.91	133.3	-1	19
3	QCSP-8-60-L3-CSB	SA-333 Gr.6	Base	219	33.75	141.0	-1	5
4	QCSP-8-60-L4-CSB	SA-333 Gr.6	Base	219	33.73	107.4	-1	157
5	QCSP-8-60-L5-CSB	SA-333 Gr.6	Base	219.9	33.74	114.8	-1	72
6	QCSP-8-90-L6-CSB	SA-333 Gr.6	Base	219	48.51	92.7	-1	62
7	QCSP-8-60-L1-CSW	SA-333 Gr.6	Weld	219	33.23	128.7	-1	45
8	QCSP-8-60-L2-CSW	SA-333 Gr.6	Weld	219	33.10	142.7	-1	12
9	QCSP-8-60-L3-CSW	SA-333 Gr.6	Weld	219	33.69	142.67	-0.5	88
10	QCSP-8-60-L4-CSW	SA-333 Gr.6	Weld	219	32.57	136.9	-1	25
11	QCSP-12-90-L1-CSB	SA-333 Gr.6	Base	324	47.40	365.5	-1	30
12	QCSP-16-120-L1-CSB	SA-333 Gr.6	Base	405	61.7	487.6	-1	20
13	QCSP-6-60-L1-SSB	SS 304LN	Base	168	32.06	83.8	-1	29
14	QCSP-6-60-L2-SSB	SS 304LN	Base	168	33.43	93.0	-1	10
15	QCSP-6-60-L3-SSB	SS 304LN	Base	168	32.91	70.2	-1	105
16	QCSP-6-60-L4-SSB	SS 304LN	Base	168	33.38	76.5	-1	40
17	QCSP-6-60-L1-SSW	SS 304LN	Weld	168	33.08	87.17	-0.87	18
18	QCSP-6-60-L2-SSW	SS 304LN	Weld	168	34.11	87.0	-1	17
19	QCSP-6-60-L3-SSW	SS 304LN	Weld	168	33.25	81.5	-1	23
20	QCSP-6-60-L4-SSW	SS 304LN	Weld	168	33.23	68.9	-1	93
21	QCSP-6-60-L1-NGW	SS 304LN	Weld	170	31.7	69.3	-1	196
22	QCSP-6-60-L2-NGW	SS 304LN	Weld	170	31.74	85.4	-1	19
23	QCSP-6-60-L3-NGW	SS 304LN	Weld	170	31.75	78.0	-1	42
24	QCSP-12-60-L2-NGW	SS 304LN	Weld	324	30.77	438.8	-1	22
25	QCSP-12-60-L3-NGW	SS 304LN	Weld	324	30.53	378.0	-1	73
26	QCSP-12-60-L4-NGW	SS 304LN	Weld	324	30.59	344.3	-1	121
27	QCSP-12-60-L5-NGW	SS 304LN	Weld	324	31.01	398.3	-1	42

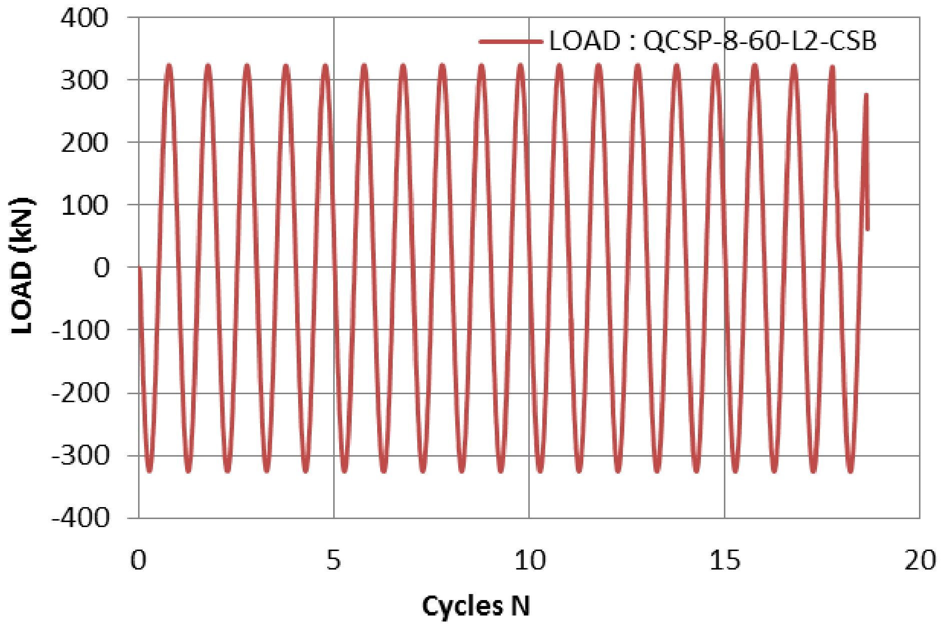

Figure 3.12: Load versus load cycles (N) curve of load controlled cyclic tearing test: QCSP-8-60-L2-CSB

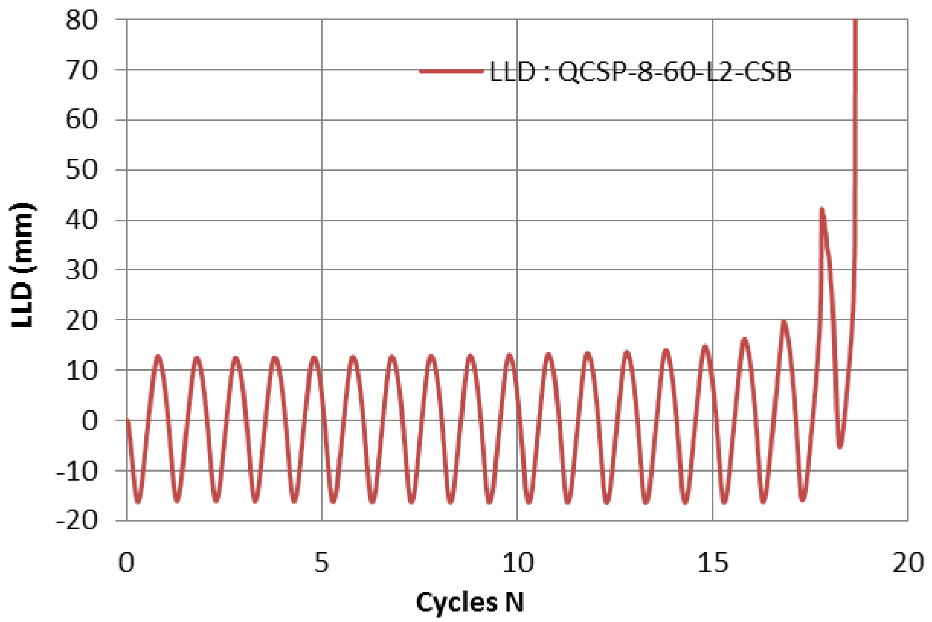

Figure 3.13: Load line displacement (LLD) versus load cycles (N) curve of load controlled cyclic tearing test: QCSP-8-60-L2-CSB

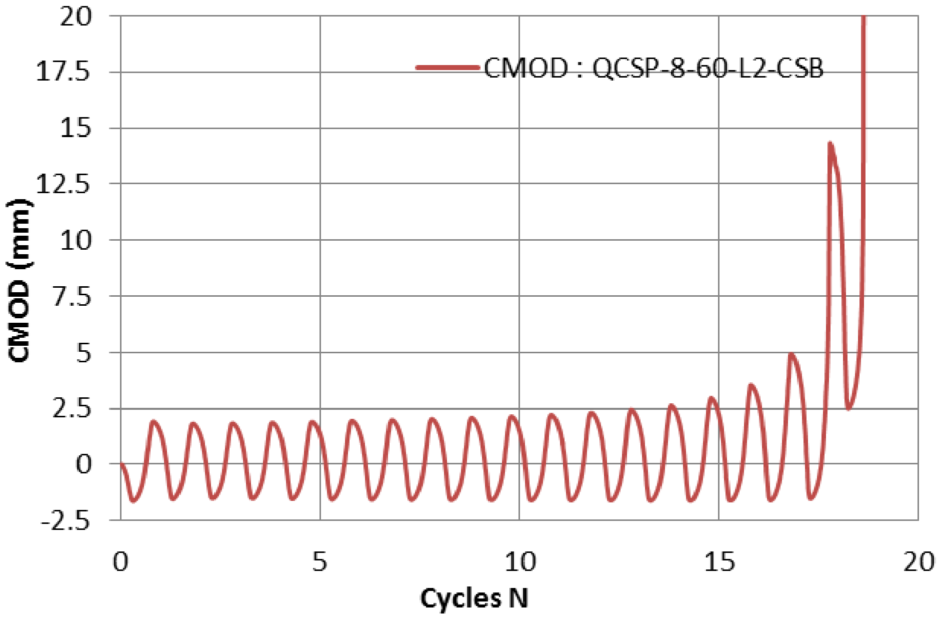

Figure 3.14: Crack mouth opening displacement (CMOD) versus load cycles (N) curve of load controlled cyclic tearing test: QCSP-8-60-L2-CSB

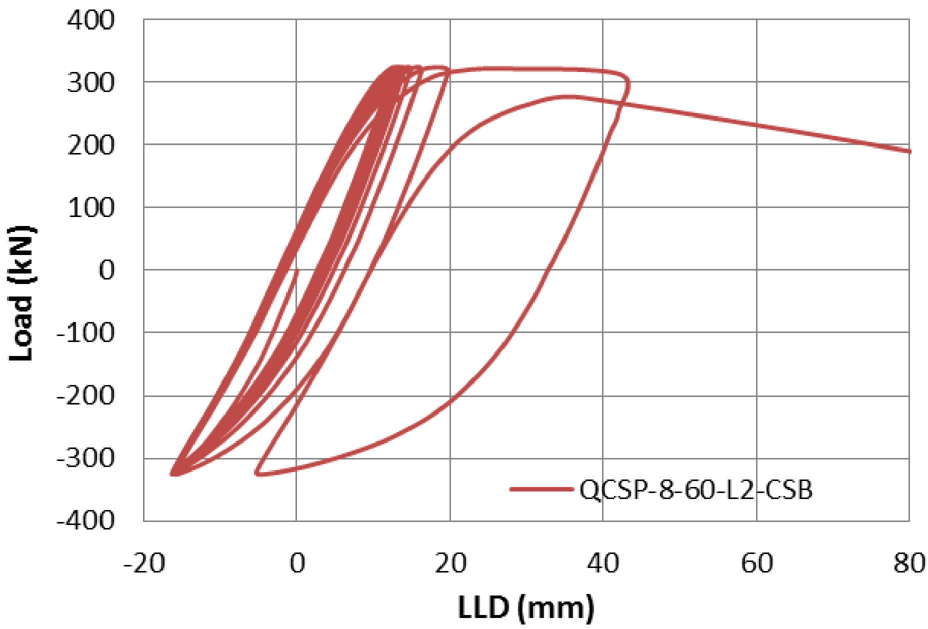

Figure 3.15: Load versus Load line displacement (LLD) curve of load controlled cyclic tearing test: QCSP-8-60-L2-CSB

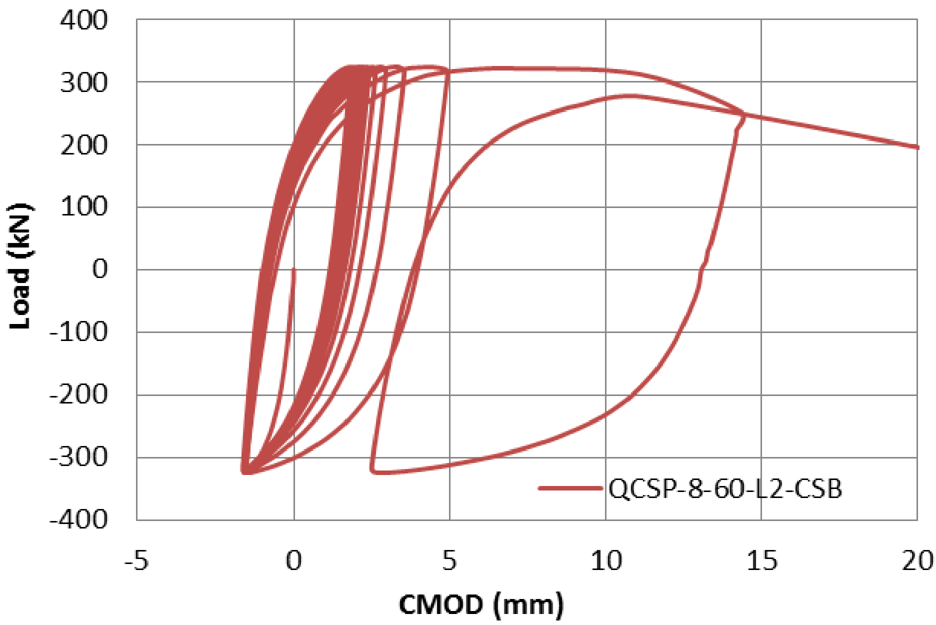

Figure 3.16: Load versus Crack mouth opening displacement (CMOD) curve of load controlled cyclic tearing test: QCSP-8-60-L2-CSB

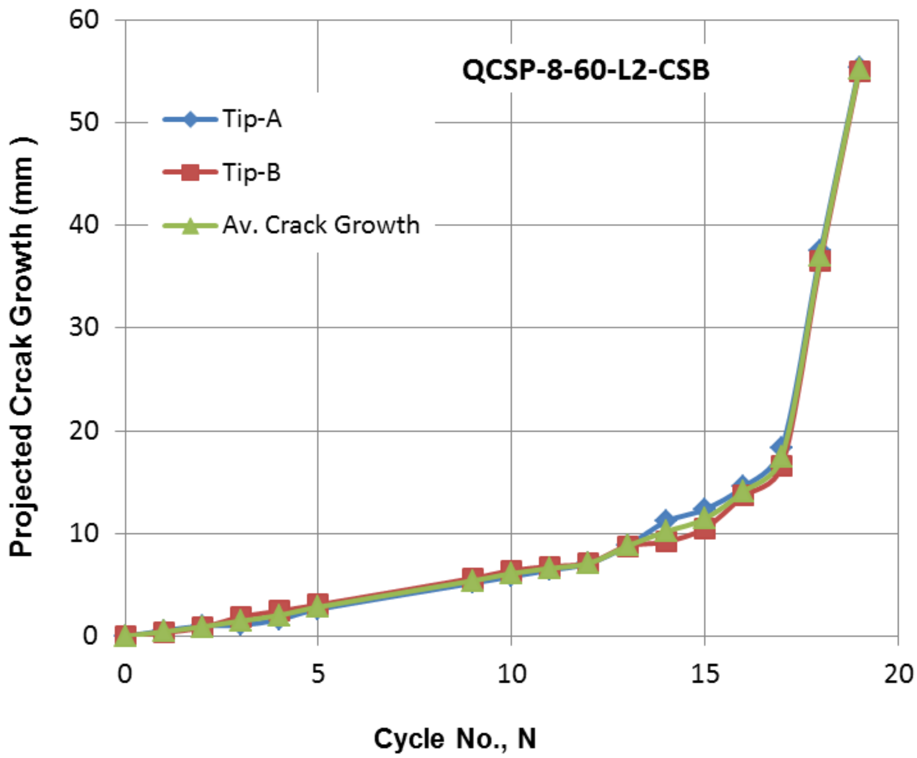

Figure 3.17: Load versus projected crack growth (on crack plane) curve of load controlled cyclic tearing test: QCSP-8-60-L2-CSB

The typical behaviour of all the 27 pipe tests is similar to the one described above. However, the tests with positive mean load have shown significant impact of mean load on the stability and number of loading cycle. The load amplitude and number of loading cycles has significant influence on the fracture stability of cracked pipe under cyclic loading application.

3.6.2 Incremental displacement controlled Cyclic Tearing Tests

The displacement controlled cyclic tearing tests results have been studied to understand the influence of reversible cyclic loading on fracture resistance and load carrying capacity of a cracked pipe. The tests in this category are conducted as per the loading scheme given in section 3.4.3. Table 3.8 gives the salient details of applied loading and results obtained from pipe tests. In order to show the typical variation of different parameters like load, LLD, CMOD, crack growth etc. complete results of an incremental displacement controlled test namely QCSP-8-60-D2-CSB have been plotted in Figure 3.18 to Figure 3.23. These figures plot evolution of load line displacement, CMOD and crack growth when an incremental displacement controlled reversible loading is applied. Figure 3.18, Figure 3.19 and Figure 3.20 respectively plot the LLD, the load and the CMOD variation with time. In every cycle the maximum LLD in crack opening direction is controlled and is increased by a constant increment while in the reverse direction the load is controlled in order to keep the load ratio as -1 and the LLD is response of pipe. The Figure 3.19 and Figure 3.21 show that the local maximum load (maxima of a cycle) initially increased with increase in the LLD, or number of cycles of incremental displacement loading but have steep drop beyond a maximum load P_{max} point (see Figure 3.19). Figure 3.23 shows large crack growth taking place beyond the P_{max} point (24th cycle). Figure 3.21 plots the load versus LLD and Figure

3.22 plots load versus CMOD behaviour of the tests QCSP-8-60-D2-CSB. These figures show the cycle by cycle evolution of hysteresis loop load versus LLD and load versus CMOD. These results are consistent and similar to those observed in IPIRG program (section 2.4.2).

The typical behaviour of all other pipe tests in this category is similar to the one described above. The summary of tests results is given in Table 3.8. These tests have shown the influence of displacement increment on the cyclic fracture load capacity M_{max}, i.e. equal to P_{max}*(Z-L)/4, of the pipe. The cycles (N_{M-max}), that is number of cycles the test took to reach the cyclic fracture load capacity (P_{max} or M_{max}), is also found dependent on applied displacement increment (δ)

Table 3.8: Results and loading details of incremental displacement controlled cyclic tearing tests (all tests at Load Ratio, R=-1, at room temperature)

Sr. No	Test No.	Material	Do mm	Half crack angle θ (deg.)	Recorded Maximum Moment M_{max} (kNm)	Disp. Increment applied in each cycle δ mm	Number of cycles, N_{M-max} to reach M_{max}	Total Number of Cycles N_f
1	QCSP-8-60-D1-CSB	SA-333 Gr.6	219	32.62	149.73	2.6	8	22
2	QCSP-8-60-D2-CSB	SA-333 Gr.6	219	32.33	142.97	0.65	24	60
3	QCSP-8-60-D1-CSW	SA-333 Gr.6	219	33.25	140.22	0.65	30	80
4	QCSP-6-60-D1-SSB	SS 304LN	168	33.16	105.23	4	5	11
5	QCSP-6-60-D2-SSB	SS 304LN	168	32.99	99.78	1	14	41
6	QCSP-6-60-D1-SSW	SS 304LN	168	33.56	91.73	0.75	20	45
7	QCSP-12-60-D1-NGW	SS 304LN	324	30.86	444.11	3	16	28

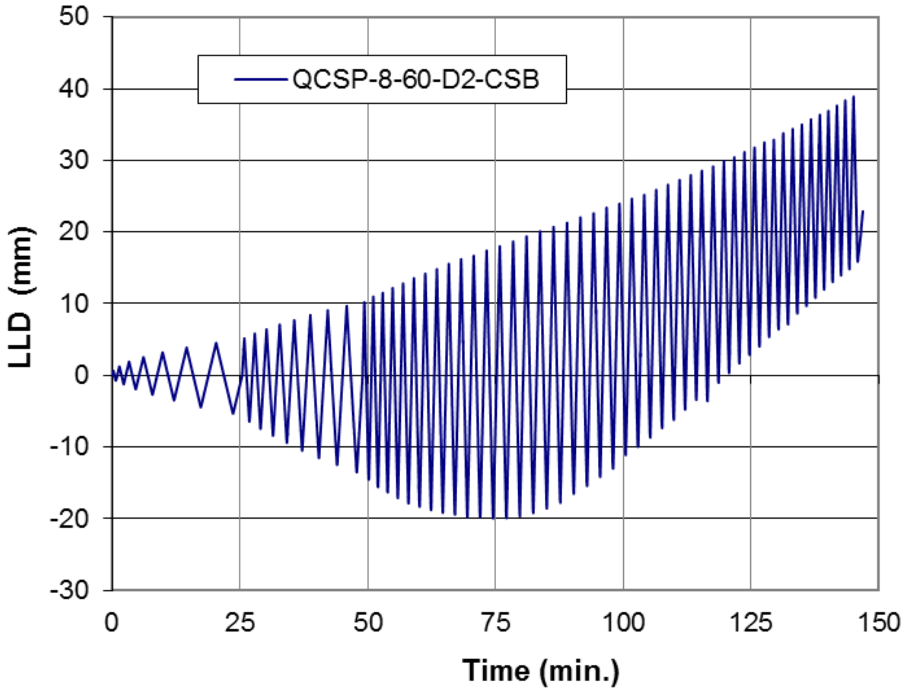

Figure 3.18: Load line displacement (LLD) versus Time curve of Incremental displacement controlled Cyclic Tearing Test: QCSP-8-60-D2-CSB

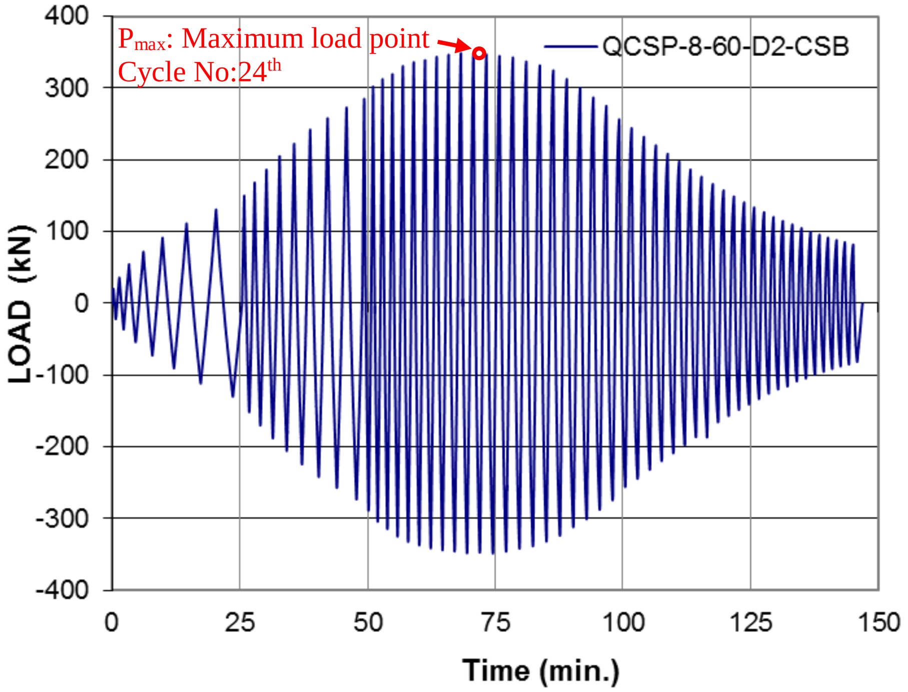

Figure 3.19: Load versus Time curve of Incremental displacement controlled Cyclic Tearing Test: QCSP-8-60-L2-CSB

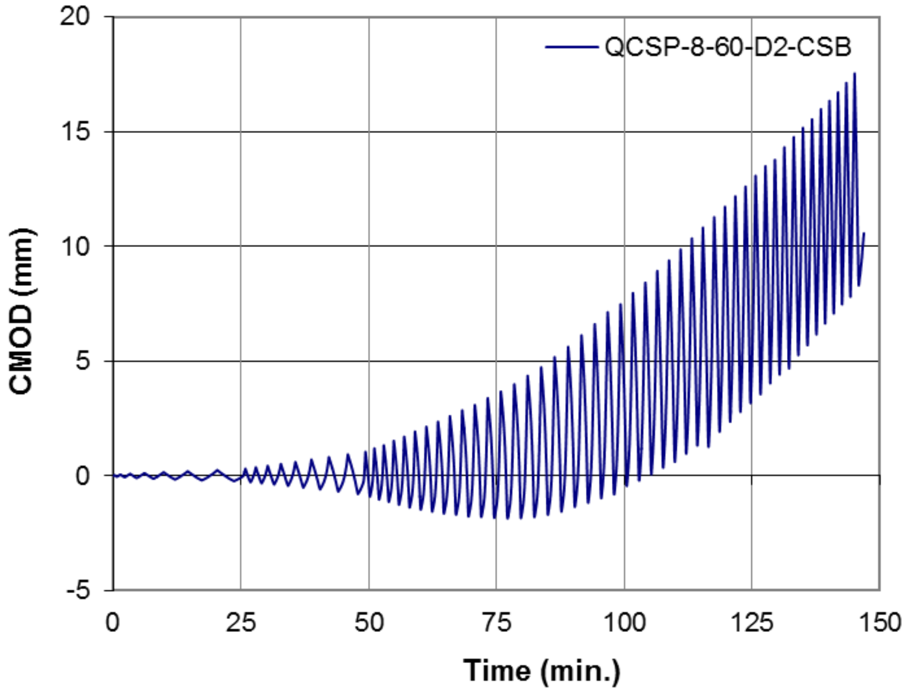

Figure 3.20: Crack mouth opening displacement (CMOD) versus Time curve of Incremental displacement controlled Cyclic Tearing Test: QCSP-8-60-D2-CSB

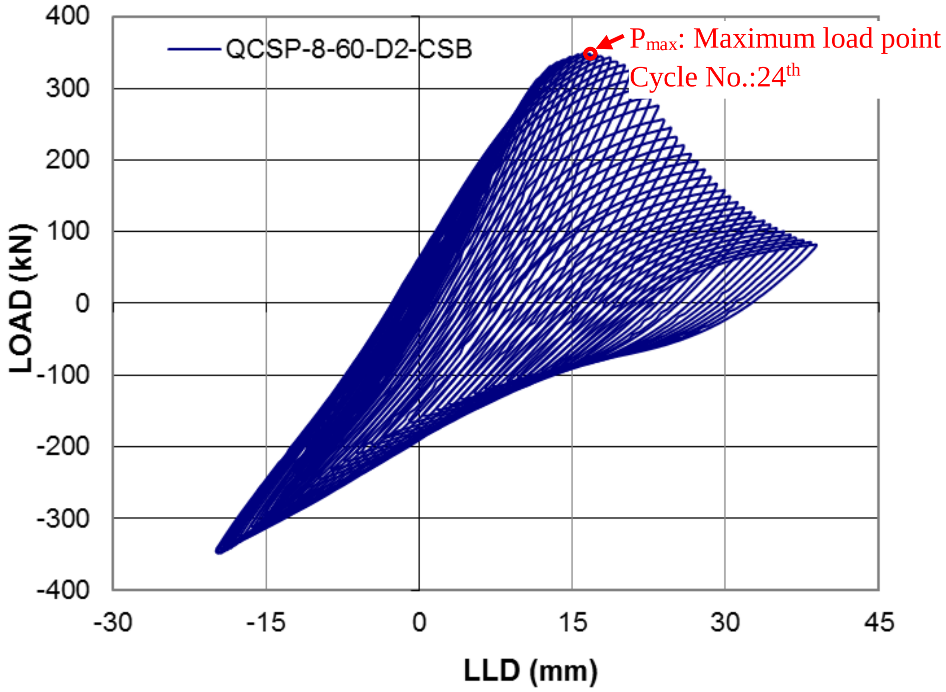

Figure 3.21: Load versus Load line displacement (LLD) curve of Incremental displacement controlled Cyclic Tearing Test: QCSP-8-60-D2-CSB

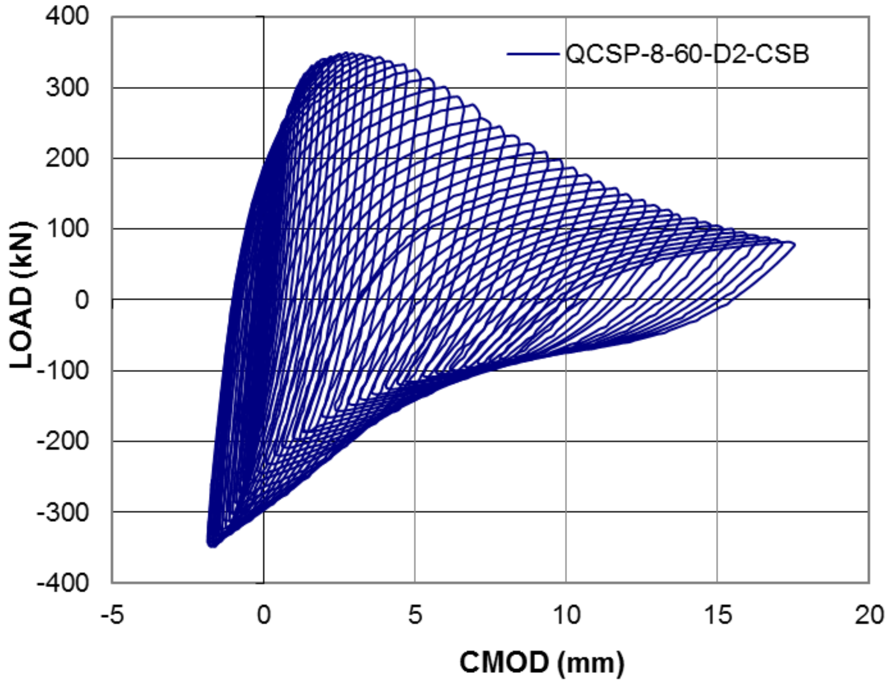

Figure 3.22: Load versus Crack mouth opening displacement (CMOD) curve of Incremental displacement controlled Cyclic Tearing Test: QCSP-8-60-D2-CSB

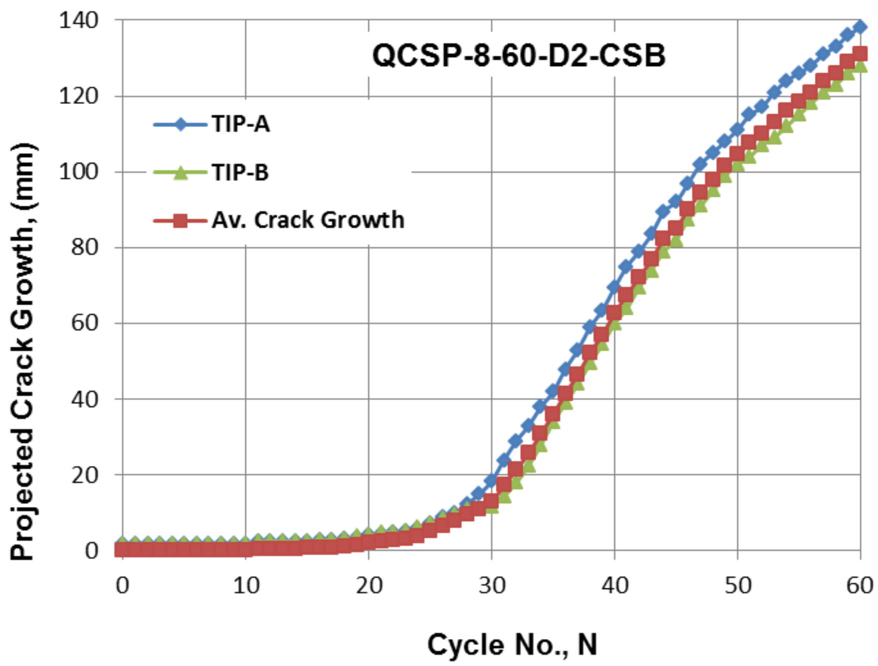

Figure 3.23: Load versus projected crack growth (on crack plane) curve of Incremental displacement controlled Cyclic Tearing Test: QCSP-8-60-D2-CSB

3.6.3 Fully reversible displacement controlled Cyclic Tearing Tests

Three numbers of cyclic tearing tests have been carried out under reversible displacement controlled loading. Here the aim is to understand the effect of reversible displacement controlled cyclic loading on cyclic tearing behaviour of cracked pipes. The tests in this category are conducted as per the loading scheme given in section 3.4.4.Table 3.9 gives the salient details of applied loading and results obtained from the pipe tests in this category. Figure 3.24 to Figure 3.29 show typical results of a reversible displacement controlled test namely QCSP-6-60-D3-SSW. Figure 3.24, Figure 3.25 and Figure 3.26 respectively plot the LLD, the load and the CMOD versus time. The amplitude of the applied LLD is kept constant throughout the test (see Figure 3.24). Figure 3.27 plots the load versus LLD and Figure 3.28 plots load versus CMOD behaviour of the tests QCSP-6-60-D3-SSW. These figures show the cycle by cycle evolution of hysteresis loop load versus LLD and load versus CMOD. They also show changes in the stiffness owing to closure of crack reverse direction loading. The Figure 3.29 plots the projected crack growth at both the crack tips and their average against the applied number of load cycles. This shows that the under reversible displacement loading conditions, large tearing may take place in few cycles of load application (about 10-30 cycles) even when the displacement amplitude is much smaller (about 20-40%) when compared with the maximum load point LLD of corresponding monotonic fracture tests. The result plots of other two pipe tests in this category are similar to the one described above. The summary of tests results is given in Table 3.9.

Table 3.9: Results and loading details of reversible displacement controlled cyclic tearing tests (all tests at room temperature)

Sr. No	Test No.	Material	Do mm	Half crack angle θ (deg.)	Recorded Maximum Moment M_{max} (kNm)	Reversible Disp. applied in each cycle, Δ_{amp}		Number of cycles, N_{M-max} to reach P_{max}	Total number of cycles N_f
						mm	% of monotonic Test Δ at P_{max}		
1	QCSP-6-60-D2-SSW	SS 304LN	168	33.96	85.8	17.25	29.3 %	2	29
2	QCSP-6-60-D3-SSW	SS 304LN	168	33.42	98.7	25	42.5 %	1	11
3	QCSP-6-60-D1-NGW	SS 304LN	170	32.02	98.3	20	25.8 %	6	26

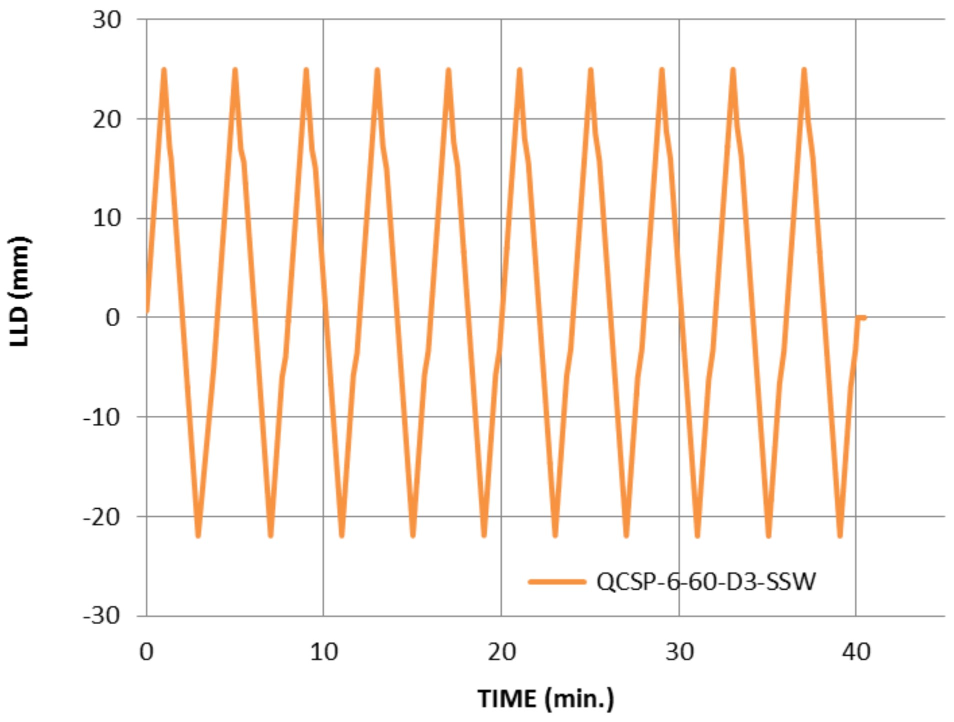

Figure 3.24: Load line displacement (LLD) versus Time curve of Incremental displacement controlled Cyclic Tearing Test: QCSP-6-60-D3-SSW

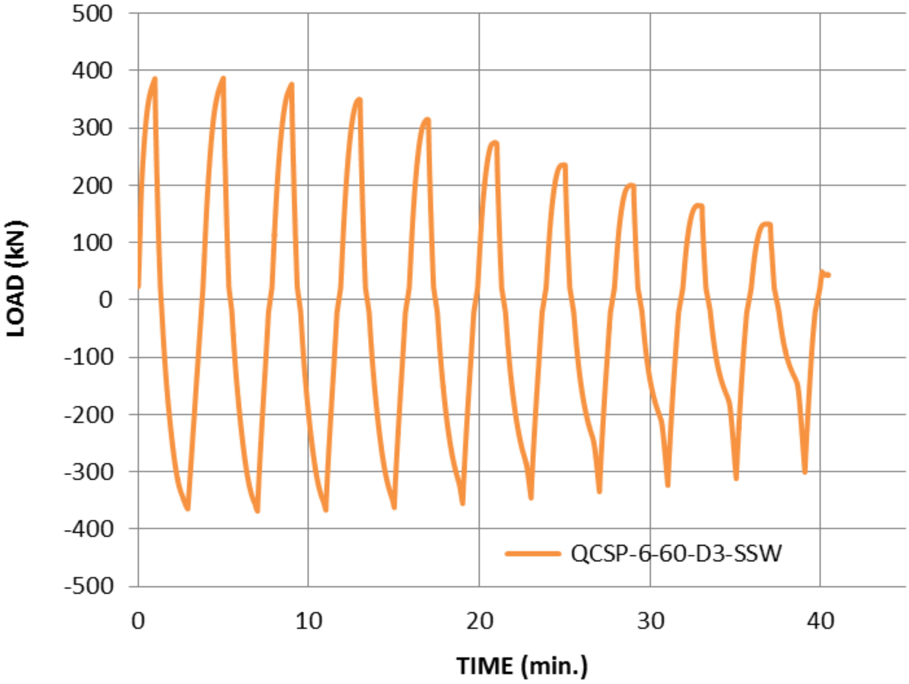

Figure 3.25: Load versus Time curve of Incremental displacement controlled Cyclic Tearing Test: QCSP-6-60-D3-SSW

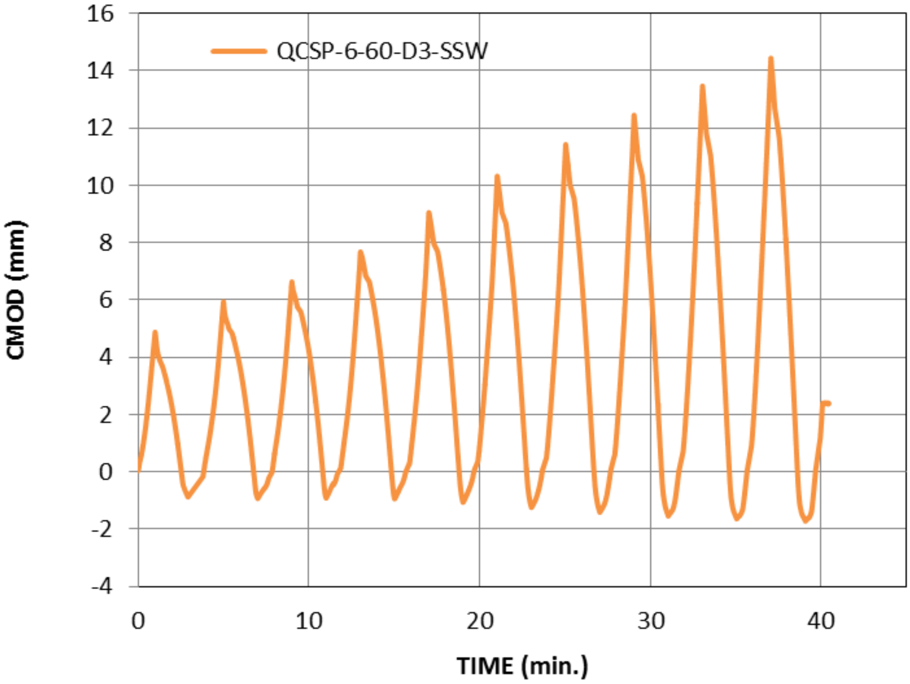

Figure 3.26: Crack mouth opening displacement (CMOD) versus Time curve of Incremental displacement controlled Cyclic Tearing Test: QCSP-6-60-D3-SSW

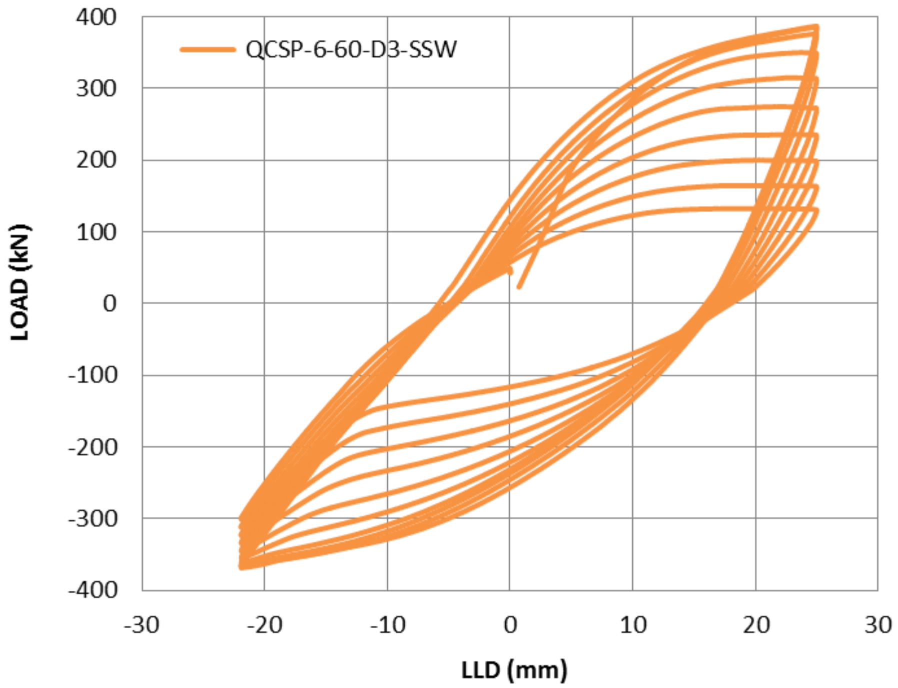

Figure 3.27: Load versus Load line displacement (LLD) curve of Incremental displacement controlled Cyclic Tearing Test: QCSP-6-60-D3-SSW

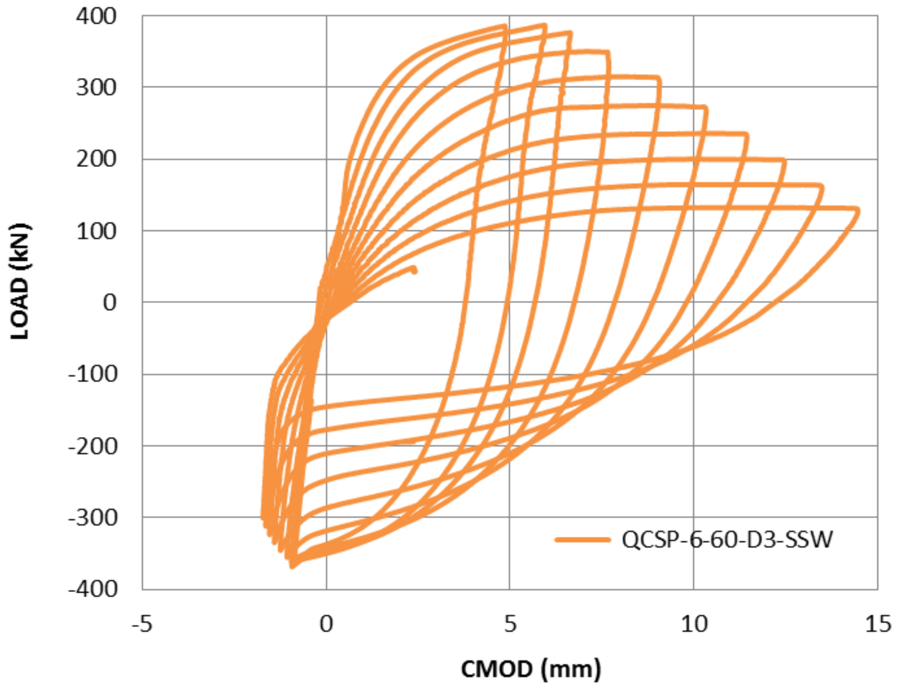

Figure 3.28: Load versus Crack mouth opening displacement (CMOD) curve of Incremental displacement controlled Cyclic Tearing Test: QCSP-6-60-D3-SSW

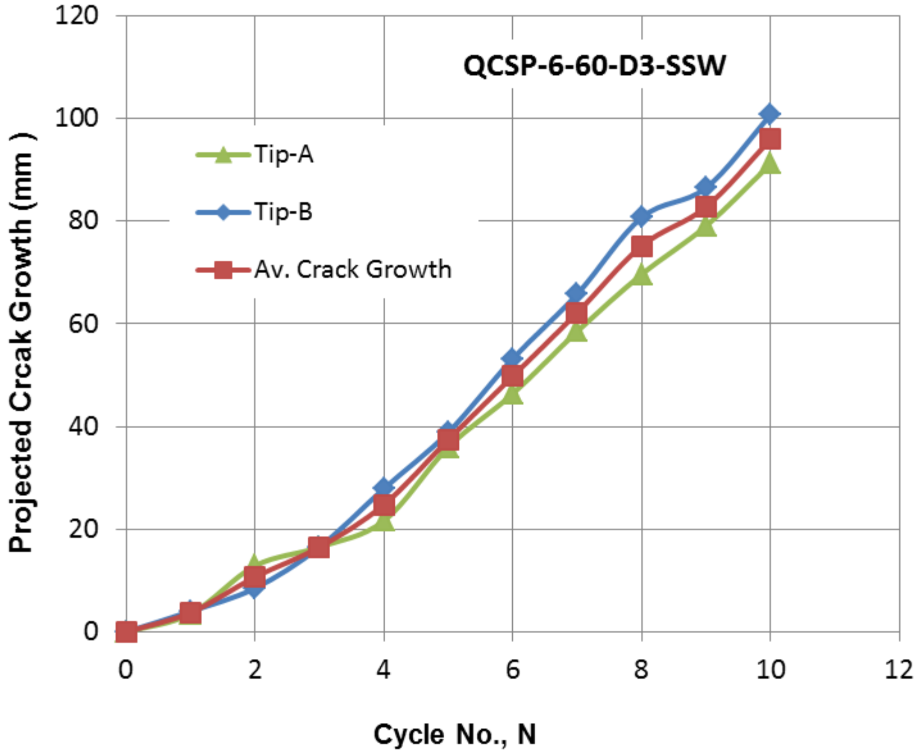

Figure 3.29: Load versus projected crack growth (on crack plane) curve of Incremental displacement controlled Cyclic Tearing Test: QCSP-6-60-D3-SSW

3.6.4 Monotonic fracture Tests

As described earlier, to obtain the load carrying capacity under cyclic load in comparison to monotonic load, the base line monotonic fracture data corresponding to category of cyclic tearing test has been key part of this investigation. The monotonic fracture tests have been conducted on the pipe sizes, material and crack sizes which are identical to cyclic fracture tests. The tests in this category are conducted as per the loading scheme given in section 3.4.5. Table 3.10, gives the salient details of applied loading and results obtained from pipe tests. The typical variation of different parameters like load, LLD, CMOD, crack growth etc. is shown in Figure 3.30 to Figure 3.34 where complete results of a monotonic fracture test namely SP-6-60-M-SSW are plotted. These figures plots evolution of load line displacement, CMOD and crack growth when an incremental displacement controlled reversible loading is applied. Figure 3.30 and Figure 3.31 respectively plot the LLD and the load versus time. Figure 3.32 plots the load versus LLD and Figure 3.33 plots load versus CMOD behaviour of this pipe test. The Figure 3.34 plots the load versus the projected crack growth at both the crack tips and their average. The maximum load point, P_{max} obtained for this crack pipe is also shown in these figures. These results are in line with the typical monotonic fracture behaviour of pipe reported in literature.

Table 3.10: Results and loading details of monotonic fracture tests, at room temperature, corresponding to cyclic fracture tests reported in Table 3.7 to Table 3.9

Sr. No.	Test No.	Material	Crack Location	Do, mm	Half crack angle,θ (deg.)	Recorded Max. Moment, $M_{max}^{Monotonic\ Test}$ (or M_{crit}) (kNm)
1[a*]	SP-8-60-M1-CSB (SPBMTWC8-1)	SA-333 Gr.6	Base	219	32.8	155.2
2[a*]	SP-8-90-M2-CSB (SPBMTWC8-2)	SA-333 Gr.6	Base	219	46.9	124.2
3	SP-8-60-M-CSW	SA-333 Gr.6	Weld	219	32.0	176.0
4	SP-12-90-M-CSB	SA-333 Gr.6	Base	324	47.8	439.5
5	SP-16-120-M-CSB	SA-333 Gr.6	Base	406	63.1	576.1
6[b*]	PB-6	SS 304LN	Base	168	21.8	126.95
7	SP-6-60-M-SSB	SS 304LN	Base	170	33.03	108.1
8	SP-6-60-M-SSW	SS 304LN	Weld	168	33.4	97.8
9	SP-6-60-M-NGW	SS 304LN	Weld	170	32.0	96.9
10	SP-12-60-M-NGW	SS 304LN	Weld	324	31.1	482.8

Note: [a] Tests data from Chattopadhayay [107-108]; [b] Test data from Singh [109].

The typical behaviour of all the monotonic fracture pipe tests is similar to the one described above. Some monotonic fracture tests data on the identical pipes were available from other tasks of BARC component integrity test programme. The summary of tests conducted and used from other BARC programmes has been given in Table 3.10. The maximum load carrying capacity $M_{max}^{Monotonic\ Test}$ has been obtained from all these monotonic fracture tests. This data would be used in quantifying the loss in the pipe capacity load under cyclic loading conditions.

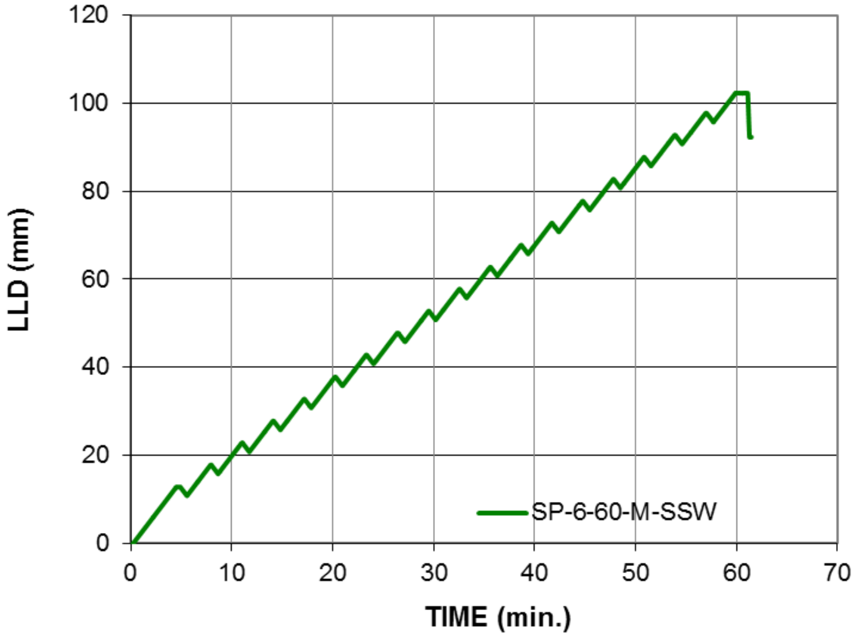

Figure 3.30: Load line displacement (LLD) versus Time curve of Monotonic Fracture Test: SP-6-60-M-SSW

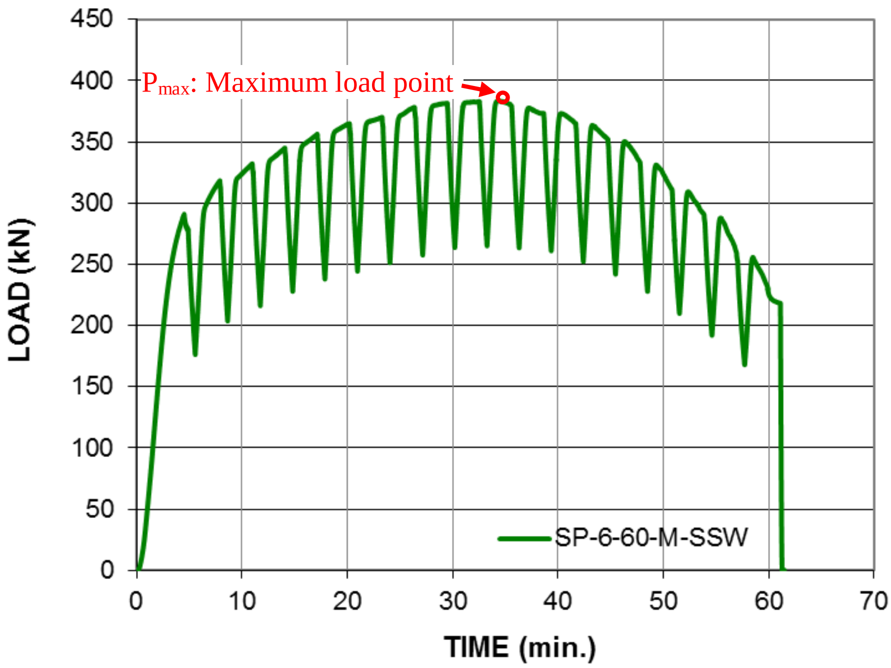

Figure 3.31: Load versus Time curve of Monotonic Fracture Test: SP-6-60-M-SSW

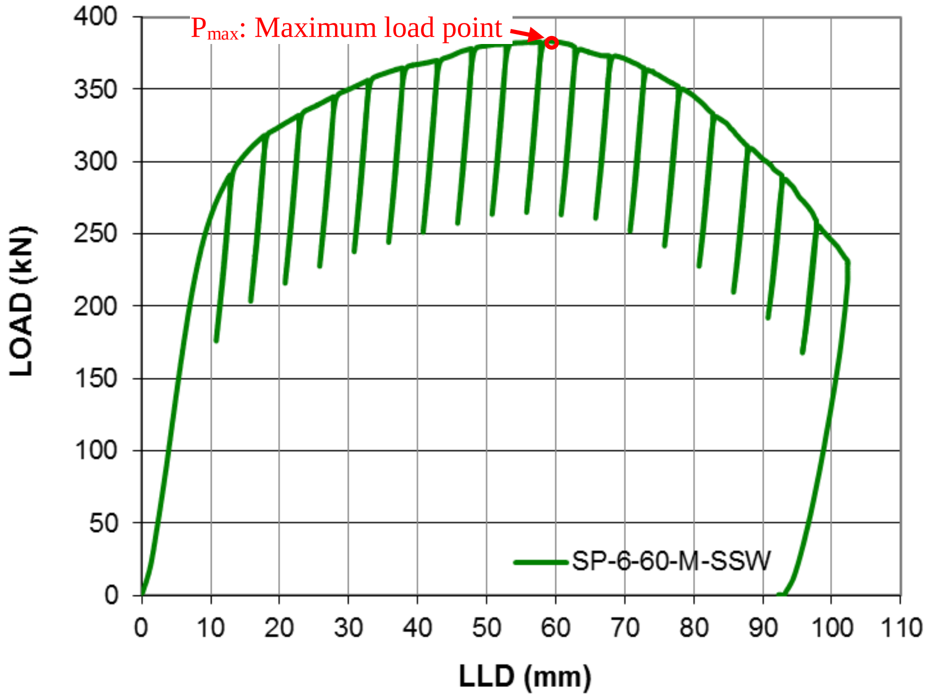

Figure 3.32: Load versus Load line displacement (LLD) curve of Monotonic Fracture Test: SP-6-60-M-SSW

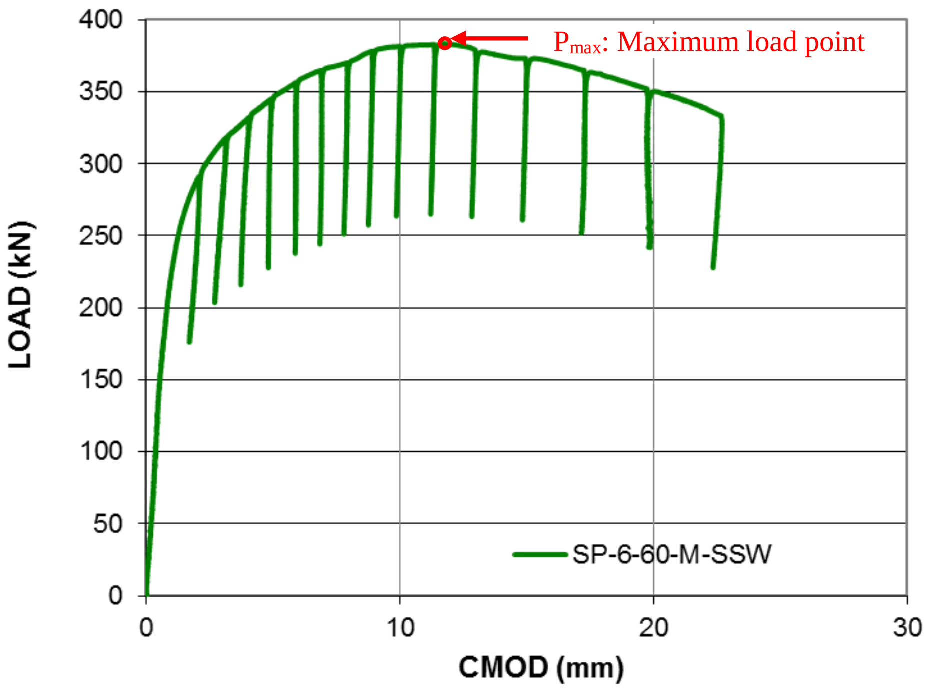

Figure 3.33: Load versus Crack mouth opening displacement (CMOD) curve of Monotonic Fracture Test: SP-6-60-M-SSW

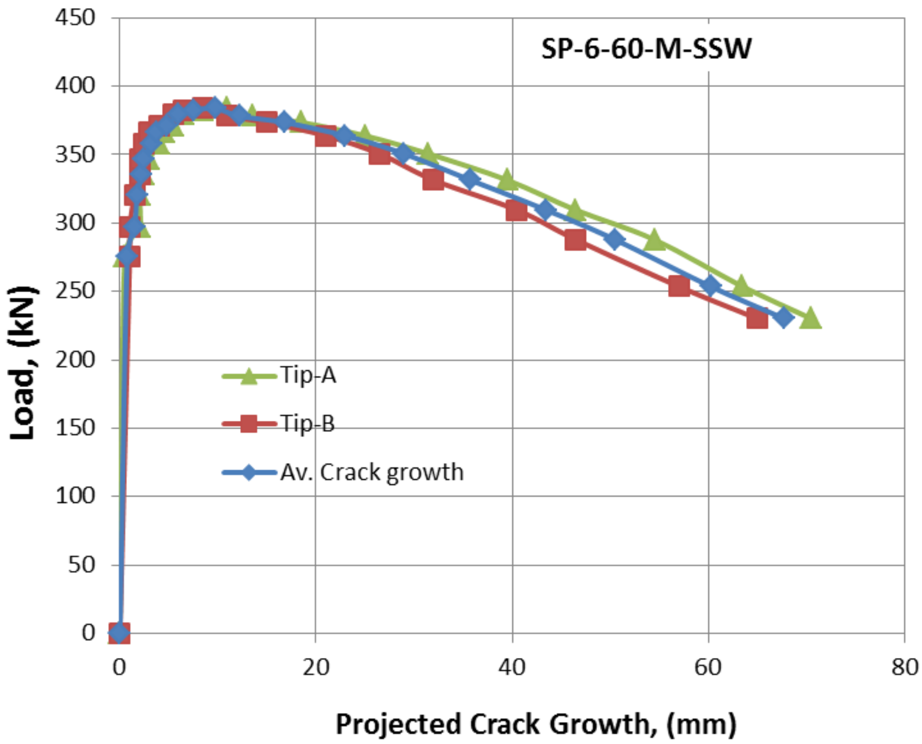

Figure 3.34: Load versus projected crack growth (on crack plane) curve of Monotonic Fracture Test: SP-6-60-M-SSW

3.6.5 Pipe fracture behaviour under different loading histories

Since the piping system is subjected to combination of loading which may be load controlled or displacement controlled or of mixed type; of monotonically increasing or cyclic in nature. In case of cyclic loading, they may be of gradually increasing or may be of constant magnitude from beginning. In view of these, tests have been conducted under four different loading history types, namely load controlled cyclic tearing tests, incremental displacement controlled cyclic tearing tests, monotonic fracture tests and a few tests under fully reversible displacement controlled loading conditions. The cracked pipe behaviour under these different loading histories may be explained by comparing their moment-rotation (M-ϕ) and moment crack growth response obtained on identical pipe tests under different loading histories. These are as follows:

3.6.5.1 Moment-rotation (M-ϕ) under different loading histories

Figure 3.35 plot the moment, M, versus pipe rotation, ϕ_{tot}, for tests on identical 8″ NB carbon steel pipes conducted under different loading conditions, namely monotonic (test name: SP-8-60-M-CSB), displacement controlled cyclic (test name: QCSP-8-60-D1-CSB) and reversible load controlled cyclic loading (test name: QCSP-8-60-L2-CSB). This figure also plots the envelop curve along with M-ϕ_{tot} history for displacement controlled cyclic tearing test. The envelope curve of M-ϕ_{tot} history is obtained by joining the maximum moment points of each cycle (in crack opening direction). Salient parameters like maximum moment (M_{max}), cycles $N_{M\text{-}max}$ (cycles to reach maximum moment M_{max}) and N_f (cycles to unstable failure in load controlled cyclic tearing tests) obtained from these tests have also been described.

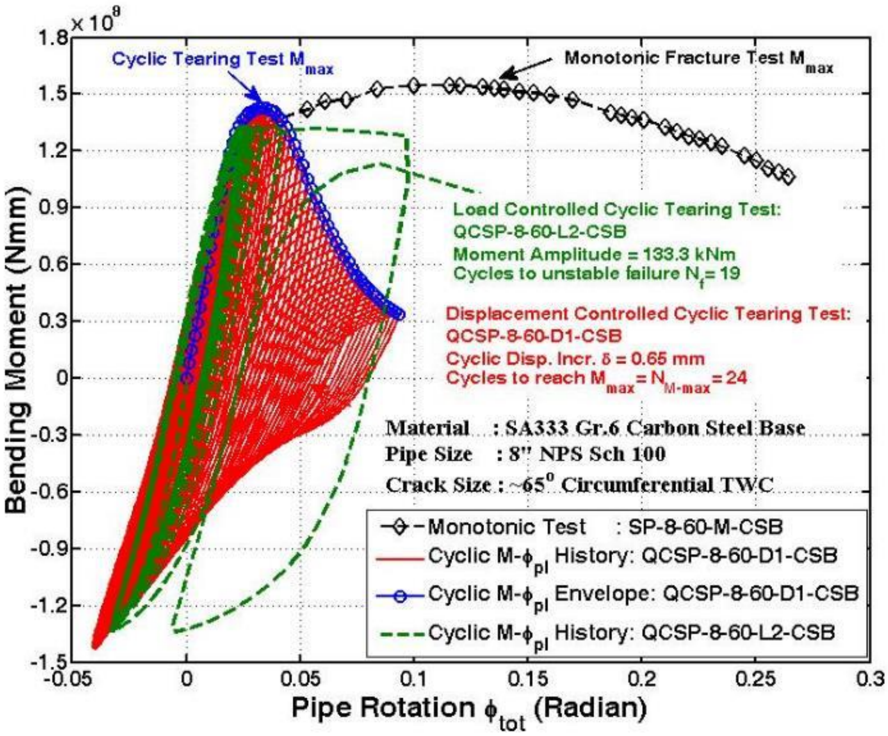

Figure 3.35: Typical plot of moment vs. total rotation for tests 6″ NB SA333Gr6 pipe with circumferential TWC (CSB) under different loading conditions

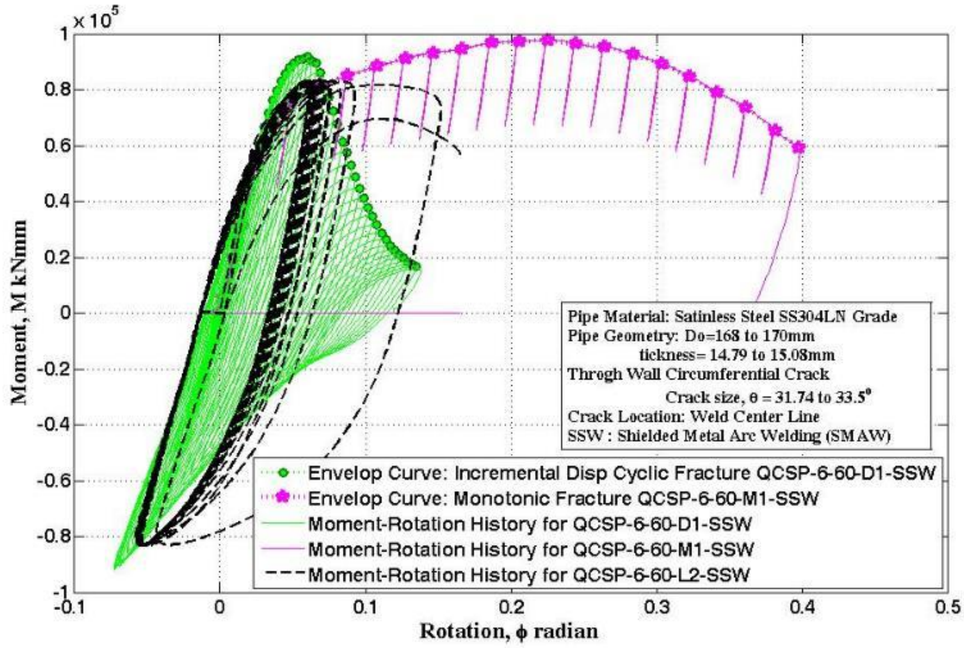

Figure 3.36: Typical plot of moment vs. total rotation for tests 6″ NB SS304LN pipe with circumferential TWC at weld centre (SSW) under different loading conditions

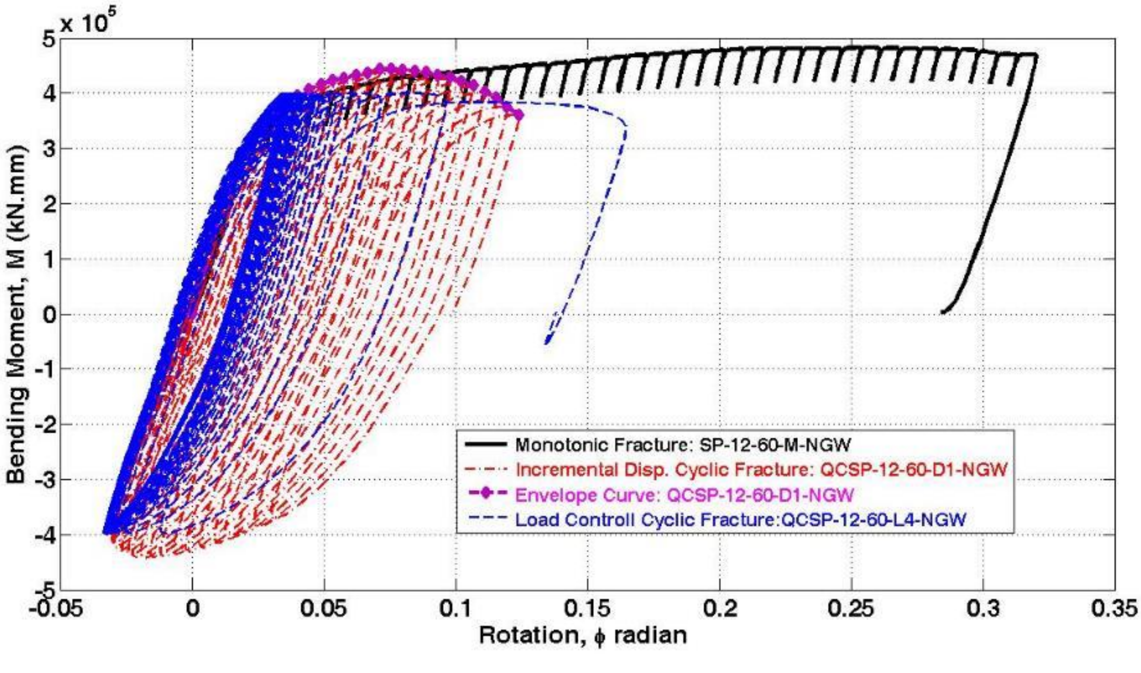

Figure 3.37: Typical plot of moment vs. total rotation for tests 12″ NB SS304LN pipe with circumferential TWC at weld centre (NGW) under different loading conditions

Likewise Figure 3.36 shows Moment (M) – total rotation (ϕ), history plots for three different loading tests on identical 6″ NB stainless steel pipes conducted under different loading conditions, namely monotonic (test name: SP-6-60-M-SSW), displacement controlled cyclic (test name: QCSP-6-60-D1-SSW) and reversible load controlled cyclic loading (test name: QCSP-6-60-L2-SSW). Figure 3.37 shows Moment (M) – total rotation (ϕ), history plots for three different loading tests on identical 12″ NB stainless steel pipes conducted under different loading conditions, namely monotonic (test name: SP-12-60-M-NGW), displacement controlled cyclic (test name: QCSP-12-60-D1-NGW) and reversible load controlled cyclic loading (test name: QCSP-12-60-L4-NGW).

In all the above three pipe cases (CSB, SSW and NGW shown in Figure 3.35, Figure 3.36 and Figure 3.37 respectively) following observations are made:

(i) In monotonic fracture tests, on increasing the applied pipe rotation, the crack imitation takes place; both the initiated crack size and the reaction moments grow further on increase of pipe rotation. After a small stable crack growth (about 5-10mm at each tip), the reaction moment reached a maximum (denoted as M_{max}) and then starts dropping. This implies that the pipe capacity has reached its full capacity and its resistance is not increasing in proportion to increase in applied loading. The large reduction in load carrying area in the cracked cross section owing to significant crack growth leads to reduction of moment.

(ii) In incremental displacement control tests the pipe rotation is incrementally building up after each cycle or fully reversible load (load ratio=-1). Here also the crack initiates after few loading cycles. The crack and peak reaction moment (of a cycle) grows with cyclic application of incremental rotation. Similar to monotonic tests, the cyclic peak reaction moment reached a maximum moment (M_{max}) in few cycles ($N_{M\text{-}max}$) of incremental rotation loading and then starts decreasing. This trend of envelope M-ϕ curve is similar to that observed in corresponding monotonic fracture tests. However, the displacement controlled cyclic tests has shown; a) A small to moderate decrease in the maximum moment (M_{max}), i.e. the capacity of pipe and b) Occurrence of the maximum moment (M_{max}) at a much smaller rotation ($\phi_{M\text{-}max}$) in comparison to that obtained in corresponding monotonic fracture tests. This is due to the presence of fatigue and reverse plasticity damages which are accumulating with each loading cycle in case of incremental displacement controlled loading tests.

(iii) In load controlled cyclic tearing test, the moment is applied while the pipe rotation, and crack growth are response of the pipe tearing behaviour. In these tests the crack initiated in 1st cycle when loading amplitude was greater than the crack initiation load (observed in monotonic test) otherwise it takes few cycles. After crack initiation, the crack further grows in each cycle load and the M-ϕ hysteresis loop size also evolves and increases. It can be clearly seen that the width of the loop increases with number of cyclic showing cycle by cycle increase in the damage including loss in stiffness owing to the increase in crack size.

3.6.6 Crack Growth patterns

In different categories of pipe tests namely CSB, CSW, SSW, SSB, and NGW, the crack has grown in different fashion. However, in all the pipe tests, crack extension, Δa, has been evaluated as the average of projected crack growth of the two crack tips onto the circumferential plane containing initial crack. The crack growth observations in different tests are described below:

Carbon Steel Base (CSB): The crack grew at some helical angle from the initial circumferential crack plane (see Figure 3.38). This observation is similar to those reported for the carbon steel pipes tested in the various USNRC programs conducted at Battelle and also by Chattopadhyay et al [107].

Carbon Steel Weld (CSW): The crack took turn and grew in base metal or along the fusion line (see Figure 3.39).

Stainless Steel Base (SSB): The crack grew straight and remained in the initial circumferential crack plane (Figure 3.40). Similar observation was also made by Chattopadhyay [110].

Stainless Steel SMAW (SSW): The crack took turn and grew along the fusion line (see Figure 3.41). In few cases it also remained in weld region. For stainless steel SMAW welded pipe tests, the crack took turn after initiation and grew along the fusion line. In few cases, it remained in weld region.

Stainless Steel narrow grove hot wire GTAW (NGW): The crack grew in the weld region or took turn and grew along the fusion line (see Figure 3.42 and Figure 3.43). For stainless steel Narrow groove hot wire GTAW welded pipe tests (NGW), the crack grew in the weld region. In many cases, after initiation, the crack took turn after initiation and grew along the fusion line

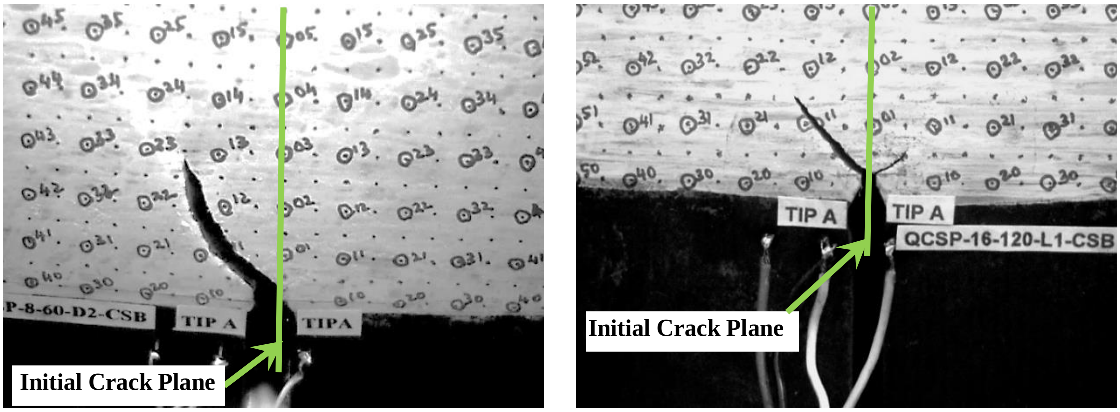

Figure 3.38: Picture showing crack growth patterns in carbon steel base (CSB) category pipe tests

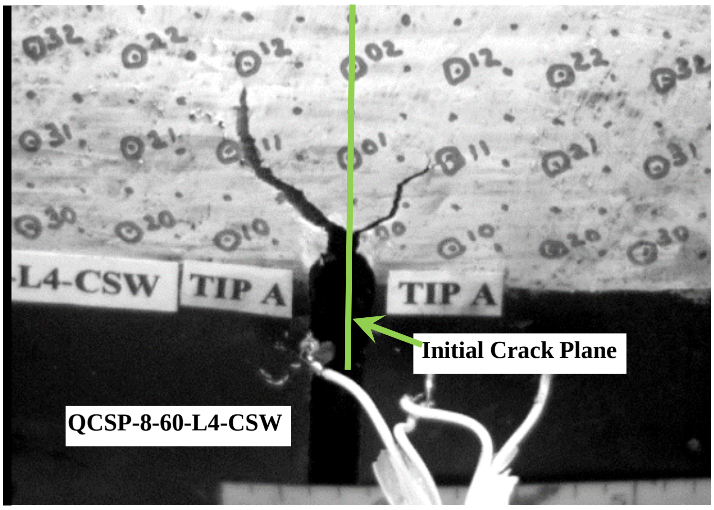

Figure 3.39: Picture showing crack growth patterns in carbon steel weld (CSW) category pipe tests

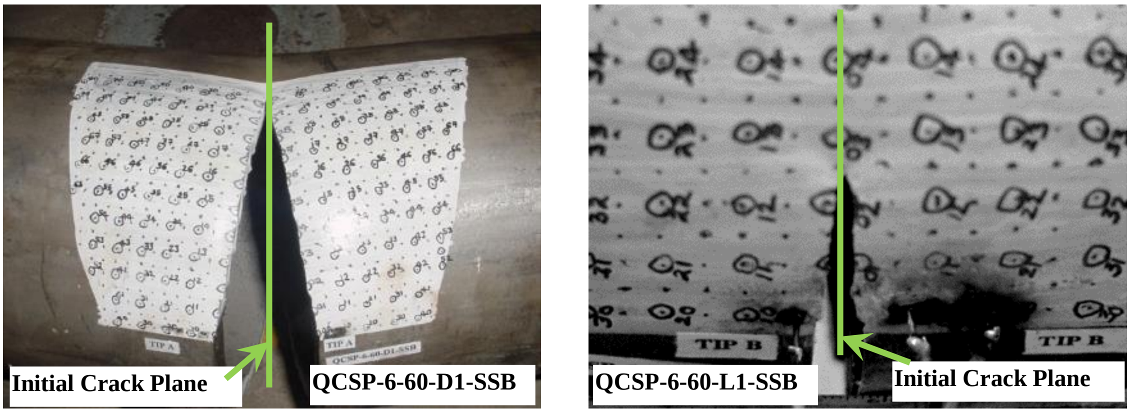

Figure 3.40: Picture showing crack growth patterns in stainless steel base (SSB) category pipe tests

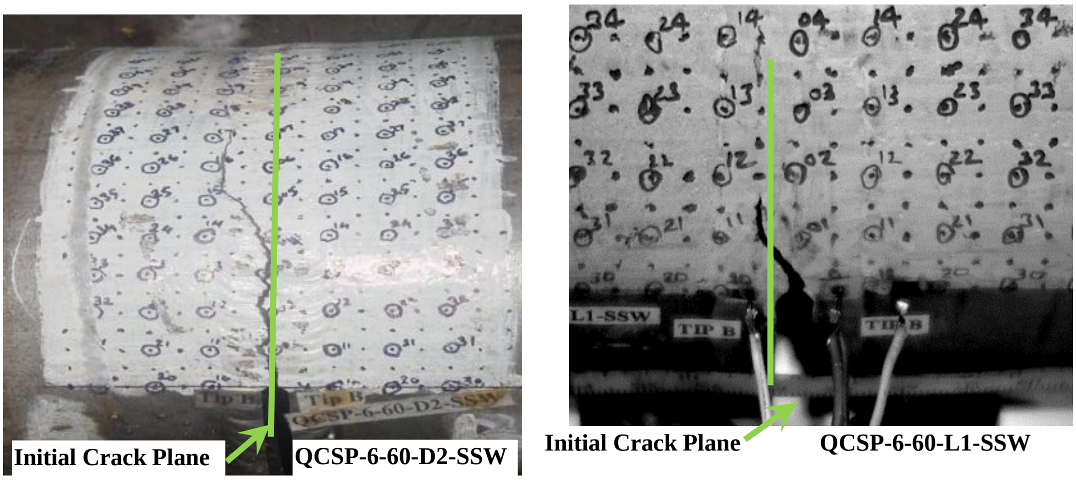

Figure 3.41: Picture showing crack growth patterns in stainless steel weld (SSW) category pipe tests

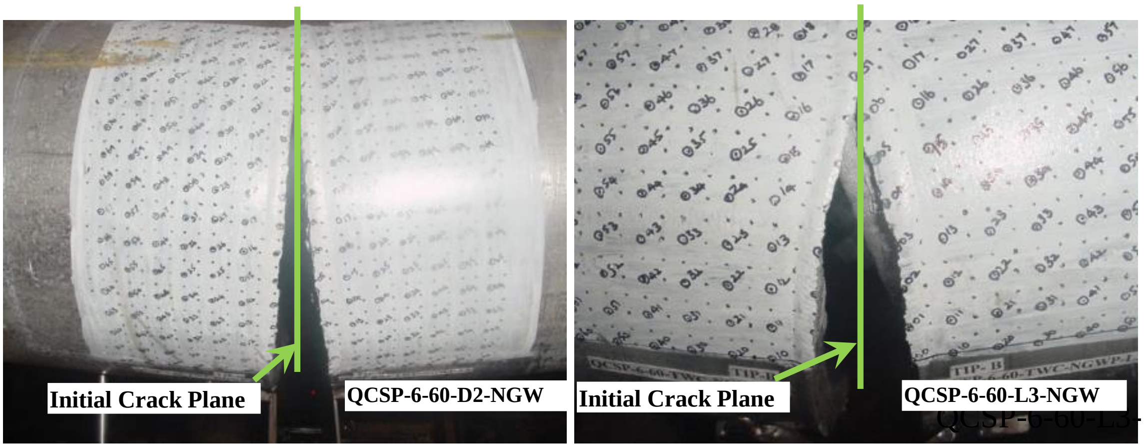

Figure 3.42: Picture showing crack growth patterns in stainless steel weld (NGW) category 6 inch pipe tests

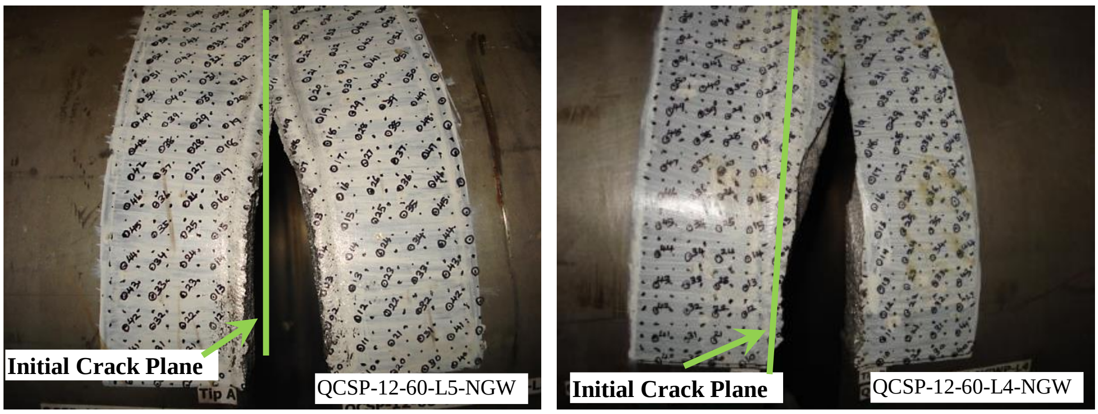

Figure 3.43: Picture showing crack growth patterns in stainless steel weld (NGW) category 12 inch pipe tests

The reason for the above observed deviations in crack growth pattern (direction / orientation) from the initial crack plane of maximum stress is the anisotropy / inhomogeneity in material toughness. The carbon steel material (material of CSB / CSW pipes) are known [114] to have toughness anisotropy due to elongated inclusions and banded microstructure. The presently used material, i.e. SA-333Gr6 carbon steel, also have ferrite-pearlite banded microstructure (see Figure 3.3) which is orientation along the pipe axis. These pipe are manufactured using hot extrusion process and hence may have elongated (along the pipe axis) non-metallic Inclusions (predominantly manganese sulphides). In case of welded pipes, the strength / toughness differences are there in the heterogeneous weld region and its transition to base material. The highest crack driving stresses were in crack plane but due to orientation dependence or spatial variation of material toughness due heterogeneity in weld specimens, the crack changes its course and goes out of initial crack plane.

3.7 Chapter conclusions

Following salient conclusion are drawn from the experimental study reported in this chapter

(a) In order to quantify the damage owing to cyclic nature, fracture tests have been conducted under both reversible cyclic and monotonically increasing loading on identical cracked pipe specimens (having same nominal size, thickness, crack size, material and having heat of material) under identical test conditions (like temperature, loading rate etc.)

(b) The test programme has covered wide range of parameters like different pipe sizes, crack size, material, material toughness, loading conditions etc. representative of those in NPPs

(i) On seamless pipes made of two different base material and three different weld configurations/combinations. These are designated as CSB, (Carbon Steel Base, SA-333 Gr.6 conforming to material specifications of PHT piping of Indian PHWRs), SSB (Stainless Steel Base, grade SA-312, type 304LN conforming to specifications of proposed material for primary loop piping of AHWR), CSW (Carbon Steel Weld, CSB Pipe joined with girth weld; root pass GTAW filler pass SMAW), SSW (Stainless Steel Weld, SSB Pipe joined with conventional girth weld; root pass GTAW filler pass SMAW) and NGW (Narrow Grove Weld, SSB Pipe joined with narrow grove girth weld; hot wire GTAW)

(ii) On wide ranges of pipe sizes and circumferential through wall crack sizes have been tested. These are 6″ NB Sch. 120, 8″ NB Sch. 100, 12″ NB Sch.100, 12″ NB Sch.120, and 16″ NB Sch.100 pipe. The circumferential through wall crack sizes (2θ) considered are 60°, 90° and 120°.

(c) The cyclic tearing tests have been conducted under both load controlled and displacement controlled loading conditions. These are two possible extremes of loading. The real piping system behaviour during an earthquake event will lie somewhere in-between and is function of piping compliance at a cracked location.

(d) Crack extension in all the pipe tests have been reliably measured using an image based technique. This image technique unlike other conventional ones (e.g., ACPD or DCPD) has provided crack-growth accurately, as it grows in-plane or out-of-plane. The image provides both component (in-plane and out of plane) of crack growth.

(e) In different categories of pipe tests namely CSB, CSW, SSW, SSB, and NGW, the crack has grown in different fashion. For CSB pipe tests, the crack grew at some helical angle from the initial circumferential crack plane (similar observation is reported in IPIRG Programme). For CSW pipe tests, the crack took turn and grew in base metal or along the fusion line. For SSB pipe tests, the crack grew straight and remained in the initial circumferential crack plane. For SSW pipe tests, the crack took turn and grew along the fusion line. In few cases it also remained in weld region. NGW pipe tests, the crack grew in the weld region or took turn and grew along the fusion line.

(f) The large number of cyclic tearing tests and corresponding monotonic fracture tests have generate a data base of the load capacities (critical loads) of a cracked pipes under cyclic (in both pure load controlled and pure displacement controlled loading conditions) as well as monotonic loading. These would be useful in quantifying the impact of cyclic load on the fracture stability and also in crack growth assessment in tearing-fatigue region under reversible cyclic loading. The critical load in a load controlled cyclic tearing test is considered for specified number of cycles to unstable failure. The maximum moment in a displacement controlled cyclic tearing test is found dependent on the applied load history parameters, e.g. displacement increment. The displacement controlled cyclic tearing tests data would help in studying the impact of cyclic loading on the fracture resistance of pipe.

(g) The comparison of monotonic and load controlled cyclic tests has shown large reduction in load carrying area in the cracked cross section owing to significant crack growth under cyclic loading conditions which, in turn, leads to unstable failure at moment much lower than the monotonic capacity of pipe.

4 Pipe fracture behaviour and J-R curves under displacement controlled cyclic loading

4.1 Introduction

The earthquake load is one of the important design-basis loading considered in designing nuclear power plants (NPPs) which induces cyclic loading in piping. The Leak-Before-Break (LBB) concept is employed in designing high energy piping of NPPs. The LBB demonstration calls for integrity assessment of a leaking (through wall cracked) pipe under design basis loading which in general are reversible cyclic loads during a design basis earthquake event. It is known (see section 2.4) that under reversible cyclic loading the crack growth occurs due to fatigue and fracture tearing (combination is termed as cyclic tearing). Further, due to fatigue and fracture synergy, the fracture resistance may reduce as compared to monotonic loading conditions. The presently used integrity assessment procedures to demonstrate LBB compliance of pipes, do not explicitly account for the cyclic tearing. Thorough understanding of the pipe fracture behaviour under both monotonic and cyclic loading conditions is essential for development suitable procedures where cyclic tearing damage can be account for in fracture assessment of pipes during integrity demonstration as required by LBB analysis. During an earthquake event, the piping system is subjected to combination of load controlled and displacement controlled conditions. The pure load controlled and pure displacement controlled conditions are two possible extremes. The real piping system behaviour will lie somewhere in-between and is function of local compliance at a cracked location and global compliance. During an earthquake event the displacement controlled cyclic loading induces due to inherent indeterminacy in piping system and due to differential movement at anchor or support locations. The earthquake time history contains finite rise time followed by strong motion and then fall time. These induced displacement controlled loads gradually builds up to maximum magnitudes during the finite rise time and strong motion period of an earthquake time history. These displacement controlled cyclic load may not cause an instability, however they may have potential to cause significantly large crack growth leading to near DEGB condition. In view of this, displacement controlled cyclic tearing tests have been conducted on pipes of various sizes/materials.

As outlined in literature survey in section 2.4.4, several investigators in past have carried out conventional small scale specimens tests to study material fracture behaviour under displacement controlled cyclic loading. In particular Singh et al [72], Roy et al [73, 74], have discussed cyclic fracture studies on CT specimens of SA333Gr6 Carbon steel and SS304LN stainless steel material respectively. These material are identical to the pipe material considered in current programme. Both have shown significant drop in cyclic J-R curve under fully reversing loads which also depends on loading history. In the present work such studies have not been perform on large scale pipe and reported in this chapter. As detailed in chapter-3, large database has been generated covering five material categories, four pipe size, three crack sizes and four loading types. The wide range of test specimens is representative of piping used in NPPs. This chapter presents details of cyclic fracture studies and evaluations under displacement controlled loading conditions carried out using the data generated by the experimental program. These studies are carried out in relation with corresponding monotonic fracture test data. The moment-rotation and crack growth behaviour of a cracked pipe subjected to certain loading condition are important response and have been examined to understand their failure behaviour under displacement controlled cyclic loading conditions. The J-R curves from both the monotonic and cyclic tearing tests have been compared to highlight the impact of cyclic loading parameters.

The work reported in this chapter is:

(i) Pipe fracture behaviour under displacement controlled cyclic loading. Here the moment-rotation (M-ϕ) and crack growth behaviour under displacement controlled cyclic loading is compared with those of identical pipe under monotonic loading

(ii) Development of a relation to quantify impact of displacement controlled cyclic loading on the maximum moment capacity of pipe

(ii) Evaluation and comparisons of monotonic and cyclic J-R curves for displacement controlled tests for all material categories

4.2 Pipe fracture behaviour under displacement controlled cyclic loading

Cyclic tearing tests under incremental displacement controlled loading (see Table 3.8) have been conducted to understand the pipe fracture behaviour. For each of the cyclic tearing test, corresponding monotonic fracture test has been conducted (see Table 3.10). The results of both cyclic as well as monotonic fracture tests have been studied. Following sections present relative comparison of the pipe fracture behaviour under the displacement controlled cyclic and monotonic loading conditions.

4.2.1 Average crack growth and Envelope M-ϕ curve

For each of the tests, crack growth is measured at both the crack tips using imaging based technique as described in section 3.5.1. The projected crack growth on the initial crack plane (i.e. Y direction component of crack growth, see Figure 3.10), have been evaluated at both the crack tips. The average value of the projected crack growth at the two tips (crack Tip-A and Tip-B) has been defined as average crack growth/extension (ACG or Δa). In both the IPIRG [46 to 61] and CRIEPI programmes [62 to 65], as well as by several other investigators [69-74], the envelope curve of the moment-rotation (M-ϕ) history (in case of specimens, it envelopes load-LLD history) is used while analysing displacement controlled cyclic tearing tests. During the pipe tests, the load and load line displacement are measured and then the moment and pipe rotations are calculated from the load and LLD data using procedure as described in section 3.5.2. The envelope curve of M-ϕ_{tot} history is obtained by joining the maximum moment points of each cycle (in crack opening direction) of loading. Figure 3.35 to Figure 3.37 plot both the M-ϕ_{tot} history as well as corresponding envelope M-ϕ_{tot} curve for different displacement controlled cyclic tearing and monotonic fracture tests.

The typical Moment (M) versus rotation (ϕ) envelope curve plots of different incremental displacement controlled cyclic tearing tests are shown in Figure 4.1(for stainless steel pipe tests) and Figure 4.2 (for carbon steel pipe tests). These figures also show M-ϕ curves from corresponding monotonic fracture test. The M-ϕ curves, in these figures, clearly show that the cyclic loading has less influence on the maximum moment (M_{max}), but there is significant loss in the energy absorbing capability of the pipes during the cyclic loading. This implies that significant reduction in the fracture resistance (evaluation based on envelope curve) under cyclic loading conditions. The M-ϕ curve drops rapidly beyond maximum moment point under cyclic loading conditions. This is due to the significant crack tearing growth, which takes place after reaching the maximum moment. These figures also show that the number of cycles, $N_{M\text{-}max}$, to reach the maximum moment.

The pipe rotation (ϕ_{tot}) versus average crack growth (Δa) and envelope M-ϕ curve have been plotted along with their corresponding monotonic fracture response for all the five material categories of pipe tests namely CSB, CSW, SSB, SSW and NGW in Figure 4.3 to Figure 4.6 respectively. Figure 4.3 plots the results for two carbon steel pipes (QPSP-8-60-D1-CSB and QPSP-8-60-D2-CSB) along with corresponding monotonic fracture test (SP-8-60-M-CSB). Figure 4.4, Figure 4.5(a), Figure 4.5(b), Figure 4.6 plot similar results for carbon steel pipes with a girth weld (CSW), stainless steel pipes with base metal (SSB), stainless steel pipe with a conventional grove girth weld (SSW) and stainless steel with a narrow grove girth weld (NGW)–respectively. The crack initiation points in all the monotonic fracture tests have also been shown in these figures.

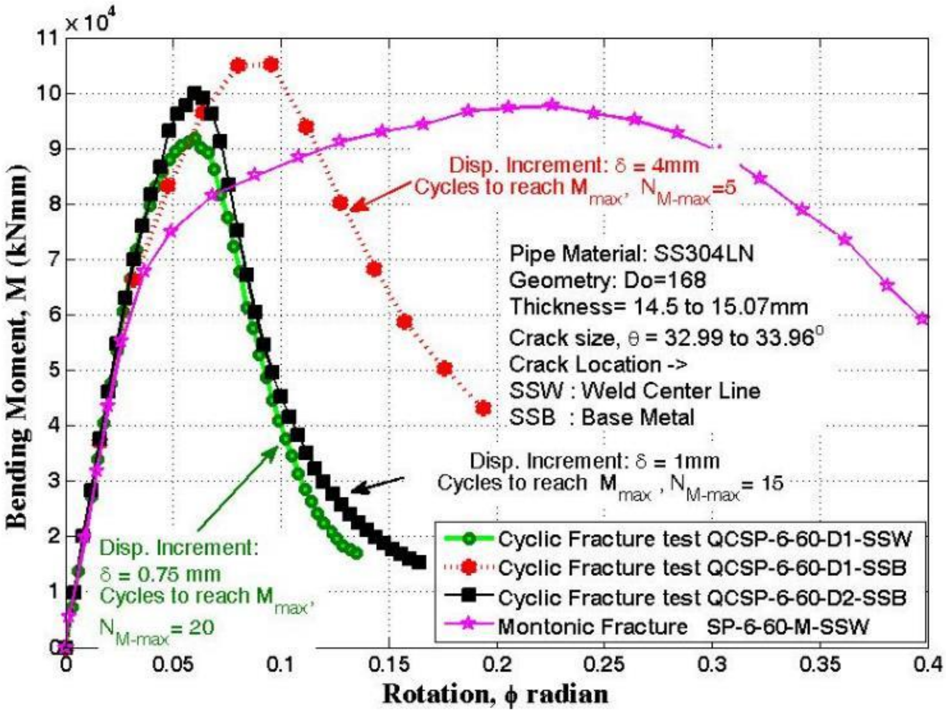

Figure 4.1: Moment Vs. Total Rotation envelope curves for Stainless Steel pipe monotonic fracture test and cyclic tearing tests with different displacement increments and different crack location

These figures show that on application of incremental cyclic rotation, the crack size and peak reaction moment (in a loading cycle) increases with number of cycles of loading. The cyclic peak reaction moment reaches a maximum value (M_{max}) in few cycles, say, $N_{M\text{-}max}$, and then it starts decreasing. This trend of envelope M-ϕ curve is similar to that observed in corresponding monotonic fracture tests. On the other hand, these figures show that the crack growth in each cycle increases gradually and becomes nearly constant (steady state) value beyond the maximum moment point.

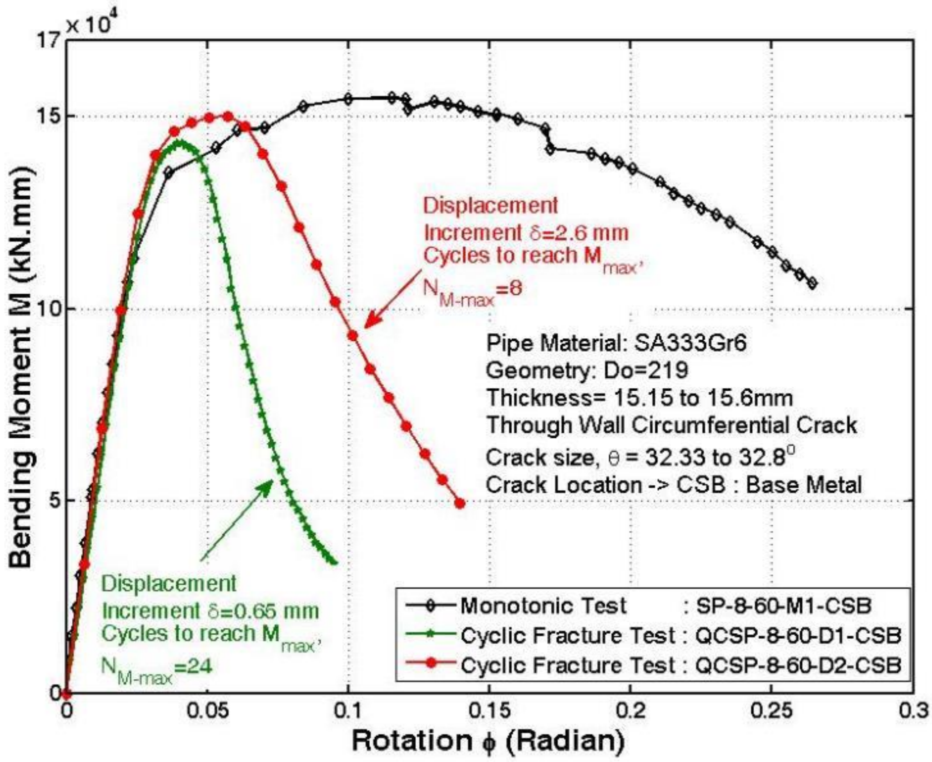

Figure 4.2: Moment Vs. Total Rotation envelope curves for Carbon Steel pipe monotonic fracture test and cyclic tearing tests with different displacement increments and different crack location

4.2.2 Pipe fracture behaviour: Incremental cyclic versus monotonic loading

The tests have been carried out under incremental cyclic as well as monotonic fracture tests on identical cracked pipe specimens under identical test conditions (like temperature, loading rate etc.). Thus pipes subjected to these two types of loading (monotonic and incremental displacement cyclic) were having same nominal size, thickness, crack size, and have same heat material. The loading scheme and test details are given in section 3.4 and 3.6. The load ratio in all the incremental displacement control cyclic tests was -1. On both type of pipe tests, the relational and comparative studies have been performed to understand and quantify the pipe fracture behaviour under incremental displacement control loading in relation to its behaviour under monotonic loading condition. Following parameters have been obtained for all the incremental displacement controlled loading tests.

i) M_{max} : Maximum moment observed in the incremental displacement controlled test and has been obtained from its envelop M-ϕ curve.

ii) $\phi_{M\text{-}max}$: Total pipe rotation corresponding to maximum moment M_{max} and has been obtained from envelop M-ϕ curve of incremental displacement controlled tests.

iii) $\Delta a_{M\text{-}max}$ = Crack extension (mm) corresponding to the maximum moment M_{max} point

iv) χ = The crack growth rate (mm/radian), $da/d\phi$, obtained beyond the $\phi_{M\text{-}max}$ point where the slope of Δa vs ϕ curve becomes nearly constant (see Figure 4.3 to Figure 4.6).

v) $N_{M\text{-}max}$: Number of cycles of incremental displacement loading to reach the maximum moment M_{max} point. It has been obtained from Load-LLD history plot (see Figure 3.19) of incremental displacement controlled tests

vi) δ_m : Displacement Increment, δ, given in term of % of the LLD at crack initiation obtained in corresponding monotonic fracture test on identical pipe.

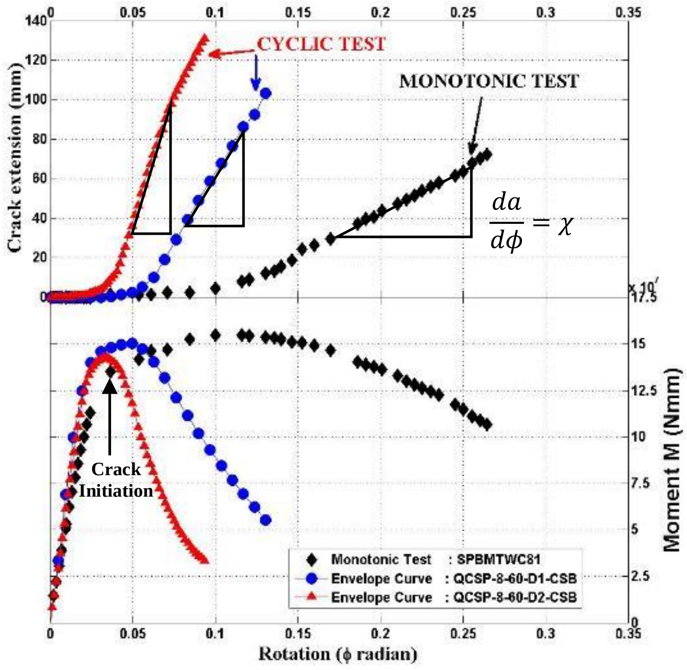

Figure 4.3: Average Crack growth and Envelope (M-ϕ) curve for incremental displacement controlled cyclic and corresponding monotonic fracture tests on CSB pipe

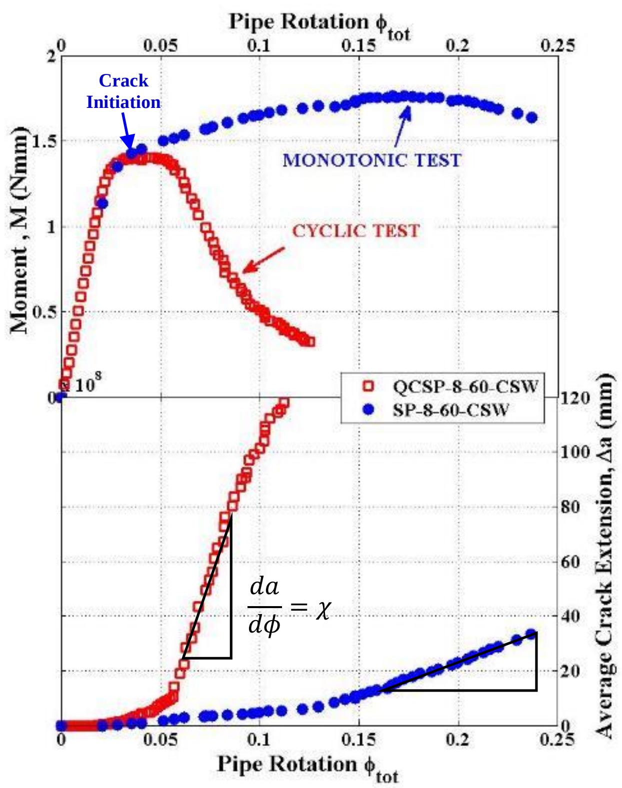

Figure 4.4: Average Crack growth and Envelope (M-ϕ) curve for incremental displacement controlled cyclic and corresponding monotonic fracture tests on CSW pipe

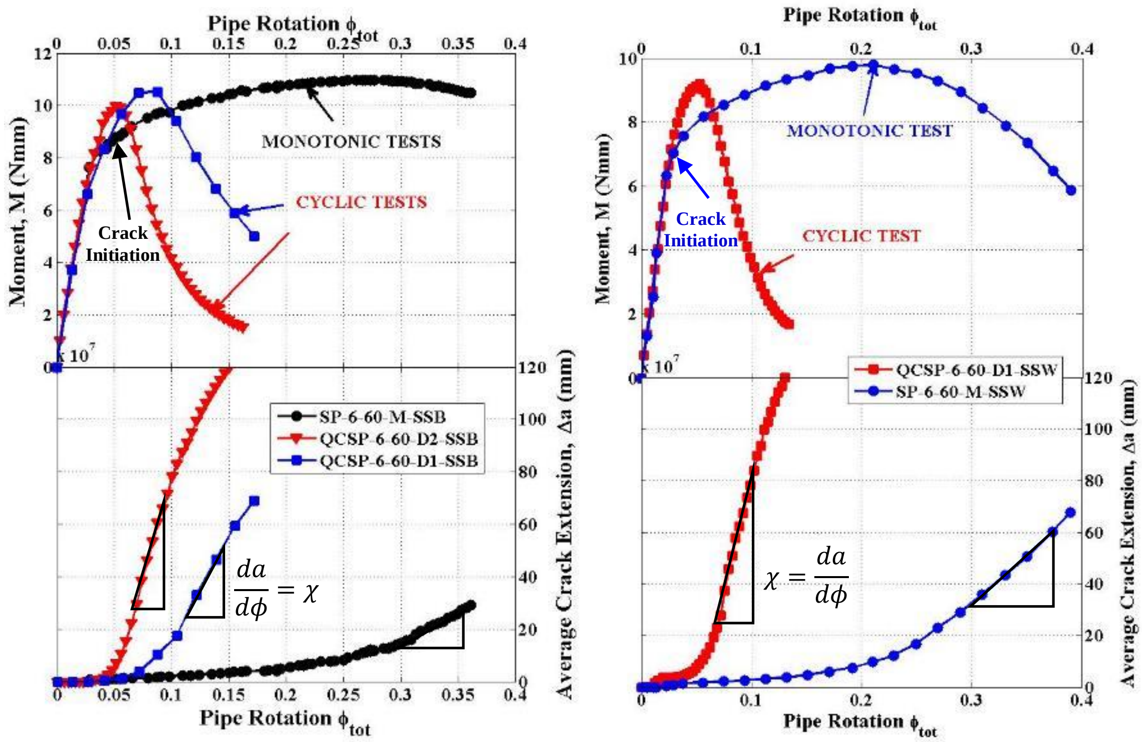

Figure 4.5: Average crack growth and envelope M-ϕ curves for incremental displacement controlled cyclic and corresponding monotonic fracture tests on SSB and SSW pipes

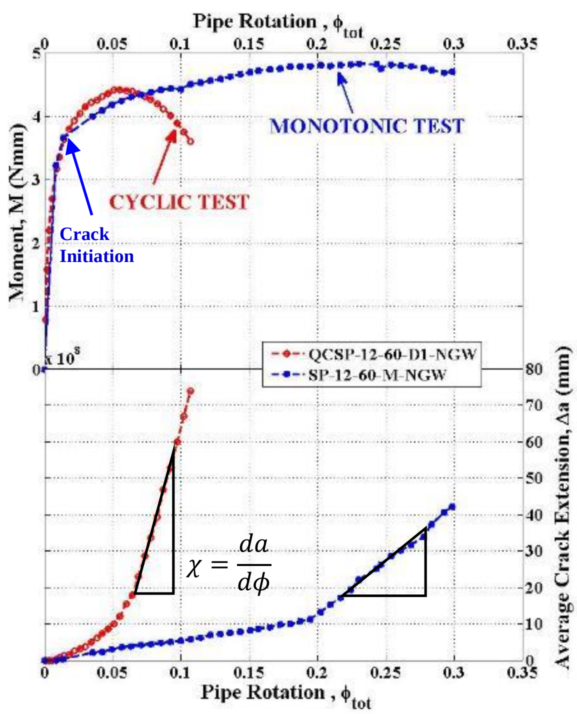

Figure 4.6: Average Crack growth and Envelope (M-ϕ) curve for incremental displacement controlled cyclic and corresponding monotonic fracture tests on NGW pipe

Table 4.1: Summary of results obtained from comparison of incremental displacement controlled test with corresponding monotonic fracture test

Material category →		**CSB**			**CSW**		**SSB**			**SSW**		**NGW**	
Test Name →		**QCSP-8-60-D1-CSB**	**QCSP-8-60-D2-CSB**	**SP-8-60-M-CSB**	**QCSP-8-60-D1-CSW**	**QCSP-8-60-D1-CSW**	**SP-6-60-M-SSB**	**QCSP-6-60-D2-SSB**	**SP-6-60-M-SSB**	**QCSP-6-60-D1-SSW**	**SP-6-60-M-SSW**	**QCSP-12-60-D1-NGW**	**SP-12-60-M-NGW**
Short name		**CSB-8D1**	**CSB-8D2**	**Monotonic**	**CSW-8D1**	**Monotonic**	**SSB-6D1**	**SSB-6D2**	**Monotonic**	**SSW-6D1**	**Monotonic**	**NGW-12D1**	**Monotonic**
Outer Diameter, Do (mm)		219	219	219	219	219	168	168	170	168	168	324	324
Thickness, t (mm)		15.6	15.2	15.2	16.6	16.2	14.8	14.5	15	15	14.8	22.3	22.2
Half crack angle, θ (deg.)		32.6	32.3	32.8	33.3	32	33.2	33	33	33.6	33.4	30.9	31.1
Displacement increment, δ	**δ (mm)**	2.6	0.65	*	0.65	*	4	1	*	0.75	*	3	*
	δ_m (%)	8.75	2.19	*	2.21	*	19.4	4.84	*	6.67	*	14.6	*
Maximum Moment M_{max}	**M_{max} (kNm)**	150	143	155	140	176	105	99.8	108	91.7	97.8	444	483
	$\%M_{max}$ (%)	96.5	92.1	100	79.7	100	97.3	92.3	100	93.8	100	92	100
Nos. of Cycle at M_{max} , $N_{M\text{-}max}$		8	24	*	30	*	5	14	*	20	*	16	*
Rotation , ϕ at M_{max}	**$\phi_{M\text{-}max}$ radians**	0.06	0.04	0.12	0.04	0.17	0.09	0.05	0.31	0.05	0.22	0.07	0.24
	$\%\phi_{M\text{-}max}$ (%)	49.3	34.2	100	24.3	100	28.5	16.9	100	23.7	100	27.6	100
Crack growth Δa at M_{max}	**$\Delta a_{M\text{-}max}$, mm**	2.1	5.1	6.9	3.9	14.4	6.9	10.2	11.3	8.9	9.75	14.9	22.1
	$\%\Delta a_{M\text{-}max}$ (%)	30.4	73.9	100	27.1	100	61.1	90.3	100	91.3	100	67.5	100
Δa at $\phi = \phi_{M-max}^{monotonic\ test}$		70	>130	6.9	>130	14.4	>70	>120	11.3	>120	9.75	>80	22.1
χ: Crack growth rate (da/dϕ) obtained beyond $\phi_{M\text{-}max}$	**χ mm/radian**	1.63	3.35	0.51	2.9	0.38	1.3	3.55	0.43	4.0	0.91	3.7	0.81
	$\frac{\chi^{Cyclic}}{\chi^{Monotonic}}$	3.18	6.52	1	7.73	1	3.06	8.35	1	4.41	1	4.55	1

The M_{max}, $\phi_{M\text{-}max}$, $\Delta a_{M\text{-}max}$ and χ are also evaluated for the corresponding monotonic fracture tests. All these parameters of both cyclic and monotonic fracture are listed in Table 4.1. The table also expressed the M_{max}, $\phi_{M\text{-}max}$, $\Delta a_{M\text{-}max}$ and χ parameters obtained in the incremental cyclic displacement tests as the % value of corresponding parameter obtained in the monotonic fracture tests conducted on identical pipe (see equation below). When any of the parameter is preceded with the % sign, it is giving the % value obtained with respect to corresponding in the monotonic fracture test.

$$\%\boldsymbol{M_{max}} = \frac{\boldsymbol{M_{max}^{Cyclic}}}{\boldsymbol{M_{max}^{Monotonic}}} * \mathbf{100} \quad ; \quad \%\boldsymbol{\phi_{M-max}} = \frac{\boldsymbol{\phi_{M-max}^{Cyclic}}}{\boldsymbol{\phi_{M-max}^{Monotonic}}} * \mathbf{100} \quad \boldsymbol{and} \quad \%\boldsymbol{\Delta a_{M-max}} = \frac{\boldsymbol{\Delta a_{M-max}^{Cyclic}}}{\boldsymbol{\Delta a_{M-max}^{Monotonic}}} * \mathbf{100}$$

Following observations have been made from the relational study of the incremental displacement controlled cyclic tearing test along with the corresponding monotonic fracture tests:

(i) Pipe Capacity in term of maximum moment (M_{max}): A small to moderate (2 to 20%) decrease in the maximum moment (M_{max} that is the capacity of pipe) has been observed in all the incremental displacement control cyclic tearing tests. For CSB material pipe tests the maximum moment M_{max} decrease w.r.t. corresponding monotonic fracture test was about 3.5% and 7.5 % for CSB-8D1 and CSB-8D2 test respectively. The δ_m (that is the δ displacement increment given as % of LLD at crack initiation in corresponding monotonic test) applied in CSB-8D1 and CSB-8D2 tests are 8.75% (or 2.65 mm) and 2.19% (or 0.65 mm) respectively. The number of cycles, $N_{M\text{-}max}$, the pipe has taken to reach the maximum moment point is 8 (for CSB-8D1) and 24 (for CSB-8D2). Likewise for SSB material pipe tests, the decrease in the maximum moment M_{max} was about 2.7% and 7.7% for SSB-6D1 and SSB-6D2 test respectively. The δ_m applied in SSB-6D1 and SSB-6D2 tests are 19.4% (or 4 mm) and 4.84 % (or 1 mm) respectively. The number of cycles, N_{M-max}, the pipe has taken to reach the maximum moment point is 5 (for SSB-6D1) and 14 (for SSB-6D2).

Both the CSB and SSB results show that the smaller displacement increment (δ) resulted in larger drop in the moment capacity M_{max} of pipe. However it takes more cycles, N_{M-max}, to reach the M_{max} point when displacement increment is smaller (see Figure 4.7).

(ii) Pipe Capacity in term of maximum rotation (ϕ_{M-max}): Significant decrease (50 to 83%) in the pipe rotation ϕ_{M-max} (corresponding to maximum moment M_{max}) is observed in all the incremental displacement control cyclic tearing tests. The rotation ϕ_{M-max} of a crack pipe, without undergoing significant tearing, is the ability to go through (absorb) the displacement/rotation loading which gradually/incrementally builds up during cyclic loading as happens in case of an earthquake event. The ϕ_{M-max} along with M_{max} is important indicator which tells about energy absorbing ability of a cracked pipe without undergoing significant tearing. In displacement controlled loading, tearing takes place after the maximum loading point as can be seen in Figure 4.3 to Figure 4.6. For CSB material pipe tests the decrease in ϕ_{M-max} w.r.t. that in corresponding monotonic fracture test is about 50.7 % and 65.8 % for CSB-8D1 and CSB-8D2 test respectively. The δ_m applied in CSB-8D1 and CSB-8D2 tests are 8.75% (or 2.65 mm) and 2.19% (or 0.65 mm) respectively. The number of cycles, N_{M-max}, the pipe has taken to reach the maximum moment point is 8 (for CSB-8D1) and 24 (for CSB-8D2). Likewise for SSB material pipe tests, the decrease was about 71.5% and 81.3% for SSB-6D1 and SSB-6D2 test respectively. The δ_m applied in SSB-6D1 and SSB-6D2 tests are 19.4% (or 4 mm) and 4.84 % (or 1 mm) respectively.

The number of cycles, $N_{M\text{-}max}$, the pipe has taken to reach the maximum moment point is 5 (for SSB-6D1) and 14 (for SSB-6D2). In all the pipe tests, the decrease in the pipe rotation absorbing capacity ($\phi_{M\text{-}max}$) is found more than 50%. In both the CSB and SSB, the decrease in $\phi_{M\text{-}max}$ is larger when the displacement increment is smaller.

A bar chart shown in Figure 4.7 plots the decrease of both the maximum moment (M_{max}), corresponding rotation $\phi_{M\text{-}max}$ in cyclic loading tests w.r.t. corresponding monotonic test. This figure also plots the applied loading cycles $N_{M\text{-}max}$ and displacement increment δ_m. High decrease in $\phi_{M\text{-}max}$ along with moderate decrease in M_{max} under cyclic displacement load implies very high loss in the energy absorbing ability of pipe.

These figures, clearly show that the smaller δ requires more number of cycles, $N_{M\text{-}max}$, to reach M_{max} which means more damage owing to cyclic loading that is due to fatigue crack growth, crack tip re-sharpening and void flattening in fracture process zone under reverse loading. This in turn leads to reduction in M_{max} when compared to that from corresponding monotonic fracture test. Due to this reason, in monotonic fracture tests, the number of unloading are generally kept small and the load ratio generally kept positive to ensure there is insignificant load drop and crack growth owing to cyclic damages.

It is observed that smaller cyclic displacement increment (δ) results in larger loss fracture resistance, and larger drop in the maximum moment. These observations are in agreement with that reported in IPIRG program and by many other investigators Marchall and Wilkowski, [69], Chang et al [70, 71] and Singh et al [72].

(iii) Crack growth ($\Delta a_{M\text{-}max}$) up to M_{max}: In all the incremental displacement cyclic tests, a small crack growth, $\Delta a_{M\text{-}max}$, between 2 mm to 15 mm has been observed at the maximum moment M_{max} point (i.e. the crack extension during the rising portion of the envelope M-ϕ curve). This is very small in comparison to the crack tearing which has taken place post the maximum loading point (i.e. the crack extension during the drooping portion of envelope M-ϕ curve). In all the incremental cyclic tearing tests, the $\Delta a_{M\text{-}max}$ is found to be lower than the corresponding $\Delta a_{M\text{-}max}$ measured during the monotonic fracture test on identical pipe. The $\Delta a_{M\text{-}max}$ observed in cyclic tests and their % value with respect to corresponding monotonic tests has been plotted in Figure 4.8. The comparison of the two tests in each CSB and SSB category has shown that % $\Delta a_{M\text{-}max}$ is higher for smaller δ that, in turn, implies higher $N_{M\text{-}max}$.

The above observations imply that in case of cyclic displacement loading tests, the presence of fatigue crack growth is not the sole cause of the reduction of the M_{max} and $\phi_{M\text{-}max}$ of a pipe. Under reversible loading, reduction in apparent fracture toughness of material due to compression of fracture process zone causing void flattening and crack tip re-sharpening during reverse loading is also responsible. This interpretation is further reinforced by the fact that large drop in M_{max} and $\phi_{M\text{-}max}$ are observed for small δ / more cycle $N_{M\text{-}max}$.

(iv) Crack growth behaviour beyond M_{max}: In all the incremental cyclic and monotonic tests, the crack growth rates, that is da/dϕ and da/dM in the drooping portion of M-ϕ (that is after the maximum moment point) becomes nearly constant. A parameter, χ, is defined as the crack growth rate (mm/radian), da/dϕ , obtained beyond the $\phi_{M\text{-}max}$ point where the slope of Δa vs ϕ curve becomes nearly constant (see Figure 4.3 to Figure 4.6). The χ for all monotonic and incremental cyclic tests is given in Table 4.1. Figure 4.9 (a) a bar chart indicating the χ for different tests along with the δ_m and $N_{M\text{-}max}$. In both the CSB and SSB tests, χ increases when the displacement increment (δ or δ_m) is reduced in a given test. Figure 4.9 (b) plots the ratio of χ obtained in a cyclic tearing tests with that obtained in monotonic fracture test on identical pipe. This figure clearly shows that the $da/d\phi$ increased 3 to 8 times when the displacement loading is applied in cyclic incremental manner while keeping the load ratio as -1. This confirms presence of significant damage taking place in the crack growth process owing to reversible cyclic nature of loading.

On the other hand the dM/da (kNm/mm that is the load drop associated with unit crack growth) in the drooping portion of M-ϕ envelope curve is also nearly constant (see Figure 4.10). The Figure 4.10 also shows that for a given pipe size and material (say 8CSB or 6SSB) the dM/da is nearly same for both the incremental cyclic tearing tests and the corresponding monotonic fracture test. Similar observation is there in all other incremental cyclic and corresponding monotonic fracture tests. This implies that the dM/da in drooping portion is nearly independent of the displacement loading history parameters. In the drooping portion of M-ϕ curve, the moment of the pipe is function of the remaining healthy ligament, which is load bearing cross section. The drop in moment is directly proportion of reduction in cross section owing to crack growth which could be due to monotonic tonic or cyclic loading. It is further noted that the dM/da in drooping portion is nearly same for the base and welds material. This is observed in both carbon steel and stainless steel tests (see Figure 4.10).

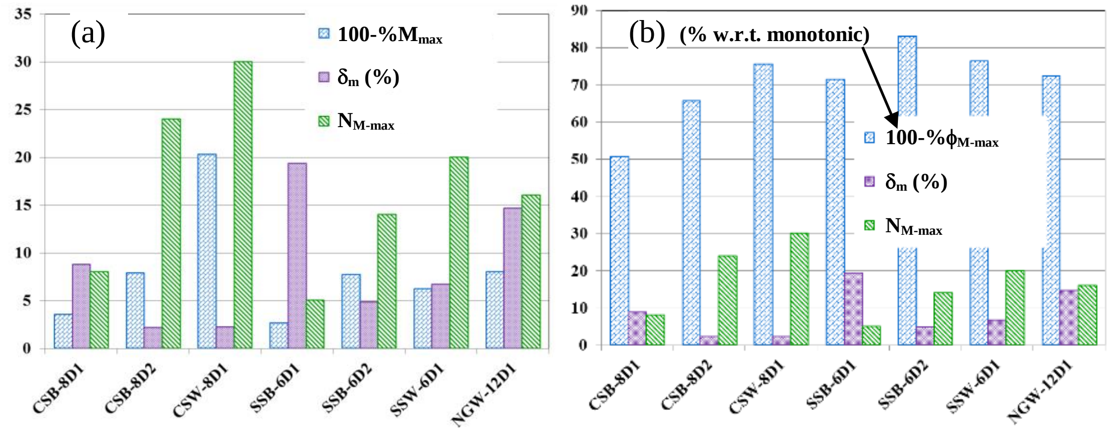

Figure 4.7: % Decrease of maximum moment, M_{max} and corresponding rotation $\phi_{M\text{-}max}$ in cyclic loading tests

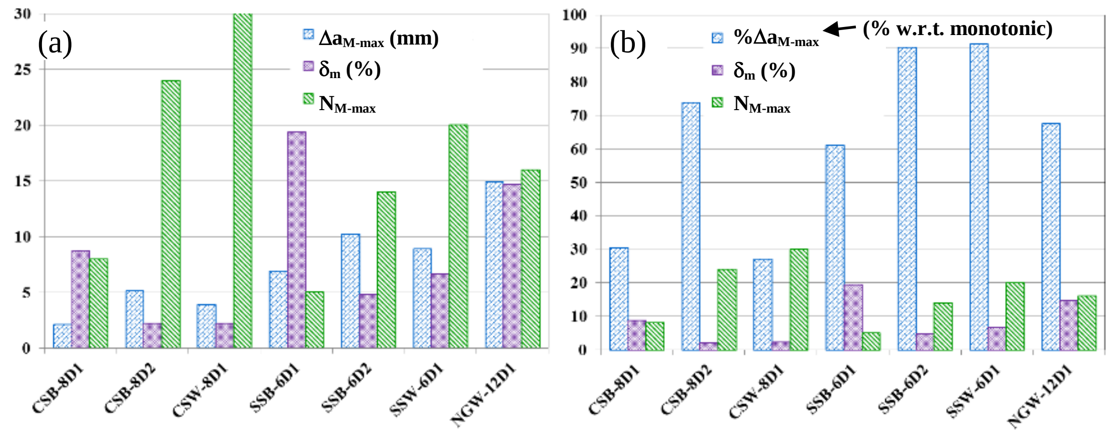

Figure 4.8: Crack growth ($\Delta a_{M\text{-}max}$) up to maximum moment M_{max} point in cyclic loading tests

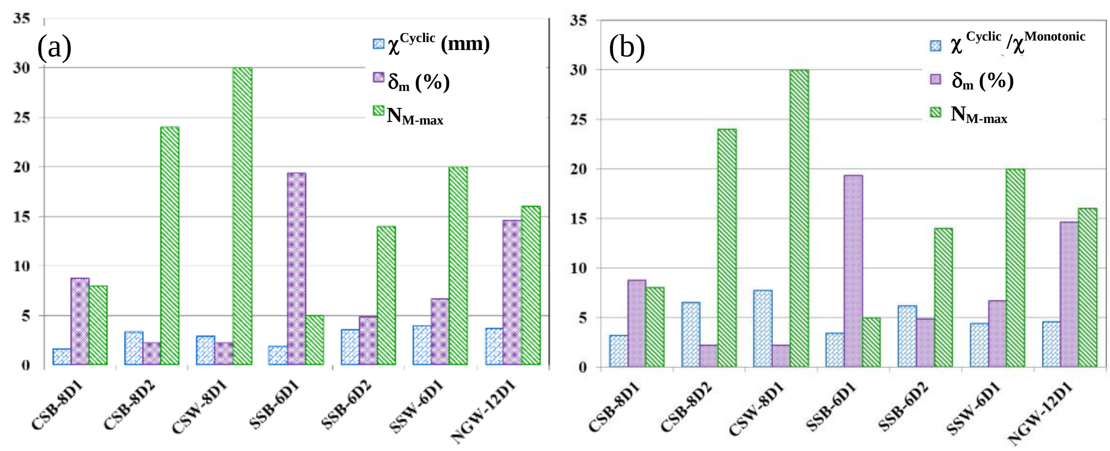

Figure 4.9: Comparison of χ, the crack extension rate ($da/d\phi$) evaluated past the M_{max} point when it becomes nearly constant

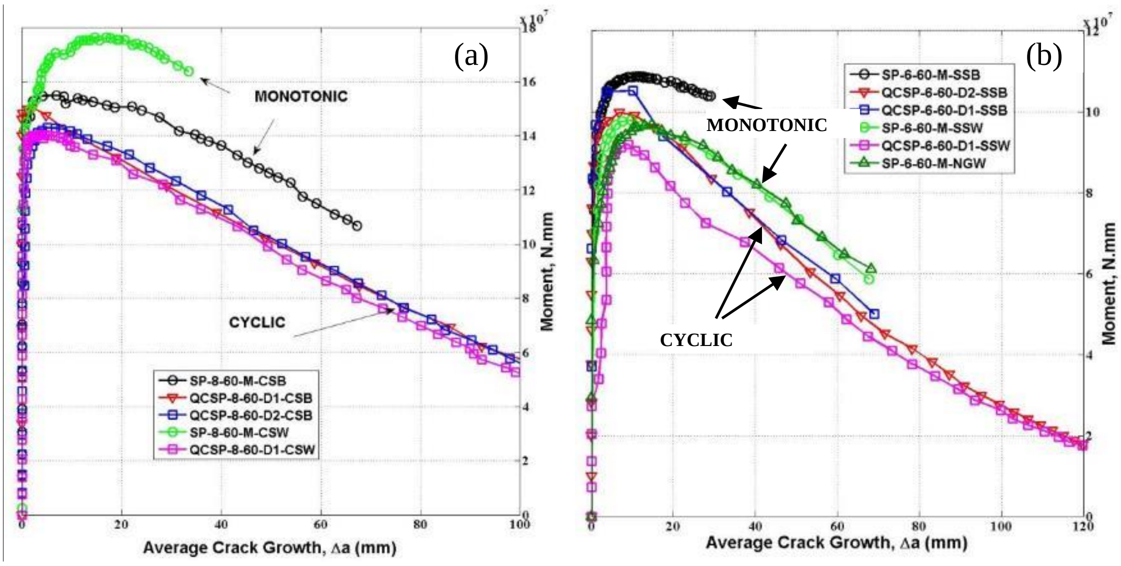

Figure 4.10: Moment vs. average crack extension plots for all incremental cyclic and monotonic test on both carbon and stainless steel base and weld material

(v) **Extent of tearing up to** $\phi_{M-max}^{monotonic\ test}$: The displacement controlled cyclic tearing tests are conducted by step wise or incrementally increasing the displacement / rotation such that the load ratio R = -1. The crack tearing observed in all these incremental displacement controlled cyclic tearing tests is several times higher than that obtained in a corresponding monotonic fracture tests when the imposed rotation in both the tests are equal to the monotonic capacity (ϕ = $\phi_{M-max}^{monotonic\ test}$, i.e. rotation at maximum moment point in corresponding monotonic test). In many of the incremental displacement tests the extent of tearing reached near DEGB at applied rotations lower than the $\phi_{M-max}^{monotonic\ test}$. This can be clearly seen by observing Figure 4.3 through Figure 4.6 and in Table 4.1. This is due to:

(i) Under incremental displacement cyclic loading tests, in addition to the fatigue crack growth the crack tip re-sharpening and the compression of fracture process zone causing void flattening also takes place. This is also reported in IPIRG programme. The Sharp crack and flattened voids enable crack extension under smaller applied rotation when compared to that required to cause similar crack extension in case of blunt crack and spherical voids present (under monotonic loading conditions).

(ii) The tests showed that smaller δ requires more number of cycles (of incremental displacement application), $N_{M\text{-}max}$, to reach the maximum moment point M_{max}. More cycles in turn means more damage owing to cyclic loading that is due to fatigue crack growth, crack tip re-sharpening and void flattening in fracture process zone under reverse loading.

4.2.3 Maximum Moment (M_{max}) Capacity of a cracked pipe under cycle loading

In previous sections (4.2.1 and 4.2.2), different displacement controlled cyclic have been investigated in relation with corresponding monotonic fracture tests and the effects of cyclic displacement loading on the maximum moment, corresponding rotations and crack tearing behaviour (in both rising and drooping portion of envelope curve) of a cracked pipe have been evaluated. Extent of crack growth is found very large when a cracked pipe subjected to gradually ratcheted rotation having value equal to $\phi_{M-max}^{monotonic\ test}$. However, these have shown that the crack growth up to the M_{max} in cyclic tearing tests is found equal or lesser than that (at $\mathrm{M}_{\max}^{\text{Monotonic Test}}$) in corresponding monotonic fracture test (see Figure 4.11). The number of cycles ($N_{M\text{-}max}$) to reach M_{max} in a cyclic test is found small when large displacement increment (δ) loading applied. For tests with smaller cyclic displacement increment,δ, (or larger $N_{M\text{-}max}$), large drop in maximum moment M_{max} (with respect to corresponding monotonic pipe fracture capacity, $\mathrm{M}_{\max}^{\text{Monotonic Test}}$) during cyclic loading is observed. Figure 4.12 plots the moment ratio ($M_{max}^{Cyclic\ test}/\ M_{max}^{Monotonic\ Test}$) and $N_{M\text{-}max}$ for all the tests conducted in present program. In this figure one of the test data plotted (on 6″ size STS410 steel pipe) is taken from NUREG-6438 report, [50].

This figure clearly shows that the load drop in displacement controlled cyclic tearing test can be correlated with number of cycles to M_{max} ($N_{M\text{-}max}$). A correlation between the moment ratio ($M_{max}^{Cyclic\ test}/\ M_{max}^{Monotonic\ Test}$) and $N_{M\text{-}max}$, has been developed. Figure 4.12 also shows the best-fit curve of data points is nearly linear (R^2 Value = 0.97). The equation of best fit curve is given below:

$$N_{M-max} = 200 * \left(1 - M_{max}^{Cyclic\ test}/\ M_{max}^{Monotonic\ Test}\right) \tag{4.1}$$

The above equation relates the number of cycles which causes limited crack growth, with the maximum moments induced under displacement controlled cyclic tearing tests. The above relation is fitted based on tests covering large variation of parameters. The developed equation can be used:

(a) To screen or to show that a cyclic displacement loading event may cause large tearing crack growth only if it's number of cycles, is significantly more than the $N_{M\text{-}max}$ evaluated from Eqn. 4.1. While evaluating $N_{M\text{-}max}$, the $M_{max}^{Disp.\ Cyclic\ test}$ is taken as maximum moment magnitude associated with the cyclic displacement loading event and the $M_{max}^{Monotonic\ Test}$ is taken equal to the monotonic capacity load of corresponding pipe.

(b) Using the incremental displacement controlled cyclic tearing tests results, The Eqn. (1) can be used to approximately evaluate the maximum moment of an identical pipe having same size crack under monotonic loading conditions.

4.3 J-R curves under incremental cyclic and monotonic loading

The material resistance to crack tearing is characterised by its J-Δa curve (generally known as J-R curve). The J-R curve of a material is obtained by carrying out fracture experiment on components or specimens of different geometry. The J-R curve evaluation procedures on standard specimens are well documented ASTM-E 1820-09 [44]. Usages of the J-R curve in ductile fracture (elastic plastic fracture mechanics) assessment of cracked structures subjected to monotonic loading are well established [32-42].

In light of this, to accesses the material's fracture resistance behaviour under cyclic loading, the concept of J-R was extended and applied under cyclic loading condition by many investigators [75 to 85]. In addition to these, the J-R curve concept is employed extensively in assessment of fracture tests conducted under both the IPIRG [46 to 61] and the CRIEPI programmes [62 to 65]. These have used the envelope curve obtained from the moment-rotation (M-ϕ) history or load-LLD history to analyse the fracture test done under cyclic loading. The J-R curve calculation methodology is identical to that used in monotonic fracture test evaluation except that in case of cyclic tests, the envelop curves as discussed above are used. The envelope curve of M-ϕ or load-LLD history is obtained by joining the maximum moment/load points of each cycle (in crack opening direction) of loading.

The monotonic pipe fracture tests carried out in this programme are analysed to evaluate the J-R curve, using the 'η and γ factor' proposed by Zahoor et. al. [32]. The cyclic J-R curves have been evaluated using the M-ϕ envelope curve of incremental displacement controlled cyclic tearing tests. The monotonic and cyclic J-R curves have been evaluated for all the five different material cases. The envelop M-ϕ_{pl} curves and M-Δa curves of all the monotonic and incremental displacement cyclic tests carried out on carbon steel and stainless materials and used in J-R curve evaluation are plotted in Figure 4.13 and Figure 4.14 respectively. The ϕ_{pl} is the plastic crack rotation evaluated using equations (sec. 3.5.2).

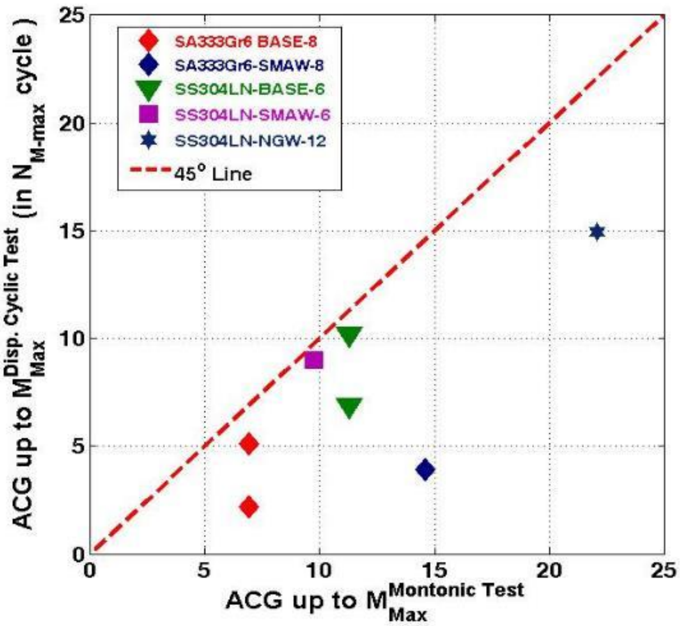

Figure 4.11: Average Crack Growth (ACG) up to M_{max} from incremental displacement controlled cyclic and corresponding monotonic fracture test

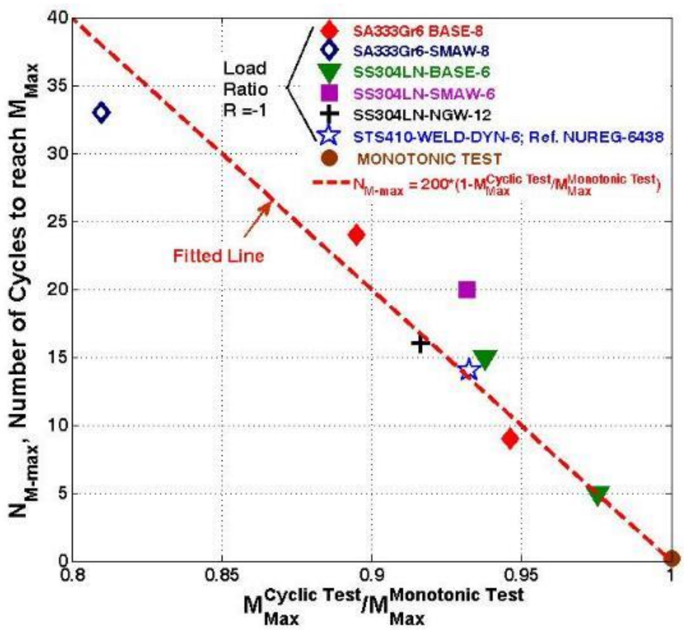

Figure 4.12:Maximum moment ratio ($M_{max}^{\text{Cyclic test}}$/ $M_{max}^{\text{Monotonic Test}}$) plotted against number of cycles, $N_{M\text{-}max}$, to reach $M_{max}^{\text{Cyclic test}}$

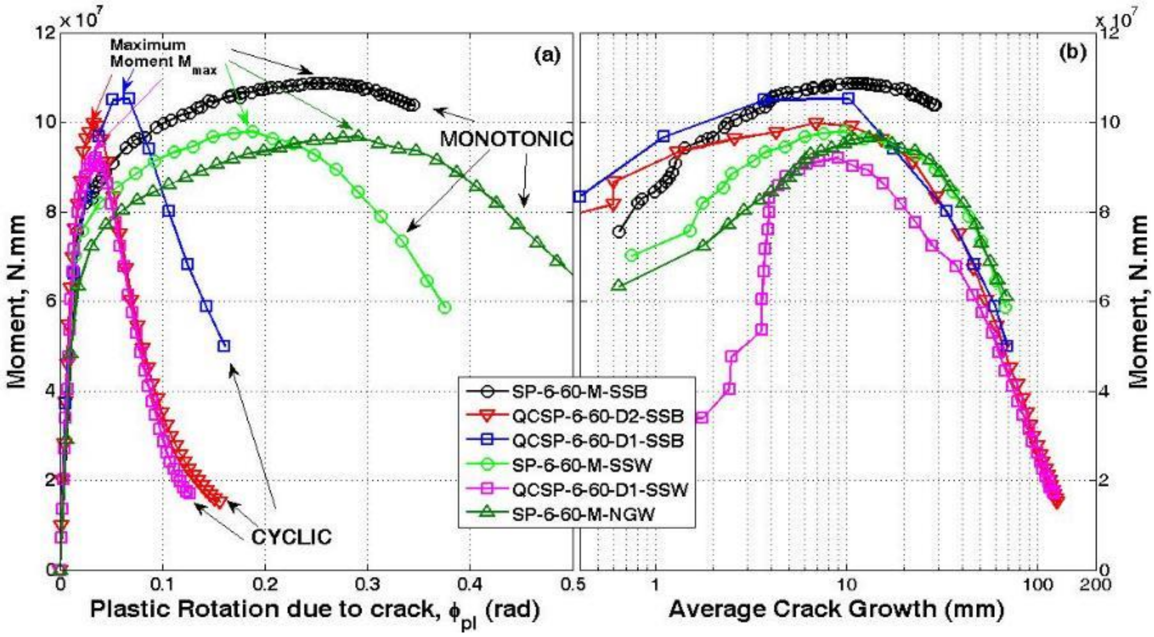

Figure 4.13: (a) Moment versus plastic crack rotation and (b) Moment versus average crack growth for different displacement controlled tests on 6″size stainless steel straight pipes

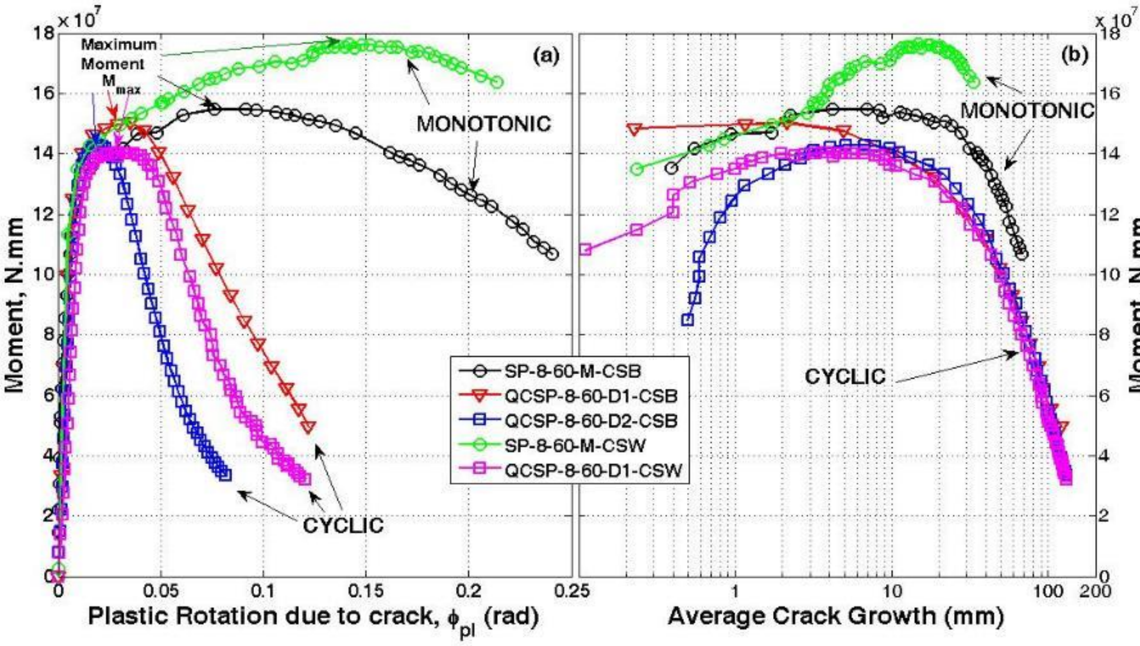

Figure 4.14: (a) Moment versus plastic crack rotation and (b) Moment versus average crack growth for different displacement controlled tests on 8″size carbon steel straight

4.3.1 Monotonic J-R Curves

The monotonic pipe fracture tests were analysed to evaluate the J-R curve under monotonic loading conditions. The current analytical procedures of ductile fracture load assessment are based on J-Integral, the crack driving force due to applied load and J_R, the material's fracture resistance to crack tearing from J-R curve. The J-R curve is generally evaluated using fracture tests on small size specimens as per the ASTM standards. However it may also be evaluated from the component fracture test in order to rule out any geometric constraint influence on the study. In the present programme, the monotonic J-R curve were evaluated from the monotonic pipe fracture tests using 'η and γ factor' proposed by Zahoor et. al.[32]. The J integral is evaluated using following equations:

$$J = J_{el} + J_{pl} \tag{4.2}$$

Here the subscript J_{el} and J_{pl} are elastic and plastic components of the J-integral. The elastic part of the J integral is given by following equation

$$J_{el} = f_b^2\left(\frac{\theta}{\pi}\right)\left(\frac{M^2}{ER_m^3 t^2}\right) \tag{4.3}$$

Here the function f_b is geometry function and available in Zahoor et. al.[32]. The Plastic part of the J-integral

$$J_{i,pl} = J_{i-1,pl} + \int_{\phi_{i-1,pl}}^{\phi_{i,pl}} \eta(\theta) M d\phi_{pl} + \int_{\theta_{i-1}}^{\theta_i} \gamma(\theta) J_{pl} d\theta \tag{4.4}$$

Where, 'θ_o' is initial half crack angle , 'θ'is current half crack angle and ϕ_{pl} is plastic load point rotation. 'i' is a data point on the M-ϕ_{pl} curve. The M and ϕ_{pl} is evaluated from the load and LLD data measured during experiment using equations/method given in section

3.5.2. The Eq. (4.4) incrementally evaluates the plastic part J-integral. The $J_{i,\,pl}$ and $J_{i-1,\,pl}$ are plastic part J-integral at ith and ith -1 points of the envelope M-ϕ_{pl} curve. The second term of the right hand side of above Eq.(4.4), represents contribution due to increase in loading magnitude, while the third term represents contribution due to increase in crack growth. The crack growth and the third term is equal to zero until crack initiation. The plastic J-integral, J_{pl}, in presence of crack growth is derived by repeating calculations using Eq.(4.4) until it converges. However for small increment in crack growth, the η and γ are evaluated at θ_{i-1} crack angle using equation given below:

$$h(\theta) = \cos(0.5\theta) - 0.5\sin(\theta) \tag{4.5}$$

$$\eta(\theta) = -\frac{h'(\theta)}{2Rt.h(\theta)} \quad \text{and} \quad \gamma(\theta) = -\frac{h''(\theta)}{h'(\theta)} \tag{4.6}$$

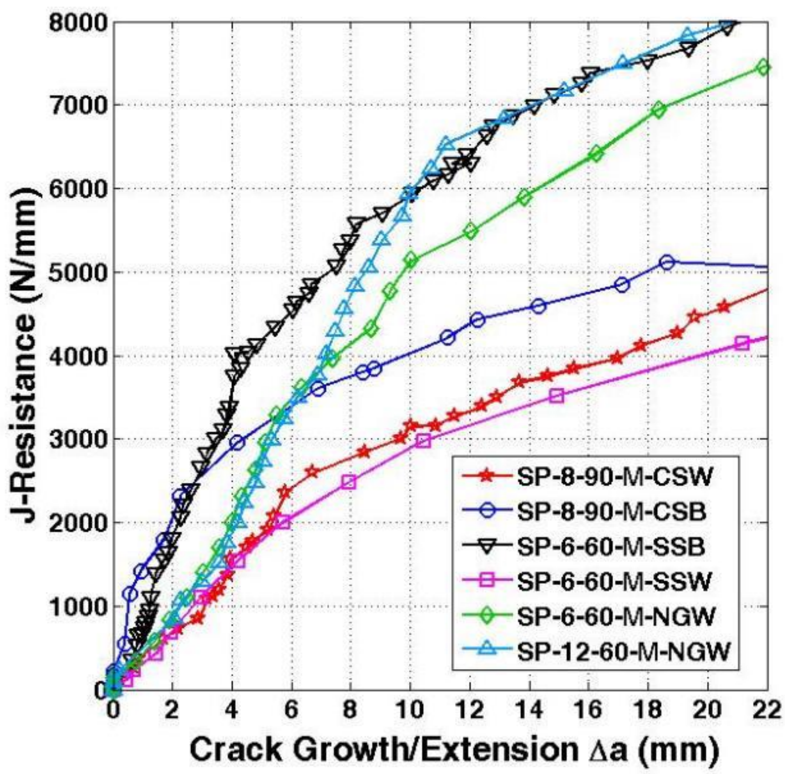

Figure 4.15: Monotonic J-R curve for different pipes.

The Moment (M) versus plastic rotation (ϕ_{pl}) curve plots of the monotonic fracture tests are shown in Figure 4.13(a) for stainless steel pipe tests and in Figure 4.14(a) for carbon steel pipe tests. The average crack growth (ACG, average of crack growth measured at the two crack tips) of these tests is plotted in Figure 4.13(b) for stainless steel pipe tests and in Figure 4.14(b) for carbon steel pipe tests. Using the M, ϕ_{pl} and ACG data along with Eq.(4.2) through Eq.(4.6), the monotonic J-R curve have been evaluated for all the 5 different pipes tested and have been plotted in Figure 4.15. It shows that the base material toughness, CSB and SSB is superior to that of corresponding weld metal, CSW and SSW. In case of SS, two different welds namely SSW (SMAW technique with conventional groove) and NGW (GTAW technique with narrow groove) were tested. The fracture toughness of NGW welded pipe was found superior to that of SMAW welded pipe.

4.3.2 Cyclic J-R curve

The initial development on application of the J-integral for fatigue crack growth modelling in presence of gross plasticity and its mathematical frame work to estimate cyclic J for 2D is available in [75 to 78]. Afterward, in IPIRG, CRIEPI and several other investigators [80-82, 69-73] have used cyclic J integral for defining cyclic J-R curve.

The IPIRG programme, NUREG/CR-6440 [53], has presented the cyclic J-R curve approach which accounts for cyclic tearing i.e. the tearing-fatigue regime crack growth. It is reported that under compressive stresses during reversible cyclic loads, the blunted crack tip re-sharpens and the round voids in fracture process zone flattens thus easing void coalescences and leading to accelerated ductile tearing in subsequent cycle load application. In addition to enhanced ductile tearing, the cyclic loading also causes the fatigue crack tearing/ growth under large scale yielding conditions. This combined tearing-fatigue regime crack growth or cyclic tearing may be accounted for in fracture assessment by using the cyclic J-R curve in place of monotonic J-R curve. In this method, the decrease in moment capacity and increased crack tearing under reversible cyclic loads is implicitly accounted for into the cyclic J-integral calculations and hence in cyclic J-R curve.

The cyclic J-R curve is evaluated using a method similar to that used in evaluation of monotonic J-R curve. Here the envelope of the moment-rotation, M-ϕ_{pl}, (see Figure 4.13 Figure 4.14) obtained from the incremental displacement controlled cyclic tearing test is used to evaluate J-integral. The test parameters namely, cyclic displacement increment (δ) and the load ratio represents the cyclic load history characteristic. The Moment (M) versus plastic rotation (ϕ_{pl}) envelope curves and the average crack growth, ACG, of cyclic and corresponding monotonic fracture tests are plotted in Figure 4.13 for stainless steel pipe tests and in Figure 4.14 for carbon steel pipe tests. The incremental displacement controlled cyclic tearing tests of all the five pipe material categories are analysed and the cyclic J-R curves have been evaluated using the M-ϕ_{pl} envelope curve and the 'η factor approach' similar to that given in section-4.3.1.

These Cyclic J-R curves with the corresponding monotonic test J-R curve have also been plotted in Figure 4.16 through Figure 4.20 for all the cases. It may be noted that both the cyclic and the monotonic J-R curve have been obtained from the incremental cyclic and monotonic tests conducted on identical pipes and under identical test conditions (temperature, loading rate etc.). Hence the difference in the cyclic J-R curve w.r.t. the monotonic J-R is only due to the cyclic nature of loading and no other reasons like geometry constraints / transferability etc. These figures clearly show that there is significant loss of the fracture resistance under the reversible cyclic loading conditions.

Figure 4.18 plots cyclic J-R curves of stainless pipe tests namely QCSP-6-60-D1-SSB and QCSP-6-60-D2-SSB which were conducted with different loading histories. The cyclic displacement increment and total number of loading cycles for QCSP-6-60-D1-SSB were 4 mm and 11 respectively while for QCSP-6-60-D2-SSB, these were 1 mm and 41 cycles. The load ratio for both the tests was -1. The cyclic J-R curve of QCSP-6-60-D2-SSB is much lower than that of QCSP-6-60-D1-SSB. Similarly Figure 4.16 plots the cyclic J-R curves of carbon pipe tests namely QCSP-6-60-D1-CSB and QCSP-6-60-D2-CSB which were conducted with different loading histories. The cyclic displacement increment and total number of loading cycles for QCSP-6-60-D1-CSB was 2.6 mm and 22 respectively while for QCSP-6-60-D2-CSB, it was 0.65 mm and 60 cycles. The load ratio for both was -1. The cyclic J-R curve of QCSP-6-60-D2-CSB is much lower than that of QCSP-6-60-D1-CSB. These observations clearly showed that the smaller displacement increment, δ, leads to larger the drop in cyclic J-R curve. This also reaffirms the observation reported in literature that the cyclic J-R curve strongly depends on loading history parameters. It may be noted here that the cyclic J-R curve included/accounted the excess crack growth due to low cycle fatigue and void flattening under reverse loading, as ductile tearing. Since the tests with smaller δ, took more number of cycles to impose a given total displacement/rotation, hence larger contribution in the crack growth comes due to fatigue and void flattening. Hence smaller displacement increment, δ, causes larger drop in cyclic J-R curves, see Figure 4.16 and Figure 4.18. In view of significant reduction of J-R curve under reversible cyclic loading w.r.t. monotonic loading, the number of unloading, in monotonic fracture tests, are generally kept small and the load ratio are kept positive to ensure there is insignificant crack growth contribution from fatigue and void flattening under reverse loading.

In view of above study and those reported in literature [69-74], cyclic J-R curve shall be evaluated for loading history which is consistent with the anticipated loads at the postulated crack location in piping system. Hence advance knowledge of the load history parameters, i.e., R-ratio, incremental cyclic plastic displacement, is required. Further these load-history parameters also may change during the course of a seismic event and also depends on plant site (seismic loading), piping layout and crack location. Hence it is practically difficult to use cyclic J-R curve in fracture assessment of a cracked pipes subjected to reversible cyclic loading.

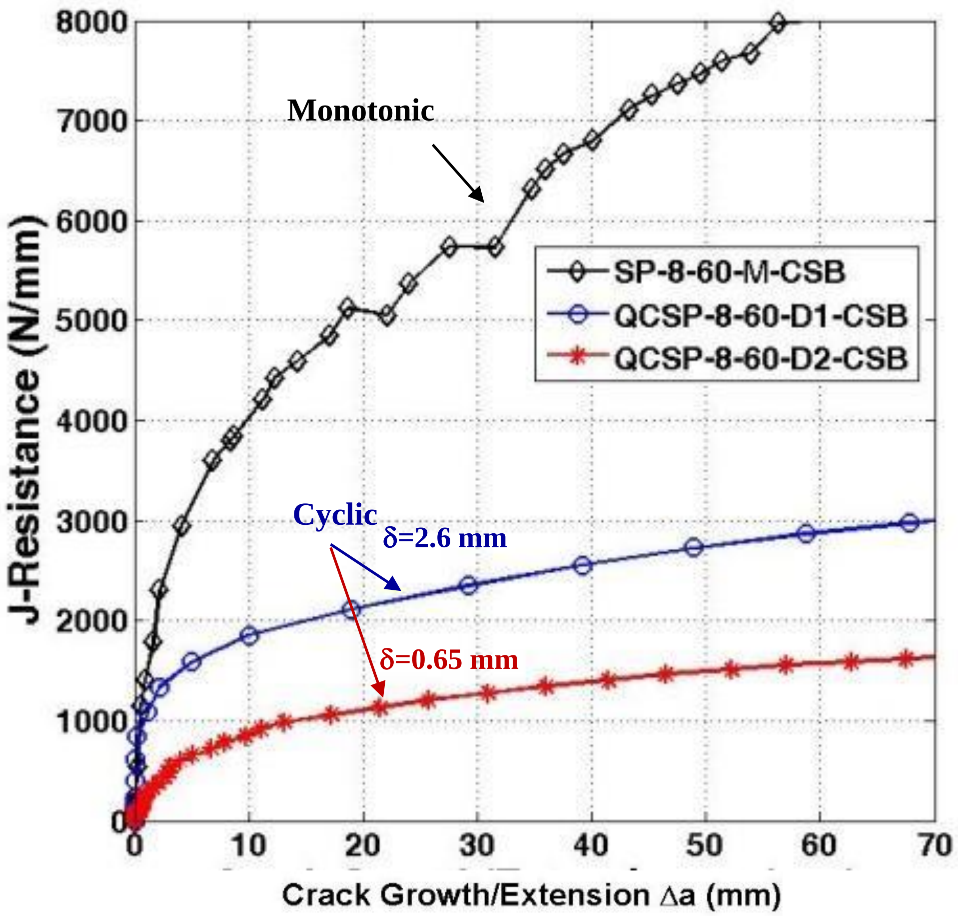

Figure 4.16: Cyclic vs. Monotonic J-R curve for carbon steel pipes (CSB)

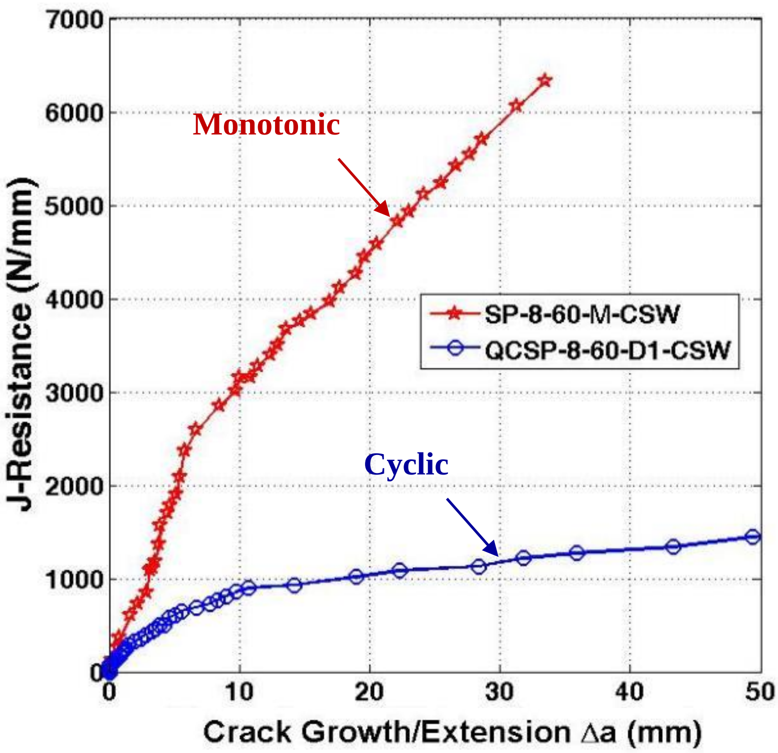

Figure 4.17: Cyclic vs. Monotonic J-R curve for carbon steel girth welded pipes (CSW)

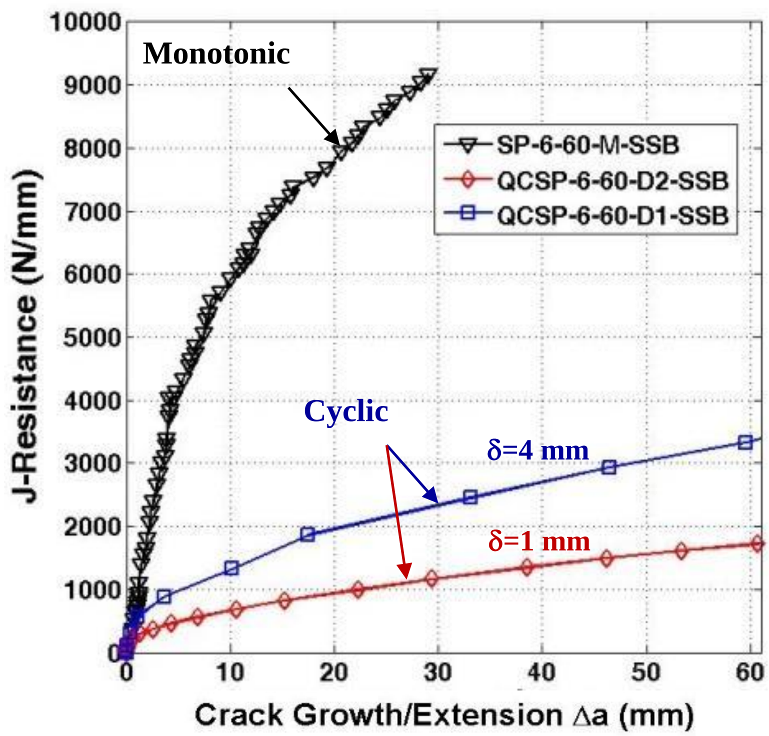

Figure 4.18: Cyclic vs. Monotonic J-R curve for stainless steel pipes (SSB)

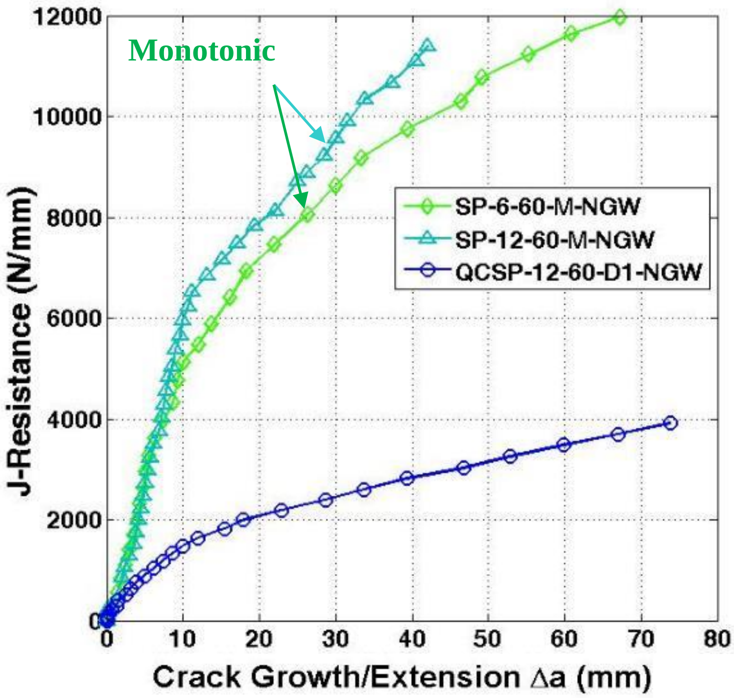

Figure 4.19: Cyclic vs. Monotonic J-R curve for stainless steel narrow gap girth welded pipes (NGW)

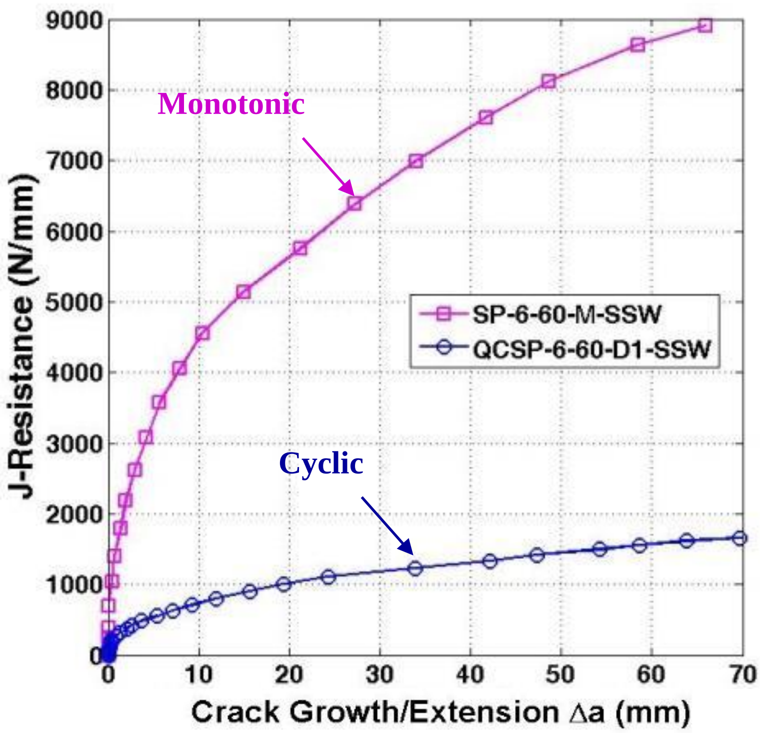

Figure 4.20: Cyclic vs. Monotonic J-R curve for stainless steel conventional grove girth welded pipes (SSW)

4.4 Reversible displacement versus incremental displacement controlled tests

These tests have been carried out to see the response of the pipe when it is subjected to reversible displacement of constant magnitude. The test details and typical results are reported in section 3.6.3. Figure 4.21 compares the response i.e. crack growth and reaction moments of the two number of reversible displacement loading pipe tests (QCSP-6-60-D2-SSW and QCSP-6-60-D3SSW) with a corresponding incremental cyclic displacement loading tests (QCSP-6-60-D1-SSW). The displacement amplitude is kept constant during the test and is equal to 17.25 and 25 mm respectively in QCSP-6-60-D2-SSW and QCSP-6-60-D3SSW. The figure shows that the crack growth is larger for larger displacement amplitude case while, the decrease in maximum moment (M_{max}) is higher in case of smaller displacement amplitude test.

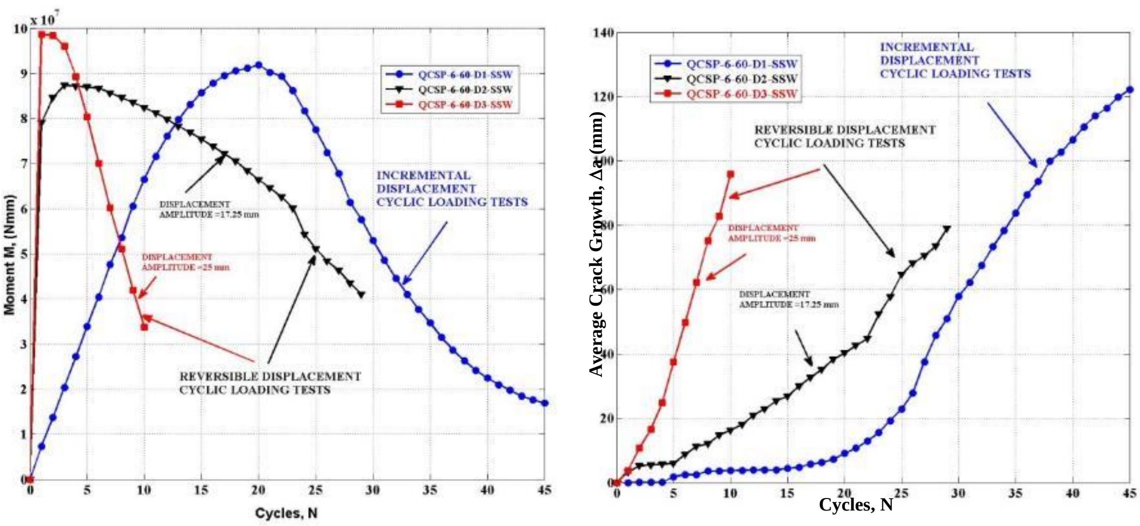

Figure 4.21: Comparison of moment and crack growth response under constant amplitude fully reversible and incremental displacement controlled loading tests on stainless steel conventional grove girth welded pipes (SSW)

4.5 Chapter conclusions

Following salient conclusions are drawn from the investigations carried out in this chapter:

(a) The results of all five material categories and of both incremental displacement controlled cyclic and corresponding monotonic fracture tests on identical pipes have been studied. The results showed significant impact of cyclic loading (load ratio=-1) on fracture behaviour pipe. Following is summary of important observations:

(i) ***Pipe Capacity in term of maximum moment (M_{max}):*** Small to moderate decrease (2 to 20% of corresponding value in monotonic tests) in the maximum moment (M_{max} that is the capacity of pipe) has been observed. The decrease was more for the tests with smaller displacement increment (δ or δ_m).

(ii) ***Pipe*** Capacity ***in term of maximum rotation (ϕ_{M-max}):*** Significant decrease (50 to 83% of corresponding value in monotonic tests) in the pipe rotation ϕ_{M-max} (value at maximum moment M_{max} point) is observed. The rotation ϕ_{M-max} indicates the cracked pipe's ability of undergoing the cyclic incremental displacement/rotation loading without any significant crack extension. The cyclic incremental displacement/rotation gradually builds up during a cyclic loading such as during an earthquake event. Smaller the displacement increment larger is the drop in ϕ_{M-max} capacity.

(iii) ***Crack growth (Δa_{M-max}) up to maximum moment point:*** Insignificant crack growth, Δa_{M-max}, observed in rising portion of the envelope M-ϕ curve (up to M_{max} point) when compared to that taken place in the drooping portion of envelope M-ϕ curve (after the M_{max} point). The crack growth (Δa_{M-max}) up to maximum moment point in incremental displacement controlled cyclic tearing tests was found little less than that recorded in corresponding monotonic fracture test.

(iv) ***Crack growth behaviour beyond M_{max}:*** The crack growth after the maximum moment point (i.e. in the drooping portion of envelope M-ϕ) is found much larger for cyclic tearing test than that in monotonic fracture test. The χ (Crack growth rate da/dϕ during the M-ϕ drooping portion) became nearly constant in all monotonic and incremental cyclic tests. For incremental cyclic loading (with load ratio = -1), the crack growth rate, χ, beyond M_{max} point is found about 3 to 8 times of that observed in corresponding monotonic tests. This confirms presence of significant damage taking place in the crack growth process owing to reversible cyclic nature of loading.

(b) **Extent of tearing in cyclic versus monotonic test (at same imposed rotation ϕ= monotonic tests ϕ_{M-max}):** The displacement controlled cyclic tearing tests are conducted by step wise or incrementally increasing the displacement / rotation such that the load ratio R ratio is -1. The extent of crack tearing is many times higher in case of cyclic condition and compared to monotonic condition when such cyclically imposed rotation / displacement equals to ϕ_{M-max} (rotation corresponding to maximum moment point in monotonic test).

(c) The ϕ_{M-max} and M_{max} together is important indicator of energy absorbing ability of a cracked pipe without undergoing any significant crack growth. High decrease in ϕ_{M-max} along with moderate decrease in M_{max} under cyclic displacement load implies very high loss in the energy absorbing ability of pipe. The smaller the cyclic displacement increment (δ) results in larger loss in energy absorbing capacity or fracture resistance.

(d) The ratio of maximum moment in displacement controlled cyclic and corresponding monotonic fracture test has been correlated with the number of cycles $N_{M\text{-}max}$. An equation has been developed correlating these two parameters. The developed equation may be used to screen/assess the number of cycles when a cyclic displacement loading event can cause large crack growth.

(f) The J-R curve assessment of all the cyclic and monotonic fracture tests has shown that there is significant drop in the J-R curve under cyclic loading conditions compared to monotonic loading. Smaller the cyclic displacement increment, larger is the drop in cyclic J-R curve. The Cyclic J-R curve is found dependent on cyclic loading parameters. Hence cyclic J-R curve shall be evaluated for loading history which is consistent with the anticipated loads at the postulated crack location in piping system.

(g) It is observed that under monotonic loading conditions, the base material toughness, CSB and SSB is superior to that of corresponding weld metal, CSW and SSW (both had conventional groove and used GTAW process for root pass and SMAW process for subsequent filler passes).

(h) Under cyclic displacement loading, the decrease (% of corresponding value in monotonic tests) in the moment capacity of pipe was found more in case of CSW pipe (about 11%) than that in CSB pipe (about 8%). While in case of stainless steel the % drop in moment capacity was nearly similar (for same % displacement increment tests).

(i) In case of stainless steel, two different welds namely SSW (conventional groove and used GTAW process for root pass and SMAW process for subsequent filler passes) and NGW (narrow groove with welding by hot wire pulsed GTAW process) were tested. The fracture toughness of NGW welded pipe was found superior to that of SMAW welded pipe.

5 Pipe crack growth and stability behaviour under load controlled cyclic loading

5.1 Introduction

The crack growth assessment of a cracked pipe is done when it is subjected to cyclic loads. The crack size at the end of cyclic loading event is evaluated considering all participating crack growth mechanisms such as fatigue, corrosion etc. With this final crack size, the stability analysis is carried out to demonstrate required safety margins between the anticipated overload (as per design basis) and the critical load (which can trigger unstable tearing or plastic collapse failure). This methodology [38] is followed during fitness for service assessment of a cracked component when a crack is detected during an in-service inspection as well as in level-2 of LBB. In the level-2 LBB assessment, the number of cycles and cyclic loading is considered in the crack growth assessment due to fatigue. However, in level-3 LBB analysis, crack growth assessment of postulated through-wall crack (called as Leakage Size Crack LSC) is not performed. The stability of pipe, with LSC crack (a maximum credible size through-wall crack) is demonstrated under postulated design basis accident event loading which in several countries, as in India also, is Safe Shutdown Earthquake (SSE) event. Here the crack growth owing to cyclic nature of SSE load is neither evaluated nor accounted in assessment of critical load in any of the present LBB practices [1-19]. In reality, the cracked pipe is subjected to large magnitude reversible cyclic load which, in turn, causes significant cyclic tearing damage [46-61,69-74]. In the piping design the earthquake induced inertial loads are conservatively considered as load controlled. In IPIRG program, [13, 56-58], the behaviour of cracked piping under inertial loading was found closer to load controlled. The nuclear piping design considers 10 cycles of equivalent maximum stress per earthquake [20, 21], in assessment of margins against fatigue and ratcheting modes of failure which are considered under cyclic loading.

In view of above, majority tests in current experimental programme (see Chapter 3) have been conducted under load controlled reversible cyclic loading. These tests have generated large data for investigation of the stability and crack growth behaviour under load controlled reversible cyclic loading. The test specimens covered wide range of parameters representative of piping used in NPPs. This chapter presents details of investigations carried out on load controlled cyclic tearing tests. These studies are carried out in relation with corresponding monotonic fracture.

The work reported in this chapter is:

(i) Pipe fracture behaviour under load controlled cyclic loading: Here the importance of the number of loading cycles (i.e. associated with an earthquake) in instability assessment; the moment-rotation (M-ϕ) and the crack growth behaviour under load controlled cyclic loading is studied. The impact of load amplitude, load ratio and mean load on stability is also investigated.

(ii) The crack growth evaluated using the methodology available in literature is compared to experimentally measured values. Finite element study on CT specimen is carried out to understand the crack tip plasticity and applicability of envelope curve methods under reversible cyclic loading.

(iii) Development a procedure for crack growth and instability assessment using a cyclic J and Dowling's ΔJ-Integral based on each cycle loading branch rather than the envelope curve

5.2 Pipe fracture behaviour under load controlled cyclic loading

Load controlled cyclic tearing test (see Table 3.7) have been conducted to understand the impact of number of loading cycles on crack growth and stability behaviour of a through wall cracked pipe. The tests in this category are conducted as per the loading scheme given in section 3.4.2. A monotonic fracture tests has been conducted (see Table 3.10) on identical pipe to general base line data corresponding to each of the cyclic tearing test. The results of both load controlled cyclic and monotonic fracture tests have been studied and following observations have been made:

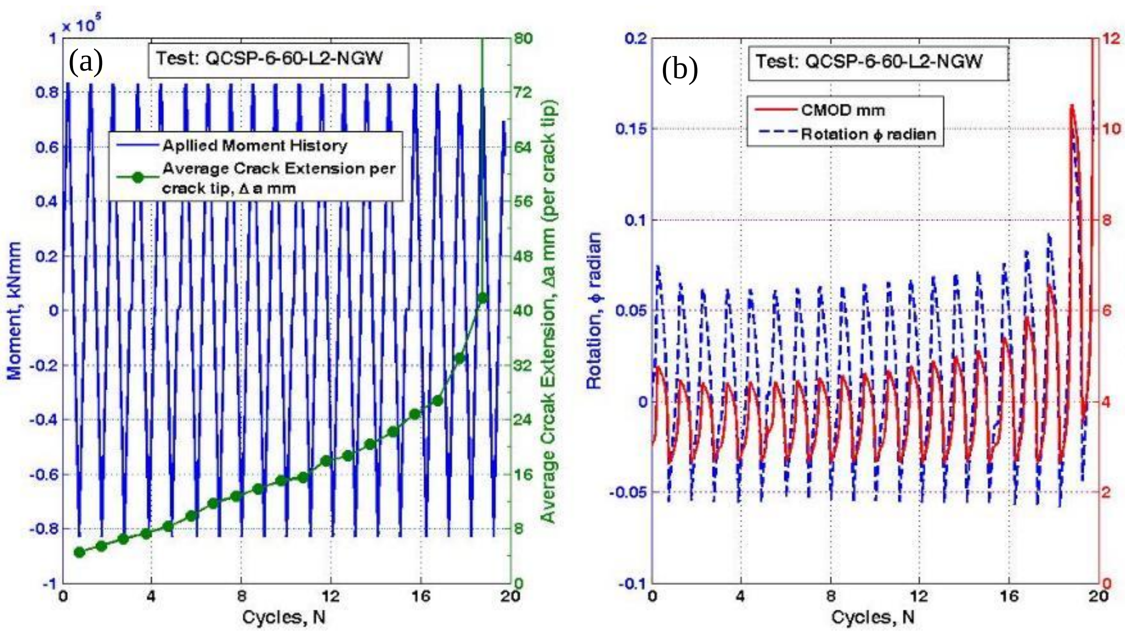

Figure 5.1: Typical Test Results for Load Controlled Cyclic Tearing Test on 6″ NB SS304LN pipe with through wall circumferential crack at weld centre (Narrow Groove hot wire GTAW) (a) Moment M & crack growth Δa vs. Cycles N, (b) Moment M & Total Rotation ϕ vs. Cycles N

Figure 5.1 shows typical test results for a load controlled cyclic tearing test on 6″ NB SS304LN NGW welded pipe. This figure shows the plot of applied load, crack extension (obtained from average of growth at two crack tip fronts), CMOD and rotation response versus number of cycles. The moment (M) versus CMOD and moment (M) versus rotation (ϕ), response are shown in Figure 5.2 (a) and (b) respectively. Figure 5.3 shows similar test results obtained from two typical load controlled cyclic tearing tests on 12″ NB SS 304LN NGW welded pipes.

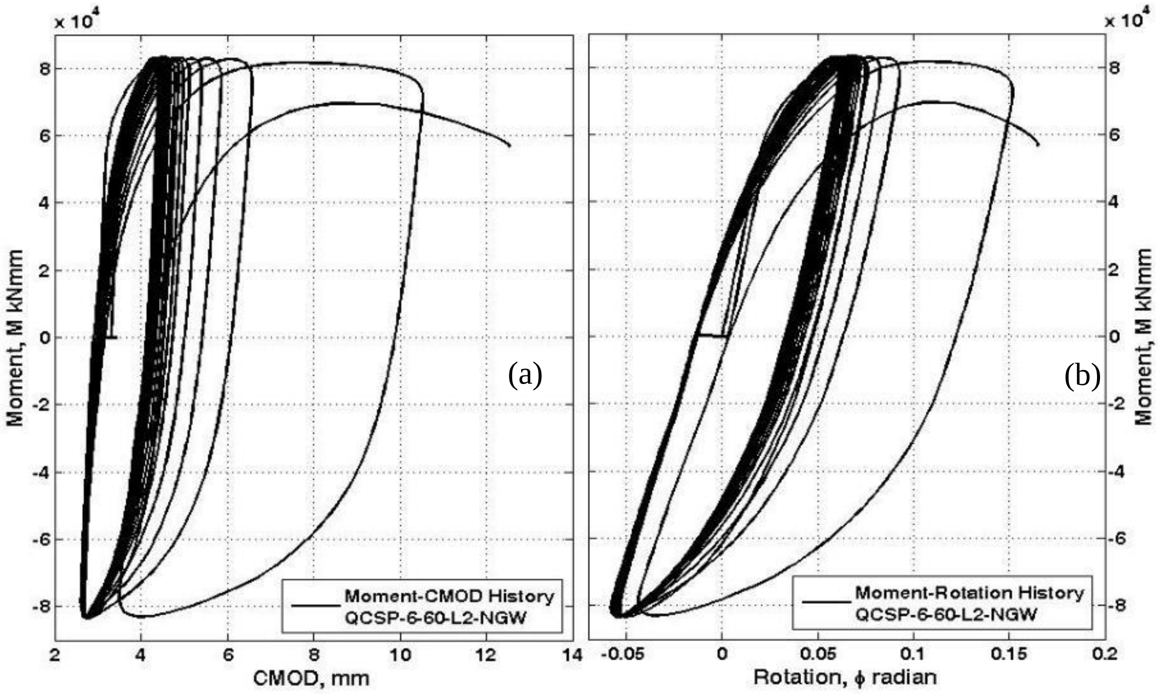

Figure 5.2:(a) Moment Vs. CMOD and (b) Moment Vs. Total Rotation plots for Load Controlled Cyclic Tearing Test 6″ QCSP-6-60-L2-NGW

Figure 5.1 (b) and Figure 5.3 (c and d) show that the maximum values of rotation / CMOD corresponding to maximum moment (when crack opens) remains nearly constant (or in some cases increase slightly) during initial cycles, while they increase rapidly in later cycles leading to instability. This shows that depending on the load amplitude, the crack growth in initial cycles is dominated by fatigue alone where ductile tearing contribution is insignificant. However, in the later cycles near to instability, in addition to fatigue crack growth, the ductile tearing also becomes significant and in fact ductile tearing-fatigue synergy governs. This can further be observed from cycle by cycle hysteresis loop evolution of moment versus rotation and moment versus CMOD, as shown in Figure 5.2(a and b) and Figure 5.3 (a and b).

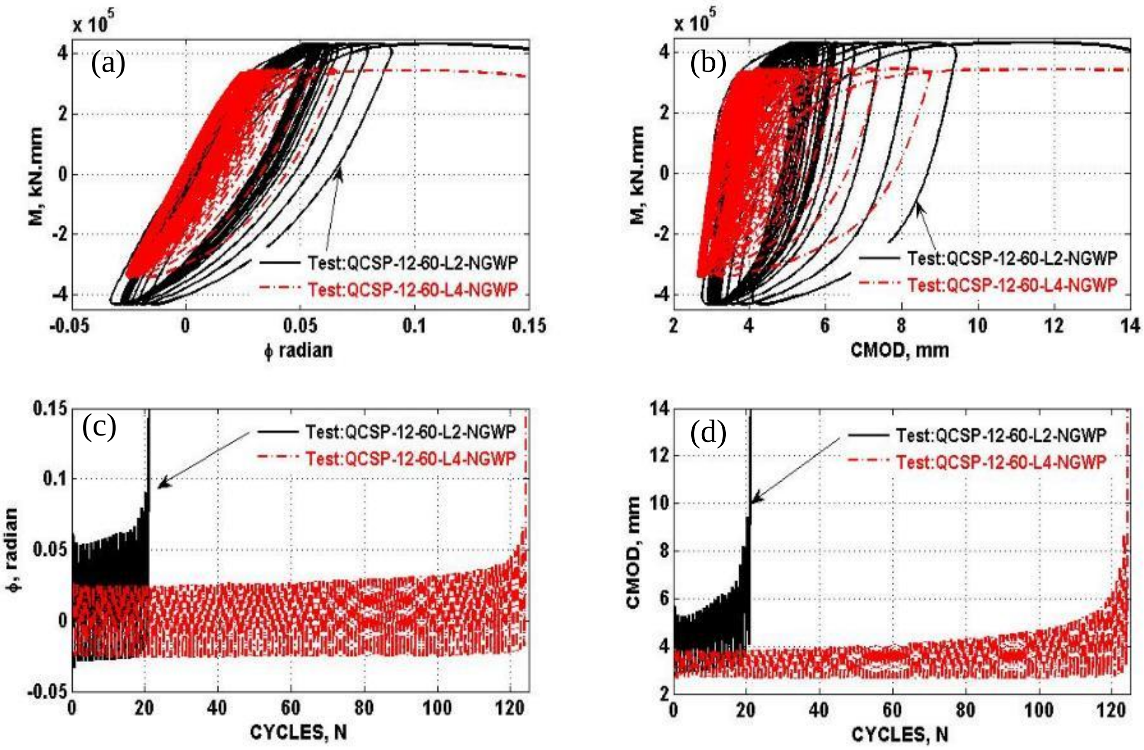

Figure 5.3: Tests results for Load controlled tests on 12″ NB SS304LN NGW pipe with circumferential TWC at weld centre

Figure 5.4 shows typical fracture surface of a load controlled cyclic tearing test conducted on SS304LN NGW 12″ NB pipe. The test pipe has stable cyclic crack growth up to 40 cycles and had unstable failure in 41st cycle when the crack size become large enough or the remaining ligament was not able to sustain the applied load. The sable crack growth, (crack growth, Δa_f, up to a cycle prior to instability) has been recorded in all the load controlled cyclic tearing tests. It can be clearly seen that there is significant amount of cycle by cycle stable ductile tearing before the instability cycle (N_f).

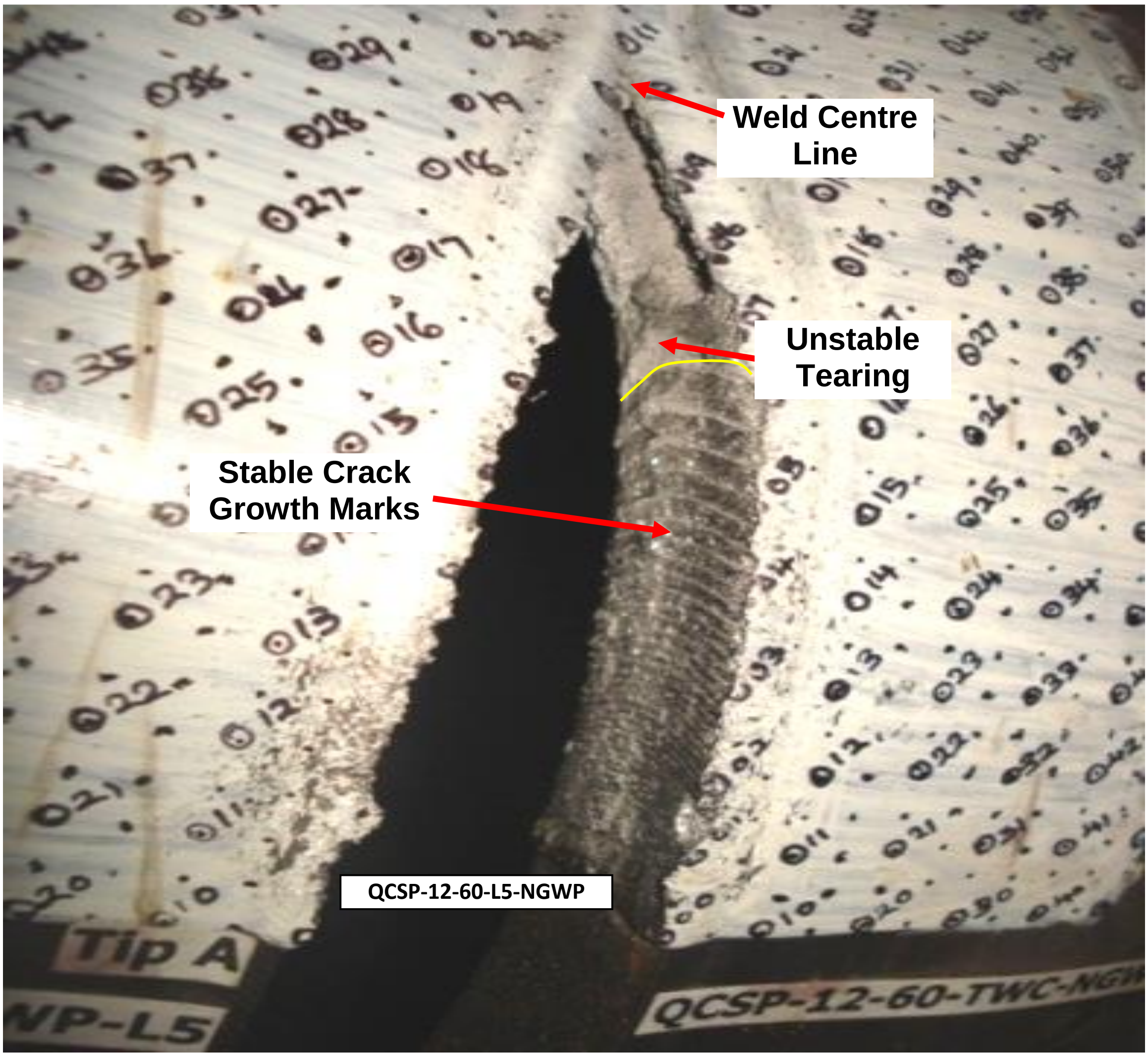

Figure 5.4: Fracture Surface showing the beach marks of the stable tearing in each cycle for load controlled cyclic tearing tests on 12″ NGW pipes

5.2.1 Stability and Crack growth behaviour

The number of cycle to instability (i.e. N_f), the stable crack growth (i.e. Δa_f) and the applied load magnitudes (M) have been studied in relation to those observed in corresponding monotonic fracture test on identical pipe.

Figure 5.5 plots a bar chart showing the magnitudes of applied moment, M, the number of cycles to instability, N_f and the stable crack growth, Δa_f, for both carbon steel base (CSB) and weld (CSW) category test on 8″ size pipes. Figure 5.6 plots a bar chart showing the magnitudes of applied moment, M, the number of cycles to instability, N_f and the stable crack growth, Δa_f, for cyclic tearing tests on both 12″ and 6″ size narrow gap welded stainless steel (SSW) pipe tests. Both these figures also plot corresponding monotonic fracture tests data. These figures clearly show:

(i) Under reversible cyclic loading, the unstable tearing leading to DEGB like failure of pipe, takes place in very few cycles (10-20) when the applied moment magnitude are 80 to 90% of the critical moment of the pipe obtained from monotonic fracture tests on identical pipe.

(ii) Significant stable crack growth (Δa_f) takes place before the unstable tearing. This crack growth increases with each loading cycle, which in turn reduces the size of healthy ligament (load bearing cross section). At certain stage, the remaining ligament becomes critical leading to unstable tearing failure.

(iii) The number of cycles, N_f, to unstable failure of pipe, increases with decrease in the applied moment magnitude.

(iv) The stable crack growth, Δa_f, increase with increase in N_f which in turn depend on applied moment magnitude. Smaller the applied moment; large would be the stable crack growth, Δa_f, prior to unstable tearing takes place.

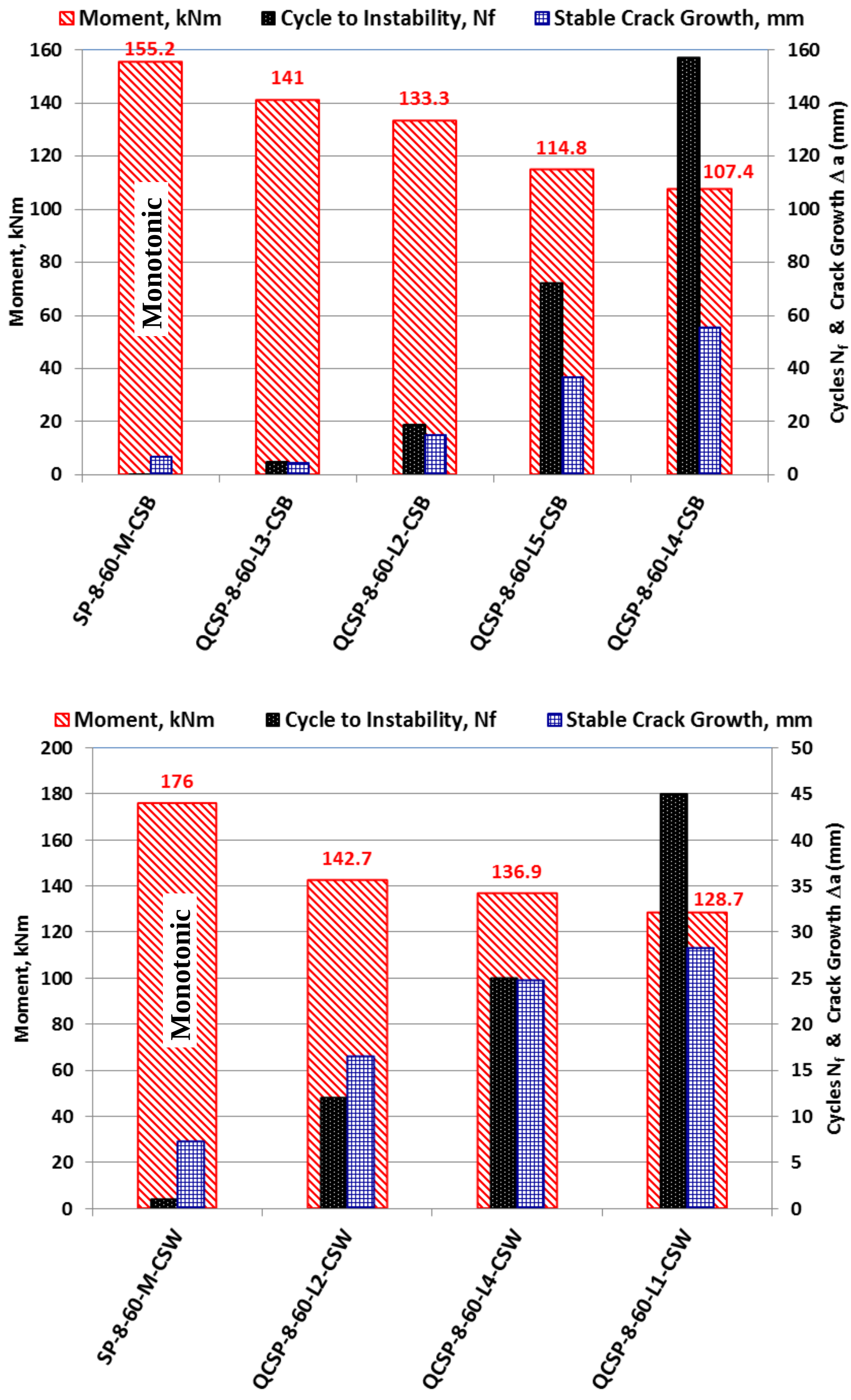

Figure 5.5. Comparison of 8″ size carbon steel base (CSB) and weld (CSW) pipe tested under monotonic and load controlled cyclic tearing (load ratio=-1) conditions

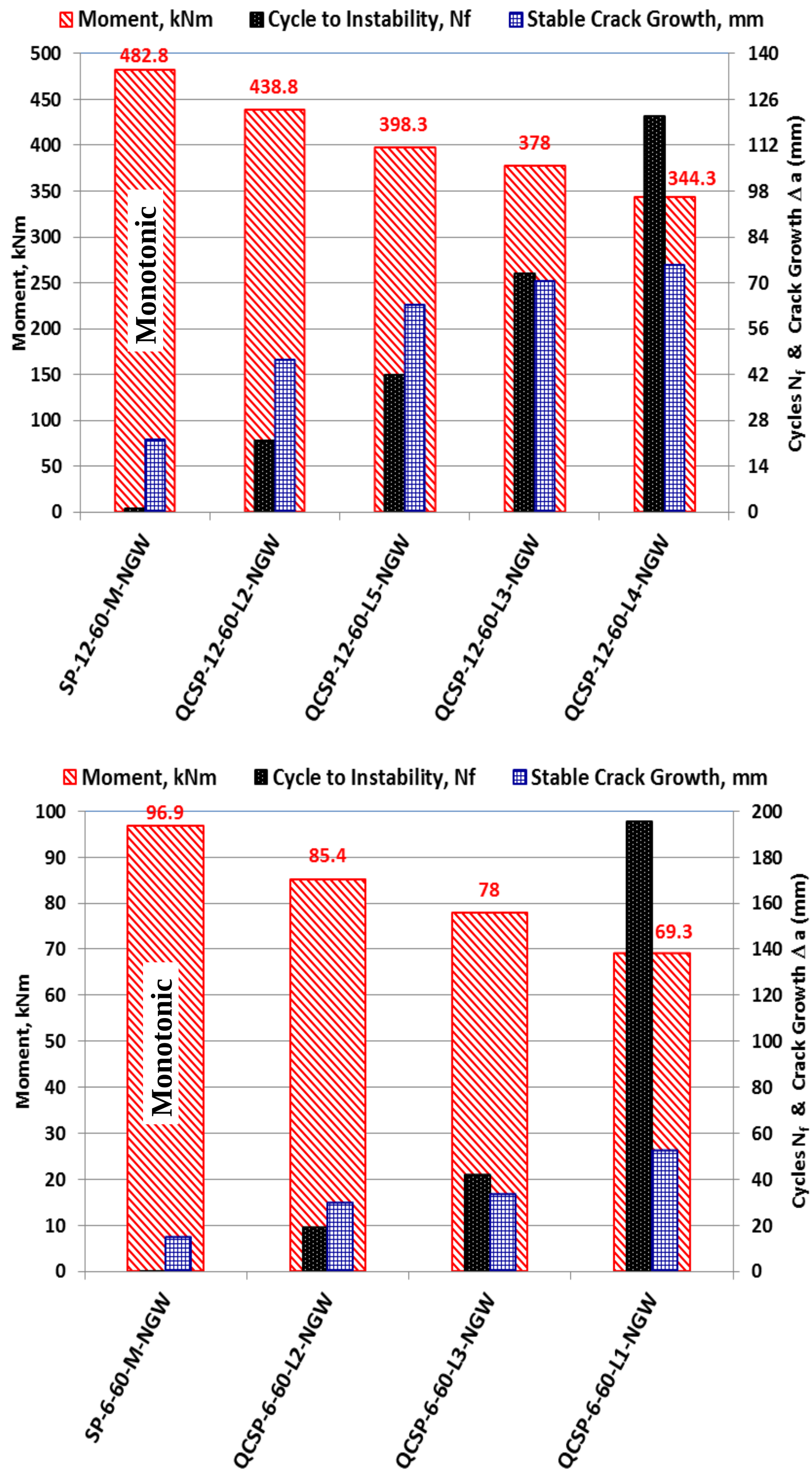

Figure 5.6. Comparison of 12″ and 6″ size stainless steel narrow gap welded (NGW) pipe tested under monotonic and load controlled cyclic tearing (load ratio=-1) conditions

Figure 5.7 shows the crack growth behaviour of different tests on pipe having same material, size and crack geometry but different crack locations, namely in base metal, in centre line of SSW and centre line of NGW. Figure 5.7(a), clearly shows that under reversible cyclic loading the crack located in SSW undergoes larger tearing/ crack growth compared to when same crack is located in base metal. Likewise, Figure 5.7(b) compares the crack growth behaviour of cases in which crack is located in NGW and SSW. The figure clearly shows that NGW has superior resistance to cyclic crack growth in ductile tearing-fatigue synergic regime. In addition, the number of cycles to instability is higher in case of NGW welded pipes as compared to not only in SSW welded pipes but base metal also. This is highlighted by comparing the results of test nos. QSSP-6-60-L1-NGW, QSSP-6-60-L3-SSB, QCSP-6-60-L3-SSW, QCSP-6-60-L4-SSW and QCSP-6-60-L1-SSB shown in Table 3.7.

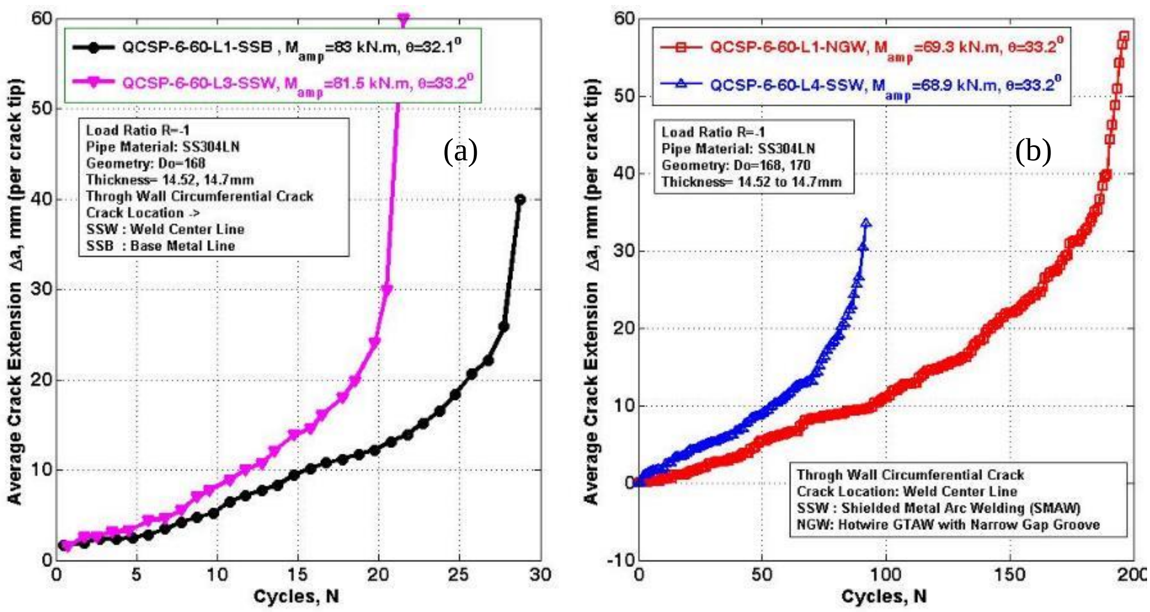

Figure 5.7: Crack growth vs. cycle's plots for Stainless steel pipes having TWC crack in Base metal, SMAW and NGW centre line. (a) SSB vs. SSW, (b) SSW vs. NGW

Figure 5.8, shows the crack growth behaviour of different tests on carbon steel pipes having same material, size and crack geometry but different loading histories in term of amplitude and mean. These results show the influence of the load ratio R, mean load and compressive plasticity on the crack growth behaviour. The observations are explained in subsequent sub-sub-sections.

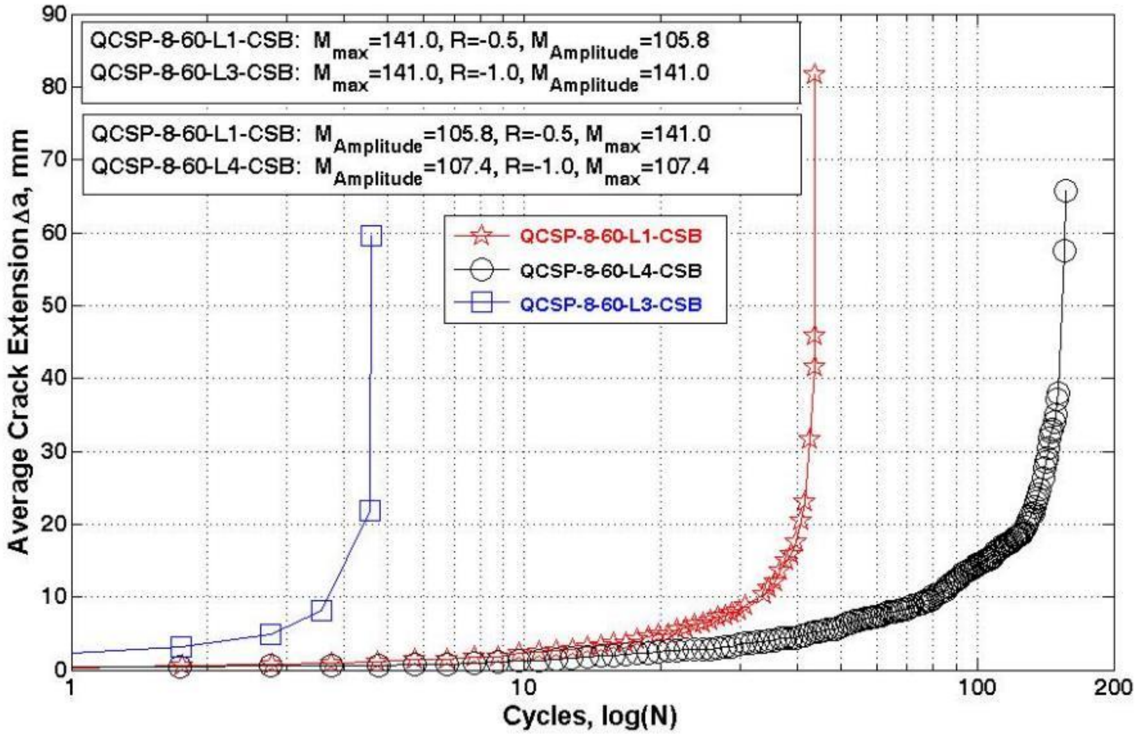

Figure 5.8: Comparison of crack growth behaviour of carbon steel pipe for same maximum load but different load ratio and for same amplitude but different load ratio

5.2.2 Effect of mean stress and stress/load ratio on cyclic fracture

Consider the two tests on carbon steel pipes (test nos. QCSP-8-60-L1-CSB and QCSP-8-60-L4-CSB, see Table 5.1), which have been conducted with same load amplitude but different load ratios. All other parameters such as crack size, pipe size, crack location and mode of loading are same in both the tests (see Table 5.1). In test no. QCSP-8-60-L1-CSB the load ratio is -0.5 (that is mean load is non-zero) whereas, in test no. QCSP-8-60-L4-

CSB the load ratio is -1.0 (that is zero mean load). The number of cycles to unstable failure was recorded as 45 (load ratio = -0.5) and 157 (load ratio = -1.0) respectively, see Figure 5.8. It shows that mean stress reduces the number of cycles to failure in comparison to zero mean stress but with same amplitude test. This is due to larger contribution of ductile tearing in crack growth owing to larger value of the maximum load (i.e. mean + amplitude; see Table 5.1) in case of non-zero mean load tests. The ductile tearing depends on the maximum load and not on the load amplitude.

Table 5.1: CSB and CSW Load controlled cyclic tearing tests on identical pipes but with different road ratio

Parameter Name	**QCSP-8-60-L1-CSB**	**QCSP-8-60-L4-CSB**	**QCSP-8-60-L3-CSW**	**QCSP-8-60-L3-CSB**	**QCSP-8-60-L2-CSW**
Do, mm	219.5	219	219	219	219
t, (mm)	15.5	15.66	16.09	15.4	16.08
θ (Degrees)	33.24	33.73	33.69	33.75	33.1
M_{max} , kNm	141.1	107.4	142.6	141	142.7
M_{amp}, kNm	105.8	107.4	107.0	141	142.7
M_{mean}, kNm	35.3	0	35.7	0	0
Load Ratio, $R=M_{min}/M_{max}$	-0.5	-1	-0.5	-1	-1
Cycles to instability, N_f	44	157	88	5	12
Tests: Same M_{amp}, Different M_{max}	⊗	⊗			
Tests: Same M_{max}, Different M_{amp}	◊		⊕	◊	⊕
Base vs Weld: Same absolute Loading	♣		♣	♥	♥

5.2.3 Effect of compressive plasticity and fatigue synergy

Consider the two typical tests on carbon steel pipes (test nos. QCSP-8-60-L1-CSB and QCSP-8-60-L3-CSB, see Table 5.1), which have been conducted with same maximum load but different load ratios. All other parameters such as crack size, pipe size, crack location and mode of loading are same in both the tests (see Table 5.1). In test no. QCSP-8-60-L1-CSB the load ratio is -0.5 whereas, in QCSP-8-60-L3-CSB the load ratio is -1.0. The number of cycles to unstable failure is recorded as 45 (load ratio = -0.5) and 5 (load ratio = -1.0) respectively, see Figure 5.8.

Similar observation is made for carbon steel weld (CSW) category pipe tests (test nos. QCSP-8-60-L3-CSW and QCSP-8-60-L2-CSW, see Table 5.1). These are conducted with same maximum load but different load ratios that is -0.5 and -1.0 respectively. All other parameters such as crack size, pipe size, crack location and mode of loading are same in both the tests (see Table 5.1). The number of cycles to unstable failure was recorded as 88 (load ratio = -0.5) and 12 (load ratio = -1.0) respectively, see Table 5.1.

The significant reduction in number of cycles in the QCSP-8-60-L3-CSB (w.r.t. QCSP-8-60-L1-CSB) and QCSP-8-60-L2-CSW (w.r.t. QCSP-8-60-L3-CSW) tests are due to:

(a) Significant reversible/compressive plasticity because of larger compressive loads, leading to significant damage in fracture process zone ahead of crack. The compressive stresses /plasticity ahead of crack tip causes:

(i) Crack tip sharpening: After each compressive unloading, crack tip re-sharpening has been observed in these tests. The sharp crack tips are known to increase the crack-tip stress intensity and promote crack extension, thus lowering the apparent fracture resistance

(i) Void flattening/crushing: In ductile fracture, the fracture process zone consists near spherical shape voids. These voids gets elongated and flattened or crushed under reverse loading (compressive load). The elongated flat and sharp voids tend to enhance void coalescence and hence lower the apparent fracture toughness.

Both, the crack tip sharpening and the void flattening are important mechanism in the cyclic degradation process causing accelerated tearing in subsequent load cycle application. These apparently accelerate fracture process in subsequent tensile loading leading to additional crack growth. Similar observations have also been reported in IPIRG programme [13, 53] and by other investigators [73]

b) Increase in the load amplitude because of larger compressive loads, leading to increased fatigue crack growth (increased range of stress intensity factor, ΔK, or range of ΔJ-integral). The contribution of fatigue crack growth is larger in the QCSP-8-60-L3-CSB w.r.t. QCSP-8-60-L1-CSB test and QCSP-8-60-L2-CSW w.r.t. QCSP-8-60-L3-CSW tests. The larger FCG would in turn further reduce the number of cycles to unstable failure.

Under large compressive loads, due to combined contribution of above both the reasons, i.e. the compressive plasticity induced damages and increased fatigue crack growth, the number of cycles to unstable failure reduce significantly.

5.3 Crack growth and stability assessment using the CRIEPI J_{max} and ΔJ integral method

In the past, fatigue crack growth in elastic plastic regions has been investigated by several researchers [69, 75-85]. In these studies, the Dowling's [76] ΔJ-integral is used to model the fatigue crack growth rates in the elastic plastic region. These studies have shown good simulation of the crack growth behaviour over wide interval of crack growth for different sized cracks. C.W. Marchall and G. Wilkowski, [69] have reviewed several experimental and analytical studies carried out to understand effect of cyclic loading on ductile fracture resistance. It is shown that the crack tearing under cyclic loading with load ratio, R, greater than 0, the total crack extension is just summation of crack extension due to monotonic ductile tearing, Δa_{mono} (obtained from a monotonic J-R curve test) and fatigue crack growth, Δa_{cyc} (estimated using fatigue crack growth analysis). While for negative R, the total crack extension exceeded above evaluated Δa_{mono}+ Δa_{cyc}. The additional tearing/degradation (that is difference in measured tearing with that of estimated tearing) is attributed to damage owing to compressive loading.

NUREG/CR-6440 [53], Rahman [85], have presented basic experimental analysis approach for low cycle fatigue crack growth assessment under reversible cyclic loading conditions that is with negative load ratio (R<0). These have evaluated the low cycle fatigue crack growth of the cyclic pipe experiments conducted under simulated earthquake loading. Here The Dowling's ΔJ-integral is used along with the extrapolated Paris law. Here the i^{th} cycle ΔJ-integral is evaluated as discussed in section 5.3.2. Then, the equivalent ΔK_i is evaluated using following equation.

$$\Delta K_i = \sqrt{\Delta J_i E} \tag{5.1}$$

The crack growth (da_i) in the i^{th} cycle then is evaluated using the effective ΔK_i and fatigue crack growth law (Paris Law).

$$\left(\frac{da}{dN}\right)_i = C(\Delta K_i)^m \tag{5.2}$$

Where, the constant C and m are generally determined from the standard fatigue crack growth tests.

During the same time as part of Japanese CRIEPI programme, Miura [62, 64-66] have proposed a cyclic J_{max} and ΔJ integral which was used in the crack growth and stability assessment of the load controlled cyclic tearing tests carried out in CRIEPI programme (similar to the load controlled cyclic tearing tests of current programme). Here the fatigue crack growth, Δa_{cyc}, is evaluated using the ΔJ-integral as described above. The static ductile tearing is evaluated using monotonic J-R curve and a cyclic J_{max} integral. It is shown that the procedure has reasonably simulated the CRIEPI programme load controlled tests carried out on 4″ size STS410 carbon steel pipes.

In view of above, the crack growth and stability assessment of load controlled cyclic tearing tests have been performed using the above CRIEPI/Miura [62, 64-66] procedure. Here cyclic maximum J-integral, J_{max} and cyclic J-integral range, ΔJ, were used for describing the crack growth behaviour in a large scale yielding region. The J_{max} and the ΔJ integrals were evaluated using experimentally measured load displacement and are discussed in following sections:

5.3.1 Evaluation of J_{max} –Integral

The cyclic J_{max}-integral, at the i^{th} cycle has been evaluated as sum of the elastic and plastic J integral using following equations as given by Miura et. al. [62, 64-66]

$$J_{max,i} = J_{max,el,i} + J_{max,pl,i} \tag{5.3}$$

$$J_{max,el,i} = f_b^2 \left(\frac{\theta_i}{\pi}\right)\left(\frac{M_i^2}{ER^3t^2}\right) \tag{5.4}$$

$$J_{max,pl,i} = \frac{1+\frac{\Delta a}{R}\gamma(\theta_i)}{1-\frac{\Delta a}{R}\gamma(\theta_i)} J_{max,pl,i-1} + \frac{2\eta(\theta_i)}{1-\frac{\Delta a}{R}\gamma(\theta_i)} U_i \tag{5.5}$$

$$U_i = \int_{\phi_{pl,i-1}}^{\phi_{pl,i}} M d\phi_{pl} \quad (5.6)$$

The U_i is the area under the envelop moment (M) versus crack plastic rotation (ϕ_{pl}) evaluated between two subsequent cycle peaks. The $\eta(\theta_i)$ and $\gamma(\theta_i)$ are evaluated using Eqs.(4.5 and 4.6). Figure 5.9(a) shows the schematic of U_i and positive half of envelope M-ϕ_{pl} curve. Here the function f_b,η and γ are geometry functions [32].

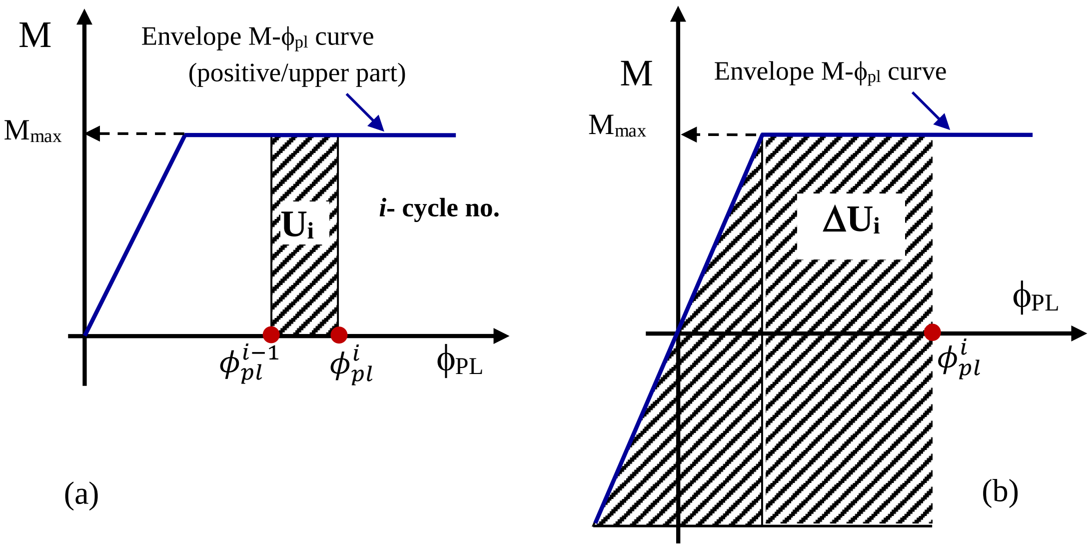

Figure 5.9: Schematic of U_i and ΔU_i Calculations from the envelope M-ϕ_{PL} curves

5.3.2 Evaluation of ΔJ–Integral

The Cyclic ΔJ-integral has been evaluated as sum of the elastic and plastic ΔJ integral using following equations as given by Miura et. al. [62, 64-66]

$$\Delta J_i = \Delta J_{el,i} + \Delta J_{pl,i} \quad (5.7)$$

$$\Delta J_{el,i} = f_b^2 \left(\frac{\theta_i}{\pi}\right)\left(\frac{\Delta M_i^2}{E R^3 t^2}\right) \quad (5.8)$$

$$\Delta J_{pl,i} = \frac{2\eta(\theta_i)}{1-\frac{\Delta a}{R}\gamma(\theta_i)}\Delta U_i \tag{5.9}$$

ΔU_i is the total area under the M-ϕ_{pl} envelope curve corresponding to ith cycle. Figure 5.9(b) shows the schematic of ΔU_i and envelope M-ϕ_{pl} curve.

5.3.3 Instability Criteria

Here the cyclic ΔJ integral along with monotonic J-R curve was used to determine the instability using equation as given below.

$$\Delta J(\Delta a) \geq J_R(a - a_o) \tag{5.10}$$

Where 'a' is the current crack length and 'a_o' is the initial crack length. For analytical cyclic tearing assessment of a cracked pipe, it was proposed to evaluate a J_{max} integral using standard analytical schemes such as GE/EPRI method etc. [32]. The J_{max} integral is the applied J-integral value of the cracked pipe evaluated corresponding to the maximum cyclic load. Then the ΔJ integral is evaluated from this J_{max} using following equation

$$\Delta J / J_{max} = \frac{4a}{2a - a_o} \tag{5.11}$$

The crack extension in ith cycle, (da_i), is calculated using the ΔJ_i using and Eq. (5.1 and 5.2). Then the crack size after ith cycle is evaluated by adding the $(da/d/N)_{i.}$ to the crack size in previous cycle that is a_{i-1}.

5.3.4 Crack growth and stability assessment of Carbon Steel Base Metal pipes

In order to assesses the suitability of the above CRIEPI with respect to current programme pipe tests, the data of five numbers of load controlled cyclic testing tests on carbon steel base metal (CSB) 8″ size pipe have been analysed. The carbon steel pipe tests are selected since it is similar to the material, STS410, used in CRIEPI programme. The envelope curve of the load-displacement history obtained from a load controlled cyclic tearing test has been used to evaluate the J_{max} and the ΔJ as described above. The constants 'C 'and 'm' used in present study, were obtained in a different test programme, Singh et. al [111], on SA333 Gr.6 carbon steel. The C and m as evaluated are 3.982×10^{-12} and 3.01 respectively. In above equation, unit of da/dN is m/cycle and ΔK is in MPa$\sqrt{m}$. These constants have been obtained as per the ASTM Standard E647 using three-point bend specimen machined from the pipe material stock of same heat as used in present program. These tests have been carried out for stress ratios of 0.1, 0.3 and 0.5. The stress ratios have negligible effect in the Paris region. The results are as given below:

(i) Figure 5.10 plots the ΔJ integral versus Δa (evaluated from test data of load-displacement and crack size). These figures also plot the monotonic J-R curve evaluated form monotonic fracture test on identical pipe having same nominal size, thickness, crack size, material and heat of material. The instability point observed in these tests is marked by a circumscribing circle. The instability point and the monotonic J-R curve (J_R versus Δa) is also plotted in Figure 5.10. This figure clearly shows that the above instability criteria, Eqn.(5.10) does not hold good for these CSB tests. Figure 5.11 plots the J_{max} integral versus Δa. This figure shows that in all the five tests, the J_{max} in the cyclic tests is below the corresponding monotonic J-integral value till instability.

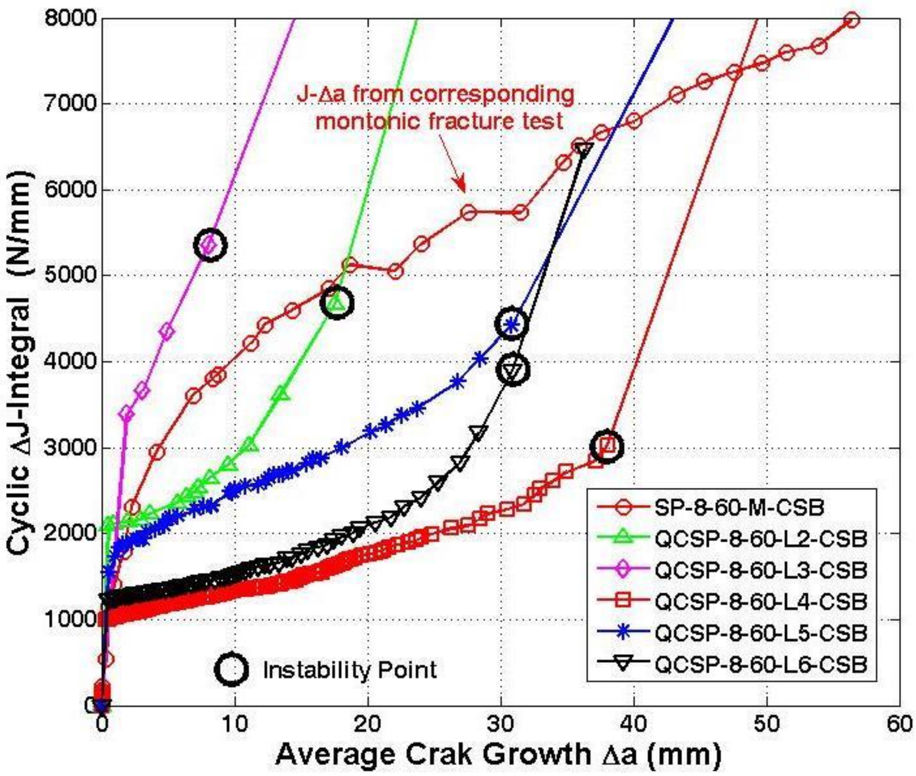

Figure 5.10: Analysis of load controlled carbon steel cyclic tearing tests on 8″ pipe: cyclic ΔJ vs. crack extension Δa and monotonic J-R curve

(ii) To investigate Eqn.(5.11) which is an important relation provided for analytical assessment of cracked pipe under cyclic loading, the parameters $\Delta J/J_{max}$ has been evaluated for all the five tests and plotted against 'a/a_o' in Figure 5.12. For tests no. L2 to L5 the initial crack size, a_o, was nearly 67° while for L6 test it was 97°. The $\Delta J/J_{max}$ as evaluated using Eq. (5.11) for these two initial a_o values is also plotted in Figure 5.12. This figure clearly shows that the $\Delta J/J_{max}$ ratio calculated from Eqn.(5.11) are not in agreement with those obtained from the test. However, the ratio $\Delta J/J_{max}$ has remained between 2 and 4 for all the tests similar to that obtained in CRIEPI programme. This clearly indicates the dependence of the ratio $\Delta J/J_{max}$, on the loading parameters in addition to a/a_o, as proposed by Miura [62, 64-66]

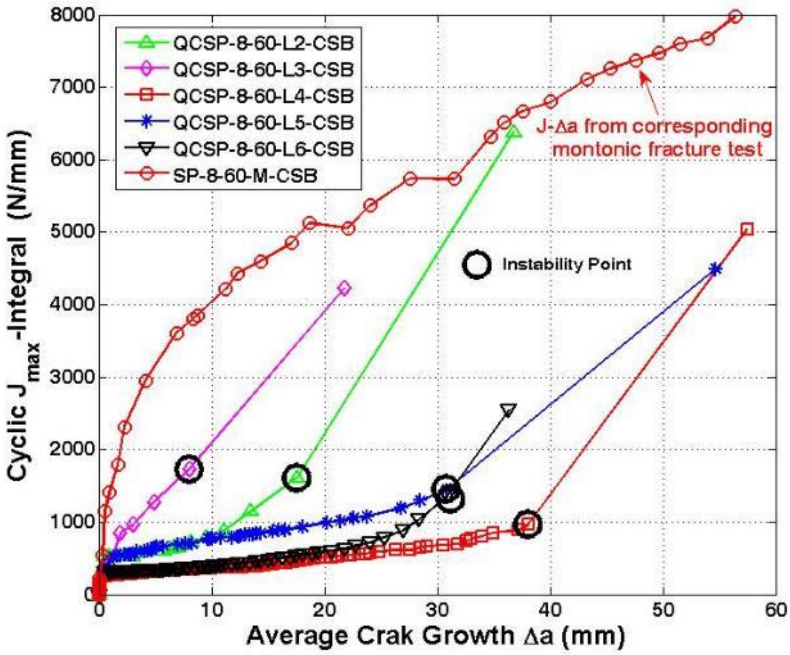

Figure 5.11: The J_{max} (load control cyclic tearing test) and J-integral (monotonic test) versus crack extension plot for carbon steel base metal 8″ size pipe load controlled cyclic tearing tests

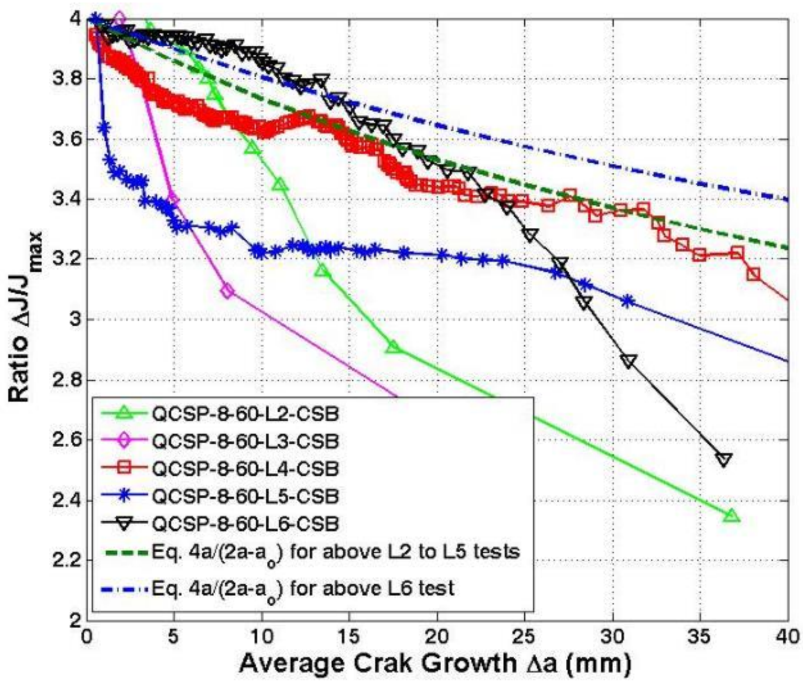

Figure 5.12: Analysis of load controlled carbon steel cyclic tearing tests on 8″ pipe ; (b) Cyclic ΔJ / J_{max} versus crack extension Δa

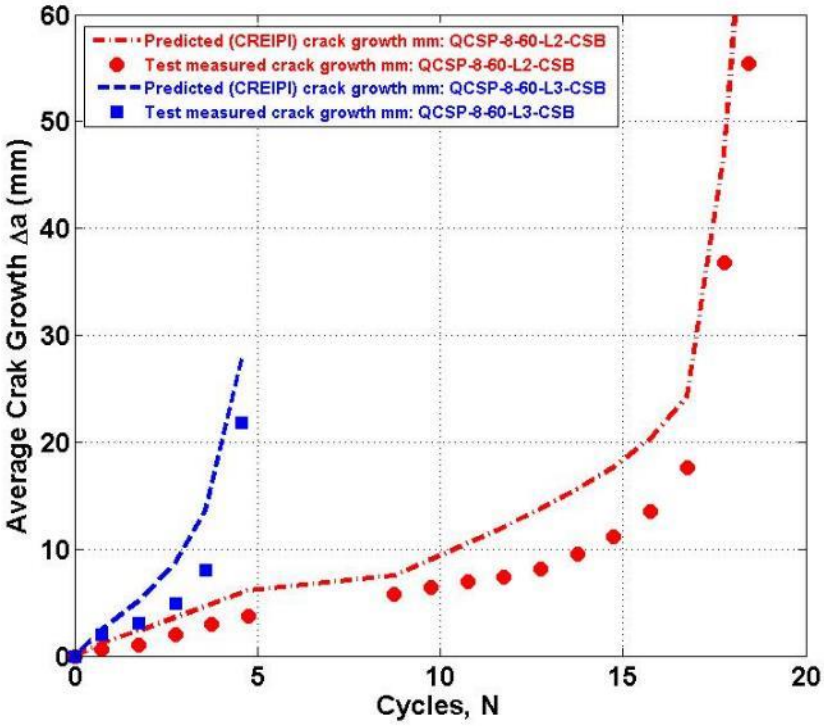

Figure 5.13:Predicted crack growth using CRIEPI method versus test measured crack extensions

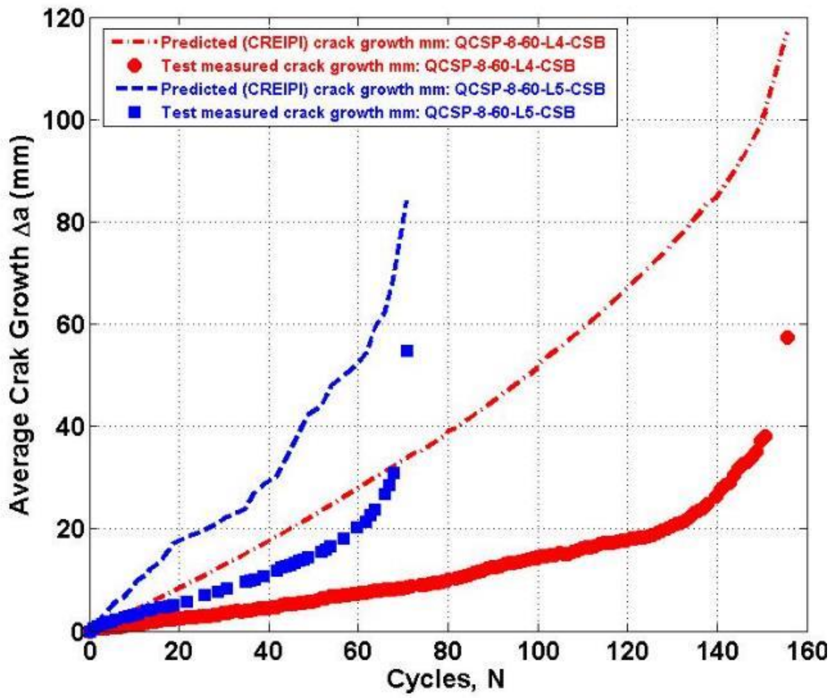

Figure 5.14: Predicted crack growth using CRIEPI method versus test measured crack extensions

(iii) The evaluated crack growth versus number of cycles has been plotted in Figure 5.13 and Figure 5.14 for all the four number of load controlled cyclic tearing tests on identical carbon steel base metal 8″ size pipes. The Figure 5.13 show that the reasonable predictions, while in Figure 5.14 the predicted crack growth was found much higher than that measured during test. Hence the above method over predicts the crack growth.

From the above evaluations and comparisons with current program tests data, it has been seen that the envelope curve based method (Miura et. al. [62, 64-66]) of assessment of cracked pipe under reversible cyclic loading the cyclic tearing test, is not universally applicable to other materials and pipe sizes. This may be due to following reasons:

(a) The procedure was developed and validated on pipe tests conducted on 4 inch size and STS410 steel. In these small size ductile material pipe tests the plastic collapse is likely to govern over ductile tearing,

(b) The procedure had used envelope curves in evaluation of the J_{max} and ΔJ integral. The use of envelop curve may not be realistic when the loading is of reversing cyclic nature (negative load ratio, $R<0$). The use of envelope curve is well established and accepted for alternating loading cases for positive load ratio $R>0$, (for example standard monotonic J-R curve tests on specimens [44] or components). However for negative load ratio, no validation / justification of envelope curve use is available in literature.

5.4 Use of Envelope curve: alternating versus reversing load

In order to assess and understand the uses of envelope curve under alternating and fully reversing loading, a study has been carried out involving the data of above analysed tests and a series of 2D finite element analysis on standard CT specimen geometry.

From study of the cycle by cycle hysteresis loops along with the corresponding envelop curves obtained from the test data used in above analyses, following observations are made:

(a) The loading branch of the M-ϕ hysteresis loop shift/ratchet towards right (in positive ϕ direction) on subsequent application of reversible cyclic loading. This can be clearly seen in Figure 5.15 and Figure 5.16.

(b) The envelope M-ϕ curve does not account for the M-ϕ_{pl} loading branch shift/ratchet towards right (in positive ϕ_{pl} direction) on repeated reversible cyclic loading. This can be clearly seen in Figure 5.16 where each cycle loading branch of M-ϕ_{pl} hysteresis and envelope M-ϕ_{pl} curve are plotted for a load controlled cyclic tearing test namely QCSP-8-60-L3-CSB. Similar observations were there for other tests also. The reason for such behaviour is that, under fully reversible loading, the pipe plastically deforms more in crack opening direction loading (positive ϕ_{pl} direction) than that in crack closing direction. This is due to asymmetry in pipe stiffness owing to crack closing/opening. Due to this asymmetric plastic deformation of pipe, and the loading M-ϕ_{pl} curve shifted in positive ϕ_{pl} direction with increase in number of load cycles, as can be seen in Figure 5.16. It becomes clear that the use of envelope curve in ΔJ_{pl} calculation (as suggested in CRIEPI program) would use a larger area for each cycle loading expect 1st cycle. This will result in over estimation of ΔJ_{pl}. Hence the ΔJ evaluated using envelope curve, after 1st cycle is larger than the actual ΔJ if evaluated from that cycle loading branch. This leads to over estimation of the crack growth (see Figure 5.14).

In order to further understand the suitability of envelope curve usage and the plasticity ahead of crack tip under alternating and fully reversing loading, elastic plastic finite element analyses on a standard size CT specimen has been carried out. Figure 5.17, plots schematic of standard CT specimen, the FE mesh, loading and boundary conditions and gap-contact elements as used in the analyses. Full domain of CT specimen has been modelled using 8 nodded 2D plane strain elements. Gap-contact element has been used to model the mating crack surfaces (Figure 5.17). Both contactor and contacting surface are taken as deformable. These contact elements would simulate the crack closure. The stress strain curve of the SA333Gr6 material (Figure 3.4a), with multi-linear kinematic hardening rule has been used to model the material. The applied load (in y-direction) is distributed over 7 nodes on one end while the y-degree of freedom of the 7 symmetric nodes on the other side, have been fixed. All these 14 nodes are in a line. The x-direction is fixed at two nodes as shown in Figure 5.17. The analyses have been carried out for two loading conditions, one alternating cyclic load (load ratio, R = 0) and the other fully reversing cyclic load (load ratio, R = -1). Figure 5.18 plots the load versus pseudo time history for these two cases. The maximum loads in the two cases are kept identical.

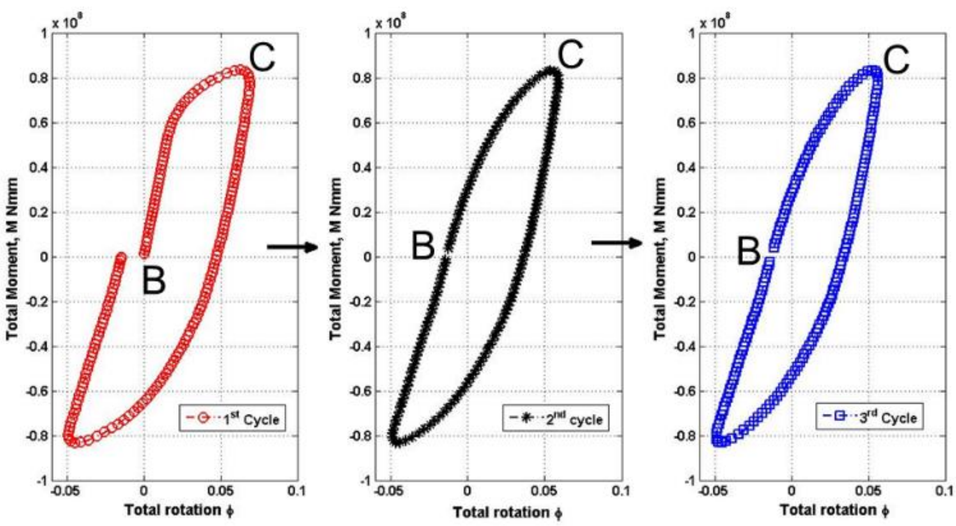

Figure 5.15: Load versus rotation for different loading cycles branch of envelop curve

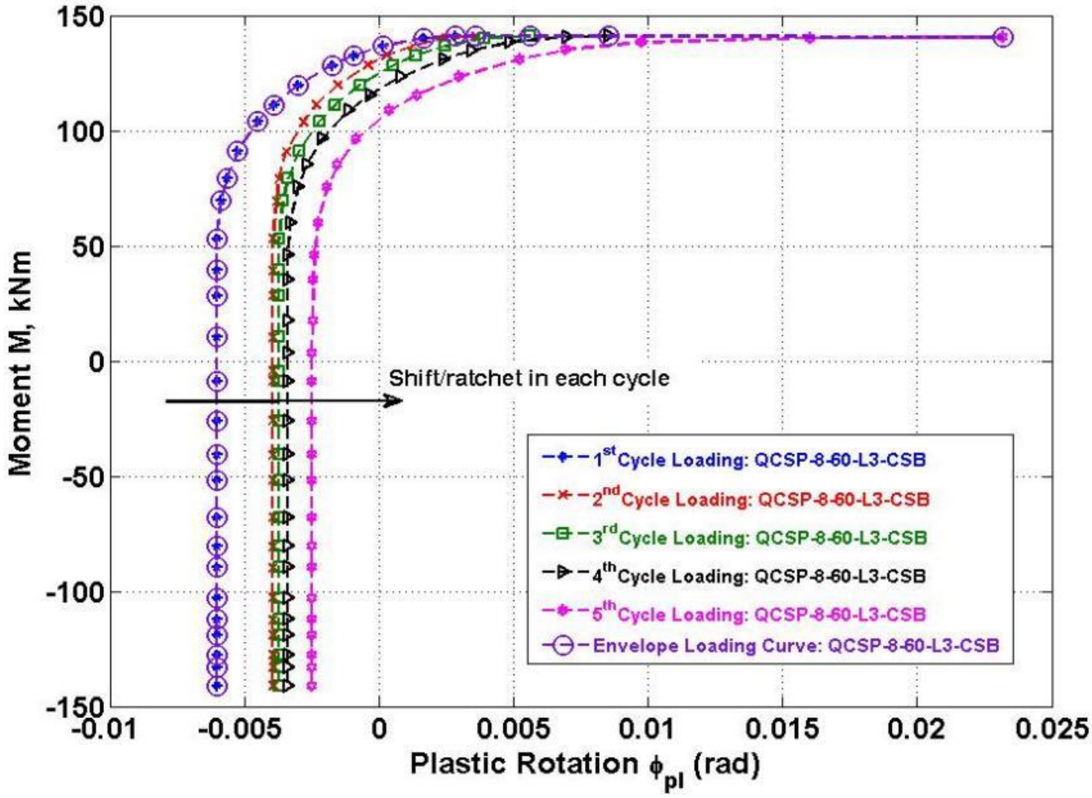

Figure 5.16: Load versus plastic load line displacement plot of different cycles loading branch and of envelop loading curve of QCSP-8-60-L3-CSB test used in cyclic ΔJ calculation

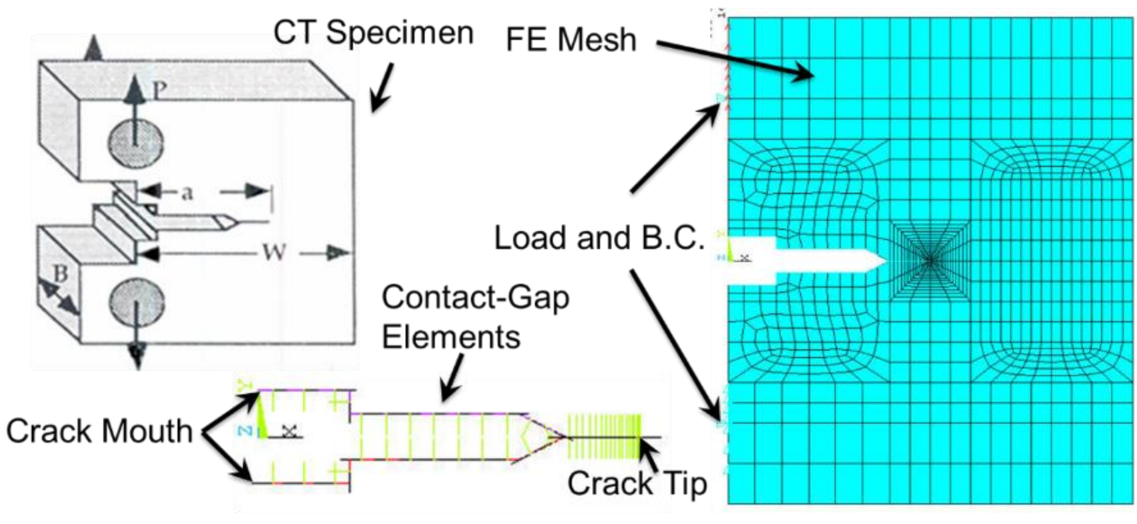

Figure 5.17: Schematic of CT specimen and the 2D finite element mesh along with gap-contact elements used for cyclic loading analyses

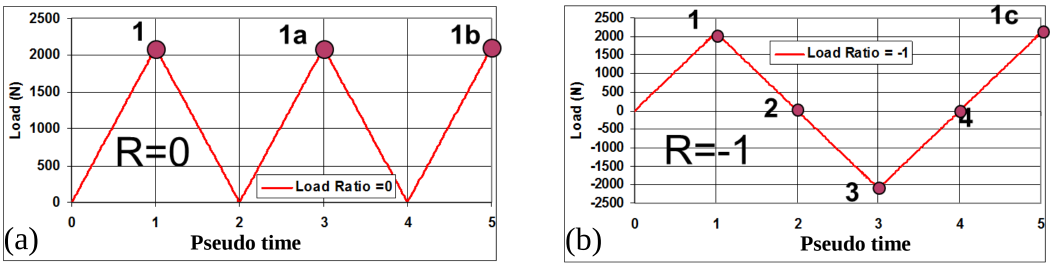

Figure 5.18: Load versus pseudo time history used in analyses (a) case-1 with load ratio R=0, (b) case-2 with load ratio R=-1

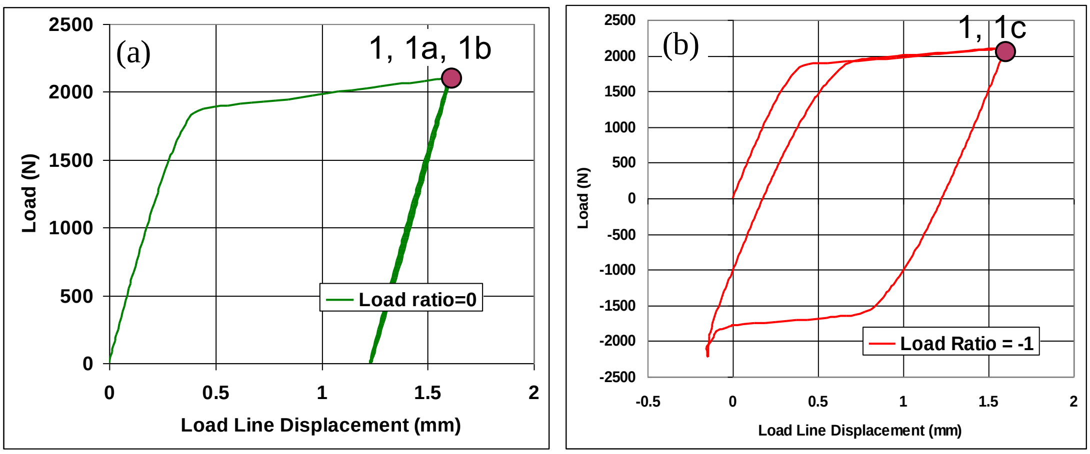

Figure 5.19: Load versus Load Line Displacement (a) for case-1 loading (Load ratio R = 0); (b) for case-2 loading (Load ratio R=-1)

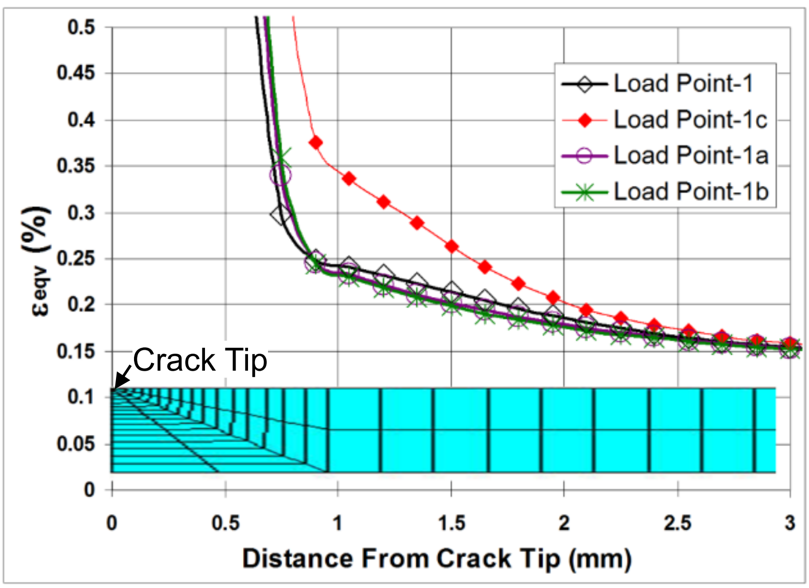

Figure 5.20: Plastic strain ahead of CT specimen crack tip at maximum load point under alternating and fully reversible cyclic loading

Figure 5.19 plots the load versus load line displacement response obtained respectively from the alternating and reversing cyclic loading schemes. It shows that the 1st load application (that is point-1), the unloading and repeat applications of load (point 1a, 1b and 1c); the load and LLD point is nearly same. However, in case of fully reversing loading, see Figure 5.19(b), the effect of crack closure and the shift in the loading branch can clearly be seen. Figure 5.20 plots the plastic strain variations ahead of CT specimen crack tip at different loading stages in both the loading cases. Following observation/conclusions are made from this:

(i) In case of the alternating cyclic loads, the plastic zone ahead of the crack tip remained nearly same on reloading to maximum load (see plot for point 1, 1a and 1b in Figure 5.20). Here on reloading the specimen to its previous maximum load level, the von-Mises plastic strains ahead of the crack in the specimen is nearly same as that before unloading. Hence, for R≥0, the envelope curve may be used to evaluate the J-integral and static tearing (as is done for monotonic fracture tests with partial unloading). Only precaution required is, if there are large numbers of unloading cycles then it is necessary to account for the fatigue crack growth.

(ii) For fully reverse loading, the CT specimen analyses has shown (see Figure 5.20) that the plasticity zone ahead of the crack tip is much larger than that before unloading. This shows that for R = -1 loading, the crack tip plasticity depends on each cycle of loading. Chang-Sung Seok et al. [71] has shown that for fully reversible loading i.e. R = -1, at the minimum load, the crack tip positive plastic strains due to previous tensile load vanishes, and the compressive plastic strains are generated at tip. On reloading to maximum load in tensile direction generates bigger plastic zone (tensile) ahead of the crack tip. Hence the crack growth assessment procedures which are based on M-ϕ envelope curve may not properly account for the elastic plastic unloading effects on crack tearing/damage on subsequent loading.

In view of above tests data and FE analyses of the CT specimen, the use of envelope curve for fracture assessment under fully reversible cyclic loading, is found unacceptable due to following reasons:

(a) The rightward shift/ratchet (in positive ϕ direction) of the loading branch of the M-ϕ hysteresis loop under repeated fully reversible cyclic loading is not accounted in the envelope M-ϕ curve approach.

(b) In case of fully reversible cyclic loading, the finite element study has shown that the crack tip plasticity and plastic zone under repeat application of load is much larger than that before unloading. This indicates increase in damage owing to reverse direction loading/unloading, on reloading up to the maximum load point and which may not be accounted in the envelope approach.

5.5 Development of a crack growth assessment procedure based on each cycle loading

The crack growth assessment of CSB pipe tests of current programme using envelope curve based procedure (section-5.3) are not in good agreement with measured values. The discussion in 5.4 has clearly shown that the use of envelope curve for simulating the fully reversible load tests is not justifiable and has no basis. In view of this, a procedure where crack growth evaluation in each cycle is based on its loading branch has been used. Here the crack growth is evaluated due to both the fatigue and the static tearing. The total crack extension in let us say ith cycle can be given by the following equation.

$$\left(\frac{da}{dN}\right)_i = \left(\frac{da}{dN}\right)_{i,fatigue} + \left(\frac{da}{dN}\right)_{i,tearing} \tag{5.12}$$

The fatigue crack growth, is evaluated using the widely accepted cyclic Dowling's cyclic J-integral range (ΔJ), while the static tearing crack growths is evaluated using a cyclic J′-integral described in section 5.5.2. Both the ΔJ and J′ integrals are evaluated for each loading cycle in place of envelop curve. The each loading cycle based calculations is used due to following reasons:

(a) In previous section, it is shown that the M-ϕ envelope curve based assessment leads to overestimation of ΔJ and hence over predicts the crack growth. Hence for fatigue crack growth assessment, the ΔJ is evaluated for each loading cycle as given in section 5.5.1

(b) The static tearing crack growth is based on J-integral which, in turn, depends on the plastic-strain field ahead of crack tip. The finite element studies on CT specimen under reversible cyclic loading, (see section 5.4) has shown that, for fully reversing load (load ratio = -1, as for the tests in current program) the crack tip plasticity and plastic zone, is much larger than that before unloading. This shows that for R = -1 loading, the crack tip plasticity is strong function of unloading and depends on each cycle loading cycle. Hence the static tearing crack growth is calculated for each cycle of loading, using a new proposed J′-integral as described in section 5.5.2

5.5.1 Crack growth due to fatigue using ΔJ integral

The fatigue crack growth calculations have used the ΔJ_i integral evaluated from each cycle loading as described below:

$$\Delta J_i = \Delta J_{i,el} + \Delta J_{i,pl} \tag{5.13}$$

Here the $\Delta J_{i,el}$ and $\Delta J_{i,pl}$ are elastic and plastic part of the total ΔJ_i integral. The elastic part $\Delta J_{i.el}$ is evaluated as given below:

$$\Delta J_{i,el} = f_b^{\,2}\left(\frac{\theta}{\pi}\right)\left(\frac{\Delta M_i^{\,2}}{ER^3\,t^2}\right) \tag{5.14}$$

The f_b is function of pipe and crack geometry and is evaluated using equations given by Zahoor [32]. ΔM_i is the moment range that is the difference of M_i^{max} and M_i^{min}. For the ith cycle, ΔJ_{pl}-integral is calculated using the loading branch of ith cyclic hysteresis M-ϕ_{pl} loop, i.e. from minimum load point ‘A’ to the maximum load point ‘C’ of loading branch (see Figure 5.21).

$$\Delta J_{i,pl} = \int_{\phi_{pl,i}^{min}}^{\phi_{pl,i}^{max}} \eta\, \Delta M d\phi_{pl} + \int_{\theta_{i-1}}^{\theta_i} \gamma \Delta J_{pl} d\theta \tag{5.15}$$

Where the $\phi_{i,pl}^{min}$ and $\phi_{i,pl}^{max}$ are the crack plastic rotations corresponding to starting and end point of the loading branch of ith cycle hysteresis loop. The Eqn.(5.15) of $\Delta J_{i,pl}$ is a non-linear equation and cannot be solved explicitly because of the second term. Within a cycle, the continuous variation of the half crack angle ‘θ’ with ‘ϕ_{pl}’, is unknown. However, the crack growth per tip in each cycle is known. If the crack growth within a cycle is small enough, then the equation for ΔJ_{pl} can be simplified as given below:

$$\Delta J_{i,pl} = \int_{\phi_{pl,i}^{min}}^{\phi_{pl,i}^{max}} \eta\, \Delta M d\phi_{pl} + \Delta J_{i,pl} \int_{\theta_{i-1}}^{\theta_i} \gamma d\theta$$

$$\Delta J_{i,pl} = \eta(\theta_i) \times \Delta U_i + \Delta J_{i,pl} \times \gamma(\theta_i) \times (\theta_i - \theta_{i-1})$$

$$\Delta J_{i,pl} = \frac{\eta(\theta_i) \times \Delta U_i}{1 - \gamma(\theta_i) \times (\theta_i - \theta_{i-1})} \quad (5.16)$$

Where the $\eta(\theta_i)$ and $\gamma(\theta_i)$ is evaluated using Eq.(4.5 and 4.6) and the ΔU_i is the area under the loading branch for the i^{th} cycle of the M –Φ_{pl} record.

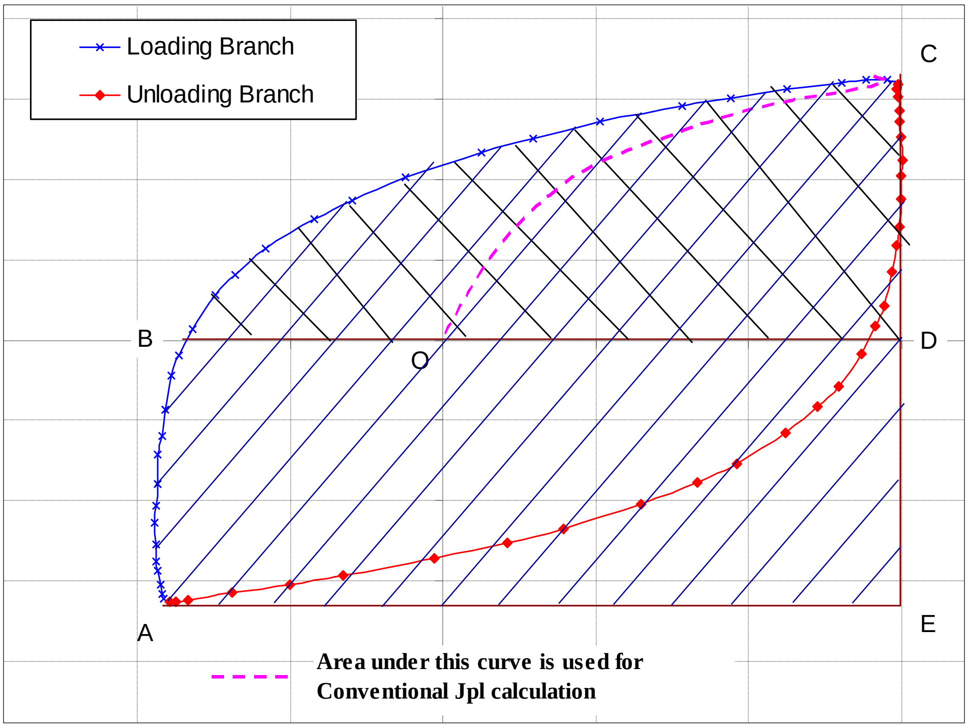

Figure 5.21: A typical moment versus plastic crack rotation hysteresis showing points A, B and C in loading path of i^{th} cycle

In Figure 5.21, ΔU_i is the area ABCDEA under the curve ABC from minimum load point ‘A’ to the maximum load point ‘C’. It is evaluated using equation given below:

$$\Delta U_i = \int_{\phi_{pl,i}^{min}}^{\phi_{pl,i}^{max}} \Delta M d\phi_{pl} \quad (5.17)$$

$$\Delta M = M - M_i^{min} \tag{5.18}$$

The M is the moment at a point in loading branch. The total ΔJ_i integral is evaluated using Eqn. (5.13 to 5.18). Then using this ΔJ_i integral, the fatigue crack extension, $(da/dN)_{i,fatigue}$ is evaluated using following equation which has been obtained from the Eqn. (5.1) and Eqn. (5.2) of section 5.3.

$$\left(\frac{da}{dN}\right)_{i,fatigue} = C\left(\sqrt{\Delta J_i E}\right)^m \tag{5.19}$$

5.5.2 Crack growth due ductile tearing using a cyclic J′ integral

A new cyclic J′-integral has been used which is calculated cycle-by-cycle from the positive half of the Moment – rotation ϕ_{pl} hysteresis. For ith the cycle J_i' is evaluated as given below

$$J_i' = J_{el,i}' + J_{pl,i}' \tag{5.20}$$

$$J_{el,i}' = f_b^2\left(\frac{\theta_i}{\pi}\right)\left(\frac{M_i^2}{ER^3t^2}\right) \tag{5.21}$$

The $J'_{i,pl}$ integral is calculated using η and γ factors from the positive part of loading branch that is from zero load point ‘B’ to the maximum load point ‘C’ of ith cycle M-ϕ_{pl} hysteresis (see Figure 5.21).

$$J'_{i,pl} = \int_{\phi_{pl,i}^{M=0}}^{\phi_{pl,i}^{max}} \eta\, M d\phi_{pl} + \int_{\theta_{i-1}}^{\theta_i} \gamma J'_{pl} d\theta \tag{5.22}$$

Where the $\phi_{i,pl}^{M=0}$ and $\phi_{i,pl}^{max}$ are the crack plastic rotations corresponding to zero moment and end point (that is maximum moment) of the loading branch of ith cycle hysteresis loop.

The Eqn.(5.22) of $J'_{i,pl}$ is a non-linear equation and cannot be solved explicitly because of the second term. However, similar to the section 5.5.1, this equation can be simplified to as given below:

$$J'_{i,pl} = \frac{\eta(\theta_i)\times U_i}{1-\gamma(\theta_i)\times(\theta_i-\theta_{i-1})} \tag{5.23}$$

Where the $\eta(\theta_i)$ and $\gamma(\theta_i)$ are evaluated using Eqns.(4.5 and 4.6) and the U_i is the area under the positive half of the loading branch for the ith cycle of the M –Φ_{pl} record of loading branch. The area under the positive part of loading curve, that is BC (see Figure 5.21) over the zero load line, is designated as energy U_i. It is evaluated using equation given below:

$$U_i = \int_{\phi_{pl,i}^{M=0}}^{\phi_{pl,i}^{max}} M d\phi_{pl} \tag{5.24}$$

The M is the moment at a point in loading branch. In Figure 5.21, it may be observed that the area 'BCDB' is more than the area 'OCDO' which one would have used in envelope curve based J_{max} integral calculation. The additional area is coming due to reversible loading which seems to account for the damage due to compressive loading.

The total J'_i integral is evaluated using Eqns. (5.20 to 5.24). Then the crack extension owing to ductile tearing in ith cycle, has been evaluated using the J'_i integral along with the monotonic fracture resistance i.e. J-Δa curve. Here if the J'_i is less than the J-initiation then there will not be any growth due to ductile tearing. However the crack will grow only due to fatigue. The monotonic J-R curve equation used is as given below:

$$J'_R = 230 + 1000\ (\Delta a)^{0.51} \tag{5.25}$$

Using Eqn. (5.12, 5.19, and 5.25), the total crack growth in i^{th} cycle may be written as

$$\left(\frac{da}{dN}\right)_i = C\left(\sqrt{\Delta J_i E}\right)^m + \left(\frac{J_i' - 230}{1000}\right)^{1/0.51} \quad (5.26)$$

It may be noted here that the second term on right hand side of above equation assumes that tearing crack growth start from the initiation toughness each cycle. Then the total crack size at end of i^{th} cycle will be given as

$$a_i = a_{i-1} + \left(\frac{da}{dN}\right)_i \quad (5.27)$$

The crack growth assessment of all the four number of carbon steel load controlled cyclic tearing tests have been carried out using the above procedure and equations, Eqn.(5.12 through 5.27). The crack growth versus number of cycles as predicted using above procedure and as measured from the experiments have been plotted in Figure 5.22 and Figure 5.23. These figures show that the crack growth predicted using above proposed equation and those measured during tests are in good agreement. This shows that the proposed analyses procedure which considers the M-ϕ loading curve of each cycle (not based on envelope curve) and also accounts for the crack growth due to both fatigue (under large scale yielding) and ductile tearing mode is reasonable and may be used for assessment cyclic tearing. However it is still not useful for analytical assessment since it required assessment of J' and ΔJ integrals. This requires generation of the cycle by cycle M-ϕ hysteresis curves by carrying out non-linear finite element analysis with simulation of crack extension (as evaluated by Eqns.(5.26 and 5.27) after each cycle.

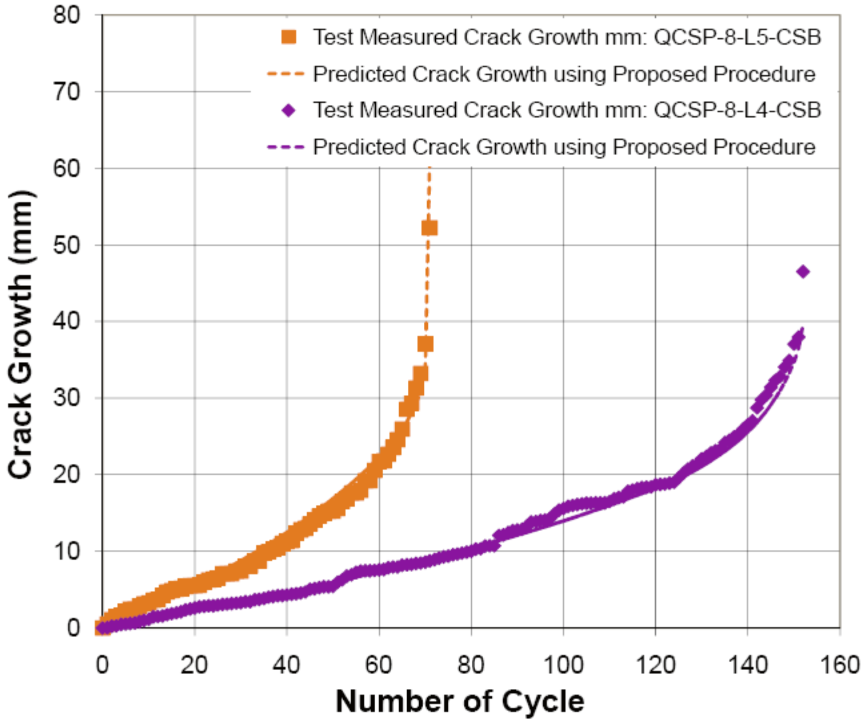

Figure 5.22: Predicted crack growth using proposed method versus test measured crack extensions

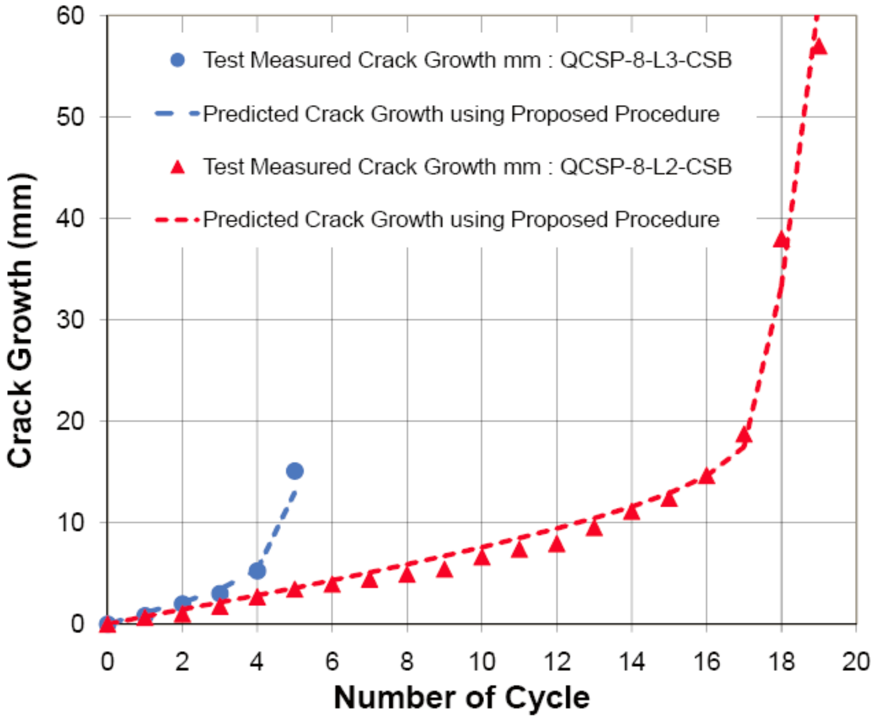

Figure 5.23: Predicted crack growth using proposed method versus test measured crack extensions

5.6 Instability Criteria for load controlled Tests

For load controlled cyclic tearing tests, peak load versus measured crack size were investigated along with monotonic load versus measured crack size. Figure 5.24 plots result from 5 load controlled cyclic tearing tests and 3 monotonic fracture tests on same material and size of pipes. A monotonic failure curve is plotted by joining the maximum load point of the 3 monotonic fracture tests which were conducted by Chattopadhayay et al [107], on the identical pipes except the initial crack size. This figure clearly shows that there is large crack growth in cyclic tests before the instability point. However in monotonic tests, there is very small crack growth up to the maximum moment (instability load). Further it also shows that the instability point of cyclic tearing tests lie close to the monotonic failure line. Hence, instability occurs when the current crack size 'a_i' in cyclic tests reaches a critical size 'a_c' for the given loading amplitude and evaluated using monotonic instability assessment. In term of load it also can be written as below

$$M_{max,\ cyclic\ load} \geq M_{Monotonic\ Capacity}(a_i) \qquad (5.28)$$

Here the a_i is the crack size in i^{th} cycle of loading and may be evaluated using Eq. (5.26 and 5.27). It includes the crack growth due to fatigue and ductile fracture as well as their synergistic damage.

The step by step procedure of assessment of cyclic tearing stability is explained in flow chart as given in Figure 5.25. Here the $M_{max,\ cyclic\ load}$ is the magnitude of reversible bending moment applied to cracked pipe. a_i is the crack size at the end of i^{th} cycle, for 1^{st} cycle calculation the initial crack size, $a_{0,}$ and the $M_{monotonic\ capacity}$ of the crack pipe evaluated using standards and established methods.

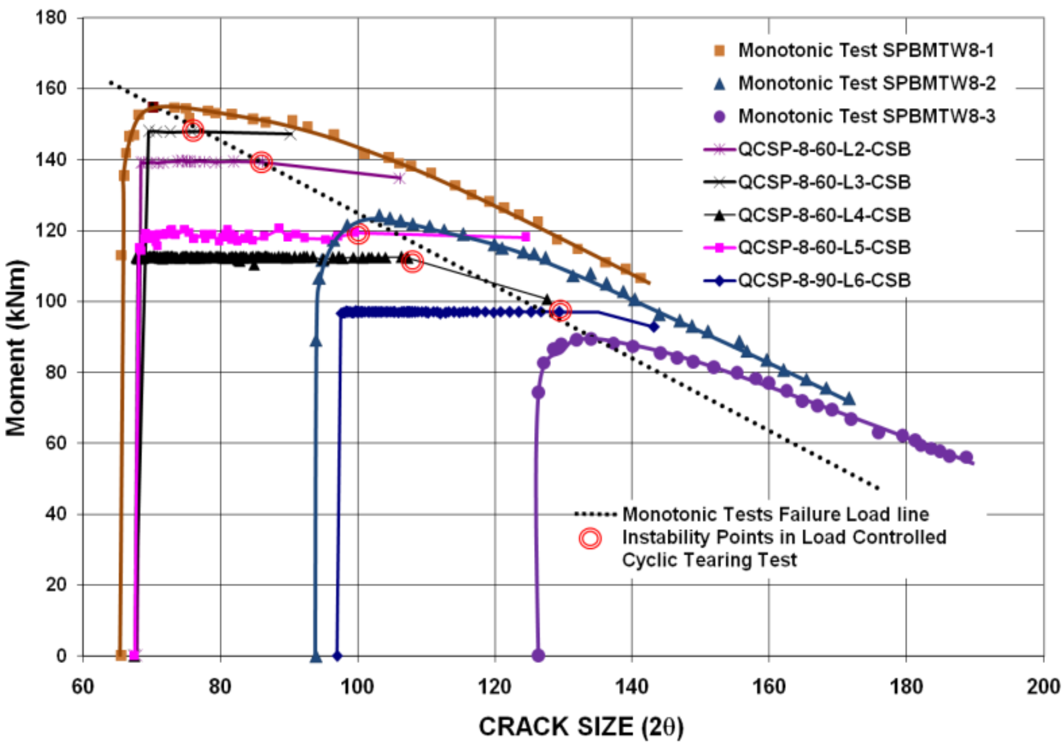

Figure 5.24: Loading versus Crack Extension from Cyclic Tearing and Monotonic Fracture Tests

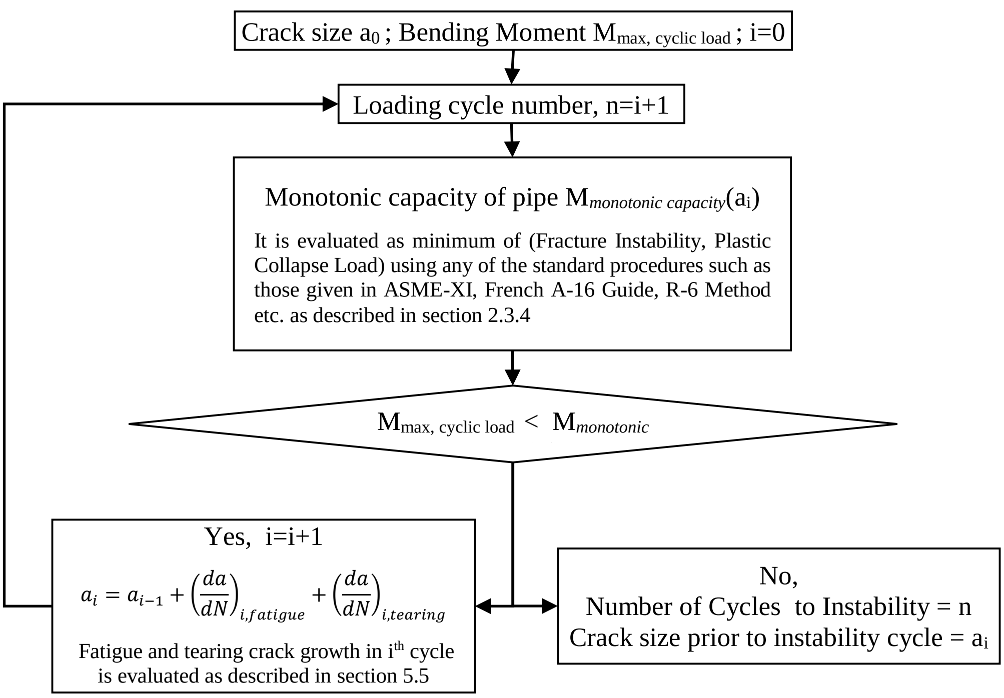

Figure 5.25: Flow chart showing the stability assessment under reversible cyclic loading conditions

5.7 Chapter conclusions

The investigations carried out to study pipe fracture behaviour under load controlled cyclic loading have revealed the following:

(a) Pipe fracture tests showed that under load controlled reversible cyclic loading, the unstable tearing leads to DEGB like failure of pipe in very few cycles (10-20) when the applied moment magnitude are 80 to 90% of the critical moment of the pipe obtained from monotonic fracture tests on identical pipe.

(b) Significant crack growth by fatigue and stable tearing precedes the instability. The crack growth increases with number of cycles which, in turn, reduces the size of load bearing ligament (cross section). After certain number of cycles, the load bearing section becomes critical resulting in unstable tearing failure.

(c) The number of cycle to unstable failure of pipe, N_f, and the stable crack growth, Δa_f increase with decrease in the amplitude of moment

(d) Under identical loading conditions on identical pipe, the crack located in SSW undergoes larger tearing/ crack growth compared to when same crack is located in base metal or in NGW weld. The number of cycles to instability is found higher in case of NGW welded pipes as compared to SSW welded pipes.

(e) The number of cycles to unstable failure of pipe depends on both the maximum moment and the load ratio. Significant reduction in number of cycles is observed in the tests for same maximum moment but with larger compressive load in reverse direction (larger negative load ratio). This is due to significant reversible/compressive plasticity that leads to significant damage ahead of crack. The compressive stress ahead of crack are known to re-sharpen the blunted crack tip, flatten the rounded voids and hence accelerates the process of void coalescence, thus leading to accelerated the tearing in subsequent load cycles. These apparently accelerate the fracture process in subsequent tensile portion of the loading cycle leading to additional crack growth.

(f) The analysis of load controlled cyclic tearing tests on carbon steel pipes using J_{max} and ΔJ integral evaluated from load-displacement envelope curve, proposed by Miura/CRIEPI program has shown that:

(i) The $\Delta J/J_{max}$ ratio, in addition to a/a_o as proposed in CRIEPI program, is found to depend on loading history also.

(ii) The $\Delta J(\Delta a) \geq J_R(\Delta a)$ criterion is unable to predict instability in the tests.

(iii) The use of envelop curve based ΔJ-integral overestimated the crack growth.

(g) The correctness of uses of envelope curve under alternating (load ration >0) and fully reversing loading (load ration = -1) is investigated using the test data and a nonlinear 2D finite element analysis on standard CT specimen geometry. The study has revealed that:

(i) In case of repetitive alternating cyclic loading (load ratio ≥0), the plastic strain field ahead of the crack tip remained nearly same on reloading to the maximum load. Hence envelope curve is justifiably used to evaluate the J-integral.

(ii) For reversed loading, (load ratio = -1) the plastic zone ahead of the crack tip on reloading to maximum load, is much larger than that before unloading. This indicates increased damage owing to unloading followed by reverse direction loading. The envelope approach doesn't account for this damage.

(iii) Further from test data (for load ratio =-1) studies it has been observed that there is ratchet/shift of zero load displacement (loading branch of load displacement hysteresis) in crack opening direction. The envelop curve procedure does not account for this and so leads to overestimation of ΔJ and crack growth.

(h) A crack growth assessment procedure under reversible cyclic loading is proposed where contributions of both fatigue and static ductile tearing are considered. The cycle by cycle crack growth, evaluated using this procedure is found to be in good agreement with the test results.

(i) An instability criteria and an algorithm is developed to evaluate number of loading cycles to unstable failure of a cracked pipe when it is subjected to fully reversible load controlled cyclic load.

6 Development of a Cyclic Tearing Failure Assessment Diagram (CTFAD) and a proposal for stability assurance for LBB analysis of nuclear piping

6.1 Introduction

This chapter deals with the existing safety margins and methodology used in designing pressurised piping for leak before break (LBB) condition, the neglect of cyclic tearing aspect (as encountered during earthquake) in stability demonstration of leaking pipes and finally development of a new proposal for stability assurance of nuclear piping for LBB analysis accounting for the cyclic tearing effect, based on exhaustive experimental data generated in the present study.

As described in section 2.2.2 , the most important and indispensable requirement for LBB is the stability demonstration of a leaking pipe under design basis loading (generally SSE loads). The piping is designed for at least 10 numbers of equivalent maximum stress cycles per earthquake [21], while the LBB level-3 stability demonstration of through wall cracked pipe is done only for one cycle where the analyses are based on monotonic fracture / plastic collapse failure modes and the equivalent maximum stress (load) is taken as a one-time applied load. The reversible cyclic loading has extremely deleterious influence on the crack tearing and stability behaviour of pipe (see section 2.4). From detailed literature survey (see Chaper-2), it is concluded that the cyclic nature of earthquake load and associated Cyclic-Tearing failure mode (tearing-fatigue regime) are not explicitly considered while demonstrating fracture stability of a through wall cracked pipe during LBB analysis using current LBB guides/practices.

In view of above, detailed investigations have been carried out to develop an independent alternative assessment approach to consider the effect of cyclic tearing damage for a specified number of cycles of a cyclic loading event (e.g. earthquake) and which could directly be implemented in existing fracture stability assessment procedures. The main objectives of the present investigations are:

(i) To single out the contribution of cyclic nature of loading on reduction in fracture load carrying capacity of a cracked pipe.

(ii) To quantify the reduction factor as function of number of load cycles.

The work presented in this chapter is an effort in this direction and aimed at developing an easily implementable method to demonstrate stability against cyclic tearing mode of failure. The outline of the work reported in this chapter is:

(i) Relational investigation on the load controlled cyclic tearing and corresponding monotonic fracture tests and quantification of the deleterious impact of cyclic nature of loading on the stability of a cracked pipe in terms of a load reduction factor.

(ii) Development of cyclic tearing failure assessment diagram (CTFAD) and a cyclic tearing based stability analysis method to account for the cyclic tearing damage into stability assessment of a cracked pipe

(iii) To understand the existing safety margins and stability assessment practiced in LBB analysis during the design of primary heat transport piping components of Nuclear Power Plant (PHWR / PWR). To develop a safety margins / procedure in combination of the existing ones for LBB demonstration taking into account the number of cycles and cyclic tearing damage.

6.2 Load capacity reduction factor (β)

The investigations reported in chapter-5 has clearly shown that load controlled cyclic loading may lead to unstable tearing resulting in DEGB like failure of pipe in 10-20 cycles, even when the applied load magnitude is much below the critical load of the cracked pipe. This aspect has also been observed in the IPIRG and CRIEPI programme.

In order to develop correlations between the fracture stability, the applied load magnitude and the number of cycles, the load-controlled cyclic tearing test results (see Table 3.7) were investigated. The objective here is to develop a parameter which accounts for the cyclic damage and may facilitate inclusion of load cycles as one of the parameters in fracture integrity assessment. The load controlled tests on carbon steel and stainless steel pipes (both base and weld) have been investigated in relation to the corresponding monotonic fracture experiments conducted on identical pipe. For each of the load controlled cyclic tearing tests, having load ratio of -1 (Table 3.7), a load reduction factor (β-factor) has been evaluated. The load reduction factor, β-factor, is defined as ratio of maximum bending moment of reversing cyclic applied in load controlled cyclic tearing test to bending moment capacity (peak bending moment) obtained under monotonic loading condition as recorded in monotonic fracture test on identical pipe, see equation given below:

$$\beta = \frac{M_{\text{max, Cyclic Load}}}{M_{\text{Monotonic Capacity}}} = \frac{M_{Max}}{M_{Crit}} \qquad (6.1)$$

Where, the $M_{\text{max, cyclic Load}}$ (or M_{Max}) is the maximum moment applied in the load controlled cyclic tearing test. The $M_{\text{Montonic Capacity}}$ (or M_{Crit}) is the monotonic load capacity which is equal to the maximum moment that can be taken by an identical pipe (having same nominal size, thickness, crack size, material and heat of material) under application of monotonically increasing load. The definition of β-factor is based on monotonic capacity because in current pipe integrity assessment procedure, engineers adopt failure assuming monotonic load as basis of evaluation, [7-8, 32-42].

Review of technical literature, codes, guides such as GE/EPRI [32, 33], R-6 [8], A-16 [7], EPRI reports [36-37] shows that monotonic moment capacity ($M_{Crit.}$) is based on minimum of the ductile fracture and plastic collapse load. These, in turn, can be evaluated using macroscopic material properties like strength or fracture resistance curves (J-R curves), for a given cracked pipe. The material properties are usually based on specimen tests. M_{Crit} evaluated using these methods may be inaccurate with respect to experimental value owing to combination of following reasons:

(a) Variation in fracture properties owing to differences in size and geometry of specimens and components pipes (transferability from specimens to pipes of different sizes).

(b) Approximation in procedures used for evaluation of failure load (plastic collapse or J-tearing analysis).

(c) Uncertainties in material tensile and fracture properties which, in turn, are attributed to intrinsic randomness (or scatter band) of properties and heat to heat variability.

In order to overcome above listed aspects, codes or standards or guides have suggested suitable factor of safety, to be used for fracture integrity or LBB assessment.

In the present study, in order to have accurate and reliable quantification of β factor, the M_{Crit} moment was taken equal to $M_{Max}^{Monotonic\ Test}$, which is directly obtained from the monotonic fracture tests conducted on identical pipe as described earlier. The β-factor has been evaluated for all the load control cyclic tearing tests conducted with load ratio -1.

Despite the fact that the cyclic tearing and corresponding monotonic test were conducted on pipes having same material and same nominal diameter and thickness, however the actual measured diameter and thickness, of as received pipes differ slightly from one pipe to another (see corresponding tests in Table 3.3 through Table 3.4). Although the differences in most cases are small but still their effect on β-factor was further minimized by appropriate scaling based on the observed fact that the M_{Crit}, in case of circumferentially cracked pipes, is approximately proportional to product R^2 t [108, 109]. Here 'R' is mean radius of pipe and 't' is the pipe wall thickness.

In addition, there are small differences in the initial crack size (due to differences in fatigue pre-cracking crack extension, see Table 3.5 through Table 3.6) of corresponding pipes subjected to cyclic tearing and monotonic fracture tests. Although the difference is very small however, even its effect on β-factor was largely minimized by considering the ratio of crack weakening function, h(θ), of circumferentially through wall cracked pipes. The h(θ) is given as follows [7-8, 32-42]:

$h(\theta) = \cos(\theta/2) - 0.5\sin(\theta)$; where, θ is half crack angle

Although very small / insignificant but above corrections are accounted and the β factor, of all load controlled cyclic tearing tests having load ratio -1 (in all 24 numbers of tests) is evaluated. The β-factor (multiply by 100 to get %) has been studied with the number of cycles to unstable failure, N_f , of the pipe. Here, the N_f is the number of cycles at which the pipe was unable to take applied load and failed by unstable tearing as can be seen in Figure

5.4. The Figure 6.1 plots the bar charts of the calculated load factor, β-factor (in %), along with the number of cycles to instable failure, N_f for all the load controlled (load ratio=-1) cyclic tearing tests on carbon steel base (CSB) and girth welded (CSW) 8″, 12″ and 16″ size pipes. Figure 6.2 plots similar bar charts for stainless steel base (SSB) and conventional girth welded (SSW) 6″pipes and Figure 6.3 for stainless steel base narrow grove hot wire full GTAW girth welded (NGW) 6″ and 12″ size pipes. These plots show that in all the tests on five material categories and four different pipe sizes, a correlation / trend between the β-factor and N_f exists. The N_f increase with the decrease in β-factor. The increase in N_f becomes steep when β-factor is the below 70%. This aspect is further studied in next section.

In addition to results of test conducted under this programme, the load reduction factor (β-factor) is also evaluated from the tests results of 6 numbers of similar cyclic tests conducted under CRIEPI, Japan, [62-65] programme. The Japanese tests were on carbon steel pipes (grade STS 410), having nominal pipe size of 4″ NB Sch.80 (outer diameter = 114.13 mm and thickness = 8.6mm) and having circumferential full crack sizes of 30° and 60°. These tests were conducted on base material. The details of cyclic and corresponding monotonic fracture tests [62-65] considered are given in Table 6.1 and Table 6.2. The β-factors for all these Japanese tests have been evaluated and plotted in Figure 6.4 along with the N_f. The figure also shows a definite trend between the β-factor and N_f and is in agreement with above observations from current programme tests.

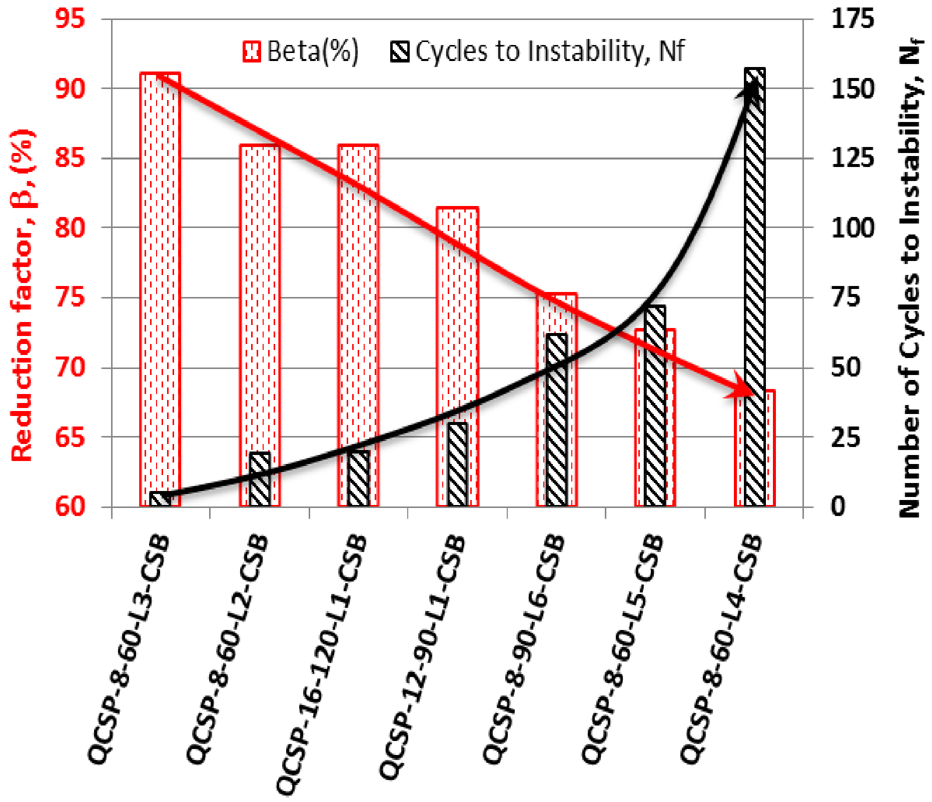

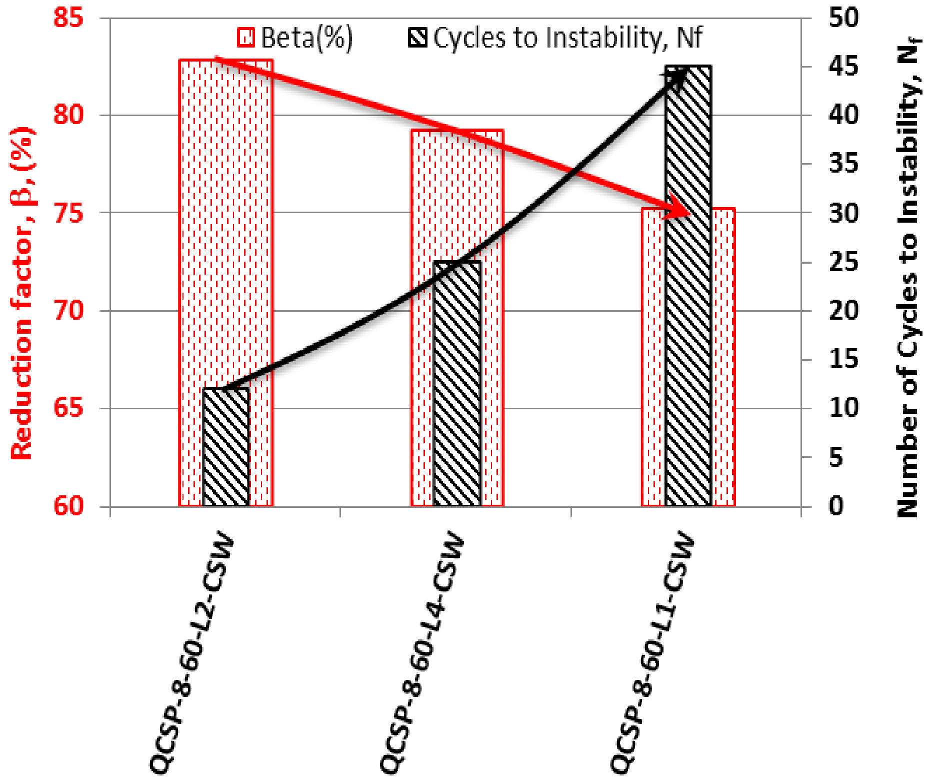

Figure 6.1: The load factor, β, and the number of cycles to instability as obtained in load controlled cyclic tearing tests on carbon steel base (CSB) and girth welded pipes (CSW)

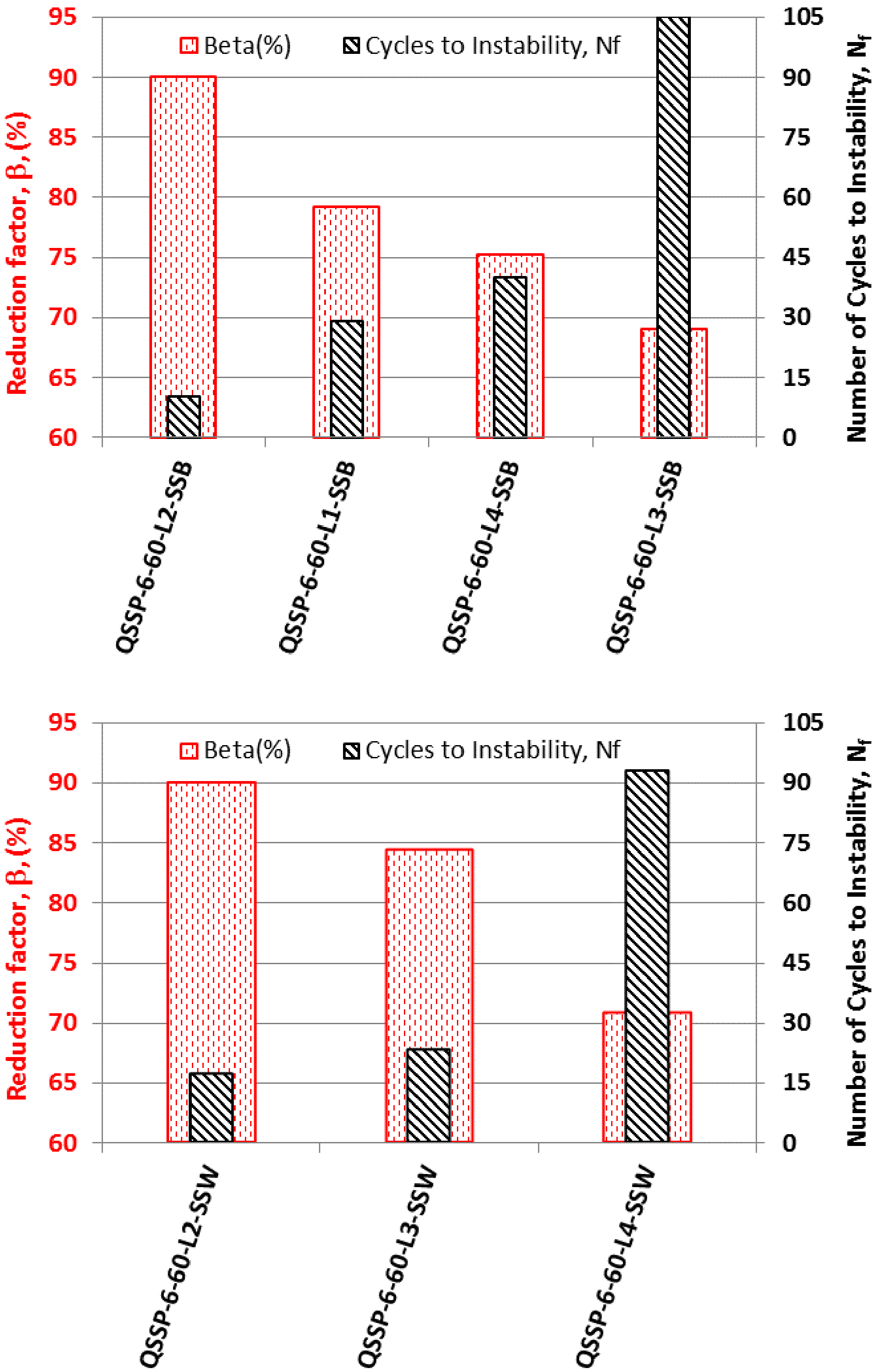

Figure 6.2: The load factor, β, and the number of cycles to instability as obtained in load controlled cyclic tearing tests on stainless steel base (SSB) and girth welded pipes (SSW)

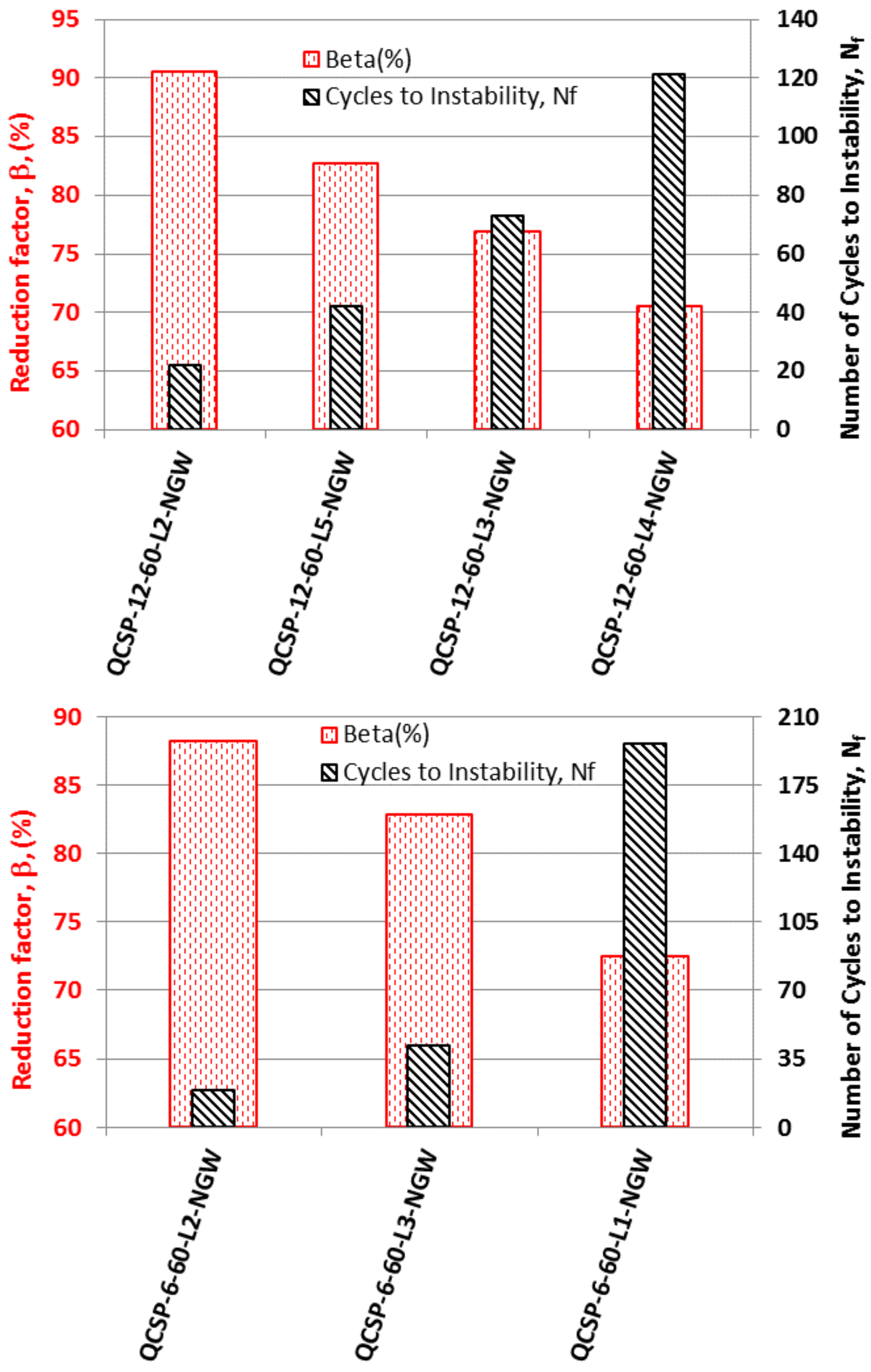

Figure 6.3: The load factor, β, and the number of cycles to instability as obtained in load controlled cyclic tearing tests on stainless steel narrow gap, full GTAW girth welded 6″ and 12″ size pipes (NGW)

Table 6.1: Geometry and loading details of monotonic fracture tests, at room temperature, corresponding to cyclic fracture tests reported in Table 6.2

Sr. No.	Test No.	Material	Crack Location	D_o, mm	Thickness, t mm	Half crack angle,θ (deg.)	Recorded Max. Moment, $M_{max}^{Monotonic\ Test}$ (or M_{crit}) (kNm)
1	M-1	STS410	Base	114.13	8.6	15.0	34.98
2	M-2	STS410	Base	114.13	8.6	30.0	29.04

Note: Tests data shown in above table is taken from by Miura et al [62];

Table 6.2: Geometry and loading details of the load controlled cyclic tearing Tests at room temperature

Sr. No	Test No.	Material	Crack Location	Do (mm)	Thickness t (mm)	Half Crack Angle θ, (deg.)	Maximum Moment applied in each cycle M_{max} (kN.m)	Load Ratio, R	Cycles to Instability, N_f
1	C-I	STS410	Base	114.13	8.6	15	29.7	-1	29
2	C-2	STS410	Base	114.13	8.6	15	26.56	-1	67
3	C-4	STS410	Base	114.13	8.6	30	26.07	-1	19
4	C-5	STS410	Base	114.13	8.6	30	23.43	-1	47
5	C-6	STS410	Base	114.13	8.6	30	20.96	-1	97
6	C-7	STS410	Base	114.13	8.6	30	20.13	-1	108

Note: Tests data shown in above table is taken from by Miura et al [62];

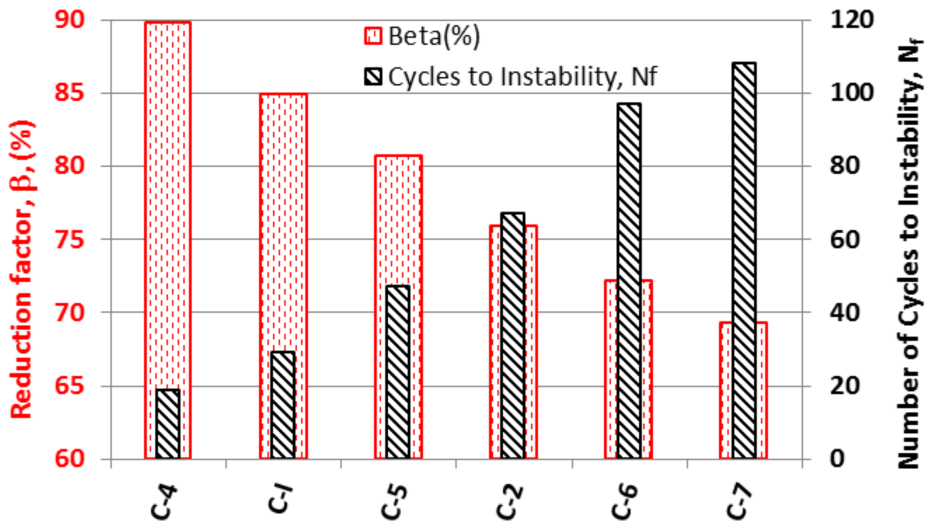

Figure 6.4: The load factor, β, and the number of cycles to instability as obtained from load controlled cyclic tearing tests of CRIEPI Programme [62-65]

6.3 Cyclic Tearing Failure Assessment Diagram (CTFAD)

The above section has described evaluation of the parameter named as load reduction factor (β-factor), directly from the cyclic tearing and corresponding monotonic fracture tests. It also has shown existence of a definite trend / correlation between β and N_f, that is number of fully reversible load cycles the pipe took before instability/unstable tearing failure.

Taking into account above corrections, the β factor, of all load controlled cyclic tearing tests having load ratio -1 (in all 24 number of tests) is plotted against the number of load cycles to instable failure (N_f), as shown in Figure 6.5. This plot has been named as "Cyclic Tearing Failure Assessment Diagram" (CTFAD). The CTFAD plot shows that initially β factor reduces rapidly with number of cycles (up to about 25 numbers of cycles). This is followed by moderate rate of reduction from 25 to 75 numbers of cycles and then finally slow rate of reduction beyond 75 numbers of cycles. In initial regime till 25 cycles, ductile tearing dominates followed by combination of tearing-fatigue in moderate regime (25 – 75 cycles) and the finally fatigue in slow reduction rate regime (beyond 75 cycles). The transition from one regime to other is fairly smooth. In addition to results of test conducted under this programme, the CTFAD plot (Figure 6.5) also includes results of 6 numbers of similar cyclic tests conducted under CRIEPI, Japan, [62-65] programme. The β-factors for Japanese tests also fall in overall trend of CTFAD.

To summarize the above, the CTFAD plots β-factor variation with number of cycles. The β-factor is directly calculated from measured loads in the reversible cyclic loading (constant load amplitude) and corresponding monotonic loading tests on identical pipe (having same nominal size, same thickness, same crack size, same material and having same heat of material). No analytical modelling / analysis is involved in β-factor calculation. As described in section-3.3, wide variation in pipe size, crack size, material strength and material fracture toughness has been considered in test programme. These reasonably cover likely variations in LBB candidate piping of PHWR type NPPs and several of PWR type NPPs. It also included data from similar cyclic tests on Japanese carbon steel pipes from CRIEPI programme.

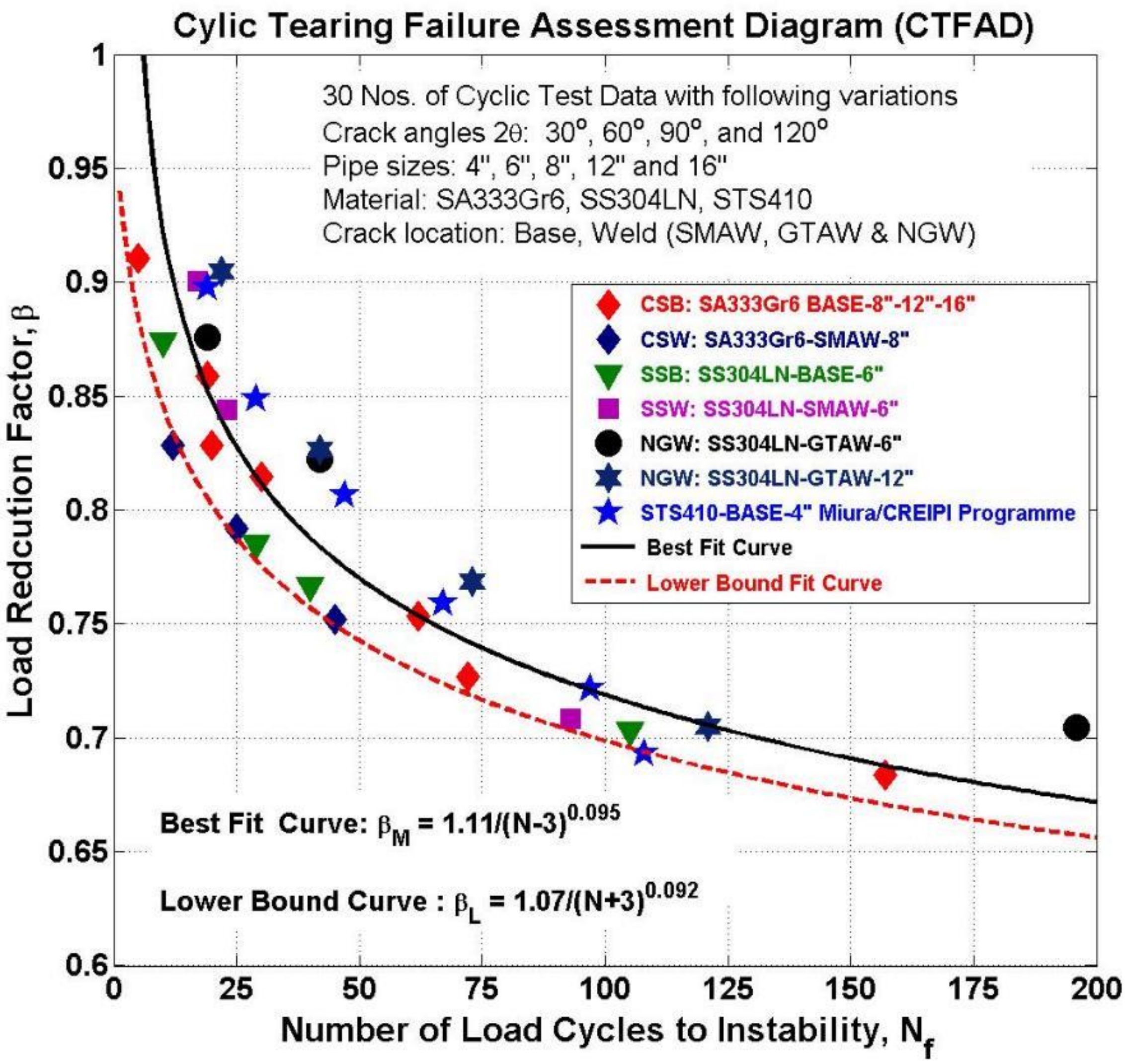

Figure 6.5: Cyclic Tearing Fatigue Assessment Diagram (CTFAD) for Cyclic tearing based stability assessment of through wall cracked pipe subjected reversing cyclic loads

Despite these large variations in crack sizes, pipe sizes, strength, fracture toughness, all the β-factor points evaluated for 30 numbers of load controlled cyclic tearing tests, lie in reasonable narrow band as presented in CTFAD (see Figure 6.5). This could be due to the fact that the β-factor is defined as ratio of load capacities of identical pipe (having same nominal size, thickness, crack size, material and heat of material) under cyclic and monotonic loading conditions. The impact of material strength, fracture toughness, crack size, pipe size etc., are obviated to a large extent. The β-factor quantifies the reduction in load capacity (under monotonic loading conditions) explicitly due to cyclic nature of loading for specified number of cycles.

CTFAD clearly shows that the cracked pipe subjected to cyclic loading will fail at load magnitude lesser than its maximum monotonic fracture load capacity. The number of cycles to failure would depend on the cyclic load magnitude in relation of monotonic load capacity (that is, β factor). Interpreting in other way leads to the conclusion that in order to ensure safety, it is essential to include number of cycles, in the loading event. This can easily be achieved by reading load reduction, β factor, from CTFAD plot corresponding to desired number of cycles. In order to facilitate this exercise, the CTFAD plot data were analysed and smooth curves were fitted to entire data. The best-fit curve (β_M versus N_f) and lower bound fit curve (β_L versus N_f) equations are as given below:

<u>Best-fit curve equation</u>: $$\beta_M = \frac{1.11}{(N_f - 3)^{0.095}} \tag{6.2}$$

<u>Lower Bound fit curve equation</u>: $$\beta_L = \frac{1.07}{(N_f + 3)^{0.092}} \tag{6.3}$$

Here β_M is load reduction factor corresponding to best-fit curve, that is, tending to median centred and β_L is load reduction factor from lower bound fit curve. All the data points do not lie on any single smooth curve**.** The observed scatter band is reasonably narrow and is attributed to effect of intrinsic scatter band in basic parameters responsible for fracture. Some of these are local variations in strength properties within the pipe and with respect to other pipes, local variations in micro-structural parameters like inclusion rating, secondary phase particle density and distribution etc. The narrow scatter band reinforces the fact that the CTFAD plot (or fitted curves) can be considered as reasonably material independent with respect to typical nuclear piping material specifications. However, consideration of lower bound curve for fracture stability analysis will account for this narrow scatter in the CTFAD data.

The lower bound CTFAD curve or the β_L equation proposed above is derived from the load controlled cyclic tearing tests at load ratio of -1. In case the load ratio is other than -1, then use of β_L equation would result in conservative assessment of load reduction factor. In the current programme, three numbers of load-controlled tests were conducted at load ratio (R) value other than -1. These are test nos. QCSP-8-60-L1-CSB (R= -0.5), QCSP-8-60-L3-CSW (R= -0.5) and QCSP-6-60-L1-SSW (R=-0.87). The β factor value evaluated using Eqn. (6.1) directly from results of these tests are 0.89, 0.83 and 0.89 respectively while those evaluated using Eqn. (6.3) corresponding to their failure cycles are 0.75, 0.71, 0.81 respectively. This clearly show that use of lower bound CTFAD curve equation for any of the load ratio is greater than -1 will lead to conservative assessment.

The use of proposed β-factor exclusively and solely accounts for the add-on damage owing to fatigue-ductile tearing synergy under reversible cyclic loading condition. The effects, if any, of other condition like temperature, pressure, loading rate , material, environment etc., shall be accounted in evaluation of monotonic critical loads(M_{Crit}) i.e. pipe load capacity under monotonic loading condition. The pressure load is an additional mechanical loading which does not change failure mode and is duly accounted in assessment of monotonic load capacity of cracked pipe. Any change in fracture toughness or failure phenomenon / mechanism owing to the loading rate (like during an earthquake event) and temperature condition, if present, is accounted in assessment of the monotonic load capacity. The IPIRG [13, 35, 53] program has shown weak interaction between the loading rate (dynamic effect) and cyclic effects and their effect on the J-R curve found nearly independent. In some temperature ranges, the fracture toughness may degrade due to dynamic strain ageing (DAS) [13, 58, 91]. Both the temperature and loading rate are not known to have any synergy with cyclic nature of loading resulting in enhanced add-on cyclic damage. Hence, the pressure /temperature /loading rate impact on β–factor obviates to a large extent owing to the fact that it is defined as ratio of load capacities under cyclic to monotonic loading under identical conditions. Hence on this basis the proposed lower bound β–factor (i.e. β_L) may be used for other conditions like temperature, pressure, loading rate, material, environment etc. if these are duly considered and accounted in evaluation of M_{Crit}. Despite this fact, use of CTFAD for materials and loading conditions which are grossly different than those included in present study – may be validated by conducting few component test .

6.4 Current LBB: safety margins in stability assessment

Currently, most widely used procedures for fracture stability and LBB assessments, are as proposed in documents like, NUREG-1061 [1], Standard Review Plan, Section 3.6.3 of NUREG-0800 [3], IAEA-TECDOC-710 and 774 [4, 5]. Russian LBB guide [6], French

A16 LBB Guide [7], and NUREG-6765 [13]. These documents recommend following safety margins for demonstrating level 3 LBB applicability against the normal operating plus design basis earthquake (like SSE) loads.

<u>Margin to Critical Crack Size</u>: Safety Factor (SF) of 2

Leakage Size Crack (LSC) $\times 2 \leq$ Critical Crack (for $\mathrm{M_{NOC}} + \mathrm{M_{SSE}}$) or

$$(\mathrm{M_{NOC}} + \mathrm{M_{SSE}}) < \mathrm{M_{Crit}} \text{ (at } 2\times\text{LSC)} \tag{6.4}$$

<u>Margin on Loads</u>: Safety Factor (SF) of √2

$$(\mathrm{M_{NOC}} + \mathrm{M_{SSE}}) \times\sqrt{2} < \mathrm{M_{Crit}} \text{ (at LSC)} \tag{6.5}$$

As per these procedures, $\mathrm{M_{Crit}}$ is ultimate failure load/moment and is generally taken for monotonic loading conditions. The Eqn. (6.4) ensures that minimum safety factor of 2 exists between critical crack size and leakage size crack (LSC). The Eqn. (6.5) ensures a safety factor of √2 on normal operating plus safe shut down earthquake (SSE) load. These safety factors are intended to account for uncertainties associated with material tensile and fracture properties, analytical procedures for assessment of monotonic critical/instability load or critical crack size, peak loads (earthquake load in this case) etc.. The individual apportionments of each of these uncertainties towards overall factor of safety are not specified in any of the referred LBB documents. It may also be noted here that these factor are not specified to account for the load history effects on material fracture behaviour.

Although the above equations are recommended to be applied for cyclic loads (as in earthquake event) however, the widely adopted analysis procedures for evaluation of the critical load or the critical crack size are done as follows:

i) the earthquake induced cyclic forces/moments are assumed as once applied monotonically increasing to its equivalent maximum magnitude value

ii) the local analysis of cracked pipe portion where the compliance effects due to its end connection to other piping components / equipment are not considered.

It may be noted that the normal operating (M_{NOC}) and SSE (M_{SSE}) moments/forces used in LBB analyses are evaluated using FE analysis of un-cracked piping system which includes the compliance effects of piping loop/system geometry, support conditions and its end connections to equipment.

From above, it is clear that neither the currently used safety factors nor the currently used analysis procedure explicitly addresses the load history effects (number of cycles and associated cyclic tearing damage) in the fracture stability assessment.

The outcome of current programme and the resulting CTFAD clearly show that for cycling loads, the effect of number of cycles on reduction in load carrying capacity, with respect to monotonic loading conditions, has to be considered. In fact even under cyclic displacement loading conditions (discussed in chapter-4) the crack growth by ductile tearing (for identical imposed rotation that is equal to monotonic $\phi_{M\text{-}max}$) is observed to be order of magnitude higher than that in monotonic loading conditions (see Table 4.1).

This highlights the need to account for the apparent damage caused by load cycling. This may be done by reducing the monotonic fracture capacity so as to account for damage due to reversible cyclic nature of load and ensure stability for specified number of cycles. Based on this, and using the developed CTFAD, a criterion / proposal has been developed to ensure fracture stability up to envisaged number of cycles (see next section).

6.5 Cyclic tearing based stability assurance in LBB analysis

Based on the lower bound CTFAD curve a criteria for fracture stability assessment under cyclic loading is proposed as given below:

$$M_{Max} < \beta_L * M_{Crit} \tag{6.6}$$

Here the 'M_{Max}' is the equivalent maximum moment magnitude of the cyclic loading event. If N is equivalent number of loading cycles of 'M_{Max}' magnitude for which stability of the cracked pipe shall be demonstrated. β_L is then evaluated from lower bound CTFAD curve Eqn. (6.3) for the 'N' number of cycles. The 'M_{Crit}' is the ultimate failure load/moment under monotonically increasing loading condition which may be evaluated experimentally or using any of the well documented existing practices or procedures [7-8, 32-42]. The Eqn. (6.6) enables the existing practices or procedures of stability assessment, to be used to demonstrate the integrity for specified number of load cycles. To account for earthquake loading condition, the Eqn. (6.4) and Eqn. (6.5), which are currently used of LBB qualification, have been modified with suitable β_L factor applied on M_{Crit}. The proposed modified equations are as given below:

Margin to Critical Crack Size : $(M_{NOC} + M_{SSE}) < \boldsymbol{\beta}_L \times M_{Crit}$ (at 2×LSC) (6.7)

Margin on Loads: $(M_{NOC} + M_{SSE}) \times \sqrt{2} < \boldsymbol{\beta}_L \times M_{Crit}$ (at LSC) (6.8)

The above LBB qualification equations may be used to demonstrate the stability for specified number of load cycles. The β_L–factor used in above equations implicitly accounts for deleterious impact due to both the fatigue-ductile tearing synergy damage and the associated number of cycles. The use of β_L–factor conservatively accounts for the drop in cracked pipe load capacity (M_{Crit}) which is solely attributed to the additional damage caused by fatigue-ductile tearing synergy under reversible cyclic loading condition. Although the β_L quantification is arrived at from pipe tests conducted at room temperature, without internal pressure load, and for quasi-static cyclic loading conditions, however it may be applied to normal operation temperature, internal pressure and dynamic cyclic loading conditions (like during earthquake) if these are considered and accounted in evaluation of M_{Crit}. The pressure /temperature /loading rate impact on β–factor obviates to a large extent owing to the fact that it is defined as ratio of load capacities under cyclic to monotonic loading under identical conditions.

Generally, 10 cycles of equivalent maximum magnitude of induced load during an earthquake event, are considered in designing the nuclear components [38, 21]. In Indian NPP, one Safe Shutdown Earthquake (SSE) event (comprising of 10 cycles) and five Operating Basis Earthquake (OBE) events (comprising of 10 cycles per event) are considered in design.

It is well known that strong earthquakes are always succeeded by large number of aftershock cycles. The exact number of cycles, experienced by components, may be difficult to quantify owing to uncertainties in associated geological processes. Consider the case of March, 11, 2011, earthquake at Fukushima, Japan. The main earthquake duration was about 300 seconds, which is considerably greater than 60 seconds duration in typical earthquakes. During this earthquake, number of cycles (including aftershocks) was greater than 100, [112]. Similarly some uncertainties are associated with the cyclic tearing damage, which are owing to intrinsic scatter of fundamental material parameters.

In view of the above, due care needs to be taken for selecting the number of cycles. From the proposed CTFAD (see Figure 6.5) or Eqn. (6.3), the β_L for different cycles is as follows:

(a) For typical earthquake comprising of 10 cycles (that is, without any significant aftershocks): β_L can be taken as 0.85

(b) For earthquake event comprising of 50 cycles (that is, including moderate number of significant aftershock cycles): β_L can be taken as 3/4 (= 0.75)

(c) For earthquake event comprising of 150 cycles (that is, including large number of significant aftershock cycles): β_L can be taken as 2/3 (=0.67)

It is observed that even for earthquake event without any significant aftershocks the β_L has to be at least 0.85. Considering the case of large duration earthquake event or earthquake with moderate number of aftershock cycles value of β_L equal to 0.75 seems to be reasonable choice. However, if stability is to be demonstrated for large number of cycles, as in case of severe earthquake followed by large number of aftershock cycles β_L can equal to 2/3 (=0.67) is suggested. As explained earlier (see section 6.3) that beyond 75 cycles the rate of reduction of β_L with cycles is very small and hence its value beyond 150 cycles may not change appreciably with further increase in number of cycles. In addition β_L equal to 2/3 will also satisfy stability under OBE events also. For any other number of cycles, the CTFAD or Eqn. (6.3) can be readily used to obtain the β_L factor as a function of number of load cycles.

The values of β_L proposed above are derived from lower bound CTFAD curve, which in turn is based on load controlled cyclic tearing tests at load ratio of -1. In case the load ratio is other than -1, then as discussed earlier (section 6.3) the resulting β_L would be slightly conservative.

6.5.1 β_L adequacy under displacement controlled cyclic loading

An earthquake event also induces displacement controlled cyclic deformations due to inherent indeterminacy in piping system and differential movement at support locations. The outcome of displacement controlled cyclic tearing tests shows that cyclic displacement loading will lead to significantly higher crack tearing growth as compared to that in corresponding fracture tests under monotonic loading conditions (see section 4.2). This is also highlighted in moment versus rotation and crack versus rotation plots (see Figure 6.6) of typical displacement controlled tests on carbon steel and stainless steel pipes. This is evident from Figure 6.6 that usage of suitable β_L factor ensures that excessive crack tearing growth is precluded. This may be further assured on revisiting section 4.2.3 where moment ratio ($= \mathrm{M}_{\max}^{\text{Disp.Cyclic test}} / \mathrm{M}_{\max}^{\text{Monotonic Test}}$), analogus to load reduction factor, β-factor, is investigated against number of cycles beyond which large ductile tearing takes place in a displacement controlled cyclic test. The Figure 6.7 (inverse plot of Figure 4.12) and Eqn. (4.1), show that application of proposed load reduction factor also ensures that under displacement controlled cyclic loading, the components will need significant cycles to reach the maximum moment beyond which large tearing crack growth takes places.

The above observations show that β-factor (derived from load cycling tests) also safeguards against excessive tearing noticed under displacement controlled conditions. Under these conditions although sudden instability may not arise, however, DEGB can still occur due to excessive stable crack tearing

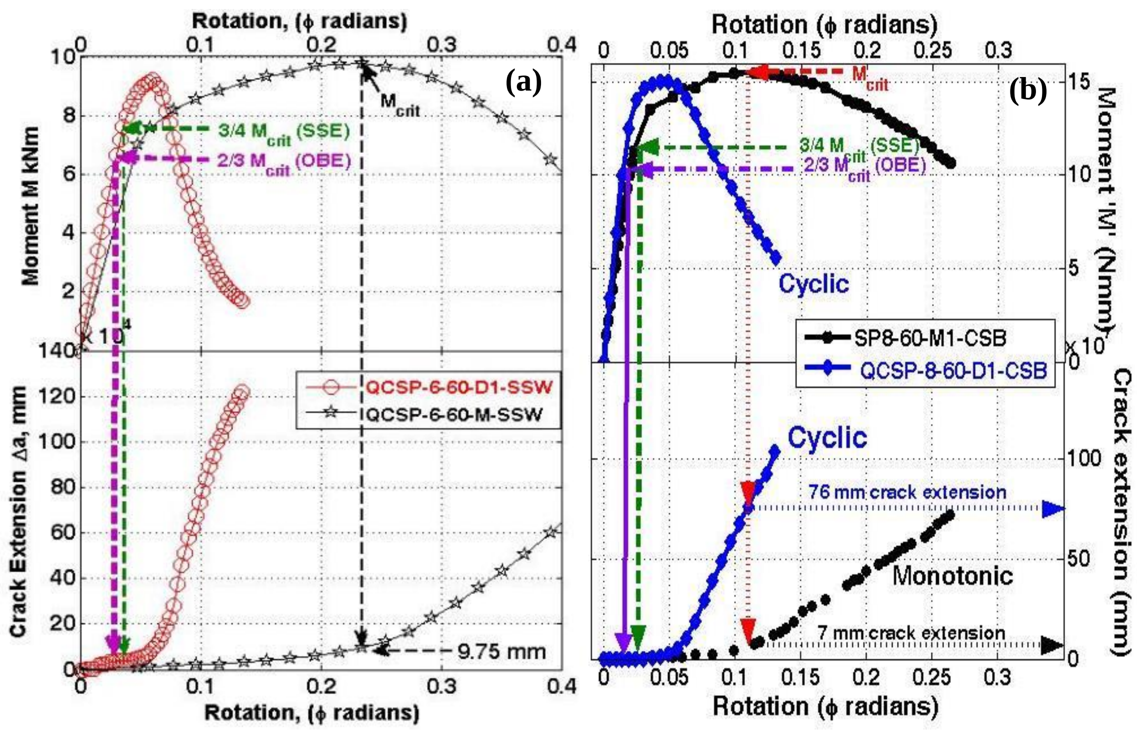

Figure 6.6: Moment versus total rotation and crack versus total rotation plots for displacement controlled cyclic tearing and corresponding monotonic fracture tests (a) SS and (b) CS material

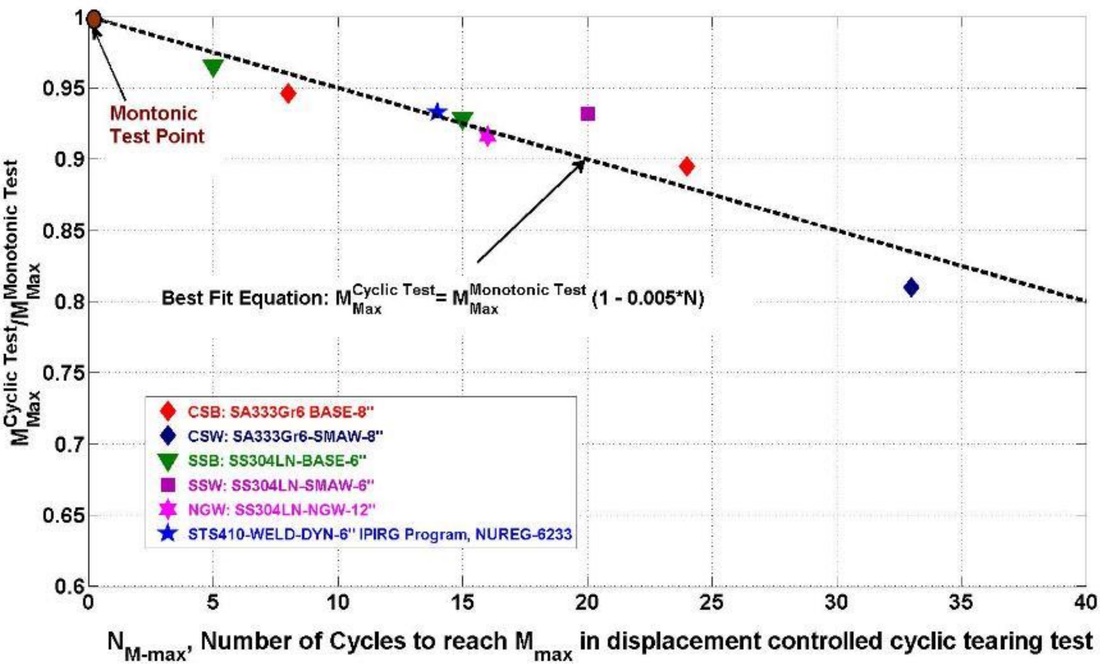

Figure 6.7. Ratio ($= M_{max}^{Disp.Cyclic\ test} / M_{max}^{Monotonic\ Test}$) plotted against number of cycles to reach the in incremental displacement controlled cyclic tearing test.

6.6 Discussion on other associated factors

As described in chapter-3, the major objective of the current experimental program is to conservatively and reliably single out and quantify the deleterious impact of cyclic nature of loading on the load carrying capacity of a cracked pipe. Further, using this, to develop a simple, reliable and easily implementable procedure to demonstrate the fracture stability of cracked pipes including the load history effects and for specified number of cycles as required in level-3 of LBB analysis. Hence the investigations carried out are very much focused to achieve these objectives. The current experimental programme has been carried out at room temperature, quasi-static cyclic loading condition and on standalone pipe that is unconnected pipe (the one having infinite system compliance). In actual LBB application the conditions are: (i) operating temperatures (250 °C – 350°C), (ii) dynamic load rate and (iii) pipes are always connected to equipment at their end (piping system, finite compliance). The following sections explain how the proposed β-factor is applicable under these conditions.

6.6.1 Nature of earthquake loads: load controlled versus displacement controlled

The piping system is subjected to combination of load controlled and displacement controlled loadings. The pure load controlled and pure displacement controlled conditions are two possible extremes. In piping design the earthquake induced loads are categorized as inertial and Seismic Anchor Displacement (SAM) loads. In general, the behaviour of SAM load is of displacement-controlled nature and the inertial loads are conservatively considered as load controlled.

In view of above the present cyclic tearing test programme included large number cyclic tearing tests in both pure load controlled and pure displacement controlled loading conditions. The β-factor (derived from constant load cycling tests) uses ensure fracture stability of cracked pipe for specified number of cycles under load-controlled loading. It is also shown that the β-factor safeguards against excessive tearing noticed under displacement controlled conditions.

6.6.2 Cyclic plasticity and crack tearing

When a cracked structure is subjected to cyclic loading, there are two possible effects: (i) material's deformation behaviour may change due to cyclic hardening or softening, dominant in initial 50 cycles (ii) crack extension may increase due to fatigue and tearing combined damage. The material's cyclic plasticity behaviour, cyclic softening/hardening and cyclic stress strain curves of both the materials SA333Gr6 and SS304LN considered in present programme, are presented in Goyal et.al.[113]. The crack growth behaviour under reversible cyclic loading has been investigated (see sections 2.5, 4.2, 5.2-5.5).

Since the proposed β-factor is derived directly from the cracked pipe tests conducted under cyclic and monotonic loading hence both the above-discussed effects of cyclic loading on cracked structure are implicitly embedded in proposed β-factor equation.

6.6.3 Piping system fracture assessment: Effect of crack, crack tearing and associated plasticity

The current understanding on the effect of piping system compliance on fracture assessment has been reviewed and discussed in chapter-2, section 2.8. As explained in section 2.8, the piping systems are always indeterminate in nature with their terminal ends at anchors or rigid equipment nozzles. Generally, the LBB analyses use the pipe moment/forces which are typically evaluated from linear elastic analysis of piping system without modelling crack. In reality the presence of a circumferential through-wall crack reduces the stiffness of piping loop and in turn changes the induced forces and moments. The magnitude of altered moment/forces can be obtained using coupled (when piping loop modelled with crack) analysis. The changes in moment/forces depend upon the piping compliance, location of the crack in piping loop, size of the crack. In case of quasi-static monotonic loading, the forces/moments would reduce at crack locations and increase at terminal/anchor end. However in case of earthquake loading, the change in the induced forces and moments in piping would depend on change in the natural frequencies and mode shapes due to postulation of through wall crack. Accounting of these effects in evaluation of forces and moments, could give more realistic LBB assessment and in many cases sufficient back-up margins may exist. However, the critical load, right hand side of Eqn. 4 & 5, would be independent of piping compliance. To utilize above benefits, a detailed analytical method was proposed in NUREG 6765 [13]. This method requires non-linear dynamic stress analysis incorporating a cracked-pipe element to represent crack section. Since actual piping test data was analysed, the load redistribution due to presence of crack and associated plasticity is implicitly taken care of in estimation of induced forces/moment at the crack location. Gupta et al [100] has proposed a J-Tearing analysis based procedure for cracked pipe stability analysis which includes the above benefits in applied J and applied tearing modulus calculation.

However, on the other, while utilizing above benefits, one shall also take the piping compliance into consideration to evaluate the Leakage Size Crack (LSC). E Smith [102-103] has shown the deleterious effect of the piping compliance on assessment of crack opening area which is important in evaluation of leakage size crack. It was shown that the LSC would be much higher for stiff piping loop as compared to unconnected pipes (i.e. the one having infinite compliance) and therefore this has potential to jeopardise any leak-before-break argument.

Both the above effects of considering the piping system compliance is contradicting, one beneficial in induced load assessments and the other deleterious in terms of leakage size crack assessment. The net effect may or may not be beneficial in term of LBB qualification and calls for computationally intensive, sophisticated and detailed calculations and system level analysis.

Moreover, the above benefits, if any, would be in the estimation of induced loads, i.e. SSE+NOC that is the left side (LHS) of the Eqn. (6.4 & 6.5). However, the present study has primarily addressed the reduction in monotonic fracture capacity under reversible cyclic loads and presented load reduction factor, β-factor, which accounts for deleterious effects of cyclic character of load on the right side of Eqn. (6.4 & 6.5). The cyclic tearing damage is bound to occur under reversible cyclic loading and independent of piping system compliance.

6.6.4 Effect of Dynamic Strain Ageing (DSA) on fracture behaviour

In chapter-2, section 2.7, the current literature status on the effect of dynamic strain ageing (DSA) on fracture assessment has been discussed. In general it has been observed that dynamic strain ageing (DSA) has detrimental effect on fracture toughness behaviour of a material. It is also observed that DSA occurs under specific combination of temperature and strain rate. Marschall, C [91], G. Wilkowski [58] and Scott P. M. [13] have shown that due to dynamic strain ageing (DSA) effects, the carbon-manganese steel (such as A106 Gr.B, A515Gr.60, A516Gr.70 etc.) may undergo additional loss in the fracture toughness, at typical plant operating temperature (i.e. 250°C-300°C) . It is known that the seismic loading involves both dynamic loading rates and cyclic loading. At these rates and the operating temperatures, there may be DSA effects present in carbon steel piping.

In the past, studies related to interaction between cyclic and dynamic effects at typical plant operating temperatures on fracture resistance have been reported in NUREG-6440 [53], NUREG-6438 [50]. These investigations have shown weak interaction between the dynamic and cyclic nature of loading. In other words, the fracture resistance during dynamic-cyclic loads can be separated and expressed as fracture resistance from the quasi-static static monotonic test multiplied by two factors, one quantifies the loss due to cyclic nature alone and the other due to the dynamic nature (see Figure 2.6, ref. [35]).

In presence of DSA conditions (temperature and strain rate), the load capacity of a cracked pipe will decrease under cyclic as well as monotonic loading. As explained earlier also, in order to minimise the effect of other variable, the proposed β-factor has been derived by taking ratio of load capacity (for given number of cycles) to load capacity of identical pipe specimen (of same heat / same WPS) under monotonic loading and under identical other condition such as temperature and loading rate etc. Hence β-factor takes care of deleterious impact of cyclic tearing damage alone. The impact of other condition like temperature, loading rate, dynamic strain ageing (DSA), environment etc., shall be accounted for in evaluation of monotonic critical loads.

6.6.5 Existing safety margin

The referred LBB guides and documents uses a safety factor (SF) of 2 on crack size (see Eqn. (6.4)) and √2 on load (see Eqn. (6.5)) as overall safety factors to take care of uncertainties associated with material properties, analytical procedures etc. It is nowhere stated that the SF of √2 on load or SF of 2 on crack size are adequate to take care of cyclic loading effect during a seismic event. The factorized contribution in SF, of uncertainties in strength, fracture toughness, peak load and modeling/analysis are not known.

In current programme, cyclic tearing damage has been singled out and its contribution in reduction of monotonic load capacity (β-factor) has been quantified (see section 6.3). For example, the load reduction β-factor required to account for tearing damage due to reversible cyclic nature of typical earthquake load comprising of 10 cycles (that is, without any significant aftershocks) is 0.85. The equivalent safety factor, SF_{cyclic} (only to take care of loss of load capacity under reversible cyclic loads) would be 1/0.85 (= 1.18). The SF_{cyclic} is less than overall SF of √2 (=1.4). However, if one considers that the margin of 1.18 is required to account for cyclic damage, is a sub safety factor of overall SF of √2, then it must be ensured with sufficient justification that the remaining margin of about 1.2 will be sufficient to take care of all other uncertainties like those associated with material toughness, analytical assessment procedures, load specification etc.

In view of above, the current proposal of using suitable β-factor to take care of cyclic tearing damage is over and above the existing SF of √2 on load or SF of 2 on crack size. Its usages would adequately take care of cyclic loading effect during a seismic event.

6.7 Chapter conclusions

This chapter presented the final outcome of the systematic experimental programme and investigations carried out in the area of cyclic tearing tests on large sized pipe components. The investigation reported in this chapter resulted in following conclusions:

(a) The load controlled cyclic tearing tests have shown that the load capacity (against unstable failure) of pipe reduces significantly under cyclic loading conditions in comparison with that under monotonically increasing loading condition. These tests highlighted the necessity and importance of inclusion of load cycles as one of the parameters in fracture integrity assessment under cyclic loading event.

(b) Based on load controlled cyclic tearing test and corresponding monotonic fracture test results, a load reduction factor (β) is evaluated which singled out and quantified only the effect of cyclic loading conditions and number of load cycles on instability. This proposed β-factor is derived by taking ratio of load capacity (for given number of cycles) to load capacity of identical pipe specimen (of same heat / same WPS) under monotonic loading and under identical other conditions such as temperature and loading rate etc...

(c) No analytical modelling / analysis is involved in β-factor calculation. The above procedure obviates, to a large extent, the uncertainties associated with analytical / numerical modelling, material properties and other effects like loading rate, temperature etc.

(d) Using evaluated β factors and number of cycles to unstable failure, a Cyclic Tearing Failure Assessment Diagram (CTFAD) is developed which plots test data from wide range of pipe sizes, crack sizes, crack location and widely used nuclear piping material. In CTFAD plot, all experiment data lie within a narrow scatter band which is attributed to intrinsic scatter band in basic material parameters.

(e) To account for this narrow scatter band, a lower bound CTFAD curve equation (β_L) is proposed for fracture stability assessment under cyclic loading. The β_L factor usage enables the existing procedures of stability assessment, to demonstrate the integrity for specified number of load cycles. Thus the CTFAD can be interpreted as follows:

(i) For any given number of cycles the β-factor gives reduction in fracture load capacity with respect to monotonic fracture load.

(ii) Alternatively one can determine the number of cycles to fracture instability for the load amplitude given as fraction of monotonic fracture load

(f) Based on the lower bound CTFAD curve and proposed equation, a procedure for cyclic tearing based stability assessment has been proposed. The proposal is simple and enables the existing practices or procedures of stability assessment to demonstrate the integrity for specified number of load cycles by additionally considering suitable load reduction factor, β.

(g) Based on the lower bound CTFAD curve and proposed equation, "Monotonic Capacity Load Reduction Factors for different earthquakes" were evaluated and the same has been recommended for fracture stability assurance and LBB qualification for specified number of cycles.

(h) The use of proposed load reduction factor (β_L) exclusively and solely accounts for the add-on damage due to both the cyclic taering damage and associated number of cycles. The use of β_L–factor conservatively estimates the drop in cracked pipe load capacity (M_{Crit}), which is solely attributed to the fatigue-ductile tearing synergy under specified cycles of reversible loading. The effects, if any, of other condition like temperature, pressure, loading rate, material, environment etc., shall be accounted in evaluation of monotonic critical loads(M_{Crit}) i.e. pipe load capacity under monotonic loading condition. However use of β_L for materials and loading conditions which are grossly different than those included in present study – may be validated by conducting few component test.

(i) It is demonstrated that the proposed "Monotonic Capacity Load Reduction Factors for different earthquakes" (derived from constant load cycling tests) also safeguards against excessive tearing noticed under displacement controlled conditions. Under these conditions although sudden instability may not arise; however, DEGB can still occur due to excessive stable crack tearing

(j) It is believed that the inclusion of proposed load reduction factors will adequately safeguard against both unstable failure and the large tearing crack growth of the leaking pipe, subjected to the design basis earthquake events. This will enhance the safety of NPP wherever credits of LBB design concept are taken.

7 Conclusion and future work-scope

This chapter presents the review of the main conclusion drawn in the preceding chapters, outcome of the experimental programme and investigations and suggest scope of future work.

Currently Leak-Before-Break (LBB) based design and fracture stability assessment considers the earthquake as once applied non-cyclic load, which monotonically increases up to its maximum magnitude. The cyclic character of earthquake load and associated cyclic tearing failure mode (tearing-fatigue regime) are not explicitly considered while demonstrating stability of a through wall cracked pipe. In past, huge efforts and investigation were made to understand, quantify and develop procedure to account for the load history effect, reversible cyclic loading into the fracture stability assessment while demonstrating the leak before break behaviour of a cracked pipe. These investigations have shown the deleterious cyclic tearing damage under a cyclic loading event. Despite the efforts, the cyclic tearing failure mode is not explicitly accounted for in present guides/practices of stability demonstration of a cracked pipe for LBB analyses. This may be due to un-availability of simple, reliable and easily implementable procedure to demonstrate the fracture stability of cracked pipes for specified number of cycles as required in level-3 of LBB analysis.

In view of this, a systematic experimental programme and investigations have been carried out in the area of cyclic tearing tests on large sized pipe components made of carbon and stainless steel materials used in the Indian nuclear power plant primary piping. The test programme have been designed for focused investigation to conservatively and reliably single out and quantify the deleterious impact of cyclic nature of loading on the load carrying capacity of a cracked pipe. Further, effort has been made to develop a simple, reliable and easily implementable procedure to demonstrate the fracture stability of cracked pipes including the load history effects using the test data generated through this programme.

The experimental programme considered pipes of two different base materials and three different weld configurations/combinations. These are, SA333Gr6 Carbon steel Pipe Base (CSB); SS Type 304LN Stainless steel Pipe Base (SSB); SA333Gr6 Carbon steel Pipe with girth weld (CSW, root pass GTAW filler pass SMAW); SS Type 304LN Stainless steel Pipe with conventional girth weld (SSW, root pass GTAW filler pass SMAW); SS Type 304LN Stainless steel Pipe with narrow grove girth weld (NGW, hot wire GTAW). These five conditions covered variation in fracture toughness. Wide range of pipe sizes, 6″ NB Sch. 120, 8″ NB Sch. 100, 12″ NB Sch.100, 12″ NB Sch.120, and 16″ NB Sch.100 pipe, have been tested. The circumferential through wall crack sizes (2θ) considered are 60°, 90° and 120°. The piping system is subjected to combination of load and displacement controlled conditions. Therefore, the cyclic fracture tests were done under pure load controlled as well as pure displacement controlled conditions. These are two possible extremes. The real piping system behaviour will lie somewhere in-between and is function of local compliance at a cracked location and global compliance. An imaging based technique is used to measure the crack growth. This image technique unlike other conventional techniques (e.g., ACPD or DCPD) has provided reliability in measurement of both component (in-plane and out of plane) of crack growth.

7.1 Major conclusions

(I) The displacement controlled cyclic tearing tests of all five material categories along with corresponding monotonic fracture tests on identical pipes have been analysed. Here two different loading histories: one named as incremental displacement controlled where, the displacement magnitudes builds up incrementally step wise such that the load ratio, R, is -1; the other named as fully reversing displacement loading where the displacement amplitude is kept constant during the test. In an earthquake, during initial motion the displacements builds up gradually and during strong motion there may be cycles of reversing constant displacement magnitude. Hence, the tests covered both conditions. These tests have shown that, the displacement controlled loading does not cause instability failure but resulted in significantly large tearing leading to DEGB type failure. The relative comparisons of the pipe fracture behaviour obtained from cyclic displacement and corresponding monotonic fracture tests lead to following major conclusions:

(a) The maximum moment (M_{max} that is the capacity of pipe) drops by a small to moderate (2 to 20%) value in comparison of the corresponding value in monotonic tests). However, significant decrease (50 to 83% of corresponding value in monotonic tests) in the pipe rotation ($\phi_{M\text{-}max}$) at maximum moment (M_{max}) is observed. This showed significant decrease in ability of cracked pipe to take cyclic displacements (which gradually build) without any significant crack extension. The $\phi_{M\text{-}max}$ and M_{max} combine is an important indicator of energy absorbing ability of a cracked pipe without undergoing any significant crack growth. High decrease in $\phi_{M\text{-}max}$ along with moderate decrease in M_{max} under cyclic displacement load implies very high loss in the energy absorbing ability of pipe. In case of smaller displacement increment (δ), the decrease in both $\phi_{M\text{-}max}$ and M_{max} is larger and hence it results in greater loss in energy absorbing capacity.

(b) Crack growth ($\Delta a_{M\text{-}max}$) up to maximum moment point (in rising portion of M-ϕ curve) in cyclic tests is found comparable or smaller than in the corresponding monotonic fracture test. Hence, the number of load cycles, to reach the maximum moment, M_{max} point (i.e. cycles in rising portion of envelope M-ϕ curve) is an important parameter and is designated as $N_{M\text{-}max}$. This implied that if the envisaged number of cycles in a loading event is smaller than $N_{M\text{-}max}$, then the extent of tearing would be insignificant. The tests also showed that smaller δ requires more number of cycles (of incremental displacement application), $N_{M\text{-}max}$, to reach the maximum moment point M_{max}. More cycles, in turn, means more damage owing to cyclic loading that is due to fatigue crack growth, crack tip re-sharpening and void flattening in fracture process zone under reverse loading.

(c) The detailed analysis of tests data has shown existence of a correlation / trend between number of cycles $N_{M\text{-}max}$ and the ratio of maximum moment in displacement controlled cyclic and corresponding monotonic fracture test (see Figure 4.12). An equation, Eqn.(4.1), relating the number of cycles, monotonic capacity of cracked pipe and maximum moment in cyclic displacement loading event is developed. This equation screens/assesses the number of cycles when a cyclic displacement-loading event can cause large crack growth.

(d) The cyclic J-R curve of all the cyclic and corresponding curve from monotonic fracture tests has shown significant decrease in fracture resistance under cyclic loading conditions. Smaller the cyclic displacement increment, larger is the drop in cyclic J-R curve. The cyclic J-R curve was found to be dependent on loading history parameters and so the cyclic J-R curve, shall be evaluated such that it is consistent with the anticipated loads at the postulated crack location in piping system. The cyclic J-R observations are in full agreement with those obtained in IPIRG and by many other investigators.

(II) The inertial loads are induced during an earthquake event and they, in general, are treated as load controlled and of fully reversing cyclic in nature. To investigate the pipe fracture behaviour under such loading, large numbers of tests have been conducted under load controlled cyclic loading condition. These tests have shown that, the load controlled cyclic loads may cause instability resulting in DEGB type failure in few cycles. Pipe failed by unstable tearing in very few cycles (10-20) even when the applied moment magnitude are lower (80-90%) than the monotonic capacity of that pipe (obtained from monotonic fracture tests on identical pipe). Significant stable crack growth occurs before the unstable failure. Both the number of cycle to unstable failure of pipe and the stable crack growth, increases with decrease in the applied moment magnitude. Significant reduction in number of cycles is observed in the tests with same maximum moment but with larger compressive load in reverse direction (larger negative load ratio). This is due to increase in cyclic damage due to crack tip re-sharpening and void-sharpening/flattening owing to larger compressive loads / compressive plasticity. These apparently accelerate fracture process in next loading cycle and results in increased ductile tearing crack growth.

(III) The fracture stability and cracked growth assessment of the load controlled cyclic tearing tests on carbon steel pipes using the Miura/CRIEPI procedure (envelope curve based) has shown that the CRIEPI procedure overestimated the crack growth. The ΔJ and

J-R based instability criteria and the $\Delta J/J_{max}$ equation showed poor agreement with the results of these tests.

(IV) The cycle-by-cycle study of evolution of the moment-rotation hysteresis has revealed that rightward (crack opening load direction) ratchet/shift of loading branch which envelope curve does not account. This leads to overestimation of ΔJ and hence over prediction of the crack growth. Suitability of use of envelope curve use under fully reversible loads is further investigated by performing elastic plastic FE analyses on CT specimen under alternating and reversing loading conditions. These have shown that under fully reversed loading, (load ratio = -1) the plastic zone ahead of the crack tip in subsequent load application is much larger than that in 1st loading. While in case of alternating cyclic loading (load ratio ≥0), the plastic strain field ahead of the crack tip remained nearly same. Hence, the use of envelope curve for cyclic tearing assessment under fully reversing loading conditions is not suitable. However, for R≥0, the envelope curve may be used to evaluate the J-integral and static tearing (as is done for monotonic fracture tests with partial unloading). Only precaution required is, if there are large numbers of unloading cycles, then it is necessary to account for the fatigue crack growth.

(V) A crack-growth evaluation procedure, based on each cycle of loading, is proposed. Here the contribution of both fatigue and ductile tearing are considered. The cycle by cycle crack growth evaluated using this procedure is found in good agreement with those measured in tests. An instability criteria and an algorithm have also been obtained from these investigation where the number of reversible cyclic load leading to unstable failure of a cracked pipe can be evaluated. The unstable failure of the pipe occurs when the cyclic load magnitude become equal to or less than the monotonic fracture capacity of the pipe with crack size, which is updated in each cycle depending on the fatigue-tearing crack growth.

(VI) In order to single out and quantify the deleterious impact of cycles and cyclic loads on the moment carrying capacity, a relational study, involving corresponding load controlled cyclic tearing and monotonic fracture tests has been performed which led to following:

(a) A load reduction factor (β-factor) is evaluated which quantifies the effect of cyclic loading conditions and number of load cycles on instability. Using evaluated β-factors and number of cycles to unstable failure, a Cyclic Tearing Failure Assessment Diagram (CTFAD), Figure 6.5, is developed. The CTFAD plots test data from wide range of pipe sizes (4″, 6″, 8″, 12″ and 16″ in diameter), crack sizes (total crack angle as 30°, 60°, 90° and 120°), crack location (in base metal and in centre of girth weld), welding technology, (SMAW, GTAW, conventional groove, narrow groove) and widely used nuclear piping material (carbon steel and stainless steel).

(b) In CTFAD plot, all experimental data lie within a narrow scatter band, which is attributed to intrinsic scatter band in basic material parameters. A lower bound CTFAD curve equation (β_L-factor), Eqn.(6.3), is proposed, which accounts for this narrow scatter band, for fracture stability assessment under cyclic loading. The β_L-factor usage enables the existing procedures of stability assessment, to demonstrate the integrity for specified number of load cycles.

(c) Based on the lower bound CTFAD curve and proposed equation, “Monotonic Capacity Load Reduction Factors (β_L values) for different earthquakes” has been evaluated and the same has been recommended for fracture stability assurance and LBB qualification for specified number of cycles. For typical earthquake comprising of 10 cycles (that is, without any significant aftershocks), the β_L has to be at least 0.85. For earthquake event comprising of 50 cycles (that is, including moderate number of significant aftershock cycles), β_L is suggested as 3/4 (= 0.75) while for earthquake event comprising of 150 cycles (that is, including large number of significant aftershock cycles) the β_L-factor can be taken as 2/3 (=0.67).

In case of cyclic loading with load ratio other than -1, the suggested β_L-factor would lead to slightly conservative assessment. The proposed β_L-factor would also limits extent of tearing under displacement controlled cyclic loading (see Figure 6.7, Figure 4.12 and Eqn. 4.1). The proposed β_L-factor to take care of cyclic tearing damage is over and above the existing safety factors of $\sqrt{2}$ on load or SF of 2 on crack size (see Eqn. 6.7 and 6.8) which are currently used in demonstrating LBB compliance.

(VII) The use of proposed β_L-factor exclusively and solely accounts for the add-on damage owing to fatigue-ductile tearing synergy under specified cycles of reversible cyclic loading. The effects, if any, of other condition like temperature, pressure, loading rate , material, environment etc., shall be accounted in evaluation of monotonic critical loads(M_{Crit}) i.e. pipe load capacity under monotonic loading condition. The pressure /temperature /loading rate impact on β–factor obviates to a large extent owing to the fact that it is defined as ratio of load capacities under cyclic to monotonic loading under identical conditions Hence on this basis the proposed β_L-factor may be used for other conditions like temperature, pressure, loading rate, material, environment etc. if these are duly considered and accounted in evaluation of M_{Crit}. Despite this fact, use of CTFAD for materials and loading conditions which are grossly different than those included in present study – may be validated by conducting few component test.

It is believed that the inclusion of proposed load reduction factors will adequately safeguard against both unstable failure and the large tearing crack growth of the leaking pipe, subjected to the design basis earthquake events. This will enhance the safety of NPP wherever credits of LBB design concept are taken.

7.2 Future work scope

The current efforts are focused on singling out and quantifying the impact of cyclic tearing on through wall cracked pipe at room temperature under pure bending loading. There are several issues that may be investigated in future. They are as follows:

(a) Despite the fact, that the impact of the loading conditions like combined pressure plus bending, loading rate, temperature, environment etc. on proposed β_L should be insignificant, still few component tests may be conducted under normal operation pressure / temperature and on circumferential through wall as well as part through wall cracks

(b) Development and modification of R-6 or FAD based analysis procedures to account for cyclic tearing. Here a series of failure curves which depend on the number of cycles of loading may be developed. However, this may require additional tests data on the highly ductile (pure plastic collapse failure mode) and brittle (pure fracture mode of failure) materials.

(c) The FEM or XFEM based analytical investigations on the cracked pipe components under reversing cyclic loading need to be carried out. These shall account the following:

(i) The cyclic plastic phenomenon i.e. cyclic softening / hardening / ratcheting which are happening in the plastic zone ahead of crack tip under cyclic loading.

(ii) The development of crack growth under cyclic loading shall be incorporated in the simulations using FEM or XFEM methods.

(d) More efforts are required on understanding of micromechanical damage behaviour under cyclic tearing and develop models for the damage and crack growth simulation.

References

1 NUREG-1061-VOL.3, 1984, Evaluation of potential pipe break, USNRC Pipe Break Task Group

2 Modification of General Design Criterion 4: Requirements for Protection Against Dynamic Effects of Postulated Pipe Ruptures, US Federal Register, Vol. 51, No. 70, Office of the Federal Register, Washington, D.C. (1986) 12502-5.

3 NUREG-0800, 2007, "Leak-Before-Break Evaluation Procedures", USNRC Standard Review Plan SRP 3.6.3

4 IAEA-TECDOC-710, 1993, Applicability of the leak before break concept, IAEA-TECDOC-710

5 IAEA-TECDOC-774, 1994, Guidance for the application of the leak before break concept, IAEA-TECDOC-774

6 Guidance for application of the "Leak Before Break" safety concept for NPP pipelines, 1999, R-TPR-01-99, RD-95 10547-99, MAE, Moscow

7 A16 LBB Guide, 2007, "Guide for Leak Before Break Analysis and Defect Assessment", RCC/MR, Section-1, Subsection-Z, Appendix A16.

8 R6, Revision 4, 2000, Assessment of the Integrity of Structures containing Defects, British Energy Generation Ltd

9 Gunther Barthome, 1997, " 'German leak-before-break concept' (description of German LBB procedures practices and applications)", Siemans/KWU Erlangen, Germany, Int. J. Pres. Ves. & Piping 71 (1997) pg 139-147

10 G. Barthome, G. Senski, R. Wellein, C. Schmidt, 1997, " Validation of simplified fracture mechanics methods by testing of real components", Siemans/KWU Erlangen, Germany, Nuclear Engineering and Design 172 (1997), pg.373-379

11 R. Bieselt, B Kuckartz, M. Wolf, 1995, "Determination of limits for smallest detectable and largest subcritical leakage cracks in piping system", Nuclear Engineering and Design, 159, pp. 29-42, 1995

12 Report- EUR 18549 EN, 2000, "European Safety Practices on the application of leak-before-break (LBB) concept", The nuclear regulator working group task force on leak before break, Directorate-General Environment, 2000

13 P. M. Scott, R. J. Olson G. M. Wilkowski, May 2002, "Development of Technical Basis for Leak-Before-Break Evaluation Procedures", U.S. Nuclear Regulatory Commission, NUREG/CR-6765, 2002

14 Jeong-Bae Lee, Young Hwan Choi, 1999, "Application of LBB to high energy pipings of a pressurized water reactor in Korea", Volume 190, Issues 1–2, Pages 191-195

15 J.Chattopadhyay, B.K.Dutta & H.S.Kushwaha, "Leak-Before-Break qualification of primary heat transport piping of 500 MWe Tarapur Atomic Power Plant", International Journal of Pressure Vessel and Piping, Vol.76, 1999, pp 221 - 243

16 LI Chengliang YANG Mengjia China Nuclear Power Design Company LTD,. Shanghai Branch, China, "Applicability of Leak-Before-Break (LBB) Technology for Primary Coolant Piping to CPR1000 Nuclear Power Plants in China", 20th International Conference on Structural Mechanics in Reactor Technology (SMiRT 20) Espoo, Finland, August 9-14, 2009 SMiRT 20-Division 2 , Paper 1884

17 Qiang Li, Peng Cen, Hongdong Zhen, "Methods and procedures of the application of LBB technology in high-power lines of nuclear power plants", Nuclear Island Division, China Nuclear Power Design Company, Shenzhen, Guangdong, CHINA, Transactions,SMiRT 21, 6-11 November, 2011, New Delhi, India Div-II: Paper ID# 352

18 Claude FAIDY, EDF-SEPTEN, France, "A new proposal on Leak Before Break for future plants", 20th International Conference on Structural Mechanics in Reactor Technology (SMiRT 20) , Espoo, Finland, August 9-14, 2009, SMiRT 20-Division 6, Paper 2596

19 S. Chapuliot*, C. Migné, "Break preclusion concept and its application to the EPRTM reactor (#333)", Areva-NP, France, Transactions SMiRT 21, 6-11 November, 2011, New Delhi, India Div-II: Paper ID# 333

20 ASME, Boiler and Pressure Vessel Code, Section III Division-1, "Rules for Construction of Nuclear Facility Components", Sub-section NB: class 1 components, 2004

21 ASME, Boiler and Pressure Vessel Code, Section III Division-1, "Rules for Construction of Nuclear Facility Components", Appendix-N: Dynamic analysis methods, 2004

22 Wells, A. A. (1961), "Unstable Crack Propagation in Metals Cleavage and Fast Fracture", Proc. Crack Propagation Symposium Cranefield, pp. 210-230

23 Rice J.R., 1968, "A path independent integral and the approximate analysis of strain concentration by notches and cracks". Journal of Applied Mechanics 1968;35:379-86

24 Shih C. F., "Relationship between the J-integral and the crack opening displacement for stationary and extending cracks.", Journal of the mechanics and physiscs of solids, Vol-29, 1981, pp. 305-3026

25 T. L. Anderson, "Fracture Mechanics,: fundamentals and applications", text book 2nd edition, CRC Press

26 Wilkowski, G. M., Marschall, C. W. and Landow, M. (1990), Extrapolation of C(T) Specimen J-R Curves for Use in Pipe Flaw Evaluations, ASTM STP 1074, Philadelphia, pp. 56-84.

27 Miller, A. G., 1988, ''Review of Limit Loads of Structures Containing Defects,'' Int. J. Pressure Vessels Piping, 32, pp. 197–327.

28 Zahoor, A., 1991, Ductile Fracture Handbook, Vol. 3, EPRI-NP-6301-D,N14-1, Research Project 1757–69, Electric Power Research Institute, Palo Alto, CA.

29 Chattopadahya, J. et. al. (2004) “Closed form collapse moment equation of through wall circumferentially cracked elbows subjected to in-plane bending moment” ASME J. of Pressure Vessel Technology, vol.126, 307-317.

30 Kim, Y. J. and Chang, S. O. (2006). “Closed form plastic collapse loads of pipe bends under combined pressure and in-plane bending”, J. Engineering fracture Mechanics, vol.-73, issue-11, pg.1437-1454

31 Suneel K. Gupta, Vivek Bhasin, K. K. Vaze and A. K. Ghosh, "General plastic collapse load equations of pipe bend with or without crack under in-plane bending Transactions, SMiRT 21, 6-11 November, 2011, New Delhi, India, Div-II: Paper ID# 730, 2011

32 Zahoor, A., “Ductile Fracture Handbook, Volume I, Circumferential Through Wall Cracks”, Report No. EPRI NP-6301-D, Electric Power Research Institute, Palo Alto, CA, 1989

33 Kumar, V., German, M.D., and Shih, C.F., “An Engineering approach for Elastic-Plastic Fracture Analysis”, Report No. EPRI NP-1931, Electric Power Research Institute, Palo Alto, CA, 1981

34 F. W. Burst, “Approximate Methods for Fracture Analyses of Through-Wall Cracked Pipes”, U.S. Nuclear Regulatory Commission, NUREG/CR-4853, 1987

35 G. M. Wilkowski, R. J. Olson, and P. M. Scott, 1997, “State-of-the-Art Report on Piping Fracture Mechanics”, U.S. Nuclear Regulatory Commission, NUREG/CR-6540, 1997

36 EPRI NP-6045, “Evaluation of Flaws in Ferritic Piping”, Electric Power Research Institute, Report No. EP-6045, October 1988

37 EPRI NP-4690, “Evaluation of Flaws in Austenitic Piping”, Electric Power Research Institute, Report No. EP-4690-SR, July 1986

38 Boiler and Pressure Vessel Code. Section XI, “Rules of In-service Inspection of Nuclear Power Plant Components.” American Society of Mechanical Engineers; New York, NY, 2007

39 Ainsworth, R.A., “Assessment of Defects in Structures of Strain Hardening Material”, Engineering Fracture Mechanics, Vol. 19, No. 4, pp. 633-642, 1984.

40 Milne, I., Ainsworth, R.A., Dowling, A.R, and Stewart, A.T., “Assessment of the Integrity of Structures Containing Defects”, Report No. : CEGB/E/H/R6-Rev.3

41 Tada H. and Paris P.C., " The Application of The Fracture Proof Design Methods using Tearing Instability Theory to Nuclear Piping Postulating Circumferential Through -Wall Cracks", NUREG/CR-3464, 1983

42 “NRC Leak-Before-Break (LBB.NRC) Analysis Method for Circumferentially Through-Wall Cracked Pipes Under Axial Plus Bending Loads,” U.S. Nuclear Regulatory Commission, NUREG/CR-4572, 1986

43 ASTM E 8M-08, (2008), Standard Test Methods for Tension Testing of Metallic Materials [Metric], ASTM, Philadelphia, PA, pp. 81–100.

44 ASTM E 1820-09, Standard Test Method for Measurement of Fracture Toughness, ASTM Philadelphia, PA, 2009.

45 ASTM E 647-03, Standard Test Method for Measurement of Fatigue Crack Growth Rates, ASTM Philadelphia, PA, 2003.

46 Marschall, C.W., Landow,M., and Wilkowski,G.M., "Loading Rate Effects on Strength and Fracture Toughness of Pipe Steels Used in Task1 of the IPIRG Program", NUREG/CR-6098, October 1993.

47 Scott, P., Kramer, G., Vieth, P., Francini, R, and Wilkowski, G., "The Effect of Dynamic and Cyclic Loading During Ductile Tearing on Circumferentially Cracked Pipe—Experimental Results", ASME PVP Vol.280, June 1994, pp. 207-220.

48 Wilkowski, G., Kramer, G., Vieth, P., Francini, R, and Scott, P., "The Effect of Cyclic Loading During Ductile Tearing on Circumferentially Cracked Pipe—Analytical Results", ASME PVP Vol.280, June 1994, pp221-240.

49 A. Hopper,G. Wilkowski, P. Scott, R. Olson, O. Rudland, T. Kilinski, R. Mohan, N. Ghadiali, and O. Paul, 1997, “The Second International Piping Integrity Research Group (IPIRG-2) Program- Final Report”, U.S. Nuclear Regulatory Commission, NUREG/CR-6452, 1997

50 D. L. Rudland, M. Scott, G. M. Wilkowski,1996, The Effect of Cyclic and Dynamic Loads on Carbon Steel Pipe, U.S. Nuclear Regulatory Commission, NUREG/CR-6438

51 C. W. Marschall, M.P. Landow, G.M. Wilkowski and A. R. Rosenfield,1995, Comparison of static and dynamic strength and J-R curves of various piping materials from the IPIRG-I program, International Journal of Pressure Vessels and Piping 62 (1995)

52 P. Scott, R. OIson,C. Marschall,D. Rudland, R. Francini,R. Wolterman,A. Hopper,and G. Wilkowski,1995,IPIRG-2 Task 1- Pipe System Experiments With Circumferential Cracks in Straight-Pipe Locations ,U.S. Nuclear Regulatory Commission, NUREG/CR-6389

53 D. L. Rudland, F. Brust, G. M. Wilkowski,1996, The Effects of Cyclic and Dynamic Loading on the Fracture Resistance of Nuclear Piping Steels ,U.S. Nuclear Regulatory Commission, NUREG/CR-6440

54 G.Kramer, P. Vieth, C.Mm-schall, R. Francini, G. Wilkowski,1997,Stability of Cracked Pipe Under Seismic/Dynamic Displacement-Controlled Stresses,U.S. Nuclear Regulatory Commission, NUREG/CR-6233 Vol-2 ; Subtask 1.2 Final Report

55 P. Scott R. Olson, G. Wilkowski, C. Marschall, R. Schmidt,1997, Crack Stability in a Representative Piping System Under Combined Inertial and Seismic/Dynamic Displacement-Controlled Stresses, U.S. Nuclear Regulatory Commission, NUREG/CR-6233 Vol-3 ; Subtask 1.3 Final Report

56 G.Wikowski, R. Schmidt, P. Smtt, R. Olson, C. Marachall, G. Kramer, D. Paul,1998, International Piping Integrity Research Group (IPIRG) Program,U.S. Nuclear Regulatory Commission, NUREG/CR-6233 Vol-4 ; Program Final Report

57 P. Scott, M.Wilson, R. Olson, C. Marschall,R. Schmidt, G. Wilkowski,1994,Stability of Cracked Pipe Under Inertial Stresses ,U.S. Nuclear Regulatory Commission, NUREG/CR-6233 Vol-1 ; Subtask 1.1 Final Report

58 G. Wilkowski, R. Olson, P. Scott, A. Hopper, 1995, "The IPIRG programs - advances in pipe fracture technology", Proceedings of the Seminar on Leak Before Break in Reactor Piping and Vessels, NUREG/CP-0155, October 9-11, page 375-399

59 R.J. Olson, B.J. Darlaston, M.E. Mayfield and R.A. Schmidt, 1993, "The IPIRG dynamic pipe loop test facility", Nuclear Engineering and Design, 144 (1993), pp. 77-90

60 R.Olson, S.Rahman, P.Scott, R.Mohan, T.Kilinski, D.Rudland, P.Krishnaswamy, A.Hopper, and G.Wilkowski, "ADVANCED LBB METHODOLOGY AND CONSIDERATIONS", Proceedings of the Seminar on Leak Before Break in Reactor Piping and Vessels, NUREG/CP-0155, October 9-11, page 601-604

61 A. Hopper, G. Wilkowski, P. Scott, R. Olson, O. Rudland, T. Kilinski, R. Mohan, N. Ghadiali, and O. Paul, 1997, "The Second International Piping Integrity Research Group (IPIRG-2) Program- Final Report", U.S. Nuclear Regulatory Commission, NUREG/CR-6452

62 Naoki Miura, Terutaka Fujioka , Koichi Kashima, Satoshi Kanno Makoto Hayashi, Masayuki Ishiwata, Nobuho Gotoh, "Low cycle fatigue and ductile fracture for Japanese carbon steel piping under dynamic loadings", Nuclear Engineering and Design 153 (1994) 57 69, 1994

63 Kalsumasa Masayuki, Satoshi Kanno, Makoto Hayashi, , Masayuki Ishiwata, Nobuho Gotoh, Naoki Miura, Terutaka Fujioka , Koichi Kashima,,1995, "Fracture Behaviour under low cycle fatigue loadings in Japanese carbon steel welded pipe joints with a defect", PVP-Vol.304, Fatigue and Fracture Mechanics

64 Naoki Miura, Terutaka Fujioka , Koichi Kashima,Kalsumasa Masayuki, Satoshi Kanno, Makoto Hayashi, Masayuki Ishiwata and Nobuho Gotoh, 1996, "Evaluation of low cycle fatigue crack growth and subsequent ductile fracture for cracked pipe experiments using cyclic J-integral", PVP-2, Fatigue and Fracture Vol-1

65 Naoki Miura, Koichi Kashima, Kalsumasa Masayuki, Satoshi Kanno ,1997, "Effect of negative stress ratio on crack growth for cracked pipe subjected to cyclic loading with large scale yielding,PVP-Vol.350, Fatigue and Fracture-1

66 Miura N., Fujioka T., Kashima K., Miyazaki K. Kanno S., Ishiwata M., Gotoh N., "Application of cyclic J-integral to low cycle fatigue crack growth of Japanese carbon steel pipe", Proceedings of the Seminar on Leak Before Break in Reactor Piping and Vessels, NUREG/CP-0155, October 9-11, page

465-471

67 K.Kinoshita, K.Murayama, M.Yokota, K.Kitsukawa, and K.Kashima, “Effect of Dynamic Monotonic and Cyclic Loading on Fracture Behavior for Japanese CarbonSteelPipeSTS410”, Proceedings of the Seminar on Leak Before Break in Reactor Piping and Vessels, NUREG/CP-0155, October 9-11, page 457-464

68 I. Milne, 2000, Observations on assessing ductile instability margins in the presence of fatigue, International Journal of Pressure Vessels and Piping 77, vol 77, pp 379-387.

69 C. W. Marschall, and G.M. Wilkowski, 1991, “Effect of cyclic loading on ductile fracture resistance”, ASME Journal of Pressure Vessel Technology, Vol.-113

70 Chang Sung Seok , Young Jin Kim, Jong Il Weon,1999, “Effect of reverse cyclic loading on the fracture resistance curve in C(T) specimen”, Nuclear Engineering and Design 191 (1999) 217–224

71 Chang-Sung Seok, K.L. Murty, 2000, A study on the decrease of fracture resistance curve under reversed cyclic loading, International Journal of Pressure Vessels and Piping 77, pg. 303-311

72 P.K.Singh, V.R. Ranganath, S. Tarafdar, Prabha Prasad, V. Bhasin, K.K. Vaze, H.S.Kushwaha, 2003, Effect of cyclic loading on elastic plastic fracture resistance of PHT piping material of PHWR,International Journal of Pressure Vessels and Piping Vol.80, pg.745-752

73 H. Roy, S. Sivaprasad, S. Tarafder, K.K. Ray, 2009, Monotonic vis-à-vis cyclic fracture behaviour of AISI 304LN stainless steel, Engineering Fracture Mechanics 76 (2009)1822 –1832

74 H. Roy, S. Sivaprasad, S. Tarafder, and K. K. Ray, 2011, Cyclic fracture behaviour of 304LN stainless steel under load and displacement control modes,Fatigue Fract Engng Mater Struct 35, 108–113

75 Lamba, H. S., “The J-integral applied to cyclic loading” Engineering Fracture Mechanics, Vol.7, pp.693-703, 1975

76 N.E. Dowling and J.A. Begley, 1976, “fatigue crack growth during gross plasticity and the J-integral” Mechanics of Crack Growth, ASTM STP 590, American Society for Testing and Materials, pp 82-103

77 K. Tanaka, “The cyclic J-integral as a criterion for fatigue crack growth”, Int J Fract, Vol.22, pp. 91–104, 1983

78 Lambert Y., Saillard P. and Bathias C., “Application of the J concept to fatigue crack growth in large scale yielding”, ASTM Special Technical Publication 969, ASTM, pp.318-329, 1988

79 Landes, J. D., Walker, H. and Clarke, A. G.(1979), Evaluation of Estimation Procedures Used in J-Integral Testing, Elastic Plastic Fracture ASTM STP 668, pp. 266-87.

80 K. Mogami, T. Hayashi, K. Ando and V. Ogura, “ Elastic-plastic fatigue crack growth and tearing instability behavior under cyclic loads”, Int J Pres Ves Pip 44, pp. 85–97, 1990

81 S Kaiser, “On Relation between stable fatigue crack growth and fatigue”, Fatigue of Engineering

Materials and Structures Vol-6 No-1 pp33-49, 1982

82 B .K. Neale and E K Priddle, “On fatigue crack growth and stable tearing”, Fatigue Fract Engng Mater Struct Vol.11 No.1, pp.31-43, 1988

83 K Obrtlik and J Polak, “ Ftaigue growth of surface cracks in the elastic plastic region”, Fatigue Fract Engng Mater Struct Vol.8 No.1, pp.23-31, 1981

84 B. Skallerud and Z.L. Zhang, “on numerical analysis of damage evaluation in cyclic elastic-plastic crack growth problems” techanical note, Blackwell sience ltd. Fatigue Frat Engng Mater Strut 23, pp 81-86, 2001

85 S. Rahman, G. Wilkowski and R. Mohan, “ Low cycle fatigue crack growth considerations in pipe fracture analyses”, Nuclear Engineering and Design, vol-168, pp. 105-118, 1997

86 Brocks W, Schimitt W. Quantitative assessment of the role of crack tip constraint on ductile tearing. In: Hackett EM, Schwalbe KH, Dodds RH, editors. Constraint Effects in Fracture, ASTM STP-1171 Philadelphia, PA: American Society for Materials and testing, 1993.,p. 64-78

87 Hiser Jr AL. “Specimen size effects on J-R curves for RPV steels”, In:Hackett EM, Schwalbe KH, Dodds RH, editors. Constraint Effects in Fracture, ASTM STP1171, Philadelphia, PA: American Society for Testing and Materials, 1993. p. 195-238.

88 Joyce JA, Hackett EM, Roe R. Effect of crack depth and mode of loading on the J±Rcurve behaviour of a high strength steel. In: Hackett EM, Schwalbe KH, Dodds RH, editors. Constraint Effects in Fracture, ASTM STP1171 Philadelphia, PA: American Society for Testing and Materials, 1993. p. 239-63

89 Roos E, Eisele U, Silcher H., “Effect of stress state on the ductile fracture behaviour of large scale specimens”. In: Hackett EM, Schwalbe KH, Dodds RH, editors. Constraint Effects in Fracture, ASTM STP1171 Philadelphia, PA: American Society for Materials and Testing, 1993. p. 41-63

90 T.V. Pavankumar, J. Chattopadhyay, B.K. Dutta, H.S. Kushwaha, 2002, “Transferability of specimen J–R curve to straight pipes with throughwall circumferential flaws”, International Journal of Pressure Vessels and Piping 79 (2002) 127-134

91 Marschall, C., Mohan, R., Krishnaswamy, P. and Wilkowski, G., 1994, “Effect of Dynamic Strain Aging on the Strength and Toughness of Nuclear Ferritic Piping at LWR Temperature”, NUREG/CR-6226, Report prepared for U.S. Nuclear Regulatory Commission.

92 C. W.Marschall, M. P. Landow, G. M. Wilkowski and A. R. Rosenfield., Int. J. of Press. Vess and Piping, vol 62, p49, 1995

93 Jin-Weon Kim, In-Sup Kim, “Effect of dynamic strain ageing on the leak before break analysis in SA106 Gr.C piping steel”, Nuclear Engineering and Design, 174, pg.59-67, 1997

94 P.K. Singh, J. Chattopadhaya, H.S. Kushwaha, S. Tarafder and V.R. Ranganath, “Tensile and fracture

properties evaluation of PHT system piping material of PHWR", Int. J of Pres. Ves & Piping, vol 75, p271 1998

95 D. Wagner, J.C. Moreno, C. Prioul, J.M. Frund, B. Houssin "Influence of dynamic strain aging on the ductile tearing of C–Mn steels: modelling by a local approach method", Journal of Nuclear Materials 300 (2002) 178–191

96 S. T. Mahmood, K. M. Al-Otaibi, Y. H. Jung, and K. Linga Murty, J of Testing and Eval., vol 18, No.5, p 332 Sept.1990

97 Nestell J. E. and Coward R. N., "Crack Growth Stability in Piping Systems with Complex Loading", Nonlinear fracture Mechanics, vol. 2, 1989, pp. 371-389

98 Yu Y.J, Kim Y.J, 1997, LBB (Leak-before-break) evaluation considering local and residual compliance of the cracked piping system, Trans. of the 14th SMiRT conference, vol. G 07/3

99 Sung-Po Liu, Kotoji Ando, 2000, "Leak-before-break and plastic collapse behaviour of statically indeterminate pipe system with circumferential crack", Nuclear Engineering and Design 195 (2000) 261-270

100 Gupta Suneel K., Vivek Bhasin, K.K. Vaze and H.S. Kushwaha, 2001, "Ductile Fracture Assessment of Piping Systems Including Compliance Effects", 16th Conference on Structural Mechanics in Reactor Technology, SMiRT-16, Washington DC, USA, paper-1427

101 Y.S. Yoo, K. Ando, 2003, "Leak-before-break behaviour of statically indeterminate piping system", Nuclear Engineering and Design, 2003

102 E Smith, 1996, "Leak-before-break: estimating the leakage area associated with a through-wall circumferential crack in a steel piping system", Int. J. Pres. & Piping, 65, 1996, pg 141-145

103 E Smith, 1997, "The effect of crack-system compliance on the leakage area for a circumferential cracked pipe subjected to combined axial and bending loadings", Int. J. Pres. & Piping, 72, 1997, pg 57-61

104 P.K.Singh, V.Bhasin, R.K.Singh, K.K.Vaze, "Improvement in Welding of Austenitic Stainless Steel Thick Pipe: Metallurgical, Mechanical & Full Scale Pipe Weld Tests" *Advanced Materials Research Vol. 794 (2013) pp 484-49*

105 P.K.Singh, V.Bhasin, K.K.Vaze, A. K. Ghosh, Kushwaha, H. S., 2008, "Structurral integirty of main heat transport system" , BARC newsletter issue 299 December 2008.

106 P.K.Singh, Punit Arora, V.Bhasin, K.K.Vaze, D.M.Pukazhendi, P.Gandhi, G.Raghava, 2013, "Fatigue crack growth and fracture resistance of narrow gap pipe welds of type 304ln stainless steel", Transactions, SMiRT-22, San Francisco, California, USA - August 18-23, Division II (Fracture Mechanics)107 Chattopadhayay, J., Dutta, B. K., and Kushwaha, H. S.,2000,Experimental and Analytical Study of Three Point Bend Specimens and Through Wall Circumferentially Cracked

Straight Pipe,”, International Journal of Pressure Vessel and Piping, vol.-77, pp. 455-471

108 Chattopadhyay J, B.K. Dutta, H.S. Kushwaha, E. Roos, K.-H. Herter,2004,Load bearing capacity of flawed piping components-comparison of experiment with calculation, International Journal of Pressure Vessels and Piping 81 (2004) 599–608

109 P. K. Singh, K. K. Vaze, A. K. Ghosh, H. S. Kushwaha, D. M. Pukazhendi and D. S. R. Murthy, “Crack resistance of austenitic stainless steel pipe and pipe welds with a circumferential crack under monotonic loading”, Blackwell Publishing Ltd. Fatigue Fract Engng Mater Struct 29, 901–915, 2006

110 J.Chattopadhyay, “Analytical and experimental studies on leak-before-break”, M.Tech. Dissertation, Indian Institute of Technology, Bombay, January,1995

111 P.K.Singh, K.K. Vaze, V. Bhasin, H.S.Kushwaha, P Gandhi, D.S. Ramchandra Murthy, 2003, “Crack initiation and growth behavior of circumferential cracked pipes under cyclic and monotonic loading” , International Journal of Pressure Vessels and Piping Vol.80, pg.629-640

112 Yoichi Fuji-ie, “A message 15 days after the 3.11 earthquake on the nuclear accident at Fukushima #1 NPS” , Journal of Disaster Research Vol.1 No.sp , 2012

113 Sumit Goyal, Suneel.K. Gupta, S. Sivaprasad, S. Tarafder, V. Bhasin, K.K. Vaze, A.K. Ghosh , “Low Cycle Fatigue and Cyclic Plasticity Behavior of Indian PHWR/AHWR Primary Piping Material, , Elsevier Procedia Engineering, 6th International Conference on Creep, Fatigue and Creep-Fatigue Interaction, Volume 55, 2013, Pages 136-143”

114 R. Mohan, C. Marschall, I. Knshnaswamy, F. Brost, N. Ghadiali, G. Wilkowski, “Effects of Toughness A.nisotropy and Combined Tension, Torsion, and Bending Loads on Fracture Behavior of Ferritic Nuclear Pipe”, USNRC, NUREG/CR-6299, April 1995